The Role of p21-Activated Kinases in Melanoma Progression

Nicholas, Nicole Stephanie

Awarding institution:
King's College London

The Role of p21-Activated Kinases in Melanoma Progression

Nicole Stephanie Nicholas

Division of Cancer Studies

King's College London

Submitted to fulfil the requirements of the degree of PhD

I declare that the work presented in this thesis is the work of the author and others' work is fully acknowledged where included

Abstract

Tumour metastasis initially requires invasion through the basement membrane and tissue migration towards the vascular system. During these stages cancer cells are thought to use actin rich protrusions called invadopodia to facilitate matrix and basement membrane degradation. p21-activated kinases (PAKs), a family of six serine/threonine protein kinases, have been linked to cell invasion and are found to be amplified/overexpressed in a wide variety of human invasive cancer cell lines and tissue. PAK1 localises in invadopodia, and PAK4 in podosomes (a closely related structure). This study looks at the role of these two PAK isoforms in invadopodia formation and cellular invasion in melanoma.

In this study a significant increase in the level of PAK1 and PAK4 expression in melanoma cell lines was demonstrated and both proteins were expressed in cell strains derived from patient samples. PAK1 overexpression correlated with melanoma cell line invasive potential, while both PAK1 and PAK4 overexpression occurred in cell lines and cell strains that formed invadopodia. Depletion of PAK1 and/or PAK4 expression resulted in a significant decrease in invasive capacity in melanoma cell lines and in an *in vivo* zebrafish invasion assay.

Protein depletion experiments point to differential roles for PAK1 and PAK4 during the invadopodia lifecycle. The data suggest that PAK1 promotes the formation of this protrusion while PAK4 is more important for the maturation and matrix degradation activity of invadopodia. This is the first time that PAK4 has been shown to be involved in invadopodia activity. Furthermore, this study has identified a signalling pathway, unique to PAK4, which suggests that this protein inhibits the function of PDZ-RhoGEF to promote the formation and degradation of invadopodia.

In conclusion, the data obtained from this study indicate that PAK1 and PAK4 play an important role in invadopodia activity and cellular invasion in melanoma. Distinct functions for each of these PAK isoforms in the invadopodia lifecycle has been established, with the identification of a novel PAK4 pathway involving the localised inhibition of PDZ-RhoGEF. PAK1 and PAK4 therefore present interesting therapeutic targets for the prevention/reduction of metastatic melanoma progression.

Acknowledgements

I owe my sincerest and deepest gratitude to my supervisor, Dr. Claire Wells, for her unwavering guidance and encouragement. I learnt and grew so much as a researcher in your lab and would not have been able to complete this project without your help, support and infinite wisdom. I cannot thank you enough. I am also grateful to my second supervisor, Dr. Katie Lacy for all the advice and suggestions throughout my PhD and for access to patient melanoma samples.

I am extraordinarily appreciative of all those who provided technical assistance and taught me a range of new research techniques. In particular, Simon Ameer-Beg for FRET, Joanna Richardson for zebrafish, Penny Morton for help with the RhoA biosensor, Panagiotis Karagiannis and Isioma Egbuniwe for patient tissue and for general help in the dermatology lab and finally the Hurlstone lab in Manchester for assistance with zebrafish xenografting and the spheroid assay.

I would like to say a big thank you to everyone in the Wells lab both past and present. In particular, Fahim, Katerina and Nouf, thank you for making the lab a fun environment, for your friendship, your support and for being there through the ups and downs of my PhD. I will certainly miss our lunches. I would also like to acknowledge Mario, Sally, Fariesha, Helen and Anna.

I am extremely grateful to all those in the office who have made the past three years a meaningful and enjoyable experience. In particular Yoli, thank you for being a good friend, for your help and support and for being there for a laugh and a chat. Ritu, I am forever grateful for your kindness, your encouraging words and for your absolute belief in my abilities. Jez, your guidance, technical support and advice were invaluable. Thank you for all your help and for being a smiling face in the lab.

I heartily thank all those who have shared their knowledge, advised, taught and guided me in the biological research field over the years - in particular, Dr. Philippa Darbre, Dr. Simon Scott, Dr. Vadim Sumbayev, Professor Shaun Thomas, Dr. David Fear and Professor Anne Ridley.

Lastly, and above all, I am extraordinarily grateful to my family. Mum, Janine and Beccy, thank you for your love and encouragement throughout my life. Sally, thank you for the past six years - for encouraging me, for believing in me, for showing me that anything is possible and for the steadfast help and support in all aspects of my life. Without you, none of this would have been possible.

Table of Contents

List of Figures

List of Tables

Abbreviations

AID	Autoinhibitory domain
BPE	Bovine pituitary extract
BSA	Bovine serum albumin
C. elegans	*Caenorhabditis elegans*
c-Src	Cellular Src
CIP4	Cdc42-interacting protein 4
CO_2	Carbondioxide
DH domain	Dbl homology domain
DHR1/2	DOCK Homology Region 1/2
DMEM F-12 Ham	Dulbecco's modified eagle's medium: nutrient F-12 ham
DMSO	Dimethyl sulfoxide
DNA	Deoxyribonucleic acid
dNTPs	Deoxyribonucleotide triphosphates
Dpf	Days post-fertilisation
Dpi	Days post injection
DQ	Dequenched
E. coli	*Escherichia coli*
ECL	Enhance chemiluminescence
ECM	Extracellular matrix
EDTA	Ethylenediaminetetraacetic acid
EGF	Epidermal growth factor
F-actin	Filamentous actin
FACS	Fluorescence activated cell sorting
FRET	Fluorescence resonance energy transfer
FLIM	Fluorescence lifetime imaging microscope
FBS	foetal bovine serum
Fwd	Forward
G-actin	Globular actin
GAPs	GTPase-activating proteins
GBD	GTPase binding domain
GDIs	Guanine nucleotide-dissociation inhibitors
GEFs	Guanine nucleotide exchange factors
GID	GEF interacting domain
H_2O	Water
HEPES	4-(2-hydroxyethyl)-1-piperazineethanesulfonic acid
HGF	Hepatocyte growth factor
HMWMAA	High molecular weight melanoma associated antigen
Hpf	Hours post-fertilisation
Hr(s)	Hour(s)
IQGAP1	IQ motif containing GTPase activating protein 1
kDa	Kilodaltons
LB	Luria-Bertani
LIMK	Lim Kinase
MAP	Mitogen activated protein
MEM	minimum essential medium
mDia	Diaphanous-related formin

Mins	Minutes
miRNA	Micro ribonucleic acid
MLC	Myosin light chain
MLCK	Myosin light chain kinase
MMP	Matrix metalloprotease
MTOC	Microtubule organising centre
MTT	Methylthiazolyldiphenyl-tetrazolium bromide
NaCl	Sodium chloride
Nck1	Non-catalytic region of tyrosine kinase adaptor protein 1
NCS	Newborn calf serum
N-WASP	N-wiskott-aldrich syndrome protein
OPCs	Oligodendrocyte progenitor cells
PAK	p21 activated kinase
$PBS^{+/+}$	Phosphate buffer saline plus calcium and magnesium
$PBS^{-/-}$	Phosphate buffer saline minus calcium and magnesium
PDGF	Platelet derived growth factor
PFA	Paraformaldehyde
PGE_2	prostaglandin E2
PH domain	Pleckstrin domain
PMA	phorbol 12-myristate 13-acetate
PTU	N-phenylthiourea
REF52	Rat embryonic fibroblast
Rev	Reverse
RGP	Radial growth phase
Rpm	Revolutions per minute
RNAi	Ribonucleic acid interference
ROCK	Rho-associated protein kinase
SCC	Squamous cell carcinoma
SEM	Standard error of the mean
siRNA	Short interfering ribonucleic acid
shRNA	Short hairpin ribonucleic acid
TAE	Tris Acetate-EDTA
TBST	Tris-buffered saline with Tween-20
TCSPC	Time-correlated single-photon counting
TE	Tris/EDTA
UV	Ultraviolet
VGP	Vertical growth phase
v-Src	Viral Src

1 Chapter 1 - Introduction

1.1 The Skin

The skin is the largest human organ and has many functions such as providing a physical barrier against pathogens, thermoregulation, sensation and vitamin production. This organ is made up of 2 layers, the dermis and epidermis, both of which serve vital functions. The epidermis is a dynamic structure, typically 0.05-0.1mm thick (Rook, 2010). It contains 95% keratinocytes and consists of multiple sub-layers, commonly referred to as stratum (Rook, 2004). Continual proliferation at the base of the epidermis (the stratum basale), moves keratinocytes outwards, until they are lost to the external environment at the outer most sub-layer, the stratum corneum (Figure 1-1) (Rook, 2010). Above the stratum basale, keratinocytes initiate the production of keratin, thus forming the layer known as the stratum spinosum. Following this, the keratinocytes produce keratohyalin granules in the stratum granulosum, and then lose their nuclei and organelles to become dead corneocytes in the stratum corneum (Rook, 2010). This process collectively called cornification, provides the strength and near impermeability of the skin.

The remaining 5% of the epidermis consists of melanocytes, Langerhans' cells and Merkel cells. Melanocytes and Merkel cells are both situated at the base of the stratum basale. Melanocytes, which account for 10% of the cell population of the stratum basale, produce melanin which is transported to the surrounding keratinocytes providing protection against ultraviolet (UV) light. Merkel cells contain mechanoreceptors which sense light tactile sensations (Maricich *et al.*, 2009). Conversely, Langerhans' cells can be found throughout the epidermis and function as antigen-presenting cells (Katz *et al.*, 1985).

The dermis, which is located below the epidermis, consists of fibroblasts, adipocytes and macrophages. The main functions of this layer are to supply gaseous and nutrient exchange to the epidermis, as well as to provide a supportive matrix to prevent any damage from environmental forces. This support, which amounts to 18-30% of the dermis volume, is primarily provided by collagen type I and III, secreted by the dermal fibroblasts (Rook, 2004). Lastly, a subcutaneous fat layer is situated below the dermis and this provides insulation. Underneath this fat layer there exists a layer of striated muscle.

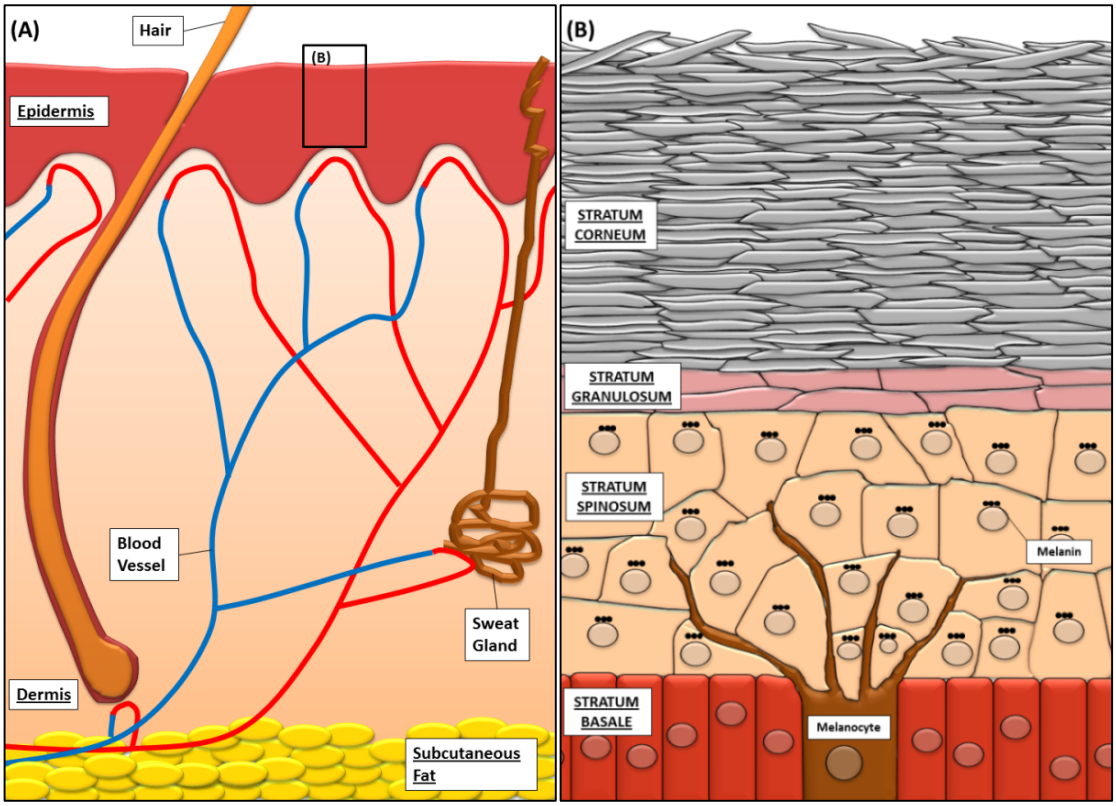

Figure 1-1: Diagrammatic representation of the human skin.
(A) The skin is made up of the epidermis and dermis, followed by a layer of subcutaneous fat. (B) The location of melanocytes in the stratum basale of the epidermis.

1.2 Cutaneous Melanoma

Melanoma arises from the neoplastic growth of melanocytes, and originates de novo or, in 50% of cases, from existing naevi (moles) (Bishop *et al.*, 2007). Despite an average age of diagnosis of 50, 20% of patients are diagnosed in adolescence (Bishop *et al.*, 2007), with a steady increase in the incidence rate from the age of 20 onwards (Cancer Research UK, 2014). Melanoma accounts for <2% of all skin cancers and has a total lifetime risk of 1 in 34 for men and 1 in 53 for women (American Cancer Society, 2014). However, it is estimated that ~79% of skin cancer deaths in 2011, in the UK, were attributable to melanoma (Cancer Research UK, 2014). Melanomas diagnosed in young individuals are most commonly found on areas that receive high intensity sun exposure, such as the trunk in men and legs in women (Whiteman *et al.*, 2011). However, when diagnosed at an older age, melanoma is more commonly found on areas that receive consistent sun exposure, such as the head and neck (Whiteman *et al.*, 2011). The main contributing factors for increased risk of melanoma are: large number of naevi (being the highest factor), having a family history of melanoma, fair skin that is susceptible to sun burning and freckling, and intense sun exposure during childhood (Whiteman *et al.*, 2011).

Initial transformation of melanocytes result in increased growth at the stratum basale in a horizontal manner, known as the radial growth phase (Figure 1-2) (Whiteman *et al.*, 2011). Following radial growth, the tumour cells develop invasive potential and can grow into the remaining upper epidermis layers (invasive radial growth phase). Finally, cells can enter the vertical growth phase, resulting in the breach of the epidermal-dermal junction and invasion into the dermis layer. The vertical growth phase brings the tumour mass within close proximity to the blood and lymphatic vasculature, greatly increasing the risk of metastasis. During this stage, tumour infiltrating lymphocytes often elicit an immune response. In some cases, this immune response can eliminate the primary tumour. However, in other cases the immune induced inflammation can drive progression of the disease.

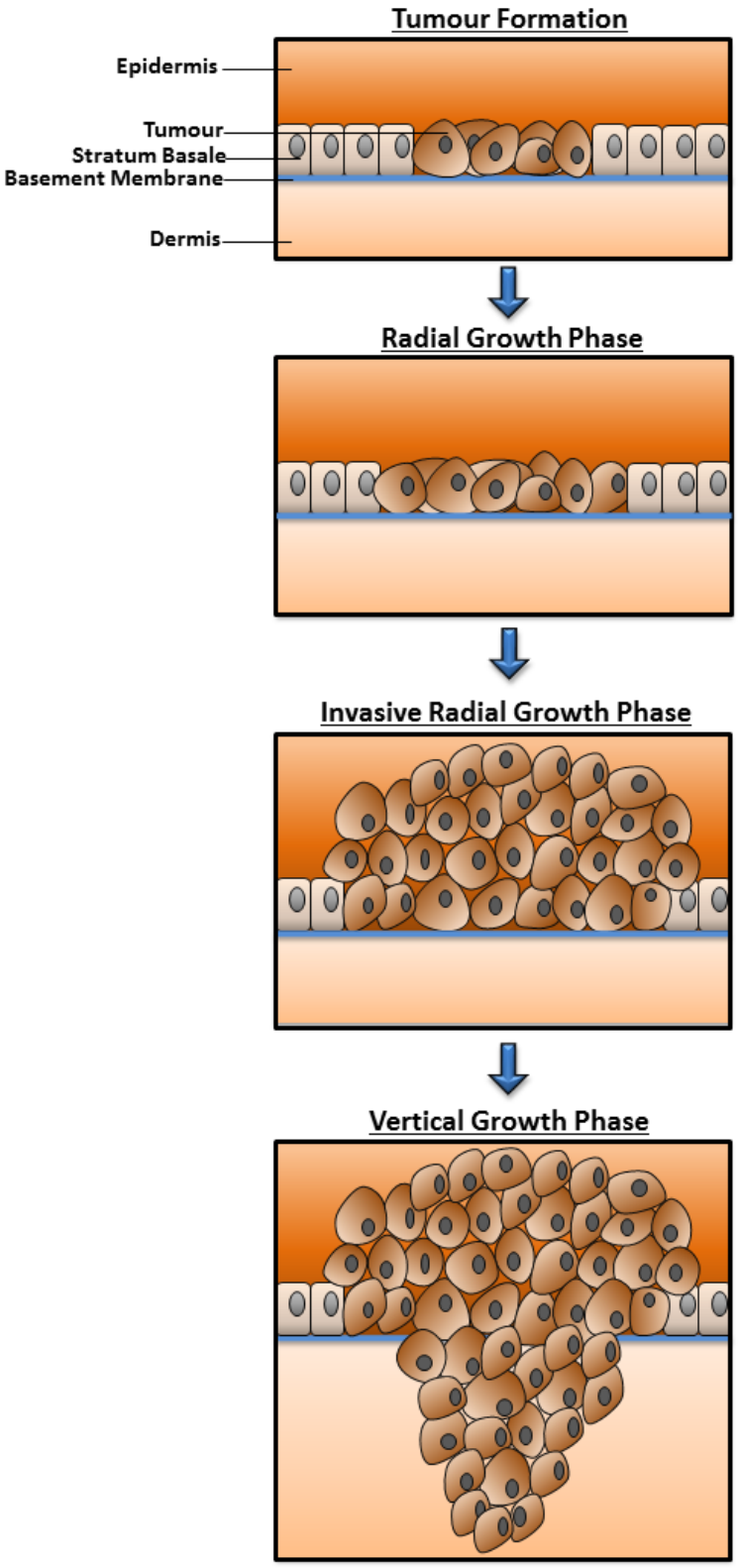

Figure 1-2: Melanoma radial and vertical growth phase.
Melanoma arises from the growth of melanocytes in the stratum basale layer of the epidermis. Melanoma grows within the stratum basale in a horizontal manner, known as the radial growth phase. Cells become invasive and grow into the epidermis (invasive radial growth phase) Following this, the cells invade through the epidermal/dermal basement membrane and grow vertically into the dermis. This is known as the vertical growth phase.

1.2.1 Diagnosis of Melanoma

As cutaneous melanomas can be seen on the exterior surface of the body, a high proportion are first identified by the patient using the well publicised 'ABCDE' monitoring guide. This guide recommends that medical advice be sought if a skin pigmentation has the following characteristics: Asymmetry; Border irregularity; Colour variation; Diameter larger than 5mm; and Evolution from the original characteristic (Neila and Soyer, 2011).

The first stage of diagnosis involves a biopsy. Unlike other cancers, the entire mass and a 2mm normal skin margin is surgically excised (Marsden *et al.*, 2010). Positive primary biopsies result in further excision of a larger margin of up to 3cm normal skin (Marsden *et al.*, 2010). Additionally, a sentinel node biopsy is performed via the injection of a radioisotope and blue dye solution directly into the excision site to identify the closest drainage lymph nodes (sentinel node). The dyed and radiation positive nodes are surgically removed and analysed for the presence of metastasis. If the sentinel nodes show evidence of the melanoma, the entire surrounding lymph nodes are removed. Diagnosed melanomas are assigned a Breslow thickness (described below) and a Staging in order to assess the relevant treatment.

1.2.2 Breslow Thickness

A direct link between melanoma thickness and prognosis was first described in 1970 by Alexander Breslow (Breslow, 1970). This was quickly adopted and the Breslow thickness is still in use today as a reliable classification of melanoma. This classification measures the thickness (in millimetres) of the tumour from the stratum granulosum to the deepest invaded tumour cells. The Breslow thickness is grouped into the following categories: <1mm; 1.01-2mm; 2.1-4mm; and >4mm. The survival rates greatly diminish in each group from a 5-year survival rate of 95-100% for <1mm to 37-50% for >4mm Breslow thickness (Melanoma Research Foundation 2011). The poor prognosis of tumours with a Breslow thickness of >4mm is due to a 50% higher risk of metastasis, compared to other thicknesses (Marsden *et al.*, 2010). This grading system is also used to indicate the clinical excision margins, ranging from 1cm for a thickness of <1mm to a 3cm margin for a thickness of >4mm (Marsden *et al.*, 2010).

1.2.3 Staging - American Joint Committee on Cancer (AJCC) TNM Staging System

The AJCC TNM staging system was first published in 2001 and has continued to be updated in subsequent years, providing relevant staging for cutaneous melanoma (Balch *et al.*, 2001; Balch *et al.*, 2009). Within this system the independent prognostic factors such as the Breslow thickness, presence of ulceration and mitotic rate, as well as the site and number of metastases provide a detailed diagnostic stage of the disease (Table 1-1) (Balch *et al.*, 2009).

Stage	Primary Tumour (T)	Lymph Nodes (N)	Metastasis (M)
IA	< 1mm, no ulceration, mitoses < 1 mm^{-2}		
IB	< 1mm, with ulceration or mitoses ≥ 1 mm^{-2} 1.01 - 2mm, no ulceration		
IIA	1.01 - 2mm, with ulceration 2.01 - 4mm, no ulceration		
IIB	2.01 - 4mm, with ulceration > 4mm, no ulceration		
IIC	> 4mm, with ulceration		
IIIA	Any Breslow thickness, no ulceration	Micrometastases 1-3 nodes	
IIIB	Any Breslow thickness, with ulceration Any Breslow thickness, no ulceration Any Breslow thickness, no ulceration	Micrometastases 1-3 nodes 1-3 palpable metastatic nodes No nodes, but in-transit or satellite metastasis/es	
IIIC	Any Breslow thickness, with ulceration Any Breslow thickness, with or without ulceration Any Breslow thickness, with ulceration	1-3 palpable metastatic nodes ≥ 4 metastatic nodes or matted nodes, or in-transit and metastatic nodes No nodes, but in-transit or satellite metastasis/es	
IV, M1a			Skin, subcutaneous or distant nodal disease
IV, M1b			Lung metastasis
IV, M1c			All other sites or any other sites of metastases with raised lactate dehydrogenase

Table 1-1: American Joint committee on Cancer (AJCC) TNM Staging System (Taken from Marsden *et al.*, 2010).

1.2.4 Treatment

The survival rate for patients suffering from early stage (no metastasis) melanoma is extremely high, with a five year survival of 98%. However, around 16% of patients presenting with melanoma will go on to develop metastatic disease (American Cancer Society, 2014). Once melanoma metastasises the available therapies provide little effective treatment with the five year survival rate decreasing to 62% for regional metastasis (the surrounding tissue) and 16% when distant metastasis has occurred (American Cancer Society, 2014). This emphasises the need for further research into new therapeutic targets for metastatic melanoma.

Metastatic melanoma has a very low median survival time of 6-9 months, with the worst survival rate of 3-4 months predicted for bone, liver and brain metastases (Becker *et al.*, 2000). Metastasis to distant lymph nodes, lungs or the skin have an increased median survival of 12-15 months, as these sites show a better response to treatments with chemotherapy medications (Becker *et al.*, 2000).

The current treatments, post-excision, for metastatic melanoma are chemotherapy: Dacarbazine, Vemurafenib and Ipilimumab. Radiotherapy is also commonly used for bone and brain metastases. Even with these treatments the patient survival rates for metastatic melanoma is less than a year. In fact, due to the lack of effective treatments for metastatic disease some patients with late stage IV disease often receive only palliative treatment.

Further investigations are therefore required to increase our understanding of metastatic melanoma such that the transition from localised to metastatic disease can be prevented.

1.3 The Metastatic Cascade

Metastasis, the growth of tumour cells at a distant site to that of the primary tumour, is the most life threatening aspect of human cancers, accounting for >90% of mortalities (Sahai, 2005; Valastyan and Weinberg, 2011). The successful metastatic growth of tumour cells is a rare occurrence, with <0.01% of the total cells which enter blood vessels resulting in the formation of a secondary tumour in animal models (Chiang and Massague, 2008). This is unsurprising as metastasis is a multistep process in which the metastatic tumour cells must survive and adapt to a wide variety of different environments. This process includes invasion through the basement membrane and surrounding tissue, entrance into blood vessels (intravasation) or

lymph vessels, exiting of the blood vessels (extravasation) into distant tissue and growth at this site (Figure 1-3) (Nguyen *et al.*, 2009). In addition, these steps rely on a multitude of pathways in which the manipulation of cell motility, cytoskeletal remodelling and cellular adhesion play prominent roles (Yilmaz and Christofori, 2009). Understanding these processes is crucial for the treatment and/or prevention of metastatic disease.

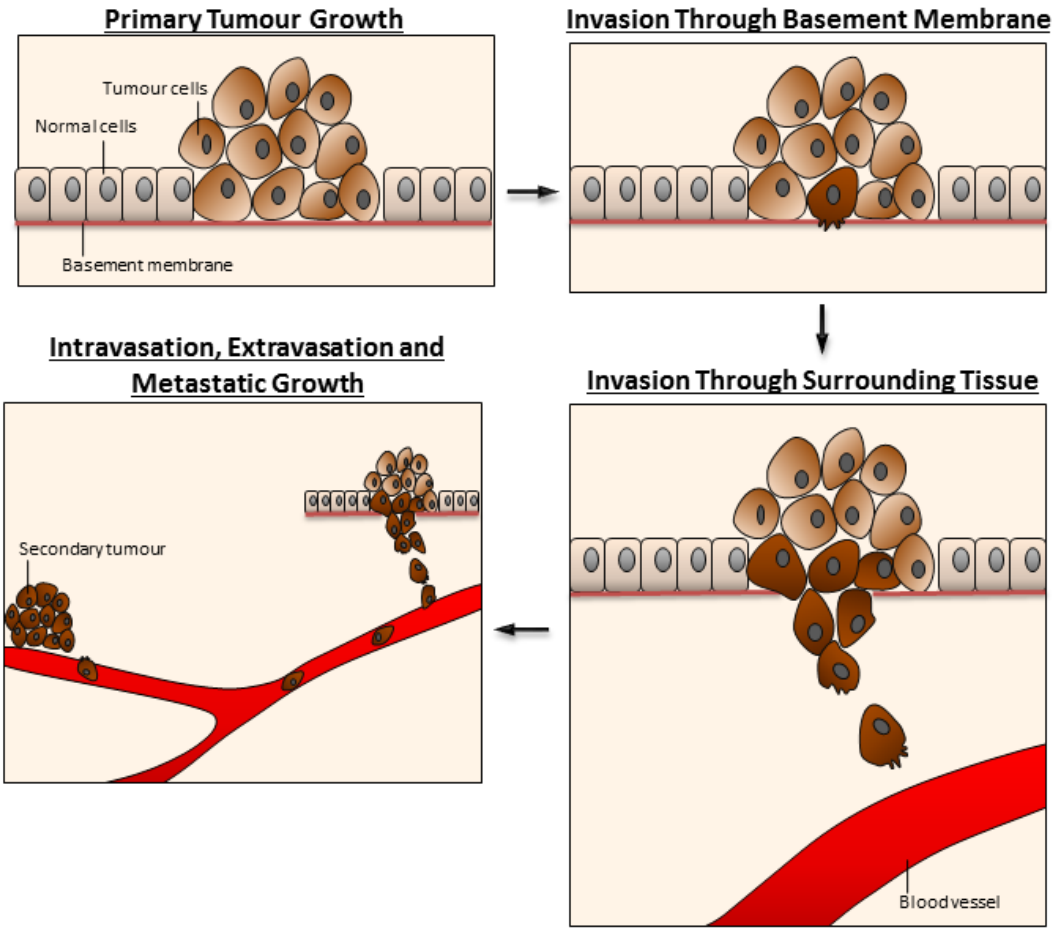

Figure 1-3: Diagram of the metastatic cascade.
Tumour cells grow at the primary site. Some cells acquire an invasive metastatic phenotype that enable the invasion through the basement membrane and into the surrounding normal tissue. These cells can intravasate into blood vessels or into lymphatic system where they disseminate throughout the body. At distant sites, cells extravasate out of blood vessels and proliferate to form a metastatic growth.

1.3.1 Mechanisms of Cell Invasion

In normal cells, migration is achieved through co-ordinated control of cytoskeleton dynamics, cell-cell status and cell-matrix adhesion turnover. To migrate, cells become polarised, producing a clear front characterised by protrusions such as filopodia (thin finger-like protrusions) or lamellipodia (broad protrusions), and a contractile rear (uropod). These protrusions are extended and anchored to the extracellular matrix (ECM) by cell adhesions that create a traction force for forward movement (Friedl and Alexander, 2011). In contrast, at the rear, the cell adhesions are dissolved and the membrane retracted to promote forward movement (Friedl and Alexander, 2011; Ridley, 2011).

During the initial stage of metastasis, cells break away from the primary mass and interact with the surrounding tissue. In order to invade through underlying tissue, cells migrate by adapting their cell shape, cell-cell adhesions and adhesions to the ECM. To reach the blood or lymph vessels, tumour cells must migrate and invade through the underlying ECM. Invasive protrusions called invadopodia (which are discussed in more detail in section 1.5) are used to degrade the ECM to aid the invasion of tumour cells through the basement membrane and the surrounding tissue. Other cell types in the tumour microenvironment can also control the invasive potential of tumour cells. For example, cells located in the surrounding stroma, such as fibroblasts and infiltrating immune cells, can secrete factors that enhance the metastatic phenotype of the invading cells (Goswami *et al.*, 2005; Joyce, 2005). In addition, these cells can directly modulate the ECM structure by the secretion of proteases to aid the invasion of tumour cells (Sahai, 2005) and guide tumour cells to the surrounding blood vessels where they also assist in intravasation (Wyckoff *et al.*, 2007).

Tumour cells are thought to migrate through the ECM via two methods, as individual cells (single cell migration) or as a collective group (collective migration) (Figure 1-4) (Friedl and Wolf, 2003; Sanz-Moreno and Marshall, 2010). These methods of migration are not mutually exclusive and can occur simultaneously in tumours (Friedl and Wolf, 2003).

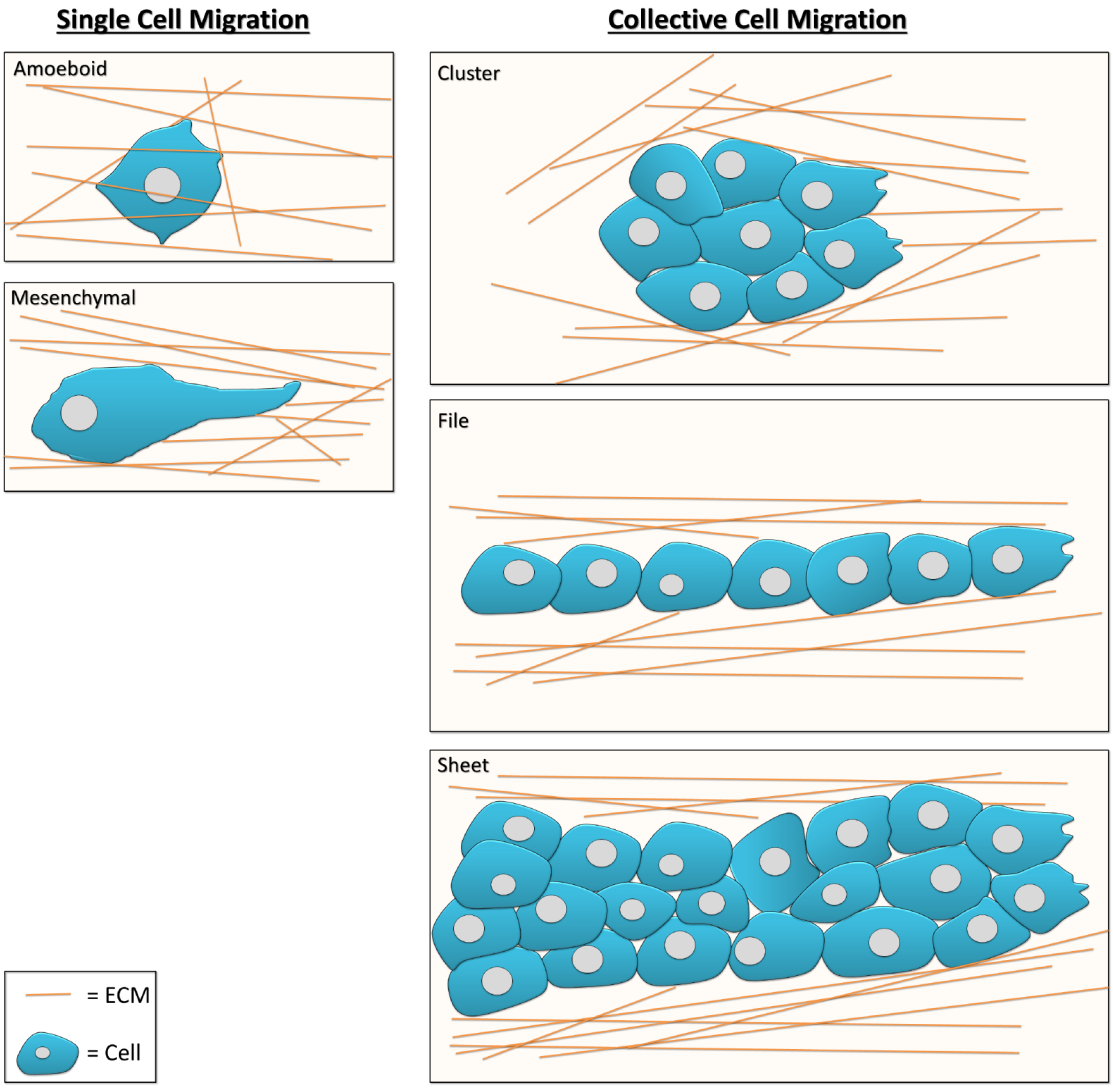

Figure 1-4: Mechanisms of single cell and collective migration.
Cells can invade either individually (single cell migration) or collectively (collective cell migration), each of which occurs via different mechanisms. Single cell migration can be separated into mesenchymal, with an elongated cell shape that uses protease degradation, and amoeboid cell movement, with a highly contractile cell shape that invades independent of protease degradation. In collective cell migration a group of cells invade in either a small cluster, file (line of cells) or a sheet, all utilising cell-cell adhesions to maintain multicellular structures during invasion.

Single cell migration utilises two interchangeable mechanisms, mesenchymal and amoeboid (Figure 1-4) (Sanz-Moreno and Marshall, 2010). Cells using mesenchymal migration have an elongated polarised cellular structure similar to that seen by migrating non-tumourigenic cells. Unlike normal cells, tumour cells that adopt the mesenchymal mechanism of migration rely on protease degradation of the ECM (via invadopodia protrusions) to enable invasion. In addition, this mode of migration is often triggered by receptor tyrosine kinases, including c-MET (by hepatocyte growth factor (HGF)).

In contrast, the amoeboid mechanism of migration is protease independent and relies on a highly contractile, rounded cell shape that allows cells to squeeze through strands of ECM. This high contractile force is often accompanied by membrane blebbing due to hydrostatic pressure that disconnects cortical actin from the plasma membrane (Lammermann and Sixt, 2009). In addition, amoeboidal cells often have weak cell-matrix adhesions, with small adhesions rather than the large stable focal adhesions used by non-tumourigenic cells.

While both forms of migration facilitate invasion, the amoeboidal mechanism is thought to be associated with an increased invasive potential compared to mesenchymal migration (Gadea *et al.*, 2008; Calvo *et al.*, 2011). These forms of migration are not fixed, and metastatic cells, especially metastatic melanoma, have high plasticity, switching between these to allow for the most appropriate mode of migration (Sahai and Marshall, 2003; Sanz-Moreno *et al.*, 2008). This plasticity is also seen *in vivo,* with cells from tumour samples exhibiting both amoeboidal and mesenchymal morphologies (Rosai and Ackerman, 2004).

Collective migration involves the movement of multiple cells which invade as a collective group. The overall structure of the collective mass can vary depending on the number of cells, the structure of the tissue that is being invaded and also the cell type, resulting in the formation of cell clusters, files or sheets (often found in melanoma) (Figure 1-4) (Geiger and Peeper, 2009; Friedl and Alexander, 2011). Within these groups, cell-cell and cell-matrix adhesion components such as cadherins and integrins, respectively, are present and aid migration (Sahai, 2005). Cadherins, which are the major transmembrane component of adherens junctions, bind adjacent cells to form cell-cell adhesions, while integrins are transmembrane proteins that bind the ECM and connect the external matrix with the cytoskeleton to form cell-matrix adhesions. The collective migration of melanoma clusters through 3D collagen I matrices are highly dependent on β1 integrin (Hegerfeldt *et al.*, 2002). In this form of migration, 'leader' cells are often found at the front of the group, and these cells exhibit similar characteristics to

mesenchymal migration, generating forward traction and using pericellular protease degradation to form a track in which the following cells can migrate (Friedl and Alexander, 2011).

1.3.2 Intravasation, Extravasation and Colonisation at Secondary Sites

In order to form a secondary tumour at a distant site cancer cells must pass from the tissue, through the basement membrane and into blood vessels (intravasation) or into the lymph ducts. Tumour cells can directly orient their migratory direction towards that of blood vessels (Sahai, 2007). This directional migration may be induced by tumour associated macrophages, that can be found clustered around blood vessels, and may provide an epidermal growth factor (EGF) chemotactic gradient that attracts tumour cells (Wyckoff *et al.*, 2007).

When at the blood vessels, tumour cells can transmigrate either between endothelial cells (paracellular) or through endothelial cells (transcellular) (Reymond *et al.*, 2013). The cell shape and mechanism of migration can influence this step of metastasis, as amoeboid cells are more efficient at transmigration than their mesenchymal counterparts (Sahai *et al.*, 2007). Cells can also exit the primary tissue through intravasation into the lymphatic system where they can form metastatic growths in the lymph nodes or drain into the cardiovascular system.

Once inside blood vessels, tumour cells must evade intracellular anchorage dependent cell death (anoikis), as well as death from shear stress and from the immune system (Valastyan and Weinberg, 2011). To reach the secondary tissue, cells have to adhere to the blood vessel wall, or become lodged in small capillaries, to become stationary. Once this occurs, cells transmigrate across the endothelial wall (extravasate) and initiate colonisation and cell growth (Reymond *et al.*, 2013).

1.4 The Rho GTPase Family

Actin cytoskeletal dynamics is an essential part of cell motility and it is regulated largely by Rho family GTPases. The Rho GTPase family are proteins of the Ras related superfamily of small GTPases and contain 20 members. These proteins interact with a range of different effectors including protein kinases, actin nucleators and phospholipases to exert their functions (Heasman and Ridley, 2008). The three most characterised Rho GTPases are Cdc42, Rac1 and RhoA, and these will be discussed in more detail herein.

The control of Rho GTPase activity is governed by guanine nucleotide exchange factors (GEFs), GTPase-activating proteins (GAPs) and guanine nucleotide-dissociation inhibitors (GDIs). Rho GTPases cycle between an inactive, GDP bound state, and an active, GTP bound state (Jaffe and Hall, 2005). GEFs catalyse the dissociation of GDP and formation of GTP bound, active Rho GTPases (Rossman et al., 2005). Most GEFs, which are part of the Dbl family, contain two representative domains; the Dbl Homology (DH) domain that functions in the catalysis of Rho GTPases; and the Pleckstrin Homology (PH) domain, which cooperates with the DH domain to aid its catalytic activity and binds phospholipids to localise the GEF to the plasma membrane (Rossman *et al.*, 2005). Other GEFs, such as the DOCK family of GEFs, have the DOCK Homology Region 1 (DHR1) which targets the protein to the membrane through phospholipid binding, and the catalytic domain DOCK Homology Region 2 (DHR2) which is responsible for the GEF activity (Goicoechea *et al.*, 2014).

Conversely, GAPs increase the rate of GTP hydrolysis to promote the formation of inactive, GDP bound Rho GTPases. These proteins are characterised by the presence of a Rho GAP domain which binds the GTP binding site of Rho GTPase when GTP is bound.

GDIs function differently to GEFs and GAPs by binding the Rho GTPases and sequestering the protein in the cytosol in the GDP bound state, thus inhibiting the activation (Rossman *et al.*, 2005). In addition, it is believed that GDIs also prevent the release of GDP and thus the binding of GTP to Rho GTPases, to further inhibit their activity (Garcia-Mata *et al.*, 2011).

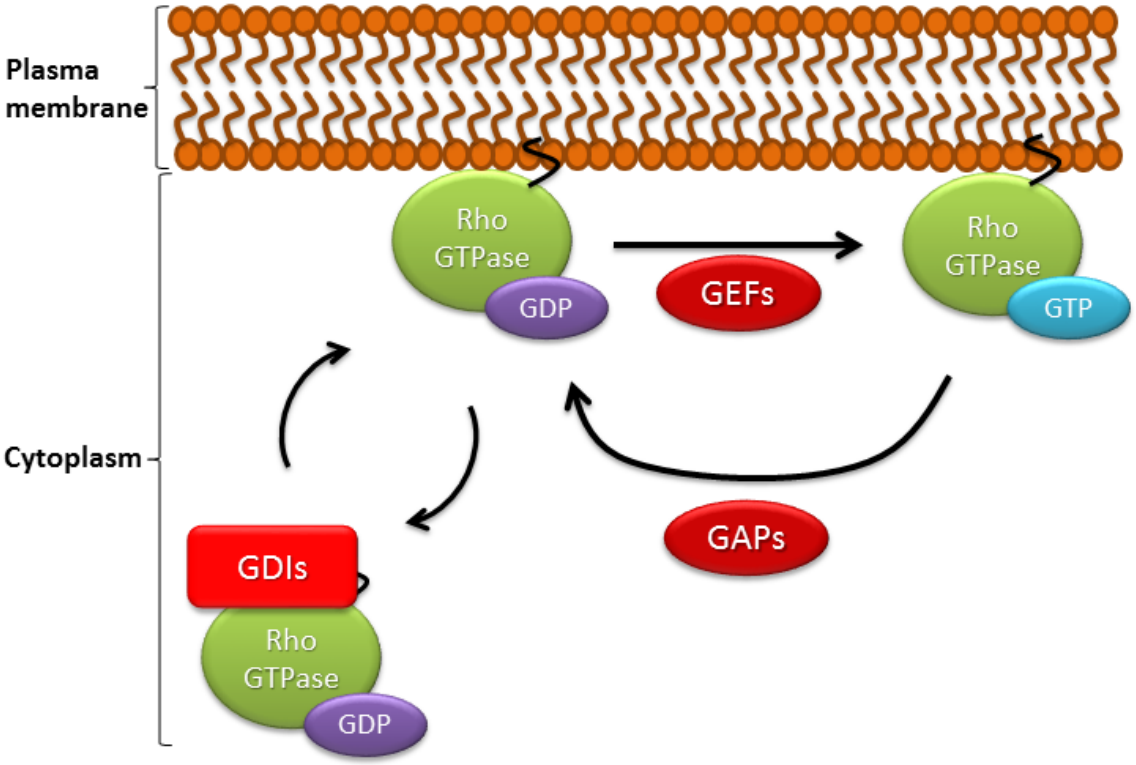

Figure 1-5: Control of Rho GTPase activity.
Rho GTPases, which are tethered to the plasma membrane, cycle between an inactivated GDP bound protein and a GTP bound activated protein. Rho GTPases are activated using GEFs and inactivated by GAPs. The GTPase activation is also inhibited by the binding of GDIs, which sequester the GTPase in the cytoplasm.

1.4.1 Rho GTPases are Major Regulators of Cell Motility

The Rho family GTPases, which include Cdc42, Rac1 and RhoA, are able to control actin polymerisation dynamics and organisation to protrude the plasma membrane and thus elicit cell movement (Jaffe and Hall, 2005).

Actin exists as either free globular actin (G-actin) monomers or as filamentous actin (F-actin) bound to other actin monomers in a polymeric fashion. Actin polymerisation consists of the addition of G-actin at sites of nucleation on actin filaments referred to as barbed ends, the result being filament elongation. The addition of the monomeric actin to F-actin is controlled by the Arp2/3 complex (which is activated by Rac1 and Cdc42) or formins such as Diaphanous-related formin (mDia) (which is activated by RhoA) (Jaffe and Hall, 2005; Le Clainche and Carlier, 2008). The polymerisation of F-actin occurs via a 'treadmilling' method involving the polarised addition

of G-actin at barbed ends along with the depolymerisation of F-actin to G-actin at the pointed end creating movement of the filament in the direction of polymerisation (Le Clainche and Carlier, 2008). The depolymerisation at the pointed end requires the actin severing protein cofilin. Cdc42, Rac1 and RhoA can all control cofilin activity. ROCK activation via RhoA can activate LIM kinase (LIMK), while Cdc42 and Rac1 can activate LIMK via PAK activation. Activated LIMK phosphorylates and inhibits the activation of cofilin.

ROCK activation via RhoA also directly phosphorylates and activates myosin light chain (MLC) and inhibits MLC inactivation by the phosphorylation and inhibition of myosin phosphatase (an inactivator of MLC) to enhance myosin induced actin contractility (O'Connor and Chen, 2013).

The control of the actin cytoskeletal dynamics, including actin polymerisation and actomyosin contraction are essential for cell movement. During migration, cells form protrusions (lamellipodia and filopodia) at the leading edge (Figure 1-6). Rac1 functions to produce broad protrusions called lamellopodia (containing branched actin filaments), and to form focal adhesions, at the leading edge of the cell (Nobes and Hall, 1995; Nobes and Hall, 1999). The formation of these focal adhesions provides a connection between the ECM and the cytoskeleton which enables cells to generate a traction force, which is translated into forward movement. Rac1 activation at the rear has also been implicated in tail retraction in motile neutrophils (Gardiner *et al.*, 2002).

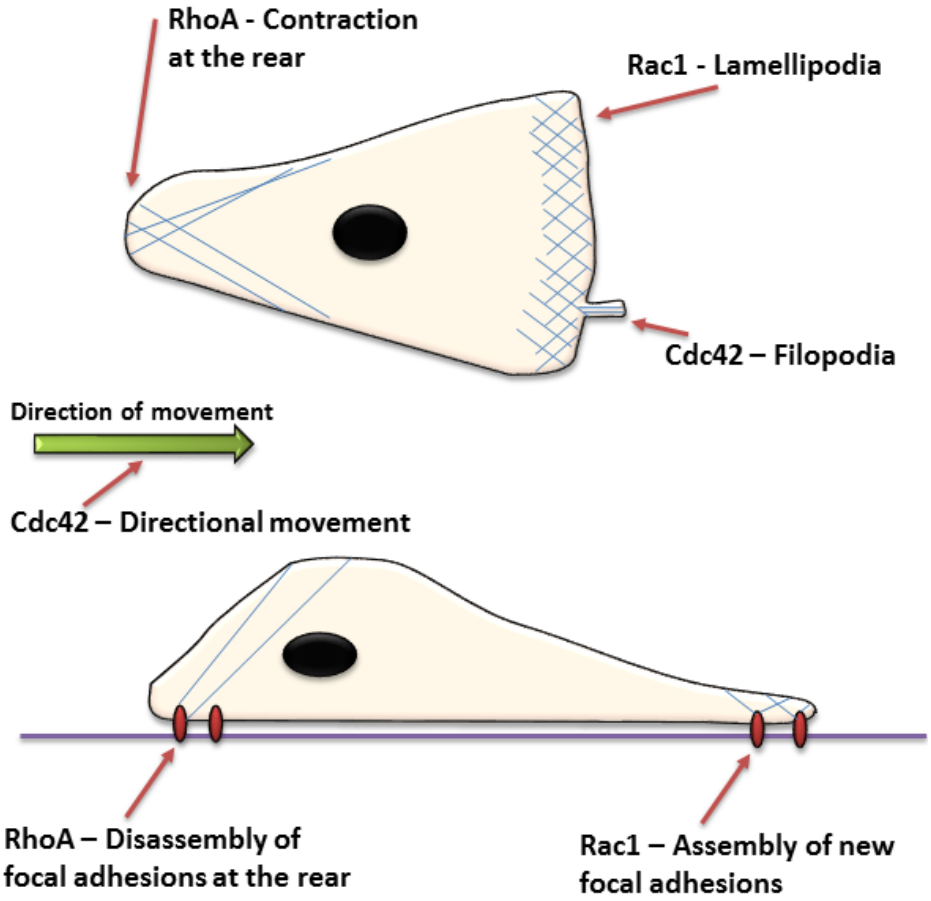

Figure 1-6: Rho GTPases in mesenchymal cell migration.
In mesenchymal cell migration, Rac1 forms lamellopodia protrusions which cause directional movement. Rac1 forms filopodia finger-like protrusions and promote the assembly of focal adhesion at the leading edge. RhoA promotes actomysin contraction at the rear of the cell and disassembly of focal adhesions.

Cdc42 promotes the formation of finger-like protrusions called filopodia which are associated with linear, unbranched actin polymerisation (Nobes and Hall, 1995). Cdc42 drives the polarity and directional movement of cells. Cdc42 also functions to position the golgi body and microtubule organising centre (MTOC) at the leading edge side of the nucleus to aid delivery of vesicles to the leading edge protrusions (Etienne-Manneville and Hall, 2003). Though Rac1, Cdc42 and RhoA all localise in lamellipodia protrusions (Machacek *et al.*, 2009), the functions elicited are dependent on their activation, which can involve a significant amount of cross talk between the proteins. Cdc42 can directly control Rac1 activation through PIX and Tiam1, which are both Rac GEFs (Li *et al.*, 2003; Cau and Hall, 2005; Pegtel *et al.*, 2007). Rac1, in turn, can inhibit the activation of RhoA through PAK induced inhibition of RhoA GEFs, including GEF-H1. In fact Rac1 and RhoA are mutually inhibitory proteins, with each protein being able to inhibit the activity of the other (Sanz-Moreno *et al.*, 2008; Machacek *et al.*, 2009).

RhoA functions in actomyosin contractility, via ROCK, and the disassembly of integrin based focal adhesions, both of which occur at the rear of a motile cell (Chrzanowska-Wodnicka and Burridge, 1996; Alblas *et al.*, 2001). The retraction and reduction of adhesions at the rear (along with protrusions at the leading edge), allows for the cell to move in a forward motion and provides membrane availability for the extension of the leading protrusion. RhoA activity is not confined to the rear of the cell, with RhoA activation having been seen in the first 2µm of cell protrusions, indicating a possible function in this process (Machacek *et al.*, 2009).

1.4.2 Rho GTPases are Central to Cancer Cell Invasion

Given their role in driving cell migration it is perhaps not surprising that Cdc42, Rac1 and RhoA all contribute to the mechanisms by with tumour cells migrate, whether it be via single or collective migration. Indeed, the mesenchymal and amoeboid mechanisms of single cell migration are finely controlled through the reorganisation of the cytoskeleton by Rac1, Cdc42 and RhoA.

The activation of Rac1 promotes mesenchymal migration, which can be induced by activators including DOCK3, or through adaptor proteins such as NEDD9 (Sanz-Moreno *et al.*, 2008). This protein also functions to simultaneously inhibit the formation of an amoeboid shape by reducing actomyosin contractility (Sanz-Moreno *et al.*, 2008). Similarly, the depletion of Rac1 can reduce cell invasion (Wheeler *et al.*, 2006), further implicating these proteins in cancer cell invasion. However, recent findings have suggested that Rac1 is required for the disassembly of invadopodia protrusions (Moshfegh *et al.*, 2014), indicating that the role played by this protein in cancer invasion is complex.

Cdc42 plays a role in both mesenchymal migration to polarise the cell and also in amoeboidal migration through PAK2 to increase MLC phosphorylation and actomyosin contractility (Gadea *et al.*, 2008). Cdc42 is also a major inducer of the invasive protrusion, invadopodia, which is thought to be used by tumour cells to invade through the ECM (Murphy and Courtneidge, 2011). In fact, the depletion of Cdc42 has been shown to reduce the metastasis of breast cancer cells *in vivo* (Reymond et al., 2012).

In contrast, the amoeboid mechanism of migration, is highly dependent on RhoA (Sahai and Marshall, 2003; Orgaz and Sanz-Moreno, 2013). The activation of this protein is responsible for the highly contractile shape that is representative of this form of migration. This occurs via the

activation of ROCK, which in turn, activates myosin light chain 2 (MLC2) to enhance myosin induced actin contraction (O'Connor and Chen, 2013). The signalling pathways that induce amoeboid motility also result in the inhibition of mesenchymal migration. This is achieved by the ROCK induced activation of ARHGAP22, which in turn inhibits the activation of Rac1 (Sanz-Moreno *et al.*, 2008).

The studies investigating the function of RhoA in cell invasion have produced contradictory results. Some studies indicate that a reduction in RhoA expression and activity results in an increase in invasion of breast and prostate cancer cell lines *in vitro* (Simpson *et al.*, 2004; Vega *et al.*, 2011). Others have found that a knockdown of this protein in breast cancer cell lines reduces *in vitro* cell invasion and lung metastases in an *in vivo* murine tail injection assay (Sahai and Marshall, 2003; Valastyan *et al.*, 2009; Sanz-Moreno and Marshall, 2010). In addition, RhoA is overexpressed in a range of different tumour types such as colon, breast and lung cancer (Fritz *et al.,* 1999; Kamai *et al.,* 2001; Sahai and Marshall, 2002). Given the key role that RhoA plays in cytoskeletal dynamics and actomyosin contractility it is unsurprising that the function of this protein in cell invasion is quite complex, and may vary depending on the cell type and/or spatiotemporal distribution of the protein. Additional studies are therefore required to further understand the specific role that RhoA plays in cell invasion.

1.5 Invadopodia

During the initial stages of invasion, cells must degrade (when amoeboid migration is not used) and invade through the basement membrane and the ECM to reach blood vessels or the lymphatic system (Nguyen *et al.*, 2009). In order to achieve this, it is thought that tumour cells form an actin rich, protease secreting invasive protrusion in the direction of movement, referred to as invadopodia (Stylli *et al.*, 2008; Buccione *et al.*, 2009; Ridley, 2011). These invadopodia degrade the ECM, promoting cellular invasion. Invadopodia are also used by tumour cells during intravasation, another important step in the metastatic process (Gligorijevic *et al.*, 2012).

Invadopodia are thought to be related to podosomes, a degradative protrusion that is formed by highly migratory, non-transformed cells of the haematopoietic lineage such as macrophages and dendritic cells (Buccione *et al.*, 2004; Yilmaz and Christofori, 2009) and which aids the migration of these cells, in and through tissue (Murphy and Courtneidge, 2011). Podosomes can be induced in endothelial and smooth muscle cells by growth factors such as platelet derived

growth factor (PDGF) and EGF (Murphy and Courtneidge, 2011). Invadopodia differ from podosomes in that they produce a more stable, longer protrusion of over 2µm (podosome protrusions are typically 0.5-2µm) that can last for hours, compared to the 2-10 minute lifespan that is typical of podosomes (Li *et al.*, 2010a; Murphy and Courtneidge, 2011; Mak, 2014).

Invadopodia and podosomes show similarities with the adhesive structure, focal adhesions and share a large proportion of their proteins such as paxillin and integrins (Hoshino *et al.*, 2013). Interestingly, recent findings have indicated that focal adhesions also have degradative capacity, further strengthening the similarities between invadopodia/podosomes and focal adhesions (Wang and McNiven, 2012). However, studies have suggested a reciprocal relationship with focal adhesion kinase (FAK) phosphorylation of Src promoting the turnover of focal adhesions and inhibition of invadopodia formation (through sequestering Src to focal adhesions) (Chan *et al.*, 2009). While the inhibition of FAK induced Src phosphorylation promotes focal adhesion disassembly and the formation of invadopodia (Vitale *et al.*, 2008; Liu *et al.*, 2010b). Similar results have been found for podosomes and focal adhesions with Yu and colleagues suggesting that they both arise from the same precursor with the resulting structure being determined by the force exerted by the matrix to stimulate stress fibre incorporation (focal adhesion) or actin polymerisation (podosomes) (Yu *et al.,* 2013),

Invadopodia structures were first described in fibroblasts transformed using the Rous sarcoma virus (which contains the oncogene v-Src) (Chen, 1989). However, it was known for many years before this that v-Src induced and localised to ventral protrusions in fibroblasts (Chen *et al.*, 1985) that had degradative capacity (Chen *et al.*, 1984), when plated on fibronectin. These structures have since been identified in a wide variety of cell lines including melanoma (Aoyama and Chen, 1990; Chen *et al.*, 1994; Mueller *et al.*, 1999; Baldassarre *et al.*, 2003), breast cancer (Chen *et al.*, 1994; Lorenz *et al.*, 2004; Artym *et al.*, 2006), prostate cancer (Desai *et al.*, 2008), colon cancer (Schoumacher *et al.*, 2010), head and neck squamous cell carcinoma (SCC) (Clark *et al.*, 2007) and glioma (Chuang *et al.*, 2004).

Invadopodia form an actin comet structure, which consists of a stationary actin cluster at the head, followed by a highly motile tail that exhibits spiral movement (Baldassarre *et al.,* 2006; Takkunen *et al.,* 2010). Protein expression in these actin comets are spatially distributed with N-WASP (neural Wiskott-Aldrich syndrome protein) localising at the base of the comet (Baldassarre *et al.,* 2006). It is thought that this actin comet provides the force needed to elongate the invadopodia.

Invadopodia are visualised in a 2D environment by plating cells on a matrix, where the protrusion forms on the ventral surface of the cell, often in the centre, underneath the nucleus (Lorenz *et al.*, 2004; Baldassarre *et al.*, 2006; Ayala *et al.*, 2008; Poincloux *et al.*, 2009). To identify the regions of degradation, the matrix, which can be native ECM proteins (such as fibronectin) or gelatin (a denatured collagen substitute), is fluorescently labelled. When these matrices are degraded, a region lacking fluorescence is produced and those regions which correspond with actin puncta are distinguished by cell staining for F-actin (Figure 1-7). These regions of actin puncta and degradation co-localisation are identified as invadopodia.

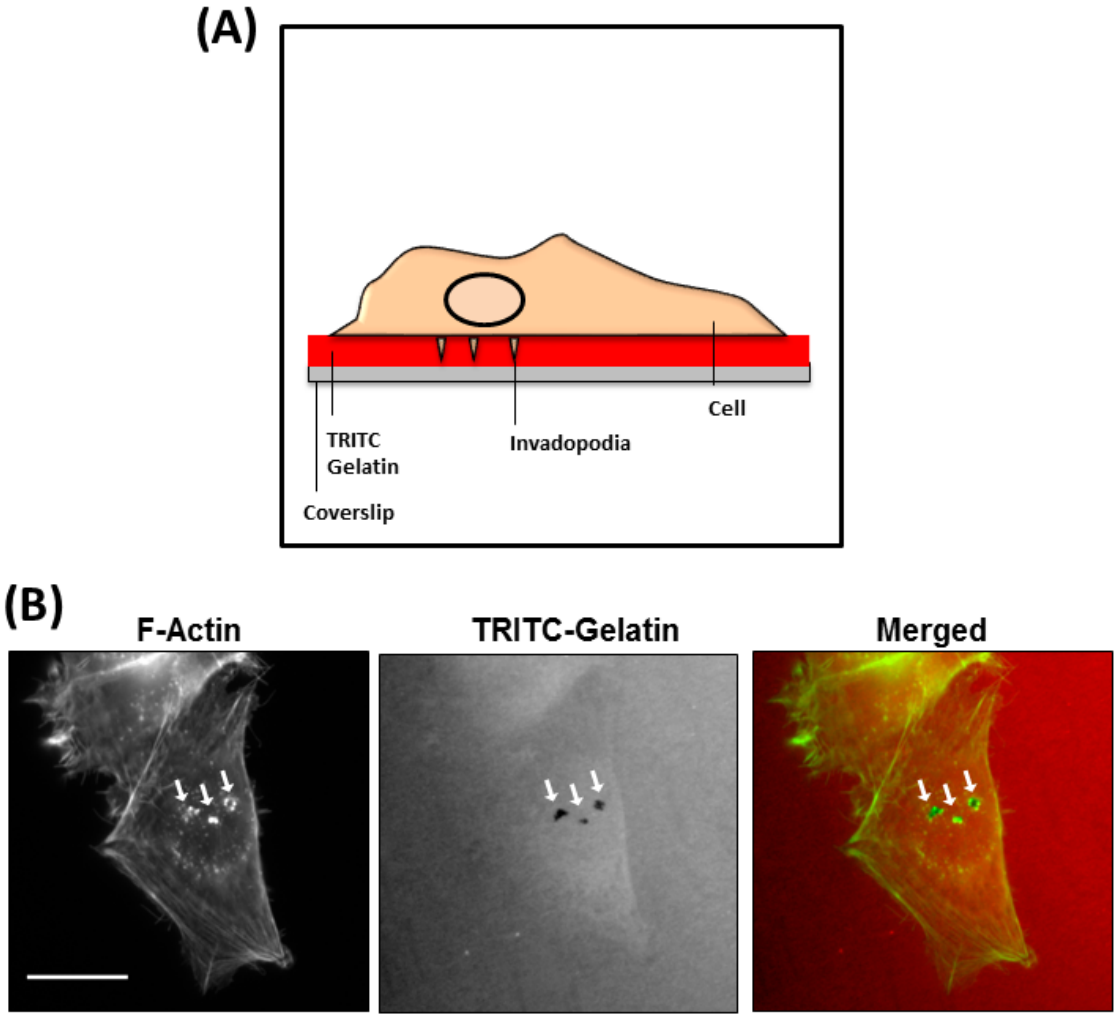

Figure 1-7: Invadopodia as visualised in a 2D assay.
(A) Invadopodia are visualised in 2D assays by plating cells on a fluorescently labelled matrix (e.g. TRITC-Gelatin) and staining for F-actin. Actin puncta that correspond with matrix degradation are classed as invadopodia. (B) Example images of an invadopodia assay (actin, TRITC-gelatin and merged images) using A-375M2 cells showing invadopodia (white arrows) (scale = 10µm).

Though invadopodia are easily visualised in an *in vitro* 2D setting, their identification in a 3D matrix and in an *in vivo* context has been challenging. In a 3D matrix, the use of dequenched (DQ) collagen, which fluoresces in areas of matrix degradation, has allowed for the identification of protrusions that have a degradative capacity, and that are believed to be invadopodia (Wolf *et al.*, 2007; Yu *et al.*, 2012; Beaty *et al.*, 2013; Moshfegh *et al.*, 2014). The introduction of the circular invasion assay (Kam *et al.*, 2008), which has been utilised by Yu and Machesky, has the added benefit of allowing for the high resolution imaging of cells in DQ collagen in which invadopodia-like structures are evident (Yu and Machesky, 2012).

In vivo, the difficulties of capturing images of invadopodia and identifying matrix degradation become even more prominent. However, invadopodia-like protrusions that were positive for cortactin (an invadopodial protein) and that showed signs of local degradation (proteolytic activity) were successfully visualised in invading tumours cells (Gligorijevic *et al.*, 2012) and in cells undergoing intravasation (Yamaguchi *et al.*, 2005b). In a recent study in *Caenorhabditis elegans* (*C. elegans*) anchor cells utilising invadopodial-like protrusions were imaged invading through the basement membrane. Thus for the first time invasive protrusions were visualised in their native environment (Hagedorn *et al.*, 2014). In addition, primary tumour cells from glioma patients have shown the ability to form invadopodia in culture, pointing to the potential relevance of this protrusion *in vivo* (Stylli *et al.*, 2008). However, this study only utilised cells from two patients and only used one cancer type. To confirm that cells from patients do in fact form invadopodia, it would be useful to conduct additional studies with a higher number of patients and also utilise cells from a different cancer type.

Despite, the difficulties associated with the *in vivo* visualisation of invadopodia in tumours, a correlation has been shown between the invasive potential of cell lines *in vivo* and *in vitro* and the ability of these cells to form invadopodia, along with the degradative capacity of these invadopodia in a 2D matrix (Coopman *et al.*, 1998; Bowden *et al.*, 1999). This highlights the importance and relevance of investigating these structures in the context of cancer metastasis.

1.5.1 Invadopodia Formation

Invadopodia formation involves the recruitment of multiple proteins, followed by actin polymerisation and elongation of the plasma membrane (Figure 1-8). While integrin and growth factor signalling proteins such as β1 integrin (Beaty *et al.*, 2013) and EGF (Bromann *et al.*, 2004;

Oser *et al.*, 2009), respectively, can initiate the signalling cascade involved in invadopodia formation (Poincloux et al., 2009), the Rho GTPase Cdc42 and cellular Src (c-Src) are the primary initiators linked to invadopodia formation. Indeed, the inhibition of either of these latter proteins prevents the formation of invadopodia. The importance of Cdc42 is further highlighted by the fact that when bound at the membrane to Cdc42-interacting protein 4 (CIP4), this protein aids in the plasma membrane curvature needed for invadopodia formation (Pichot *et al.*, 2010).

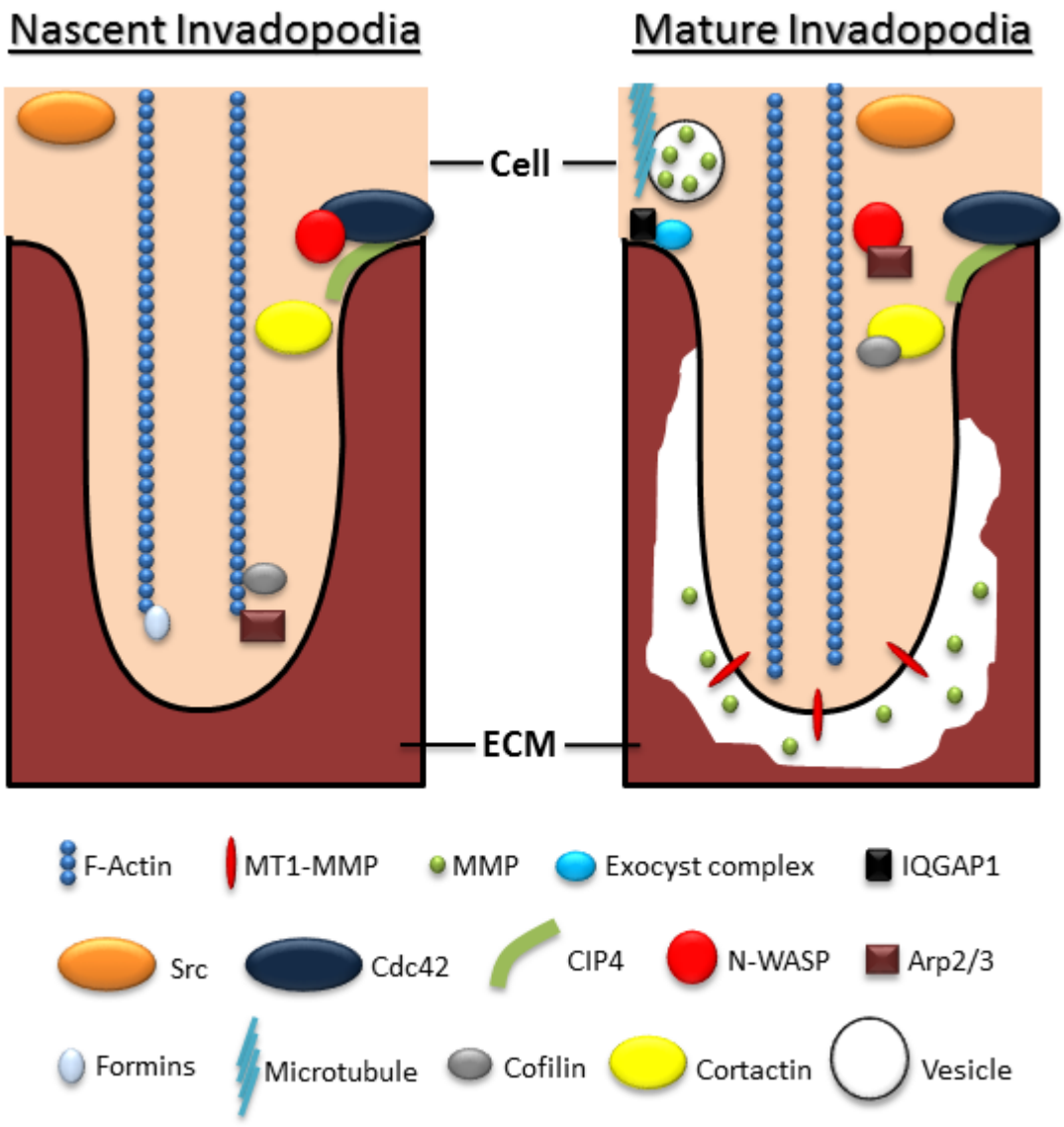

Figure 1-8: Diagrammatic representation of a nascent and mature invadopodia.
Diagram showing proteins in nascent and mature invadopodia. Nascent invadopodia protrude into the ECM. After this, the protrusion stabilises and becomes a degradative mature invadopodia. Additional protein other than those represented in this diagram are also involved in nascent and mature invadopodia protrusions.

Substrates of Cdc42 (including N-WASP and formins) and c-Src (including cortactin) contribute to the formation of invadopodia in several ways. Cortactin accumulates at invadopodia where it is bound in an inhibitory complex with cofilin (Bowden et al., 1999). Cofilin binds and severs actin filaments, allowing the binding of proteins such as formins, for linear actin polymerisation (Lizarraga et al., 2009), and the Arp2/3 complex, for branched actin filament polymerisation (Buccione *et al.*, 2004). During the formation of invadopodia, it is thought that cortactin becomes phosphorylated, which results in the release of cofilin, allowing the actin filaments to be severed, thus creating free barbed ends for actin polymerisation (Oser *et al.*, 2009). Activation of the N-WASP protein occurs either through Cdc42 or via phosphorylated cortactin which promotes the interaction and activation of N-WASP by Nck1 (non-catalytic region of tyrosine kinase adaptor protein 1) (Tehrani *et al.*, 2007). N-WASP then activates the Arp2/3 complex to promote actin polymerisation.

After the formation of invadopodia, cortactin is de-phosphorylated and exerts an inhibitory function on cofilin, leading to invadopodia stabilisation (Yamaguchi *et al.*, 2005a; Oser *et al.*, 2009). Some debate exists over the function of cofilin in invadopodia, with another study suggesting that the activity of cofilin also plays a role in the turnover of invadopodia. Indeed, active cofilin was essential for the formation of discrete invadopodia-like protrusions *in vivo* and the promotion of actin recycling (to provide a pool of free actin for new invasive protrusion formation) in *C. elegans* (Hagedorn *et al.*, 2014). However, whether this activation is via cortactin or another protein is unknown. As cortactin is a prominent player in invadopodia function, localising to invadopodia through the entire life cycle (Artym et al., 2006), this protein is used by many, along with F-actin, as a marker of invadopodia *in vitro* (Lorenz *et al.*, 2004; Baldassarre *et al.*, 2006; Ayala *et al.*, 2008; Poincloux *et al.*, 2009).

Other members of the Rho GTPases such as Rac1 and RhoA may be involved in invadopodia formation. However, studies investigating the roles played by these proteins provide conflicting results. Initial studies have implicated Rac1 in the formation of invadopodia with active mutants enhancing a diffuse-type degradation from invadopodia (Nakahara *et al.*, 2003), and the depletion of Rac1 in glioma cell lines reducing the formation of invadopodia (Chuang *et al.*, 2004). However, a recent study, using a Rac1 FRET biosensor, has found low activity during invadopodia formation with increased activity evident during the disassembly of the protrusion suggesting the importance of Rac1 for invadopodia dissolution (Moshfegh *et al.*, 2014). Similar contradictory data have also been found regarding the role of RhoA in invadopodia. Bravo-Cordero and colleagues, detected no localised variation in RhoA activity at invadopodia

structures (Bravo-Cordero *et al.*, 2011). A decrease in RhoA expression in this study reduced invadopodia formation and degradation suggesting RhoA activity may be important for invadopodia function. In contrast, other studies using active and dominant negative RhoA mutants have suggested that this protein has no effect on invadopodia degradation (Nakahara *et al.*, 2003). Therefore, to further understand the role that RhoA plays in invadopodia function, additional investigation is required.

1.5.2 Invadopodia Maturation

The maturation of invadopodia produces a stable, prolonged protrusion with degradative capacity. During this maturation, the de-phosphorylation of cortactin occurs, leading to the reformation of the cofilin complex, and preventing actin polymerisation (Oser et al., 2009). Mature invadopodia contain vimentin filaments and microtubules that are thought to play a role in invadopodia elongation and the transport of matrix degrading enzymes to the plasma membrane respectively (Schoumacher et al., 2010). The actin bundling protein, fascin, is important in the stabilisation of invadopodia (Machesky and Li, 2010), with fascin depleted cells exhibiting more transient and smaller invadopodia (Li *et al.*, 2010a).

The degradative stage of invadopodia maturation involves the transport and exocytosis of extracellular matrix degrading enzymes. The most prominent matrix degrading enzymes present at invadopodia are the MMPs, primarily membrane type 1 MMP (MT1-MMP), MMP-2 and MMP-9 (Nakahara et al., 1997; Poincloux et al., 2009). MT1-MMP is a membrane bound enzyme that can degrade a range of matrices, including fibronectin, gelatin, vitronectin, as well as collagen I, II and III (Overall and Dean, 2006). MMP-2 and MMP-9 are both enzymes that are secreted into the extracellular matrix as inactive pro-MMPs where they are activated by membrane bound receptors such as MT1-MMP (Poincloux et al., 2009). MMP-2 and MMP-9 can degrade collagen type IV, one of the most abundant basement membrane components (Poincloux et al., 2009). It is believed that the accumulation of actin and cortactin stimulates MT1-MMP localisation to invadopodia, as well as MMP-2 and MMP-9 secretion at this protrusion (Artym et al., 2006; Clark et al., 2007; Clark and Weaver, 2008).

Integrins play an important role in invadopodia degradation by activating MMPs, including MMP-2 (integrin $\alpha v\beta 3$) and seprase (integrin $\alpha 3\beta 1$) (Mueller et al., 1999; Gimona et al., 2008). Indeed, the activation of $\beta 1$ integrin can increase invadopodia induced degradation (Nakahara

et al., 1998), while reduction in levels of this protein inhibits the formation of invadopodia (Destaing *et al.*, 2010).

MMPs are thought to be delivered to invadopodia by transportation from the golgi body, in vesicles, down microtubules to the invadopodia (Schnaeker et al., 2004). Electron microscopy found that invadopodia protrusions form proximal to the golgi body, suggesting an important role for this complex in this structure (Baldassarre *et al.*, 2003). The exocyst complex has been shown to be important in MMP localisation to invadopodia (Sakurai-Yageta *et al.*, 2008). RhoA activity promotes the interaction of the exocyst complex, with IQ motif containing GTPase activating protein 1 (IQGAP1) to aid the tethering of vesicles (containing MMPs) to the invadopodia plasma membrane for matrix degradation (Sakurai-Yageta et al., 2008).

Fusion of the vesicle and plasma membranes result in the release of MMPs. This leads to degradation of the extracellular matrix, thus facilitating cellular invasion. Inhibition of the RhoA effectors, ROCK and myosin II, has been shown to inhibit this invadopodia degradation (Alexander *et al.*, 2008).

Subsequent removal of MMPs from invadopodia occurs via endocytosis, followed by recycling back to the plasma membrane. The endocytosis and thus removal of MT1-MMP at invadopodia is prevented by the formation of a FAK/c-Src complex which inhibits endophilin A2 (a membrane curvature protein essential for endocytic vesicle formation) (Wu *et al.*, 2005).

Non-MMP proteins such as dynamin 2 (a protein localised to the invadopodial cytoplasm) are also important for invadopodia degradation. The expression of dominant negative dynamin 2 mutants were found to decrease both the number of degrading cells as well as the size of the degradation area (Baldassarre *et al.*, 2003).

1.6 p21-Activated Kinases

There are many known effectors of the Rho GTPases, the most well characterised being the p-21 activated kinase (PAK) family of serine/threonine kinases (King *et al.*, 2014). PAKs are involved in several cellular processes including gene transcription, proliferation, changes in cell morphology, cell motility and cancer cell invasion (King *et al.*, 2014). These kinases are highly conserved across a wide range of organisms including, yeast, flies and humans (Bokoch, 2003). Human PAKs consist of 6 isoforms, which are separated into two groups according to their

sequence and structural homology: group I, containing PAKs 1-3; and group II, containing PAKs 4-6 (Figure 1-9).

Deletion of the PAK gene in mice has varying effects on viability and phenotype depending on which PAK isoform has been depleted. PAK1, PAK5 and PAK6 show no obvious developmental requirement as knockout mice are viable (Li and Minden, 2003; Arias-Romero and Chernoff, 2008; Nekrasova *et al.*, 2008). However, PAK2 and PAK4 knockout mice are embryonically lethal, showing the necessity for these 2 isoforms during embryonic development (Qu *et al.*, 2003; Arias-Romero and Chernoff, 2008). Uniquely, PAK3 knockout mice are viable but show defects in synaptic plasticity, suggesting a key role for PAK3 in neural differentiation (Meng *et al.*, 2005).

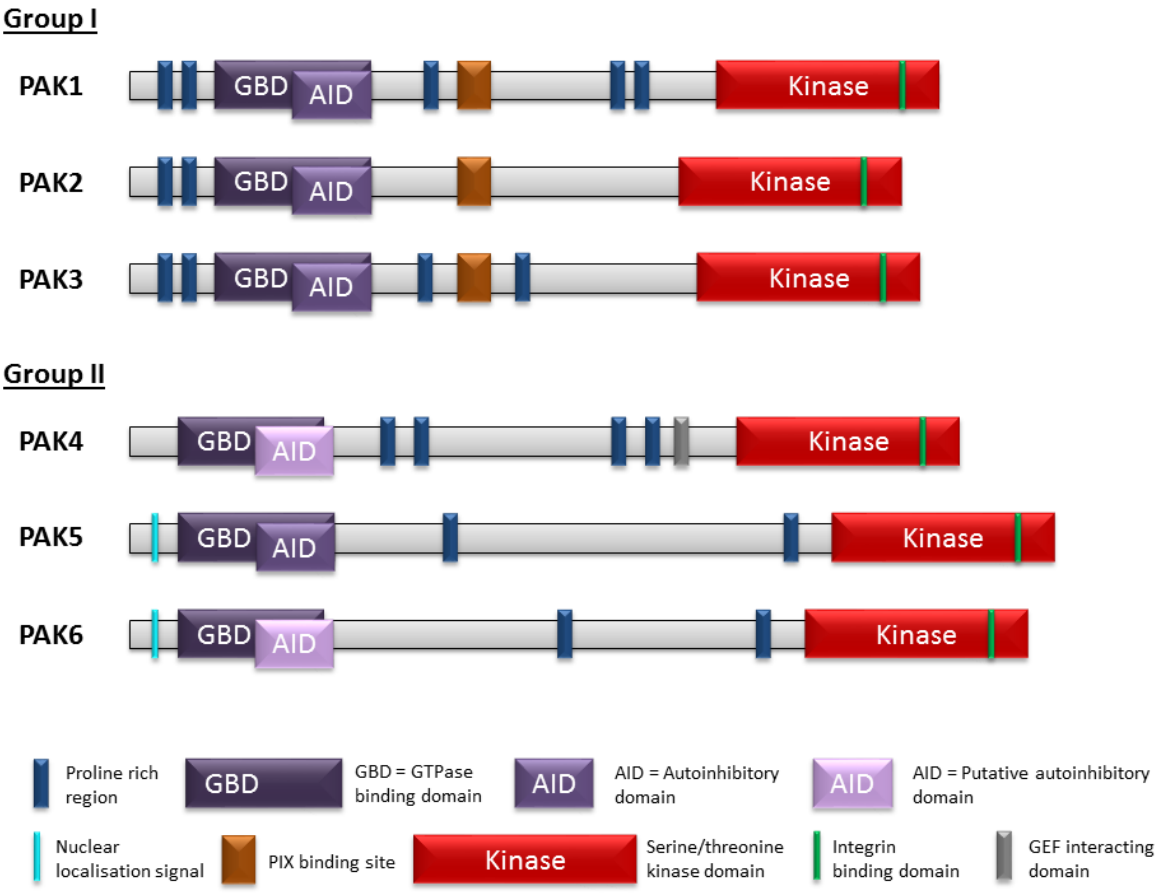

Figure 1-9: Domain Structure of PAKs.
PAK family kinases consist of 6 isoforms, divided into two groups according to their sequence homology. Protein sizes: PAK1, 68kDa; PAK2, 62KDa; PAK3, 65KDa; PAK4, 68KDa; PAK5, 80KDa: and PAK6, 75KDa (Wells *et al.*, 2002) (Figure adapted from (King *et al.*, 2014)).

1.6.1 PAK Domain Structure and Regulation of Activity

All the PAK isoforms contain a highly conserved N-terminal GTPase binding domain (GBD) and a C-terminal kinase domain (Dummler et al., 2009). However, the central intervening sequences differ greatly across and within the two groups. Group I PAKs and PAK5 (a group II PAK) contain an autoinhibitory domain (AID) in the GBD that blocks protein activation (Lei et al., 2000).

Group I PAKs have a low basal kinase activity which is increased by the binding of Cdc42 and Rac1 to the GBD (Figure 1-10). In the inactive state, group I PAKs form a homodimer in a trans-inhibitory conformation, with the AID of one protein binding to the kinase domain of the other to block protein activation (Lei *et al.*, 2000; Parrini *et al.*, 2002). Although PAK2 and PAK3 dimerisation has not previously been investigated it is assumed (due to the sequence homology within the binding sites), that these proteins also form homodimers (Lei *et al.*, 2000).

The binding of active Cdc42 and Rac1 to the GBD dissociates the AID from the homodimer, allowing autophosphorylation to occur at Thr^{423} (in PAK1), Thr^{402} (PAK2) or Thr^{421} (PAK3), resulting in kinase activation (Zenke *et al.*, 1999; Arias-Romero and Chernoff, 2008). Uniquely, the PAK3 gene has splice exons located in the GBD/AID region, resulting in four splice variants. Three of these have constitutive kinase activity (Kreis *et al.*, 2008), with the splice variant PAK3a, preferentially binding PAK1 to form a heterodimer rather than a homodimer (Combeau et al., 2012).

In contrast, regulation of group II PAK activity is more complex and to date is not fully understood. PAK5 is the only group II PAKs to contain an AID, similar to that used to regulate group I PAK activity (Ching *et al.*, 2003). Conflicting studies exist regarding the mechanism of PAK4 regulation. A 1998 report suggests that PAK4 has a high basal kinase activity that is not affected by the binding of the activated small GTPases, Cdc42 and Rac1 (Abo et al., 1998). However, more recent studies suggest that the regulation of PAK4 activity occurs via one of two alternative mechanisms. One such mechanism involves a putative AID, located in the N-terminal domain (amino acid 20-68) that maintains PAK4 in an inactive confirmation until binding of activated Cdc42 occurs (Baskaran et al., 2012). In the second PAK4 regulatory process an N-terminal autoinhibitory pseudosubstrate motif binds the kinase domain (Ha *et al.*, 2012). This pathway has in fact been validated via nuclear magnetic resonance (NMR), which identified an AID, incorporating the autoinhibitory pseudosubstrate motif, that occupies the entire kinase cleft to achieve autoinhibition (Wang *et al.*, 2013).

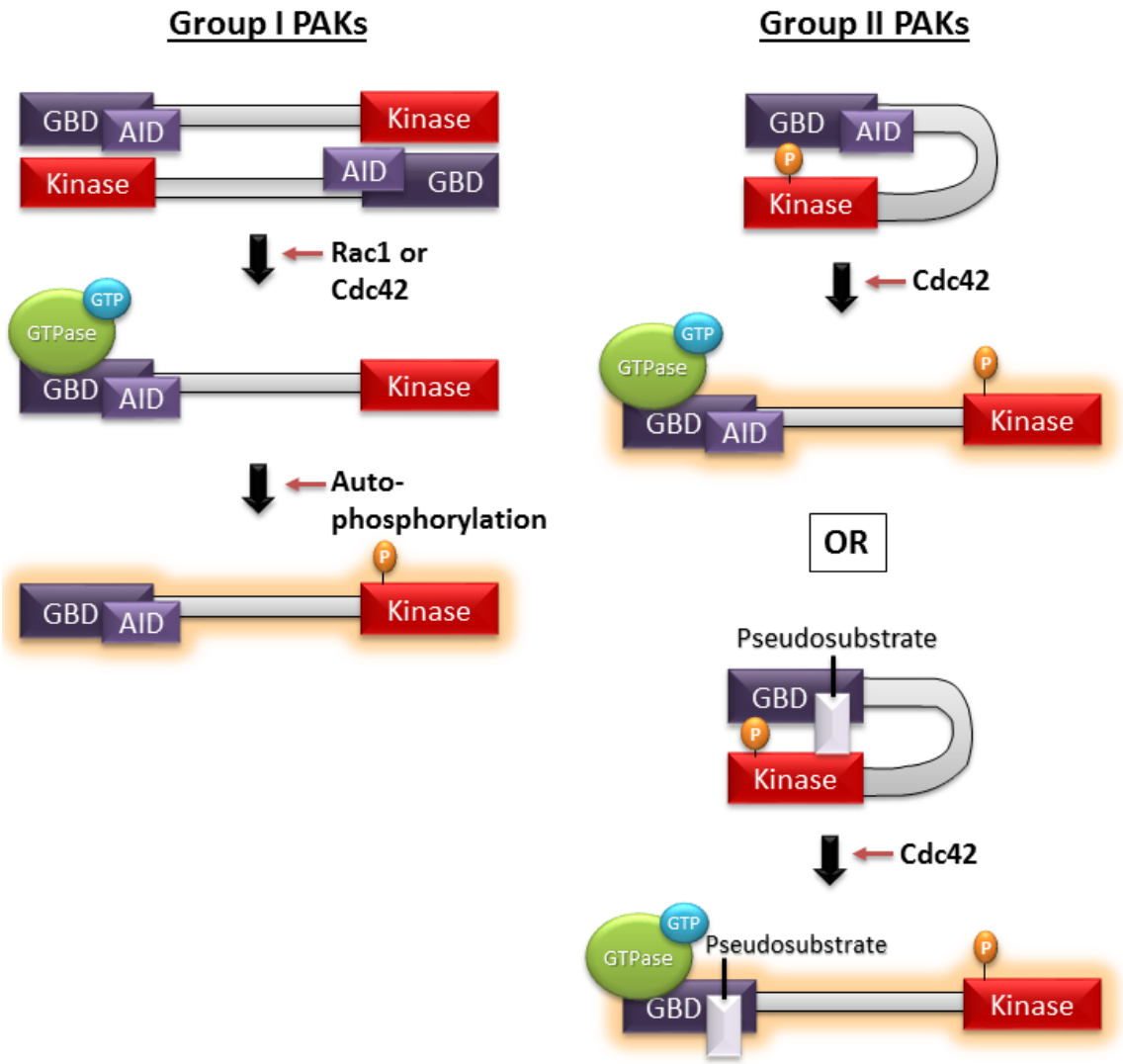

Figure 1-10: Activation of group I and group II PAKs.
Group I PAKs forms an inhibitory homodimer where the AID of one protein binds in trans to the kinase of another. The binding of Rac1 or Cdc42 to the GBD dissociates this dimer and allows for PAK autophosphorylation and thus activation. There are currently two possibilities for activation of group II PAKs. PAK4 may have an inhibitory conformation with a putative AID domain that blocks the kinase domain. The binding of Cdc42 to the GBD results in a conformational change that releases the kinase domain from the inhibitory domain resulting in activation of the protein. Alternatively, PAK4 may use a pseudosubstrate, located in the GBD to block the substrate binding site in the kinase domain thus inhibiting protein function. The binding of Cdc42 changes the conformation, releasing the pseudosubstrate from the kinase domain and thus activating the protein.

These reports indicate that PAK4 activity is controlled by conformational changes mediated by the AID and not by the autophosphorylation of PAK4 at Ser^{474} (used previously as an indicator of PAK4 activity), which is in fact likely to be constitutively phosphorylated at this site. In addition, as this region is highly conserved in all group II PAKs it is highly probable that this method of regulation is also adopted by PAK5 and PAK6 (Ha *et al.*, 2012; Wang *et al.*, 2013).

The regulation of PAK kinase activity occurs not only through the interaction of Cdc42 and Rac1 GTPases, but also through a range of different proteins and pathways. For example, activation of phosphoinositide 3-kinase (PI3K), results in the PI3K induced phosphorylation of PAK1, leading to increased cell motility (Adam *et al.*, 1998). PAK1 can also be activated by growth factors, with stimulation of platelet derived growth factor (PDGF) resulting in 3-phosphoinositide-dependent kinase-1 (PDK1) phosphorylation of PAK1 at the Thr^{423} autophosphorylation site (King *et al.*, 2000). Furthermore, PDGF induced cell activation results in the binding of the SH3 domain adapter protein Nck to the N-terminal proline rich site of PAK1 (Figure 1) (Bokoch *et al.*, 1996). Nck translocates PAK1 to the plasma membrane where it is activated by receptor tyrosine kinases. This leads to the downstream activation of the MAP kinase cascade similarly seen with Cdc42 and Rac1 induced PAK1 activation (Galisteo *et al.*, 1996; Lu *et al.*, 1997). PAK1 can also be translocated to focal complexes by the binding of PIX guanine nucleotide exchange factor to a centrally located proline rich site in group I PAKs (PIX binding site; Figure 1). This translocation enhances the activation by Cdc42 and Rac1 at focal complexes (Manser *et al.*, 1998).

Further studies into the regulation of group II PAKs have demonstrated the presence of an integrin binding domain on PAK4 which binds to the β5 subunit of the αvβ5 integrin. This integrin is involved in the motility and movement of cells on the extracellular matrix protein, vitronectin. The PAK4-αvβ5 integrin interaction leads to the translocation of PAK4 to lamellipodia and promotes cell motility and migration (Zhang *et al.*, 2002). All 6 PAK isoforms have high homology at the corresponding location of the PAK4 integrin binding domain, making it very likely that similar integrin interactions do occur across the PAK family members.

Given the key role played by the PAK family of kinases in several cellular pathways one would expect their activity to be tightly controlled by inhibitors or negative regulators. The latter have in fact been identified for group I PAKs.

One form of negative regulation involves the phosphorylation and inhibition of PAK1 activation by Protein Kinase A. This PAK inhibition can inhibit the activation of anchorage independent

growth signalling through the MAP kinase cascade (Howe and Juliano, 2000). Additionally proteins such as PAK interacting proteins (PIP) and Nischarin can bind PAK1, forming a complex which blocks phosphorylation and downstream signalling (Xia *et al.*, 2001; Alahari *et al.*, 2004). The partners of PIX1 (POPX1) and PIX2 (POPX2) employ a different mechanism of inhibition which involves the dephosphorylation and thus inactivation of PAK1 (Koh *et al.*, 2002). In yet another PAK1 inhibitory pathway, Rac1 activated PAK1 has been shown to phosphorylate Merlin at Ser^{518}, with the resulting activated Merlin protein subsequently competitively binding to PAK1, preventing Rac1 induced activation (Kissil *et al.*, 2003). This negative feedback mechanism allows tight regulation of Merlin-PAK1 signalling, which in turn leads to tight regulation of cell growth. While most of the regulators and inhibitors have been discovered through the use of PAK1, inhibitory pathways also exist for other group I PAKs (Zhan *et al.*, 2003) and play a vital role in controlling the activity of these kinases and the key downstream pathways in which they signal.

1.6.2 PAK Expression in Cancer

Given the involvement of PAKs in cell cycle control, proliferation, cell movement and apoptosis, it is not surprising that this family of kinases also plays a role in cancer growth and progression. The overexpression of group I PAKs is evident in a wide variety of cancers, with the PAK1 isoform being the most commonly overexpressed. Increased levels of this protein have been observed in human cancer tissue from breast (Holm *et al.*, 2006; Ong *et al.*, 2011), liver (Ching *et al.*, 2007), lung (Ong *et al.*, 2011), colorectal (Li *et al.*, 2010b) and also in a subset of melanoma (Ong *et al.*, 2013). PAK2 overexpression is found in breast (Li *et al.*, 2011) and lung cancer tissue (Kikuchi *et al.*, 2012), while increased levels of PAK3 has to date only been found in thymic neuroendocrine tumours (Liu *et al.*, 2010a).

In group II PAKs, PAK4 is the most commonly overexpressed in tumour tissues including breast (Liu *et al.*, 2008), gastric (Ahn *et al.*, 2011) and ovarian cancer (Siu *et al.*, 2010a). In addition PAK4 is the only isoform to date where overexpression of the wildtype protein (in NIH3T3 cells) induces tumour formation when injected in athymic mice. For all other PAKs, only phospho PAK1 is tumourigenic with an activated mutant being required for tumour formation. In fact PAK4 tumour formation took longer to occur when wildtype protein was expressed versus an activated mutant (wildtype = 44 days; Activated = 16 days) (Liu *et al.*, 2008). Overexpression of PAK5 and PAK6 occurs less often than PAK4, but has been found in colorectal (PAK5) (Gong *et*

al., 2009), prostate (PAK6) (Kaur *et al.*, 2008) and breast cancer cell lines (PAK6) (Kaur *et al.*, 2008), as well as in hepatocellular carcinoma tissue (PAK6) (Chen *et al.*, 2014).

An alteration of the phosphorylation state of various PAKs isoforms has also been found in human cancers. An increase in PAK1 phosphorylation (pPAK1) is found in tumour tissues including colorectal cancer (Li *et al.*, 2010b; Liu *et al.*, 2013), with an increase of pPAK1, pPAK2 and pPAK4 being evident in ovarian cancers (Siu *et al.*, 2010a; Siu *et al.*, 2010b). Interestingly, a constitutively active PAK1 mutant can induce mammary gland tumours in mice (driven by the β-lactoglobulin promoter) indicating that PAK1 kinase activity has the ability to induce tumour development (Wang *et al.*, 2006).

In addition to protein overexpression and increased protein kinase activity, genomic amplification is also observed for some PAK isoforms, in particular PAK1 and PAK4 in bladder (Ito *et al.*, 2007) and ovarian cancer (Davis *et al.*, 2013), respectively.

Taken together these data suggest a key role particularly for PAK1 and PAK4 in tumour formation and development.

In cutaneous melanoma specifically, increased PAK1 protein expression is observed in primary melanoma tissue that lack a common BRAF mutation, when compared to primary melanoma tissue with this mutation (Ong *et al.*, 2013). However, little is known about the expression of PAK1 protein in metastatic melanoma (irrespective of BRAF mutation status). At the transcriptional level, PAK4 mRNA is overexpressed in melanoma cell lines, while no increase in PAK6 mRNA is seen (Callow *et al.*, 2002). In addition, no increase in PAK2 or PAK3 gene expression was observed in primary melanoma tissues (Ong *et al.*, 2013). However, it is unclear whether the gene expression or mRNA transcription of these PAK isoforms corresponds to an increase, or lack thereof, of protein expression in melanoma cells.

1.6.3 PAK1 and PAK4 in Invasion

As PAKs are the downstream effectors of the Rho GTPases Cdc42 and Rac1, and therefore play a key role in cell motility, it is not surprising that these kinases can influence tumour cell invasion. As the most commonly overexpressed isoforms in cancer, PAK1 and PAK4 in particular play a key role in tumour invasion in some cancers (Callow *et al.*, 2002; King *et al.*, 2014).

For PAK1, this role in cell migration involves the regulation of lamellipodial protrusions, cell directionality (Sells *et al.*, 1999; Sells *et al.*, 2000), as well as focal adhesion assembly and dissolution (Manser *et al.*, 1997; Nayal *et al.*, 2006). In a study utilising an ovarian cancer cell line, the depletion of PAK1 expression reduced migration and invasion, while the overexpression of PAK1 enhanced migration and cell invasion (Siu *et al.*, 2010b). Similarly, cellular invasion was blocked in a breast cancer cell line with a kinase dead PAK1 mutant. This indicates a dependency on kinase activity in PAK1 induced invasion (Adam *et al.*, 2000). The level of PAK1 expression correlates directly with cell invasion and therefore disease progression. In a range of uveal melanoma cell lines, PAK1 overexpression correlated with invasive potential (determined *in vitro*), with the depletion of PAK1 expression resulting in a corresponding reduction in cellular invasion (Pavey *et al.*, 2006). Furthermore, the inhibition of PAK1 and PAK2 expression simultaneously in primary melanoma cell lines (lacking a BRAF mutation) reduced cell migration, indicating that one (or both) of these isoforms can promote melanoma cell motility (Ong *et al.*, 2013). However, to elucidate which PAK isoform is contributing to the melanoma cell migration, investigations using isoform specific PAK inhibitors are required.

In addition, through various signalling pathways PAK1 plays a role in the inhibition of E-cadherin expression, a key protein in cell-cell adhesion. Data obtained using cells with dominant negative and depleted PAK1 demonstrated that this protein is required for Rac1 induced disassembly of E-cadherin junctions (Lozano *et al.*, 2008). Additionally, PAK1 has been found to phosphorylate Snail resulting in its translocation to the nucleus and subsequent inhibition of E-cadherin expression (Elloul *et al.*, 2010). This diminished expression promotes cell-cell dissociation and the epithelial-mesenchymal transition in ovarian cancer cell lines, thus promoting cell migration and tumour invasion. In non-small cell lung cancer cells PAK1 phosphorylates CRK-II to reduce E-cadherin and p120-catenin expression, both components of cell-cell junction, thus increasing cell invasion (Rettig *et al.*, 2012), while reduced PAK1 expression prevents the dissociation of cell-cell junctions in prostate cancer cells (Bright *et al.*, 2009).

Like PAK1, PAK4 can be involved in tumour cell invasion, with the level of PAK4 expression being indicative of disease prognosis in some cancers. PAK4 expression is found at a higher level in metastatic compared to primary gastric tumours (Guo *et al.*, 2014), and overexpression of PAK4 in this cancer type is associated with a lower overall survival compared to patients that lack PAK4 overexpression (Ahn *et al.*, 2011). Similarly, PAK4 expression was further increased in more advanced serous and clear cell ovarian cancer tissue samples and was associated with lower overall patient survival (Siu *et al.*, 2010a). This is due to the greater invasive capacity of tumour

cells with increased levels of PAK4 as has been demonstrated in multiple studies. Expression of constitutively active PAK4 mutants in pancreatic ductal cell lines, (Kimmelman *et al.*, 2008), and overexpression of wildtype PAK4 in choriocarcinoma cell lines, both resulted in enhanced cell invasion (Zhang *et al.*, 2011). Conversely the depletion of PAK4 expression reduced cell migration and invasion in glioma (Kesanakurti *et al.*, 2012), SCC (Zanivan *et al.*, 2013), choriocarcinoma (Zhang *et al.*, 2011) and breast cancer cells (Wong *et al.*, 2013).

PAK4 aids cell migration and invasion through the promotion of focal adhesion turnover. Reduced PAK4 expression increases the number of focal adhesions present (Wells *et al.*, 2010), therefore increasing cellular adhesion and reducing invasion. This PAK4 induced adhesion turnover is thought to be facilitated through the phosphorylation of paxillin (Ser^{272}) (a key focal adhesion associated protein) and through the phosphorylation of β_5 integrin which reduces cell-matrix attachment and promotes cell migration (Li *et al.*, 2010c).

Therefore, both PAK1 and PAK4 have been linked to invasion in a range of human cancers. However, very few studies focus on the role these kinases may play in melanoma progression, which could prove vitally important given the significant difference in survival rates between primary and metastatic melanoma.

1.6.4 Expression and Localisation of PAK1 and PAK4

The distribution and cellular localisation of PAK1 and PAK4 vary in normal tissue. PAK1 are highly expressed in various tissues including the brain (common feature for group I PAKs), muscle, heart and liver (Arias-Romero and Chernoff, 2008). While PAK1 is concentrated in the cytosol, certain stimuli can also cause localisation to different regions of the cell, including at filopodia and lamellipodia protrusions, (Sells *et al.*, 2000; Nayal *et al.*, 2006), cortical actin (Dharmawardhane *et al.*, 1997), focal adhesions (Manser *et al.*, 1997; Delorme-Walker *et al.*, 2011), cell-cell adhesions (Zegers *et al.*, 2003) and the nucleus (Li *et al.*, 2002; Rayala and Kumar, 2007).

PAK4, is thought to be expressed ubiquitously with higher protein levels in certain tissues such as colon, testis and prostate (Callow *et al.*, 2002). PAK4 is also localised to the cytosol and targeted to different subcellular locations when stimulated, including filopodia protrusions (Abo *et al.*, 1998), cell focal adhesions (Zhang *et al.*, 2002; Wells *et al.*, 2010) and the nucleus (Li *et al.*, 2012).

1.6.5 PAK1 and PAK4 Substrates

The group I and group II PAKs, to which PAK1 and PAK4 belong, respectively, differ in several ways including protein sequence. All PAK isoforms contain a conserved N-terminal p21 binding domain (PBD) and a C-terminal kinase domain (Dummler et al., 2009). However, there is less than 40% and 54% homology between the PBD and the kinase domain sequences respectively, of group I and II PAKs (Jaffer and Chernoff, 2002). These differences in sequence suggest that PAK1 and PAK4 could have differing substrates in cells which could drive divergent functions (Jaffer and Chernoff, 2002). In fact a positional scanning peptide library study by Rennefahrt and colleagues showed differing optimal phosphorylation sequences between PAK1 and PAK4, suggesting differential substrate specificities (Rennefahrt et al., 2007).

These two proteins are rarely directly compared, however some studies suggest that PAK1 and PAK4 share the majority of their substrates, with little evidence to date suggesting that these isoforms are involved in different pathways (Arias-Romero and Chernoff, 2008). However, differences do exist, with wildtype PAK4 having a tumourigenic capacity, while PAK1 can only bring about this transformation with constitutively active mutants (Wang *et al.*, 2006; Liu *et al.*, 2008). The signalling pathways that may be contributing to this difference in phenotype are unknown.

A unique feature of the PAK4 protein, that is not present in PAK1, is the GEF interacting domain (GID) (Figure 1-9) (Callow et al., 2005). Through this domain, PAK4 phosphorylates GEF-H1 at Ser^{885}, which inhibits the GEF function. Due to the lack of GEF-H1, RhoA remains inactive leading to the dissolution of stress fibres (Callow et al., 2005). Indeed, PAK4 can inhibit the formation of prominent actin fibres via the phosphorylation of GEF-H1, inhibiting the activation of RhoA in prostate cancer cells (Wells et al., 2010). However, the results found with PAK1 are less consistent, with some studies demonstrating that phosphorylation of GEF-H1 at Ser^{885} by PAK1 inhibits the GEF activity towards Rho (Zenke et al., 2004; Tian et al., 2014), while others report no activation of RhoA when PAK1 expression is depleted (Coniglio et al., 2008).

PAK1 and PAK4 have differential binding to another GEF, PDZ-RhoGEF - whilst PAK1 does not bind, PAK4 both binds and inhibits protein function (Barac et al., 2004; Rosenfeldt et al., 2006). However, while exciting, this data is preliminary and has not been linked to distinct PAK1 or PAK4 cellular processes.

One study indicates a separation in PAK1 and PAK4 signalling in the phosphorylation of MLC. In NIH3T3 fibroblasts, constitutively active PAK4 mutants are unable to phosphorylate MLC while PAK1 activated mutants increase the MLC phosphorylation (Qu *et al.*, 2001). However, the functional implications of this remains to be investigated.

There may be other distinct substrates for PAK1 and PAK4, however, the substrates or signalling pathways of these two isoforms are rarely directly compared in the same cell type. Given the key role that both proteins play in tumour formation and invasion, a direct comparison of the substrates and signalling pathways of these PAKs could prove invaluable in furthering our understanding of cancer progression. This could be achieved through phospho proteomic arrays (using cells with depleted PAK1 and PAK4 protein expression) that may detect differential phosphorylated substrates.

1.6.6 PAK1 and PAK4 in Invadopodia

Given the potential role of PAK1 and PAK4, in tumour invasion and the fact that invadopodia are also implicated in this process, it is not surprising that several studies demonstrate a potential involvement of PAKs in invadopodia function. PAK1 has been shown to localise to invadopodia protrusions (as demonstrated in MTLn3 rat mammary adenocarcinoma cells) (Moshfegh *et al.*, 2014), and can also phosphorylate cortactin at Ser^{113}, thus activating this protein which is vital for invadopodia formation (Ayala *et al.*, 2008). However, studies in which PAK1 activity is reduced have produced conflicting results, with one study demonstrating that PAK1 activity is required to sustain invadopodia formation and activity during the invasion of the A375MM cell line (Ayala et al., 2008), while a more recent study indicates that PAK1 is involved in invadopodia dissolution, in MTLn3 and MDA-MB-231 cells (Moshfegh *et al.*, 2014). Therefore, to fully understand the role that PAK1 plays in invadopodia function, additional studies are required.

Much less is known about the involvement of PAK4 in invadopodia formation with studies indicating that this protein may be involved in podosome (protrusions that often share the same signalling pathways with invadopodia (Murphy and Courtneidge, 2011)) formation/activity. PAK4 has been shown to localise to podosomes in bone-marrow-derived mouse dendritic cells (Wells and Jones, 2010) and primary human macrophages (Gringel *et al.*, 2006). In addition studies in macrophages involving the depletion and enhancement of PAK4 activity suggest that this kinase enhances podosome size and number (Gringel *et al.*, 2006). These studies implicate

PAK4 in podosome formation, and highlight the need for studies to investigate a possible role for PAK4 (and other PAK isoforms) in invadopodia formation.

PAK1 and PAK4 have been implicated in matrix degradation pathways, with both proteins influencing MMP expression and secretion in a variety of cell lines. Recent studies involving PAK1 suggest that this protein has different effects on different MMPs. PAK1 was shown to induce the secretion of MMP-1 and MMP-3 in breast cancer cells and downregulate the expression and secretion of MMP-9 in collagen I, and MMP-2 in collagen IV (Rider *et al.*, 2013). The effect of PAK4 on MMPs is more straightforward with overexpression enhancing MMP-2 expression (Siu *et al.*, 2010a), and knockdown down regulating MT1-MMP expression in CCA choriocarcinoma cells (Zhang *et al.*, 2011). Therefore, PAK1 and PAK4 may also impact invadopodia induced degradation, through their effect on MMP expression and secretion.

1.7 Aims

The aims of this project are to address the following questions:

1. What is the invasive capacity of a panel of melanoma cell lines and patient derived cell strains?
2. Are the PAK isoforms expressed in melanoma cells, and if so, does this expression correlate with the invasive characterisation?
3. Do PAKs play a role in melanoma invasion?
4. What are the mechanistic pathways of PAKs in melanoma invasion?

2 Chapter 2 - Materials and Methods

2.1 Materials

2.1.1 General Materials

Reagent	Company
152mm glass capillary, with a central filament	World Precision Instruments, USA
4-(2-hydroxyethyl)-1-piperazineethanesulfonic acid (Hepes)	GIBCO®, Invitrogen, UK
4', 6-diamidino-2-phenylindole (DAPI)	Sigma-Aldrich, UK
96-well, U-bottomed, suspension culture plate	Greiner, UK
96 well, V-bottomed, plate	Sigma-Aldrich, UK
Acetic acid	Sigma-Aldrich, UK
Acrylamide (30%)	Severn Biotech Ltd, UK
Agarose	Sigma, UK
Ammonium persulfate (APS)	Sigma-Aldrich, UK
Ampicillin	Sigma-Aldrich, UK
Aprotinin	Sigma-Aldrich, UK
Bovine serum albumin (BSA)	VWR International, UK
Bromophenol blue	Bio-Rad, UK
Calcium phosphate transfection kit	Sigma-Aldrich, UK
Control siRNA oligonucleotide (non-silencing)	Qiagen Ltd, UK
Crimson *Taq* polymerase	New England Biolabs, UK
Cell dissociation solution	Sigma-Aldrich, UK
DAPI	Invitrogen, UK
Deoxyribonucleotide triphosphate (dNTPs) mix	New England Biolabs, UK
DH5α™ Competent *Escherichia coli* (*E. coli*) Cells	Invitrogen, UK
Dimethyl sulfoxide (DMSO)	Sigma-Aldrich, UK
Dithiothreitol (DTT)	Sigma-Aldrich, UK
DMEM (Dulbecco's Modified Eagle's Medium)	Sigma-Aldrich, UK
DMEM (1x) Powder, High Glucose	PAA, UK
DMEM (High Glucose)	PAA, UK
DMEM F-12 (Dulbecco's modified eagle's medium: nutrient F-12 ham)	Lonza, UK
Dulbecco's Phosphate buffered saline (PBS) without Calcium & Magnesium	PAA, UK
Enhanced chemiluminescence (ECL) Plus western blotting detection system	Amersham Biosciences, UK
Ethidium bromide	Thermo Fisher Scientific, UK
Ethyl 3-aminobenzoate methanesulfonate (MS222)	Sigma-Aldrich, UK
Ethylenediaminetetraacetic acid (EDTA)	Sigma-Aldrich, UK
Fibronectin	Sigma-Aldrich, UK
FluorSave™ Reagent	Calbiochem, UK
Flexitube siRNA HsPAK4 (PAK4 Oligo 2)	Qiagen, UK
Foetal bovine serum (FBS)	GIBCO®, Invitrogen, UK
Falcon™ 5ml polystyrene round-bottom tubes	BD Biosciences, UK

Gateway® LR and BP Clonase™ enzyme kit (including proteinase K)	Invitrogen, UK
Gelatin- Type A from porcine skin	Sigma-Aldrich, UK
Gentamicin	Sigma-Aldrich, UK
Glutaraldehyde solution, Grade I, 25%	Sigma-Aldrich,UK
Glycerol	Sigma-Aldrich, UK
Glycine	Sigma-Aldrich, UK
HiPerfect transfection reagent	Qiagen Ltd, UK
Human Adult Epidermal Melanocytes	TCS CellWorks, UK
Illustra GFX PCR DNA and gel band purification kit	GE Healthcare, UK
Kanamycin	Invitrogen, UK
L-glutamine	Lonza, UK
Leupeptin	Sigma-Aldrich, UK
Lipofectamine 2000	Invitrogen, UK
Lithium chloride (LiCl)	Fisons Scientific Apparatus, UK
Low Melting Point Agarose	Invitrogen, UK
Luria-Bertani agar (LB-agar)	Sigma-Aldrich, UK
Luria-Bertani broth (LB-broth)	Invitrogen, UK
Magnesium chloride ($MgCl_2$)	Sigma-Aldrich, UK
Melanocyte Growth Medium Package including epidermal melanocyte growth supplement	TCS CellWorks, UK
Methylene blue	Thermo Fisher Scientific, UK
Methylcellulose	Sigma-Aldrich, UK
Minimum essential medium Eagle (MEM) media	Sigma-Aldrich, UK
Mini-Proteinase inhibitor cocktail tablet	Calbiochem
Methylthiazolyldiphenyl-tetrazolium bromide (MTT)	Sigma-Aldrich, UK
Newborn calf serum (NCS)	Sigma-Aldrich, UK
Non-fat milk powder	Marvel, UK
N-phenylthiourea (PTU)	Sigma-Aldrich, UK
Octylphenoxypolyethoxyethanol/Nonidet™ P40 substitute (NP-40)	Sigma-Aldrich, UK
One Shot® TOP10 Chemically Competent *E. coli* Cells	Invitrogen, UK
OptiMEM	GIBCO®, Invitrogen, UK
Roswell Park Memorial Institute (RPMI)-1640 medium	Sigma-Aldrich, UK
PAK1 siRNA Oligo 1	Dharmacon, Thermo Fisher, UK
PAK1 siRNA Oligo 3	Dharmacon, Thermo Fisher, UK
PAK4 silencer pre-designed siRNA (PAK4 Oligo 1)	Ambion, Invitrogen, UK
Paraformaldehyde (PFA)	Sigma-Aldrich, UK
pDONOR™ 207	Invitrogen, UK
Penicillin/Streptomycin	Sigma-Aldrich, UK
Phalloidin CruzFluor™ 647 Conjugate	Santa Cruz
Phenylmethylsulfonylfluoride (PMSF)	Sigma-Aldrich, UK
Phusion® HF	New England Biolabs, UK
Phosphate buffered saline (PBS) tablets	Oxoid Limited, UK
Pierce® ECL western blotting substrate	Thermo Scientific, USA
Protein G Sepharose™ 4 Fast Flow beads	Amersham Biosciences, UK

Precision Plus Protein Marker	Bio-Rad, UK
ProLong® Gold antifade reagents	Life Technologies, UK
Protran Nitrocellulose hybridization transfer membrane	Perkin Elmer, USA
PureCol Collagen Type I Solution 3mg/ml	Nutacon, NL
Purelink™ Hi Pure Plasmid mini-prep kit	Invitrogen, UK
Puromycin	Sigma-Aldrich, UK
Q5™ High-fidelity DNA polymerase	New England Biolabs, UK
QIAGEN Plasmid maxi-prep kit	Qiagen Ltd, UK
QIAGEN Plasmid midi-prep kit	Qiagen Ltd, UK
Quick-Load® 100bp DNA ladder	New England Biolabs, UK
Quick-Load® 1kbp DNA ladder	New England Biolabs, UK
Rhodamine B Isothiocyanate	Sigma-Aldrich,UK
Roswell Park Memorial Institute (RPMI)-1640 medium	GIBCO®, Invitrogen, UK
Slide-A-Lyzer® dialysis cassette	Thermo Fisher Scientific, UK
Sodium borohydride	Sigma-Aldrich,UK
Sodium chloride (NaCl)	Sigma-Aldrich, UK
Sodium dodecyl sulphate (SDS)	Sigma-Aldrich, UK
Sodium fluoride (NaF)	Alfa Aesar, UK
Sodium hydroxide (NaOH)	Sigma-Aldrich, UK
Sodium orthovanadate (Na_3VO_4)	Sigma-Aldrich, UK
Sodium pyrophosphate	BDH Chemicals, UK
Sucrose	Sigma-Aldrich, UK
T4 DNA ligase	Promega, UK
Tetramethylrhodamine isothiocyanate (TRITC)-Phalloidin	Sigma-Aldrich, UK
Tris-base	Sigma-Aldrich, UK
Triton X-100	VWR International, UK
Trypsin/EDTA	GIBCO®, Invitrogen, UK
Tween 20	VWR International, UK
X ray film	Scientific Laboratory Supplies
X-tremeGENE HP transfection reagent	Roche, UK
Borosilicate glass capillary, 1.0mm outer diameter x 0.78mm inner diameter	Harvard Apparatus, USA
Zebra Channel Device	MMB Foundry, USA

Table 2-1: General Reagents.

2.1.2 Cell lines

Cell line	Source
A-375M2	Dr. Erik Sahai, London Research Institute
A-375M2 RhoA	Dr. Penny Morton, King's College London
Adult Melanocytes	TCS CellWorks, UK
HaCaT	Dr. Victoria Sanz-Moreno, King's College London
Neonatal Melanocytes (1)	Dr. Katie Lacy, King's College London
Neonatal Melanocytes (2)	TCS CellWorks, UK
NIH3T3	Dr. Maddy Parsons, King's College London
SK-MEL-2	Dr. Katie Lacy, King's College London
SK-MEL-28	Dr. Katie Lacy, King's College London
WM-115	Dr. Katie Lacy, King's College London

Table 2-2: Cell lines.

2.1.3 Antibodies

Antibody	Species	Dilution	Application	Company
Anti-β-Actin	Mouse	1:10,000	Western Blotting	Sigma-Aldrich (#A5441)
Anti-c-Myc	Mouse	1: 500	Western Blotting	Santa Cruz (#sc-40)
Anti-Cortactin	Mouse	1:50	Immunofluorescence	Upstate (#05-180)
Anti-GAPDH	Mouse	1: 20,000	Western Blotting	Millipore (#MAB374)
Anti-GEF-H1	Rabbit	1:1000	Western Blotting	Cell Signaling Technology (#4076)
Anti-HMWMAA (0.9µg/µl)	Human	1:600	FACs	Gift from Dr. Sophia Karagiannis, King's College London
		1:50	Immunofluorescence	
Anti-p-GEF-H1 (Ser^{885})	Rabbit	1:500	Western Blotting	Abcam (#ab94348)
Anti-PAK1	Rabbit	1: 1000	Western Blotting	Cell Signaling Technology (#2602)
Anti-PAK2	Rabbit	1: 1000	Western Blotting	Cell Signaling Technology (#2608)
Anti-PAK3	Rabbit	1: 1000	Western Blotting	New England Biolabs (#2609)
Anti-PAK4	Rabbit	1: 1000	Western Blotting	In-house affinity purified (Wells *et al.*, 2002)
Anti-PAK4/6	Rabbit	1: 500	Western Blotting	Cell Signaling Technology (#3242)
Anti-PAK5	Goat	1: 500	Western Blotting	Santa Cruz (#sc-22155)
Anti-PAK6	Rabbit	1: 500	Western Blotting	Calbiochem (#ST1108)
IgG1 Isotype Control (0.25µg/µl)	Human	1:166	FACS	Stratech, UK (#044887-USB)

Table 2-3: Primary Antibodies.

Antibody	Species	Dilution	Application	Company
Alexa Fluor® 488 anti-human IgG	Goat	1:200	FACs	Dr. Sophia Karagiannis, King's College London
		1:100	Immunofluorescence	
Alexa Fluor® 488 anti-mouse IgG	Goat	1:200	Immunofluorescence	Invitrogen (#A11001)
Alexa Fluor® 488 anti-rabbit IgG	Goat	1:200	Immunofluorescence	Invitrogen (#A11008)
Horseradish peroxidase (HRP)-conjugated anti mouse	Goat	1: 1000 - 1: 10,000	Western Blotting	Dako (#P0447)
Horseradish peroxidase (HRP)-conjugated anti goat	Rabbit	1: 1000	Western Blotting	Dako (#P0449)
Horseradish peroxidase HRP-conjugated anti rabbit	Goat	1: 1000 - 1: 2000	Western Blotting	Dako (#P0448)

Table 2-4: Secondary Antibodies.

2.1.4 Plasmids

Construct	Source
GFP Alone	Clontech, UK
GFPPAK4	Produced by lab of Dr. Claire Wells
GFPPAK1	Produced by lab of Dr. Claire Wells
GFPPAK1r	Made by author
GFPPAK4r	Produced by lab of Dr. Claire Wells
mTFP Alone	Gift from Maddy Parsons, King's College London, UK
pDONR™207	Invitrogen, UK
pEGFP-C1 Destination vector	Clontech, UK
myc-PDZ-RhoGEF	Gift from John Masters, University College London (UCL), UK
myc-PDZ-RhoGEFΔDH	Gift from John Masters, UCL, UK
RhoA Biosensor	Gift from Maddy Parsons, King's College London, UK

Table 2-5: Plasmid Constructs.

2.1.5 Buffers

Buffer	Composition
Blocking solution	5% w/v milk powder or 5% w/v bovine serum albumin in TBS-Tween
Collagen I matrix	1.617mg/ml Purecol collagen type I, 3mM NaOH, 10% FBS in DMEM
DNA loading buffer	5% w/v glycerol, 0.04% bromophenol blue (w/v) in H_2O
Cell lysis buffer	0.5% NP-40, 30mM sodium pyrophosphate ($Na_4O_7P_2$), 50mM Tris-HCl pH7.6, 150mM NaCl, 0.1mM EDTA, 50mM sodium fluoride (NaF), 1mM sodium orthovanadate (Na_3VO_4), 1mM phenylmethylsulfonyl fluoride (PMSF), 10µg/ml leupeptin, 1µg/ml aprotinin and 1mM dithiothreitol (DTT) in H_2O
PBS-Tween	PBS + 0.1% Tween-20
SDS-PAGE running buffer	192mM glycine, 19mM Tris Base + 0.1% w/v SDS in H_2O
SDS-PAGE sample buffer	100mM Tris pH 6.8, 10% w/v SDS, 30% v/v glycerol, 0.2% w/v bromophenol blue in H_2O
SDS-PAGE transfer buffer	192mM glycine, 19mM Tris base + 20% methanol v/v in H_2O
Stripping buffer	25mM glycine pH2 + 1% SDS in H_2O
TAE buffer	40mM Tris-HCl, 10mM EDTA in H_2O
TBST	50mM NaCl, 0.1% v/v Tween, 25mM Tris pH7.6 in H_2O
E3 media	5mM NaCl, 0.17mM KCl, 0.44mM $CaCl_2$, 0.68mM $MgSO_4$ in H_2O
FACS Buffer	$PBS^{-/-}$ + 5% FBS

Table 2-6: Solutions and buffers (working concentrations).

2.2 Methods

2.2.1 Cell Line Culture

The melanoma cell lines A-375M2, SK-MEL-2 and SK-MEL-28 were grown in Dulbecco's modified eagle's medium: nutrient F-12 ham (DMEM F-12) (containing 2.5mM L-glutamine), and the WM-115 cell line was grown in minimum essential medium (MEM) (containing 2.5mM L-glutamine). The HaCaT keratinocyte cell line was grown in Dulbecco's modified eagle's medium (DMEM) (containing 2.5mM L-glutamine). All the growth media above were supplemented with 10% foetal bovine serum (FBS), 100U/ml penicillin and 100µg/ml streptomycin sulphate. The NIH3T3 fibroblast cell line was grown in DMEM (high glucose (4.5g/L))) supplemented with 10% newborn calf serum (NCS), 2.5mM L-glutamine, 100U/ml penicillin and 100µg/ml streptomycin sulphate. Human melanocytes were cultured in epidermal melanocyte basal growth medium to which was added epidermal melanocyte growth supplement (5µg/ml bovine insulin, 0.18µg/ml hydrocortisone, 3µg/ml heparin, 10ng/ml phorbol 12-myristate 13-acetate (PMA), 5µg/ml

bovine transferrin, 3ng/ml basic fibroblast growth factor, 0.5% (v/v) FBS, 0.2% (v/v) bovine pituitary extract (BPE)) and antibiotic supplement (25µg/ml gentamicin and 50ng/ml amphotericin B). Cells were maintained in a humidified incubator at 37°C, with 5% CO_2. Cells were sub-cultured using 0.5% trypsin/ 0.2% ethylenediaminetetraacetic acid (EDTA) when the culture flasks were ~80% confluent.

2.2.2 Thawing and Freezing Cells

To thaw cells, cryovials (from liquid nitrogen) were rapidly warmed in a 37°C water bath and transferred into 10ml (T-75 flask) or 5ml (T-25 flask) of cell specific media in a tissue culture flask. The media was changed the following day and cells were cultured using the method described in 2.2.1.

When freezing, cells were trypsinised and transferred into cryovials in a 90% FBS and 10% DMSO solution. Cryovials were placed in a cryo freezing container at -80°C, overnight, to ensure slow freezing, then stored long term in liquid nitrogen tanks.

2.2.3 Preparation of Ethanol Washed Coverslips

13mm round glass coverslips were rocked in 70% ethanol for 30 mins at room temperature, after which the process was repeated for a further 30 mins in 96% ethanol. Following this, coverslips were air dried in a sterile tissue culture hood. The ethanol washed coverslips were stored in a sealed 10cm^2 plate for later use.

2.2.4 Immunofluorescent Staining

Cells were seeded onto the ethanol washed coverslips (Section 2.2.3) at a density of 2x10^4/ml. The following day, cells were fixed with 4% (w/v) paraformaldehyde (PFA) for 20 mins at room temperature, or overnight at 4°C. Cells were permeabilised for 5 mins using 0.2% (v/v) triton X-100. Following this, cells were washed three times with phosphate buffer saline plus calcium and magnesium ($PBS^{+/+}$). Non-specific binding was blocked by incubating for 30 mins at room temperature with 3% bovine serum albumin (BSA):$PBS^{+/+}$. After blocking, coverslips were

incubated for 2 hrs at room temperature with the primary antibody diluted in 3% BSA:$PBS^{+/+}$. The unbound antibody was removed by washing three times with $PBS^{+/+}$ and cells were incubated for 1 hr at room temperature with the appropriate fluorophore conjugated secondary antibody and fluorophore conjugated phalloidin (to stain for F-actin) in 3% BSA:$PBS^{+/+}$. When staining only for F-actin, cells were incubated with phalloidin for 1 hr at room temperature directly after permeabilisation with triton X-100. When required, nuclei were stained by adding 100µM DAPI:$PBS^{+/+}$ to the cells for 5 mins at room temperature prior to mounting. The coverslips were then washed three times with $PBS^{+/+}$ fixed to microscope slides using Fluorsave™ reagent. The fluorescence was visualised using an Olympus Ix71 microscope with Image-Pro Plus 7.0 software. Confocal images were taken using a Nikon Eclipse Ti confocal microscope or Nikon A1R Si Spectral confocal microscope with NIS Element 64bit software. Image analysis was performed using ImageJ software.

2.2.5 Establishment and Isolation of Patient Derived Cell Strains

The human melanoma tumour tissues were obtained with written informed consent and all work was approved by the Guy's Research Ethics Committee, Guy's and St. Thomas' NHS Trust (reference number 08/H0804/139, approval date 15/10/2008).

Patient tissue was collected (submerged in $PBS^{-/-}$) the day of surgery from St. John's Institute of Dermatology. The adhesive surfaces of a 6 well plate were scratched using a scalpel and coated with 10ng/ml fibronectin:$PBS^{-/-}$. The patient tissue was diced and placed into the 6 well plate. Using the padded inner compartment from a 1ml syringe, the patient tissue was firmly pressed and spread across the scratched surfaces. The tissue was left to dry and attach for 5 mins at room temperature before RPMI 1640 media was added to each well. Once proliferative populations were visible, cells were trypsinised and transferred to a new fibronectin coated 6 well plate and allowed to grow. When the cells were next sub-cultured $2x10^4$ cells were removed and stained for high molecular weight melanoma associated antigen (HMWMAA) to assess the purity of melanoma cells in the cell population. Thereafter, fluorescence activated cell sorting (FACS) by flow cytometry was used to isolate the melanoma cells (FACSAria™ II Cell Sorter) or confirm a pure melanoma population (using a BD FACSCanto™ II system). All the experiments using the patient derived cell strains were performed within 6 months of the initial seeding to reduce culture induced gene/phenotypical alteration.

2.2.6 Fluorescence Activated Cell Sorting (FACS)

>$5x10^4$ cells (in FACS buffer) were added to each well of a 96 well V-bottom plate and centrifuged at 1000rpm for 5 mins at 4°C. The supernatant was removed by inverting the plate and the cell pellet was dislodged by briefly vortexing. Cells were incubated in 50µl anti-HMWMAA primary antibody/anti-IgG isotype control antibody (1.5µg/ml in FACS buffer) for 1 hr at 4°C. Cells were washed by centrifugating at 1000rpm for 5 mins at 4°C, inverting the plate, vortexing and adding 100µl FACS buffer. A further two washes were performed before 50µl secondary antibody (in FACs buffer) was added for 90 mins at 4°C, in the dark. To remove the unbound secondary antibody the cells were washed three times with FACS buffer. Cells were transferred in 4ml FACS buffer containing 0.5% PFA to a Falcon™ 5ml polystyrene round-bottom tube. Samples were subject to FACS by flow cytometry within 24hrs.

2.2.7 MTT Assay

$4x10^3$ cells were plated in a 96 well plate and left to grow for 4 days. Media was removed and replaced with 50µl 5mg/ml methylthiazolyldiphenyl-tetrazolium bromide (MTT) solution:$PBS^{-/-}$ and incubated at 37°C, in 5% CO_2, for 4 hrs (in the dark). The MTT solution was then removed and 50µl DMSO was added. The cells were mixed thoroughly and the absorbance at 570nm was measured using an Alpha-Fusion plate reader.

2.2.8 Adhesion Assay

The adhesion assay was performed either on ethanol washed glass coverslips (Section 2.2.3) lacking any additional coating or coated with collagen I. The collagen I coated coverslips were prepared by adding 200µl 50µg/ml collagen I in 20 mM acetic acid and incubating for 1 hr at room temperature. The unbound collagen was removed by washing the coverslips three times with $PBS^{-/-}$.

Cells were seeded on the coverslips at a concentration of $1x10^5$. All melanocytes were seeded at a density of $5x10^4$ when plated on collagen I, due to reduced cell quantity. After 1 hr and 8 hrs, cells were washed twice with $PBS^{+/+}$, fixed with 4% PFA and stained for F-actin using the immunofluorescent staining protocol (Section 2.2.4). Images were taken at five evenly spaced

sites on the coverslip using an Olympus Ix71 microscope with Image-Pro Plus 7.0 software (x10 objective). The total number of cells in each site were counted using ImageJ software. Cell adherence was calculated as a percentage of cells that were adhered at 1 hr compared to the cells at 8 hrs.

2.2.9 Cell Morphology Analysis

Cell morphology was analysed using ImageJ software. Within ImageJ, the actin images were inverted and the threshold adjusted to fully highlight one cell. Using the Wand Tool, the highlighted cell was selected and the cell area, perimeter and elongation was measured. This process was repeated for 90 cells over three experiments. The cell elongation was calculated as a relative value of the longest axis to the shortest axis of a cell, subtracted from 1 (Ahmed *et al.*, 2008). Cells classed as having prominent actin fibres were those with at least two prominent actin fibres that crossed over the nucleus.

2.2.10 Invadopodia Assay

Rhodamine conjugated gelatin was prepared by incubating 2mg/ml Type A Gelatin (from porcine skin) in H_2O at pH 9.3 (with 61mM sodium chloride (NaCl) and 50mM sodium borohydride ($NaBH_4$)) for 1 hr at 37^oC. 36ng/ml Rhodamine B isothiocyanate was added and the mixture was rocked for 4 hrs at room temperature in the dark. Large precipitations were removed by filtering the rhodamine gelatin through a 0.45µm filter. The filtrate was injected into a Slide-A-Lyzer® dialysis cassette and dialysed for 4 days in $PBS^{+/+}$ at 4°C in the dark. The $PBS^{+/+}$ was replaced three times each day. The rhodamine gelatin was removed from the cassette and centrifuged at 4000rpm for 2 mins at room temperature to remove any additional precipitations. 20mg/ml sucrose was added and the rhodamine gelatin was stored at 4°C until use.

Ethanol washed coverslips (Section 2.2.3) were coated with 300µl rhodamine conjugated gelatin (pre-warmed to 37°C) and incubated at room temperature for 10 mins. The coverslips were then inverted onto 120µl 0.5% gluteraldehyde:PBS minus calcium and magnesium ($PBS^{-/-}$) and incubated for 15 mins at room temperature. The coverslips were washed three times using

$PBS^{-/-}$ and incubated at room temperature for 3 mins with 132mM sodium borohydride:$PBS^{-/-}$. Coverslips were again washed three times with $PBS^{-/-}$ and sterilised using 70% ethanol for 5 mins at room temperature. After this, the ethanol was removed and the coverslips were air-dried for

10 mins. DMEM media was added to the coverslips, which were then incubated for 1 hr at 37°C. Cells were detached from 6 well plates using cell dissociation buffer for 10 mins at 37°C. The DMEM media was removed from the gelatin coated coverslips and $2x10^4$ cells were seeded and incubated at 37°C for 3 hrs in 5% CO_2 (unless otherwise stated). Cells were fixed using 4% PFA and stained for the desired protein and F-actin using the immunofluorescent staining protocol (Section 2.2.4).

2.2.11 Gelatin Degradation Analysis

The gelatin degradation area was measured for invadopodia producing cells using the gelatin degradation plug-in with ImageJ software (kind gift from Laura Machesky, Beatson Institute for Cancer Research, Glasgow). Each actin cell image and corresponding gelatin image was cropped to contain only one cell and converted to an 8-bit format using Adobe Photoshop. The actin and gelatin images were compiled into two separate image stacks (all actin images in one and gelatin in another). The stacks were opened using the ImageJ gelatin degradation plug-in to measure the degradation area per cell (in pixels). The values were multiplied by the pixel area to convert values to real degradation area (μm^2).

2.2.12 Fluorescence Intensity Co-Localisation Analysis

The co-localisation of proteins and gelatin degradation was calculated by measuring the fluorescence intensity using ImageJ software. Confocal single Z-plane fluorescent images were opened in ImageJ, saved as a stack and a single line was drawn across the invadopodia to be analysed. The intensity was measured along this line using the Plot Profile tool and exported to Microsoft Excel. A plot profile was generated for each channel in the stacked image to show the co-localisation of fluorescence intensity.

2.2.13 3D Spheroid Invasion Assay

Spheroids were formed by adding $2.5x10^2$-$5x10^2$ cells in 100µl of cell specific media, containing 5% FBS and 0.32% methylcellulose, into a 96-well U-bottomed suspension culture plate. Cells were incubated at 37°C in 5% CO_2, for 3 days to enable a spheroid mass to form. On the 3rd day,

collagen I matrix (from bovine hide) was prepared on ice and 400µl was added to a 24 well plate and allowed to polymerise for 2 hrs at 37°C in 5% CO_2. Following this, another 400µl of collagen I matrix was added onto the polymerised collagen I layer and the spheroid was transferred directly into this layer. The collagen/spheroid layer was allowed to polymerise for 2 hrs at 37°C in 5% CO_2. Images were taken at day 0 and day 3 or 4 using an Olympus Ix71 microscope with Image-Pro Plus 7.0 software (x10 objective).

2.2.14 Transfection

WM-115 and A-375M2 cells were plated into a 6 well plate with the cell specific media (without antibiotic) at least 24hrs prior to transfection. For WM-115 cells, 2µg DNA and 2µl XtremeGENE HP transfection reagent were incubated in 100µl optiMEM for 30 mins at room temperature. To transfect A-375M2 cells, 3µg DNA and 3µl Lipofectamine 2000 transfection reagent were incubated in 100µl optiMEM for 30 mins at room temperature. Following this, the DNA and transfection reagent mix was added, drop wise, to the cells and incubated at 37°C for 48 hrs in 5% CO_2 prior to any further experiments or fixation.

2.2.15 RNA Interference (RNAi)

When transiently knocking down a protein, $2x10^4$ cells were seeded into a 6 well plate. The following day, 3µl short interfering RNA (siRNA) oligonucleotides and 12µl HiPerfect transfection reagent were added to 97µl optiMEM and incubated at room temperature for 30 mins. When two oligonucleotides were used to achieve a double knockdown, 3µl of each oligonucleotide was added to the transfection mix (total of 6µl). This mixture was then added, dropwise to the cells. Experiments were performed 4-7 days after transfection. The siRNA oligonucleotides used in this study (including the target sequence) are shown in Table 2-7.

To create stable knockdowns of PAK1 or PAK4 A-375M2 cell lines, one T-25 flask (at 70% confluency, in media without antibiotic) was transfected with 4µg short hairpin RNA (shRNA) DNA construct and 4µl Lipofectamine reagent using the transfection protocol (Section 2.2.14). The shRNA constructs used in this study (including the target sequence) are shown in Table 2-7. Puromycin selection antibiotic, at a concentration of 1µg/ml, was added to the media 3 days post-transfection. Cells were cultured in 1µg/ml puromycin from here onwards to maintain the protein knockdown.

siRNA/shRNA	Target Sequence (5'-3')	Company
Control siRNA	AATTCTCCGAACGTGTCACGT	Qiagen Ltd, UK (1022076)
PAK1 Oligo 1	AGAAATACCAGCACTATGA	Dharmacon, Thermo Fisher Scientific, UK (D-003521-07)
PAK1 Oligo 3	CATCAAATATCACTAAGTC	Dharmacon, Thermo Fisher Scientific, UK (D-003521-03)
PAK4 Oligo 1	GGTGAACATGTATGAGTGT	Ambion, UK (AM16708)
PAK4 Oligo 2	CGAGAATGTGGTGGAGATGTA	Qiagen Ltd, UK (SI02660315)
Control shRNA (pGIPz)	CTTACTCTCGCCCAAGCGAGAG	Open Biosystems, Thermo Fisher Scientific, UK (RHS4346)
PAK1 shRNA 1 (pGIPz)	GCCTAGACATTCAAGACAA	Open Biosystems, Thermo Fisher Scientific, UK (V2LHS_152618)
PAK1 shRNA 2 (pGIPz)	TATTGTCACTCTTGATGTC	Open Biosystems, Thermo Fisher Scientific, UK (V2LMM_68590)
PAK4 shRNA 1 (pGIPz)	TCTTGATGAAGTTGTCCAG	Open Biosystems, Thermo Fisher Scientific, UK (V2LHS_197812)
PAK4 shRNA 3 (pGIPz)	CTTCGGACATTCATGATCG	Open Biosystems, Thermo Fisher Scientific, UK (V3LHS_646396)

Table 2-7: siRNA oligonucleotides and shRNA constructs used in this study.

2.2.16 Cell Lysates

Cells were seeded into 6 well plates and when at 90% confluency were lysed using cell lysis buffer. Cell debris was removed by centrifugation at 13,000rpm for 10 mins at 4°C. The supernatant was placed in 1.5ml eppendorf tubes and gel sample buffer was added. Samples were boiled for 3 mins and stored at -20°C until use.

2.2.17 Western Blotting

Lysate samples were thawed, boiled for 3 mins and solubilised proteins were then separated by electrophoresis at 125V for 1-2 hrs on a 6.5 - 10% (w/v) polyacrylamide-SDS gel, submerged in SDS-PAGE running buffer. 5µl precision plus protein marker was used as a size indicator. Proteins were transferred onto protran nitrocellulose hybridization transfer membranes using SDS-PAGE transfer buffer at 100V for 1-1.5 hrs. Blots were placed in Tris-buffered saline with Tween-20 (TBST), containing 5% (w/v) non-fat milk powder or 5% BSA (w/v) for 1 hr at room temperature

to block non-specific binding. The membranes were incubated overnight at 4°C in primary antibody in TBST with 1% (w/v) non-fat milk powder or BSA. To remove unbound primary antibody, the membranes were washed three times for 10 mins each, in TBST. When probing the membranes with the polyclonal rabbit anti-PAK5 antibody the wash time was increased to 15 mins per wash. Following this, membranes were incubated for 1 hr at room temperature with the respective secondary antibody conjugated with horseradish peroxidase at double the dilution of primary antibody in TBST with 1% (w/v) non-fat milk powder or BSA. Proteins were detected using Pierce® enhance chemiluminescence (ECL) western blotting substrate and analysed using ImageJ software. The western blots shown in figures are exposure copies and may not be film that was used for analysis.

To remove the antibodies to allow for another protein to be detected (used for phosphorylated and total protein levels), the blot was rocked twice, each for 15 mins in fresh stripping buffer. The unbound antibody was washed for 5 mins with PBS-Tween. The membrane was blocked with TBST containing 5% (w/v) non-fat milk powder or 5% BSA (w/v) for 1 hr at room temperature and the western blot protocol was repeated.

2.2.18 Fluorescence Resonance Energy Transfer (FRET)

$2x10^4$ A-375M2 cells, stably transfected with a RhoA biosensor, were seeded onto ethanol washed glass coverslips (Section 2.2.3). The following day, cells were fixed, permeabilised and washed, using the immunofluorescent staining protocol (Section 2.2.4). To quench the autofluorescence, often caused by the PFA, the cells were incubated in 1mg/ml sodium borohydride:$PBS^{+/+}$ for 15 mins at room temperature. Coverslips were then washed three times with $PBS^{+/+}$ and mounted onto glass slides using ProLong® Gold antifade reagent. FRET was measured using a multiphoton, time-correlated single-photon counting (TCSPC) fluorescence lifetime imaging microscope (FLIM). FRET efficiency was analysed using TRI2 software (Barber *et al.*, 2009).

2.2.19 Polymerase Chain Reaction

When PCRs were performed for diagnostic techniques the PCR sample contained 10ng of template DNA, 100ng of each primer, 1 unit crimson *Taq* DNA polymerase and 2.5µl crimson *Taq*

reaction buffer, in a final volume of 25µl. The primers used in this study are shown in Table 2-8. The PCR program was as follows: 94°C for 2 mins; thereafter 30 cycles consisting of: 94°C for 30 secs (denaturing phase); 55°C for 30 secs (annealing phase); and 72°C for 1 min per kilobase pair (kbp) of DNA to be amplified (elongation phase). Lastly, an additional incubation at 72°C for 5 mins was performed to ensure all PCR fragments were fully elongated.

When PCR fragments were required for further molecular cloning techniques, the *Taq* polymerase-containing mixes were substituted for 2.5 units of the proof reading enzyme Phusion® HF or Q5™ high-fidelity DNA polymerase and a 800µM dNTP mix in the corresponding buffer. Negative controls contained no template DNA. Positive controls contained a plasmid with the correct primer binding sites to produce the desired PCR product.

Primer	**Use**	**Sequence (5'-3')**
PAK1 Fwd	Construction of PAK1 rescue construct	GGGGACAAGTTTGTACAAAAAAGCAGGCTTGATGTCAAATAACGGCCTAGAC
PAK1 Rev	Construction of PAK1 rescue construct	GGGGACCACTTTGTACAAGAAAGCTGGGTCTTAGCTGCAGCAATCAGTGGA
PAK1Rescue Fwd	Construction of PAK1 rescue construct	CCGATGAGAAATACGAGCACCATGATTGGAGC
PAK1Rescue Rev	Construction of PAK1 rescue construct	GCTCCAATCATGGTGCTCGTATTTCTCATCGG

Table 2-8: The sequence of the primers used in this study.

PCR samples were visualised by gel electrophoresis. The Quick-Load® 100bp DNA ladder or Quick-Load® 1Kb DNA ladder was included in all gels. Electrophoresis gels consisted of 1% agarose and ethidium bromide (1:100,000 dilution) in Tris-acetate-EDTA TAE buffer. 1% low melting point agarose containing gels were used when band excision was required for use in further cloning experiments. Gels were submerged in TAE buffer and run at 60-90 Volts for 45 mins. DNA fragments were visualised with a Gel Doc-It™ TS Imaging System. Excised bands were visualised using a UVP dual intensity transilluminator and removed with a sterile scalpel. PCR fragments were purified from electrophoresis gels by using the Illustra GFX™ PCR DNA and gel band purification kit.

2.2.20 Site Directed Mutagenesis

To produce the PAK1 Oligo 1 siRNA resistant mutant, two PCR reactions were performed to produce one fragment from the 5' PAK1 (flanked by the *att*B1 site) to the mutated sequence and one fragment from the mutated sequence to the 3' (flanked by the *att*B2 site) PAK1 sequence. The resulting two PCR products were mixed and used as template DNA in a further PCR reaction to produce the full length PAK1 gene containing the desired mutations. The Gateway® Technology system (Invitrogen, UK) was used to clone the PAK1 mutated fragment into a GFP tagged vector using two recombination reactions, the BP and LR reaction.

Firstly, an entry clone was created in the BP reaction by incubating 120ng PAK1 fragment (flanked by *att*B sites), 150ng pDONR™207 vector and 4µl BP clonase in TE buffer to a total volume of 20µl, for 1 hr at room temperature. 2µl proteinase K was added to stop the reaction and incubated for 10 mins at 37°C.

DNA was then transformed in *Escherichia coli* (*E. Coli*). 5µl of the reaction mix was added to 25µl chemically competent *E. coli* cells (DH5α strain) and incubated on ice for 30 mins. Following this, cells were heat shocked at 42°C for 20 secs and again placed on ice for a further 2 mins. Cells were added to 500µl Luria-Bertani (LB) broth and placed in a shaking incubator for 1 hr at 37°C. After this, 250µl of incubated cells were spread on LB agar plates containing the appropriate antibiotic (100µg/ml ampicillin or 50µg/ml kanamycin) and incubated overnight at 37°C. Colonies were screened by adding a proportion of the colony into 10µl H_2O, incubating for 10 mins at 95°C and then inserting into a PCR reaction. The positive colonies were amplified and purified using a Mini or Midi prep or kit. The vectors were sequenced to screen for any mutations that may have been produced during PCR amplification. Purified DNA was diluted to 100ng/µl in a total volume of 15µl. Primers were diluted to 2pmol/µl, with a total volume of 15µl. DNA was sequenced by Eurofins MWG (London, UK).

Secondly, 100ng of the resulting entry clone was incubated, in the LR reaction, with 150ng pEGFP-C1 destination vector and 4µl LR clonase in TE buffer, in a total volume of 20µl. The LR reaction mixture was incubated for 1 hr at room temperature, the 2µl proteinase K was added and incubated for 10 mins at 37°C. The reaction mix was transformed in *E. Coli* and the resulted GFPPAK1rescue (GFPPAK1r) expression vector was purified using a maxi prep kit.

2.2.21 Zebrafish Embryo Maintenance

All work that was conducted using zebrafish were performed under the UK Home Office project licence PPL 70/7912 and approved by the King's College Ethical Review committee.

Adult zebrafish were maintained in H_2O produced by a reverse osmosis system at 28°C and exposed to a light:dark cycle of 14:10 hrs. Embryos were obtained by placing one male and female in a gated breeding tank (containing a grated inner tank and a lower collection tank) the evening before embryos were required. The following morning the gate was removed from the breeding tank, enabling the adults to spawn. Embryos were collected 2 hours after the gate removal.

To collect the embryos, the zebrafish were removed from the breeding tank and the lower collection tank H_2O was poured through an inverted sieve, where the embryos were caught. The embryos were transferred from the sieve to a 10cm petri dishes containing E3 media with 0.0002% methylene blue. Faeces and debris was removed from the media and the embryos were stored at 28°C. 6-8 hours post-fertilisation (hpf), unfertilised cells were removed to prevent the apoptosis of fertilised embryos. 1 day post-fertilisation (dpf) the chorion (the capsule enclosing the embryo) was removed from each embryo, to prevent curling of the embryo during development. After the completion of experiments or after 6 dpf (whichever was sooner) embryos were killed, via exposure for 1 hr to an anaesthetic overdose of 15mM Ethyl 3-aminobenzoate methanesulfonate (MS222).

2.2.22 Zebrafish Yolk Invasion Assay

Injection needles were prepared using a P-87 flaming/brown micropipette puller. Each borosilicate glass capillary (1.0mm outer diameter x 0.78mm inner diameter) was pulled at both ends away from a central heating element until the glass had extended to create two fine needles.

A-375M2 stably transfected cells were detached from a T-75 flask using dissociation buffer and $2.1x10^7$ cells/ml were added to $PBS^{-/-}$, in at total volume of 50µl, and placed on ice. 2 dpf embryos were submerged in 3.5mM MS222, 50 units/ml penicillin and 50µg/ml streptomycin and placed in a V-shaped grooved 2% agarose (in H_2O) mould. The cells were loaded into a borosilicate glass capillary needle and approximately 500 A-375M2 cells were injected into the embryo yolk sac

using a Nikon SMZ-U zoom 1:10 Picospritzer II microinjection station. Injected embryos were placed in E3 media (containing 50 units/ml penicillin and 50µg/ml streptomycin) and incubated at 28°C for 1 hr to recover, then transferred to 35°C for the remainder of the experiment. 4 hrs post-injection, embryos that lacked a clear tumour mass within the yolk sac or that had cells outside of the yolk sac were removed and humanely killed using 15mM MS222. The percentage of embryos with A-375M2 cell tail invasion was calculated 4 days post-injection. The embryos were then humanely killed by the addition of 15mM MS222 for 1 hr.

2.2.23 Imaging of Zebrafish Embryos

To obtain representative fluorescent and brightfield images, the embryos were firstly anaesthetised with 3.5mM MS222. Embryos were placed, on their side, in a V-shaped grooved 2% agarose (in H_2O) mould, submerged in reverse osmosis H_2O (containing 3.5mM MS222 and 200mM PTU) and imaged using a Nikon SMZ1500 dissecting microscope. Alternatively, for the tiled images, embryos were placed in a zebra channel device (containing 3.5mM MS222 and 200mM PTU) and imaged using an Olympus Ix71 microscope with Image-Pro Plus 7.0 software. After imaging, the H_2O was replaced with fresh H_2O (lacking MS222) and the embryos were carefully removed from the mould and returned to the incubator.

2.2.24 Statistical Analysis

An unpaired, two-tailed *t*-Test was used to measure all statistical significance, except for the FACS efficiency significance, where a Kolmogorov–Smirnov test was used. Data was considered significant if the P value was < 0.05, indicated in the result figures as *. The error bars show SEM values.

3 Chapter 3 – Characterisation of Melanoma Invasion

3.1 Introduction

The survival rate for patients suffering from early stage melanoma is extremely good (5 year survival of 98%). However, around 16% of melanoma patients are diagnosed with metastatic disease (American Cancer Society, 2011; American Cancer Society, 2014). Once melanoma metastasises, the available therapies provide little effective treatment with a 5-year survival rate of 62% for regional metastasis (the surrounding tissue) and 16% when distant metastasis has occurred (Whiteman *et al.*, 2011; American Cancer Society, 2014). This highlights the need to improve knowledge regarding the mechanisms by which melanoma metastasises with a view to identifying new therapeutic targets and prognostic tools.

Tumour metastasis involves multiple steps - breaking through the basement membrane, invasion through the surrounding tissue, intravasation into blood or lymph vessels, extravasation into surrounding tissue and ultimately cell growth at distant sites (Chambers *et al.*, 2002). During the initial stages of metastasis, cancer cells are thought to use actin rich protrusions called invadopodia to degrade the basement membrane and surrounding extracellular matrix (Stylli *et al.*, 2008; Buccione *et al.*, 2009; Ridley, 2011) and inhibition of proteins associated with invadopodia function can inhibit tumour cell invasion both *in vitro* and *in vivo* (Yamaguchi *et al.*, 2005a; Gligorijevic *et al.*, 2012; Paz *et al.*, 2013). Indeed, the formation of invadopodia is often used as a marker of invasive potential (Yamaguchi, 2012). However, the regulation and co-ordination of these proteins in invadopodia protrusions are not fully understood, and in particular, the function of serine/threonine kinases remains unknown.

This chapter characterises the morphology and invasive properties (using both 2D and 3D assays) of a variety of melanoma cell lines and patient derived cell strains, and compares these properties to melanocyte wildtype controls. These studies are designed to inform and complement the subsequent studies of PAK family isoform expression presented in chapter 4.

3.2 Results

In order to investigate the role of PAKs in melanoma invasion (Chapter 4 and 5), the level of invasiveness of the cell lines used in this study needs to be established. The use of a single cell line to investigate the pathways involved in cancer cell invasiveness is not ideal, as the data obtained could be specific to the cell line in question and not be representative of the more general cancer signalling pathways. This chapter, therefore aims to rank the relative cell invasiveness of the chosen melanoma cell lines compared to melanocyte controls. As such, a range of assays were employed, including cell morphology, 2D invadopodia and the 3D spheroid assay. Therefore in this study a number of different cell lines were utilised to conduct these invasive studies.

3.2.1 Characterisation of Melanoma Cell Lines

Four melanoma cell lines were selected for this study: two from primary origins (SK-MEL-28 and WM-115); and two from metastatic origins (A-375M2 and SK-MEL-2). Melanocytes from both neonatal (from two sources, named (1) and (2)) and adult origins were used as wildtype controls.

3.2.1.1 Cell Morphology

Cell shape has previously been used as an indicator of cell invasiveness (Friedl and Wolf, 2003). Cell morphology may therefore be an indicator of invasive potential and thus this characteristic was studied in the melanoma cell lines.

To determine their shape, cells were seeded on glass coverslips, incubated overnight, then fixed and stained for F-actin. The cell area, cell perimeter and cell elongation were calculated for each cell line and melanocyte control using ImageJ software (Figure 3-1). All the cell lines had significantly different cell areas, when compared to neonatal melanocytes (1), with the exception of the SK-MEL-2 cells (Figure 3-1). Cell area also varied between the various cell lines. Variations in cell area between the normal melanocyte controls were also documented.

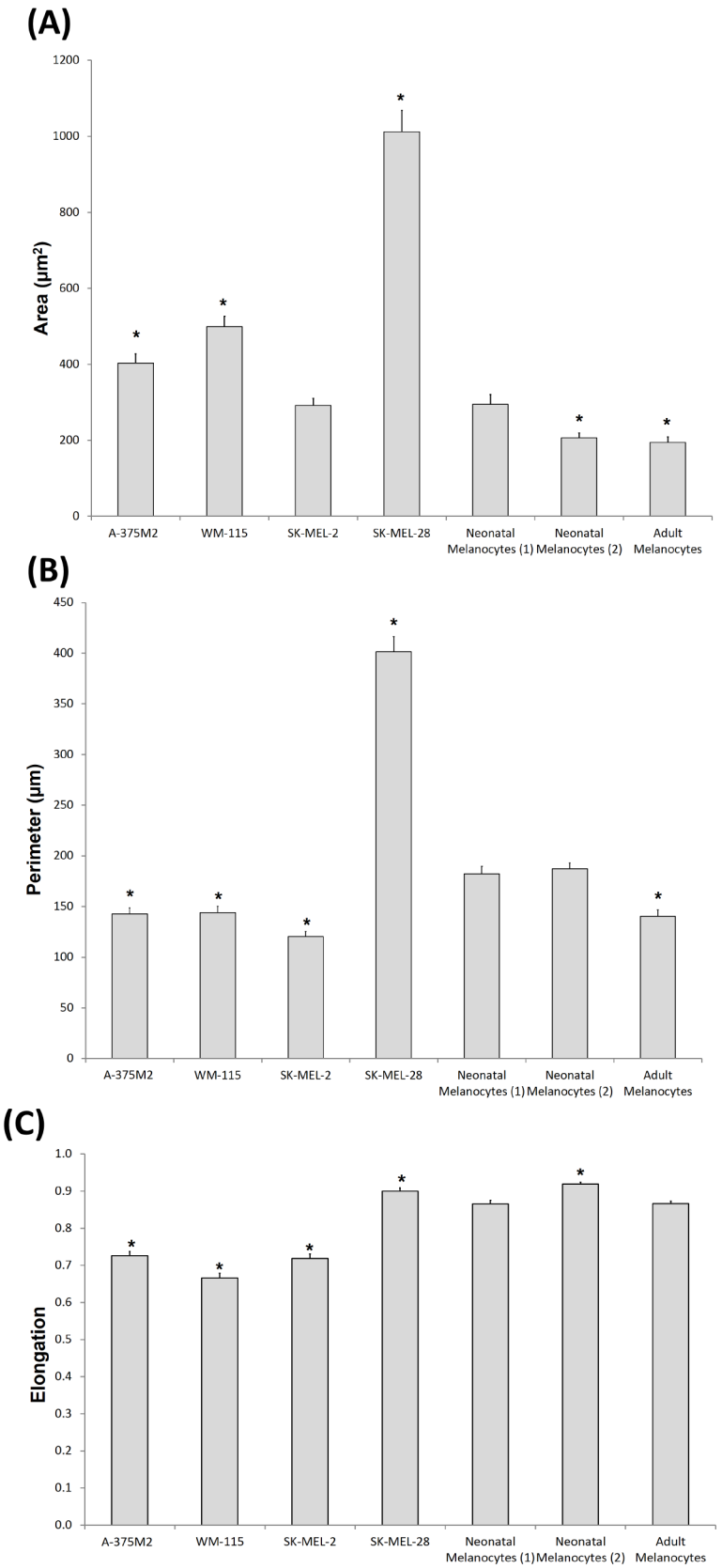

Figure 3-1: Cell shape analysis of melanoma cell lines and normal melanocytes.
Cells were seeded on glass coverslips and stained for F-actin. The cell area (A), cell perimeter (B) and cell elongation (C) were calculated for 90 cells over 3 independent experiments. Cell elongation was represented as a scale from 0 to 1 where 0 = circular and 1 = straight. Significance was calculated to neonatal melanocyte (1). Data are mean values ± S.E.M.; * = $P < 0.05$.

The A-375M2, WM-115 and SK-MEL-2 cell lines exhibited a reduced cell perimeter and cell elongation compared to the melanocyte controls (Figure 3-1B and C). This indicates that these cell lines are more circular with potentially less ruffles or protrusions at the cell membrane. In contrast the SK-MEL-28 cell line exhibited an increased cell perimeter and elongation compared to the melanocyte controls. However, this increased perimeter is likely accounted for by the large cell area of these cells.

During the cell shape analysis (which was performed on F-actin stained cells) a difference in the number of cells with prominent actin fibres was noted. Therefore, the nature of actin fibre formation in these cells was examined. The presence of prominent actin fibres has been linked to cell rigidity and a reduction in invasion (Friedl and Wolf, 2003).

Normal melanocytes from all three populations had prominent actin fibres (Figure 3-2). However of the melanoma cell lines only WM-115 cells showed a significant reduction in prominent actin fibres compared to the melanocyte control. This suggests that the WM-115 cell line may be less rigid compared to melanocyte controls and could exhibit an increased invasive potential.

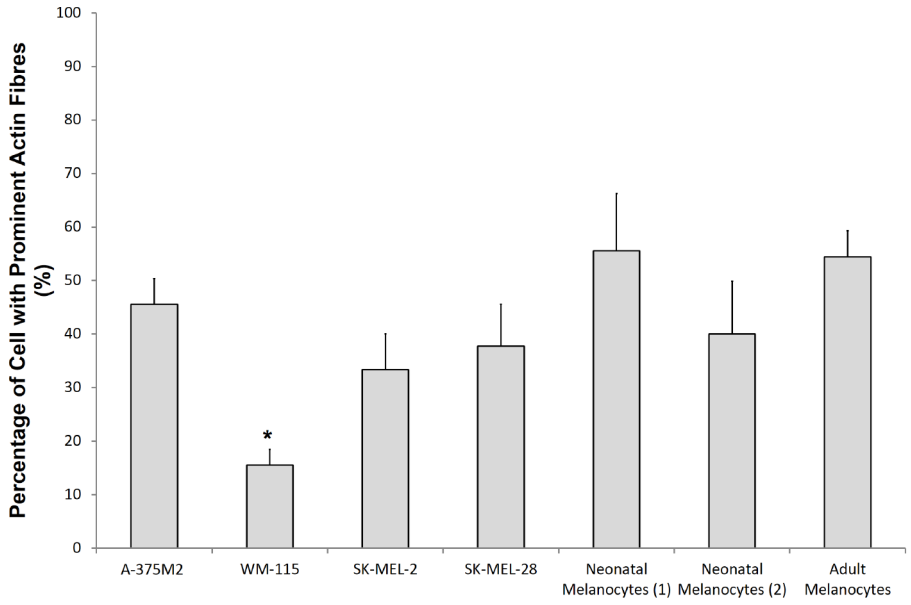

Figure 3-2: Quantification of the percentage of cells with prominent actin fibres.
Cells were seeded on either glass coverslips and stained for F-actin. Significance was calculated to neonatal melanocyte (1). Data are mean values ± S.E.M. of 150 cells, over 3 independent experiments; * = $P < 0.05$.

3.2.1.2 Invadopodia Assay as a Measure of Cell Invasiveness

A 2D invadopodia assay was utilised as part of our cell characterisations. Actin rich protrusions were identified by F-actin staining and were confirmed to be invadopodia structures by their degradative capacity and ability to co-localise with the invadopodia localising protein cortactin (Figure 3-3). Confocal images were taken and fluorescence intensity plots through an invadopodia structure were measured, both of which showed co-localisation of cortactin and F-actin at regions of gelatin degradation. Thus confirming these structures were in fact invadopodia.

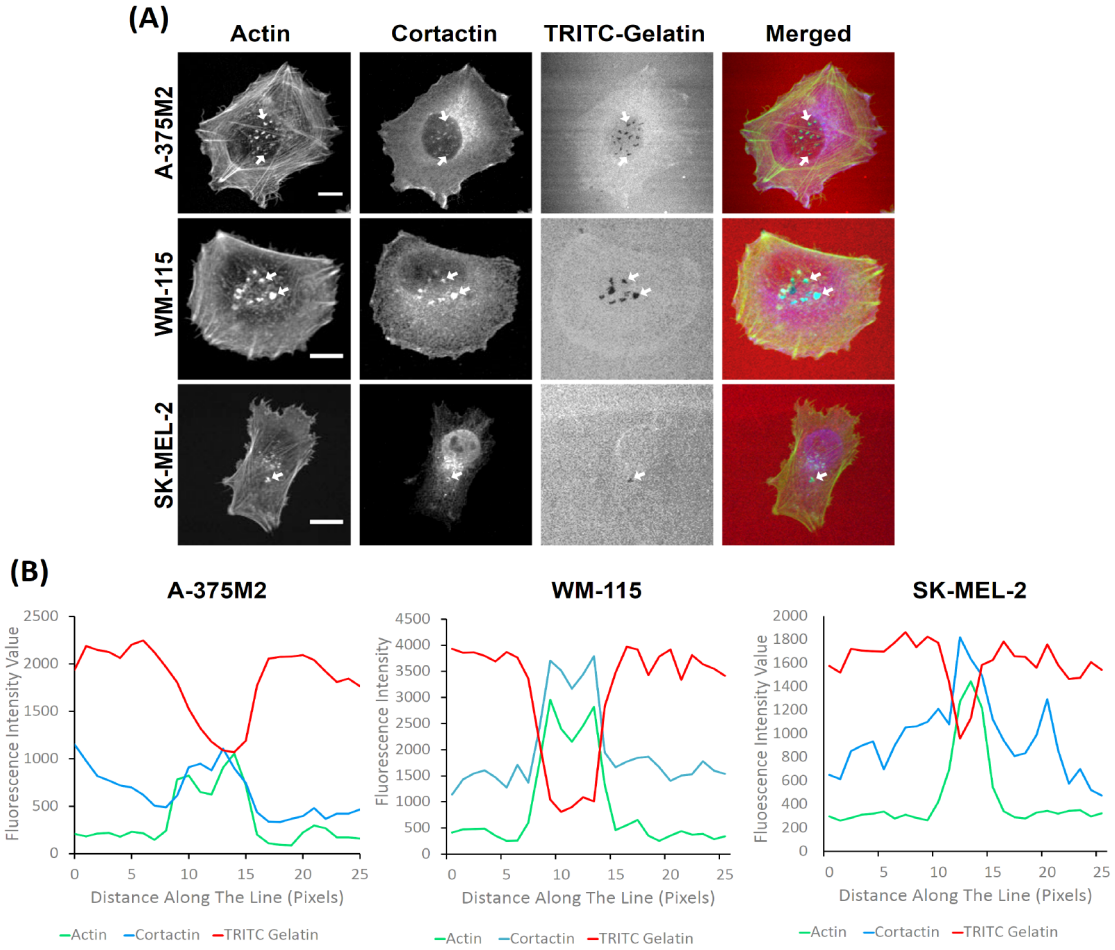

Figure 3-3: Co-localisation of cortactin with F-actin and TRITC gelatin degradation.
A-375M2, WM-115 and SK-MEL-2 cells were seeded on TRITC gelatin coated coverslips for 3 hrs and then fixed and stained for F-actin and cortactin. (A) Representative confocal images showing co-localisation of F-actin, cortactin and gelatin degradation. Scale bar = 10µm. (B) A representative fluorescence intensity plot for each cell line showing co-localisation of cortactin, F-actin and gelatin degradation. Fluorescence intensity was measured at each image pixel along an arbitrary line that crossed through an invadopodia structure.

The number of cells with invadopodia protrusions was measured, as well as the area of gelatin degradation per cell (when appropriate), for each melanoma and melanocyte cell line (Figure 3-4 and Figure 3-5). As expected, none of the melanocyte controls were able to make invadopodia (Figure 3-5A). Of the melanoma cell lines, a significant number of cells belonging to the A-375M2, SK-MEL-2 and WM-115 cell lines produced invadopodia. Interestingly, the WM-115 primary cell line not only formed invadopodia, but had a significantly higher percentage of cells with these structures, compared to the other invadopodia forming cell lines. This was also true for the area of degradation, where the invadopodia producing WM-115 cells had a higher degradative capacity than both the A-375M2 and SK-MEL-2 cells (Figure 3-5B). Less than 1% of cells produced invadopodia in the primary melanoma cell line SK-MEL-28, and this was not statistically significant when compared to the neonatal or adult melanocytes. This data shows that the A-375M2, WM-115 and SK-MEL-2 cell lines produce invadopodia and can be classed as invasive in the 2D invadopodia invasion assay.

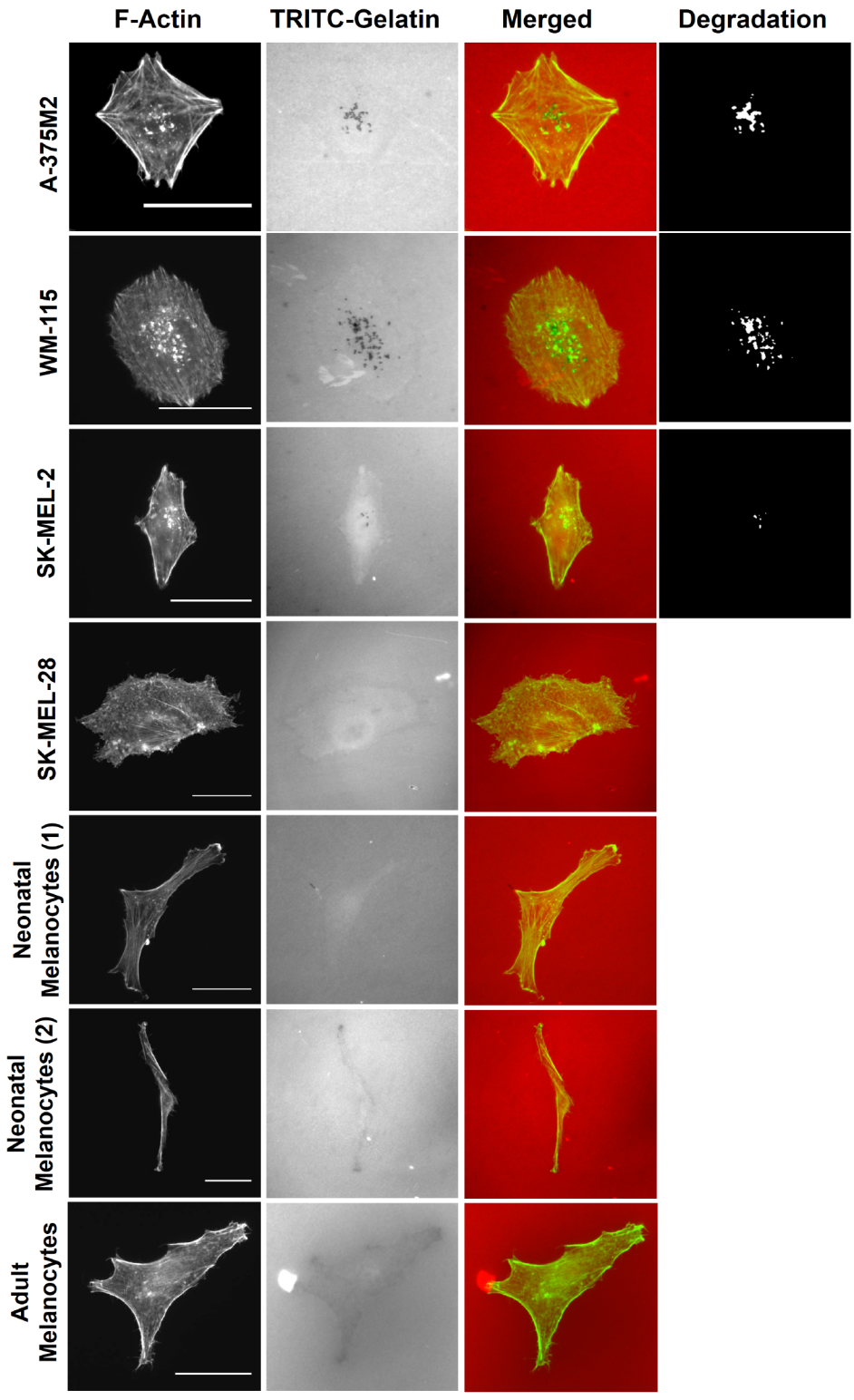

Figure 3-4: Representative invadopodia assay images of melanoma cell lines and melanocyte controls. Cells were seeded on rhodamine conjugated gelatin for 3 hrs and stained for F-actin. Only actin rich dots that corresponded with gelatin degraded dots were counted as invadopodia. The degradation was measured using ImageJ software. Scale bars = 20µm.

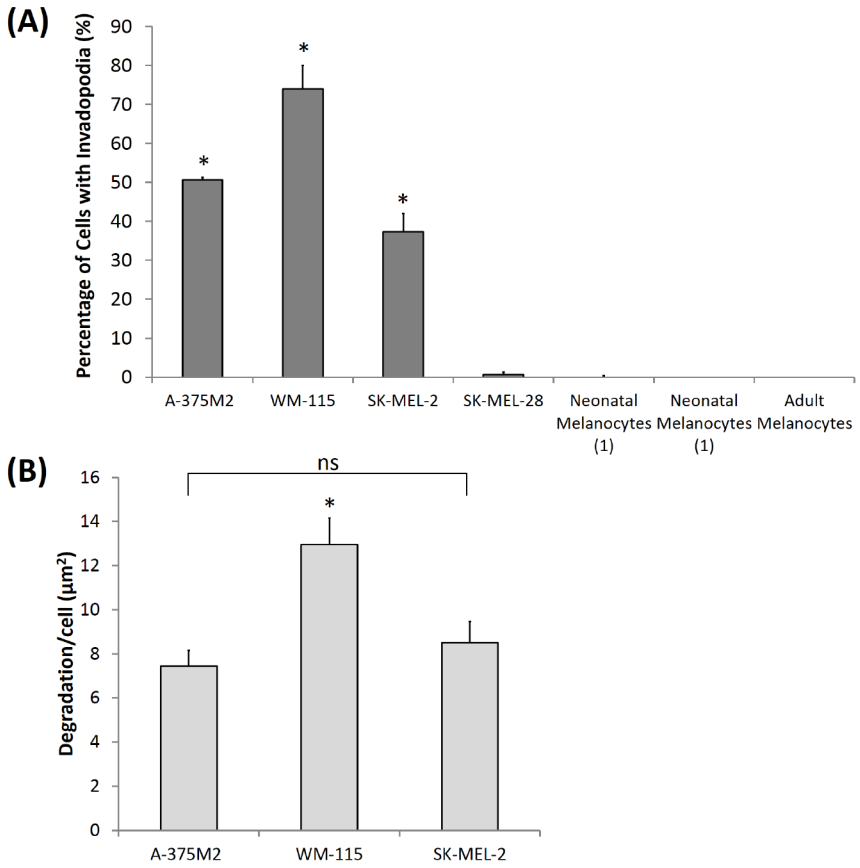

Figure 3-5: Invadopodia assay of melanoma cell lines and melanocyte controls.
(A) The percentage of cells with invadopodia. Significance was calculated to neonatal melanocytes (1) and between all melanoma cell lines. Data are mean values ± S.E.M. of 150 cells, over 3 independent experiments; * = $P < 0.05$. (B) The area of degradation from invadopodia per cell. Significance was calculated between all cell lines. Data are mean values ± S.E.M. of 90 invadopodia producing cells, over 3 independent experiments; * = $P < 0.05$, ns = not significant.

3.2.1.3 Characterisation of Cellular Adhesion

Cellular adhesions play a functional role in invadopodia structures as well as cell motility (Friedl and Wolf, 2003; Beaty *et al.*, 2013), and as such, the intrinsic adhesive properties of the various cell lines were investigated to identify any differences between primary and metastatic melanoma. In addition, the adhesion to collagen I was investigated due to the in vivo relevance (the dermal extracellular matrix surrounding melanoma cells *in vivo* being comprised mostly of collagen I) (Rook, 2010) and to validate the use of this matrix in the 3D spheroid invasion assay (section 3.2.1.4). Melanoma cell lines were plated on glass or collagen I coated coverslips and allowed to adhere for 1 or 8 hrs. Adherence was calculated as the number of cells adhered at 1 hr compared to 8 hrs (taken at 100%) (Figure 3-6).

Interestingly, on glass coverslips all the cell lines and the melanocyte controls had similar adherence values, except for A-375M2 and SK-MEL-2 cells, which were reduced (Figure 3-6). However, on a collagen I matrix all cell lines (including melanocyte controls) adhered equally well.

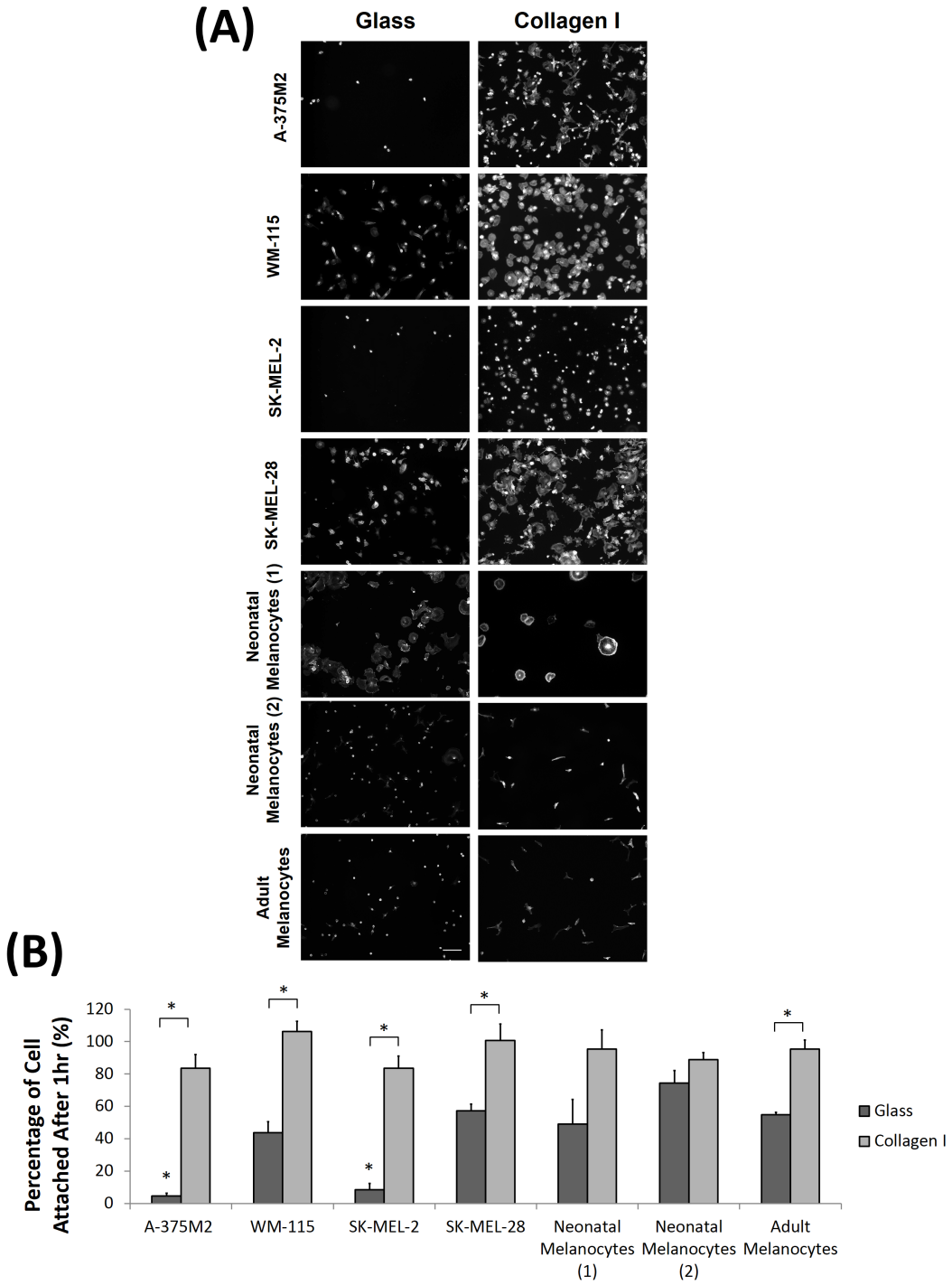

Figure 3-6: Adhesion assay on glass and collagen I.
Cells were plated at $1x10^5$, fixed and stained for F-actin 1 hr and 8 hrs after seeding. Melanocytes were plated at $5x10^4$ per well when plated on collagen I. (A) Representative F-actin images of cells at 1 hr post-seeding on glass or collagen I. Scale bar = 100µm. (B) The percentage of cells attached at 1 hr compared to 8 hrs after seeding. Significance was calculated to neonatal melanocyte (1) and between plastic and collagen I of the same cell line. Data are mean values ± S.E.M. over 3 independent experiments; * = $P < 0.05$.

3.2.1.4 3D Spheroid Invasion Assay using Melanoma Cell Lines

Cells can exhibit phenotypic differences in 2D environments, when compared to 3D (Sahai, 2007). Thus, to complement 2D experiments many scientists also employ 3D assays to investigate invasion in environments that would more closely resemble that seen *in vivo* (Zaman *et al.*, 2006; Yamazaki *et al.*, 2009). One such 3D assay that has been used reliably in the past is the spheroid invasion assay (Wolf *et al.*, 2007; Sabeh *et al.*, 2009; Wiercinska *et al.*, 2011). In this assay, spheroid tumour masses are created and encapsulated by a 3D matrix, such as collagen I, to represent the primary tumour mass and the surrounding tissue. Over time, the tumour cell invasion away from the spheroid mass can be measured.

The dermis extracellular matrix (often the site where melanoma invasion occurs) is comprised predominantly of collagen I (Rook, 2010). Data from the previously described adhesion assay (Figure 3-6) revealed that all the tested melanoma and melanocyte cell lines adhered to a collagen I matrix. Therefore, the 3D spheroid invasion assay was chosen as a suitible model to quantify cellular invasion in a 3D environment.

Cells were firstly submerged in methylcellulose media for 3 days to allow for the formation of the spheroid mass. They were then transferred into a collagen I matrix, where the level of invasion was quantified after 4 days.

During assay optimisation, the diameter of the A-375M2, SK-MEL-2 and SK-MEL-28 spheroids dramatically increased when in the collagen I matrix for 4 days, while the diameter of the WM-115 cell line derived spheroid and the melanocyte derived spheroids did not change. These differences in spheroid diameter could indicate differences in cell proliferation rates. Therefore, an MTT assay was performed, over the length of 4 days, to estimate the difference in proliferation between the A-375M2, SK-MEL-2, SK-MEL-28 and WM-115 cells (Figure 3-7). The MTT assay confirmed that the A-375M2, SK-MEL-2 and SK-MEL-28 cell lines had significantly higher proliferation when compared to the WM-115 cells (Figure 3-7). It was deduced from the MTT assay that the WM-115 cells had a 40% reduction in proliferation rate. Thus the seeding number of the other cell lines was reduced by 40% to deliver spheroids of the same size.

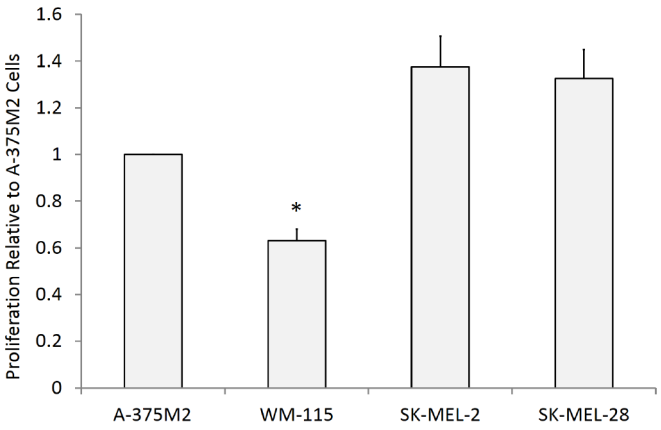

Figure 3-7: MTT assay of the melanoma cell lines.
Cells were grown over 4 days to simulate the time that the spheroid would spend in the collagen I matrix in the 3D spheroid invasion assay. Cells were incubated in MTT solution and solubilised in DMSO. The absorbance was measured using a plate reader and normalised relative to A-375M2 cells. Significance was calculated between all cell lines. Data are mean values ± S.E.M., over 3 independent experiments; * = $P < 0.05$.

Subsequent cell invasion was measured in two ways: the number of cells that exhibited clear spatial separation from the spheroid mass (see red arrows in Figure 3-8) and the number of cells that had migrated further than 100µm from the spheroid edge.

Using the 3D spheroid invasion assay it was demonstrated that all the melanoma cell lines had a higher number of invading cells when compared to neonatal melanocytes (1) (Figure 3-8A and B).

Interestingly, when the number of cells that invaded further than 100µm was calculated (Figure 3-8C), only the A-375M2 and WM-115 cell lines were found to be significantly different compared to the neonatal melanocytes (1). Thus, in this assay the WM-115 cell line is the most invasive melanoma cell line, followed by A-375M2, SK-MEL-2 and then SK-MEL-28. These results phenocopy those seen in the 2D invadopodia assay (Figure 3-5), suggesting that there is a good correlation between the 2D and 3D invasion assays, chosen for this study (Table 3-1).

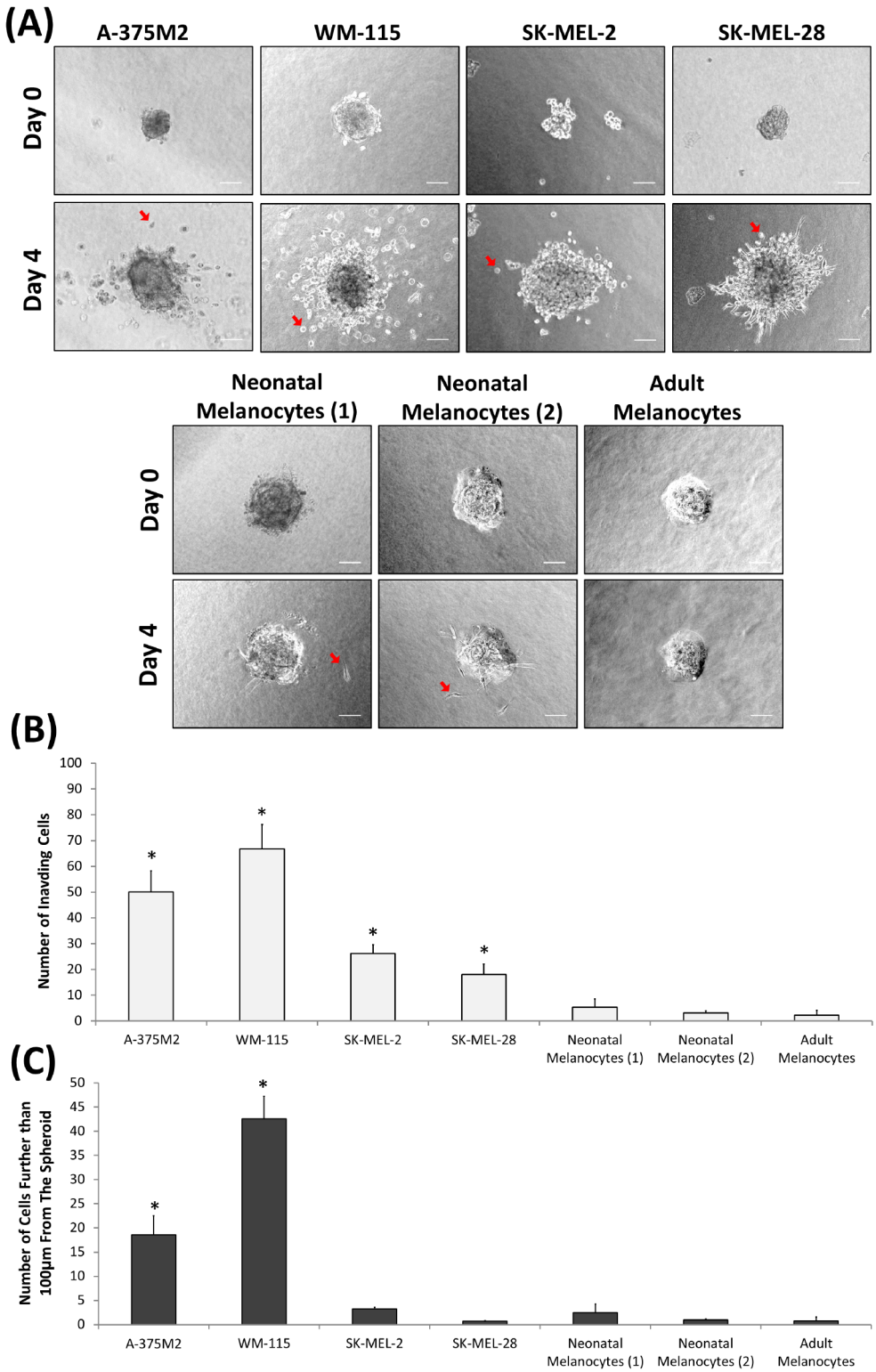

Figure 3-8: 3D spheroid invasion assay of melanoma cell lines.
Spheroid were produced in methylcellulose for 3 days, then submerged in a collagen I matrix. The cell invasion was measured at day 4 commencing when the spheroids were placed in the collagen I matrix. (A) Representative phase contrast images of the spheroids at day 0 and 4. Examples of invading cells are indicated by red arrows. Scale bar = 100µm (B) The number of cell that had invaded away from the spheroid mass. Significance was calculated to neonatal melanocytes (1). Data are mean values ± S.E.M., of 9 spheroids over 3 independent experiments; * = $P < 0.05$. (B) The number of cells that invaded further than 100µm from the spheroid mass. Significance was calculated to neonatal melanocytes (1). Data are mean values ± S.E.M., of 9 spheroids over 3 independent experiments; * = $P < 0.05$.

Cell Line	Invadopodia Assay	3D Spheroid Invasion Assay (Number of invading cells)	
		Total	>100µm from the Spheroid
WM-115	+++	+++	+++
A-375M2	++	++	++
SK-MEL-2	+	+	ns
SK-MEL-28	ns	+	ns
Neonatal Melanocytes (1)	¥	¥	¥
Neonatal Melanocytes (2)	ns	ns	ns
Adult Melanocytes	ns	ns	ns

Table 3-1: Collation of the melanoma cell line and melanocyte invasive phenotypes in the 2D and 3D invasion assay.

The trend in invasion is depicted by the number of + symbols (+ = low invasion, +++ = highest invasion). The number of + symbols indicates the trend in invasiveness and may not necessarily indicate significant differences in invasion to other cell lines with the + symbol. ¥ indicates the control cells to which significance was calculated: ns= not significant ($P > 0.05$).

3.2.2 Characterisation of Melanoma Patient Derived Cell Strains

Most commercially available cell lines have been established many years ago and cultured through several passage numbers. As such these cell lines may have acquired differing phenotypes to that present in the patient. In addition, it is not known whether melanoma cells, recently derived from patient tissue, can form invadopodia and/or invade collagen I matrices. Therefore, to complement the cell line findings, cell strains from melanoma patient primary and metastatic lesions were established and utilised in various experiments in parallel with the commercially available cell lines.

Surgical biopsies of primary and metastatic melanoma tissue are used for histological testing, but, when possible, small samples can also be used for scientific research. The excised melanoma tissue samples contain a range of cell types along with the melanoma cells, including fibroblasts and keratinocytes. Thus, melanoma cell isolation is required.

In this study six patient derived cell strains were established from both primary (M133, M460 and M586) and metastatic (M581, M575 and M35) patient tissue with associated clinical data.

3.2.2.1 Establishing Patient Derived Cell Strains

Tissue from patients with primary and metastatic melanoma were grown on fibronectin coated plates and a small number were removed and stained for high molecular weight melanoma associated antigen (HMWMAA) in order to estimate the percentage of melanoma cells present. The A-375M2 cell line was used as a positive control. In addition, the NIH3T3 fibroblast cell line and HaCaT keratinocyte cell line were used as a negative control for HMWMAA staining (Figure 3-9). Those samples in which the initial immunofluorescent stain suggested over 90% of HMWMAA positive cells were further analysed via FACS to obtain a more accurate cell count (Figure 3-10). All other patient strains were FACS sorted to isolate the HMWMAA positive cells. The successfully established patient derived cell strains, with associated patient clinical data, are listed in Table 3-2.

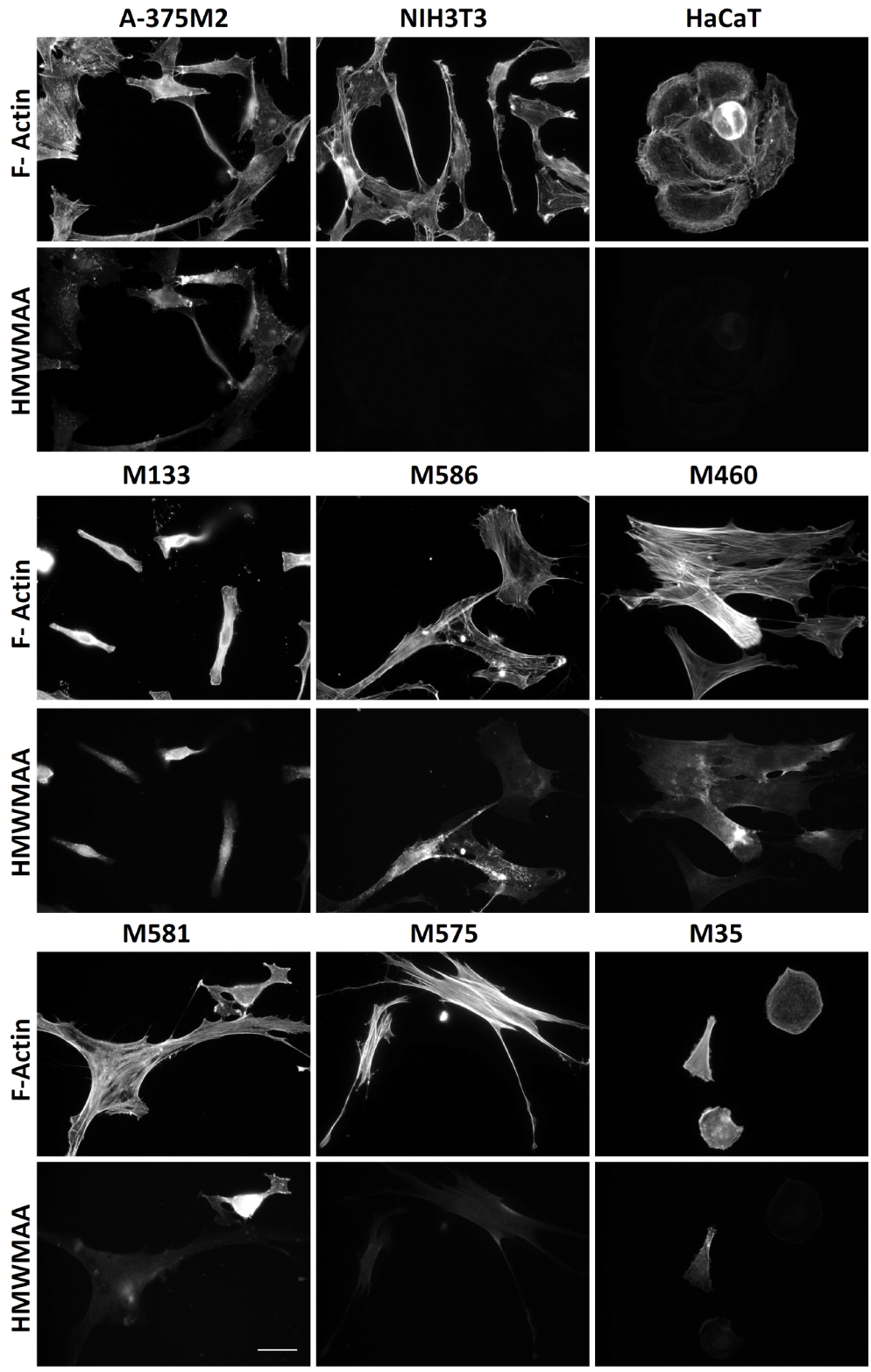

Figure 3-9: HMWMAA staining of patient derived tissue populations.
The cells grown from patient tissue were stained for HMWMAA and F-actin to identify and estimate the population of melanoma cells. A-375M2 (positive), NIH3T3 (negative) and HaCaT (negative) were stained as controls. Scale bar = 20µm.

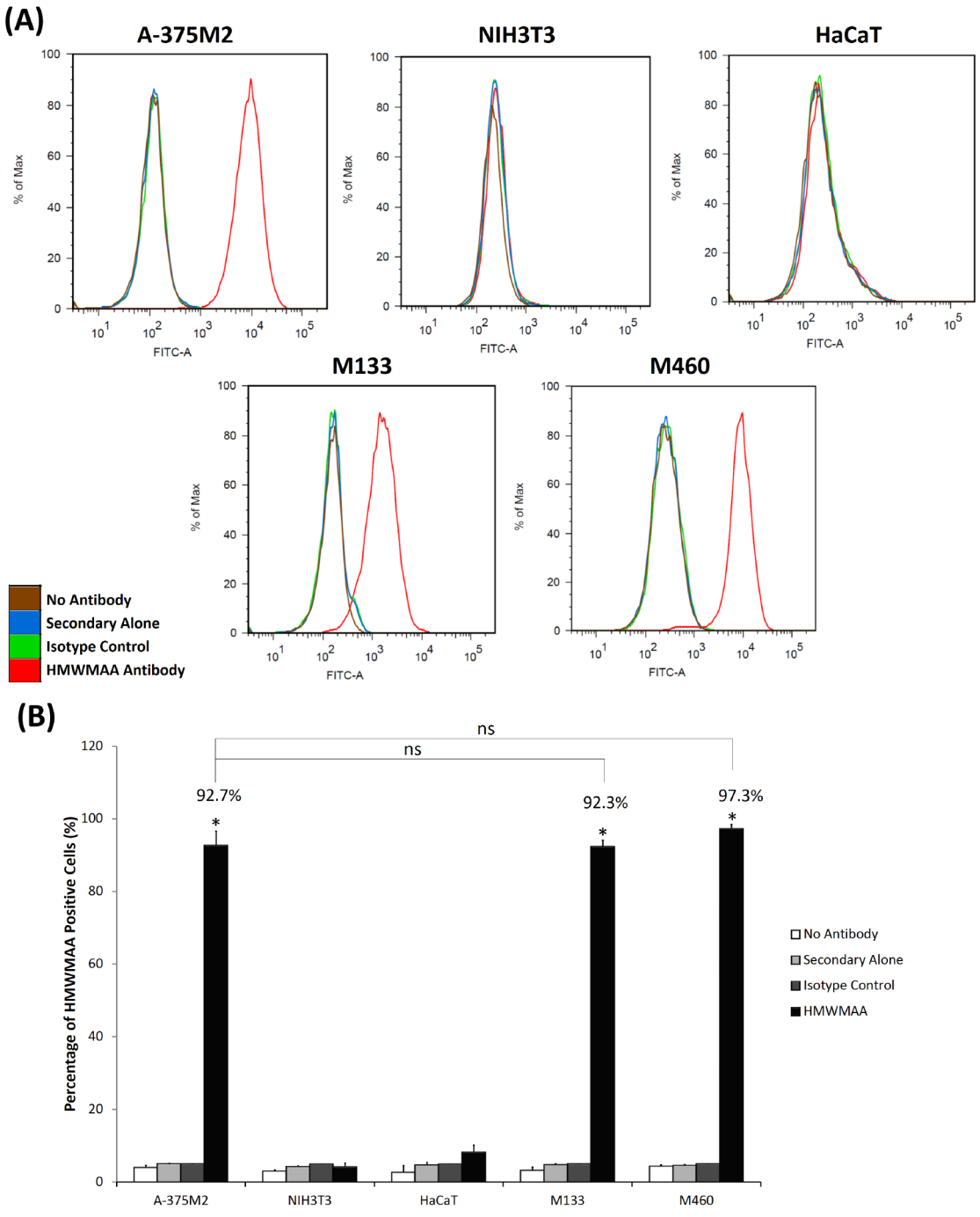

Figure 3-10: Fluorescence activated cell sorting (FACS) confirming the purity of melanoma cell in patient derived cell strains.

(A) FACS fluorescence intensity histograms (fluorescence intensity plotted against the number of events) of the patient derived cell strains, the positive control (A-375M2) and two negative control (NIH3T3 and HaCaT) cell lines. (B) The percentage of HMWMAA positive cells in the cell population. Data are mean values ± S.E.M., of 30,000 cells over 3 independent experiments; * = $P < 0.05$, ns = not significant.

Patient	When Tissue Was Taken		Date Tissue Was Taken	Current Stage	Patient Outcome
	Primary/ Metastatic	Stage			
M133	Primary	IIC	11/2009 (cells then frozen)	IIC	Died 02/2010 (carcinomatosis bronchus)
M586	Primary	IIC	01/2013	IIC	Alive
M460	Primary	IIIA	03/2012	IV	Died 10/2013 (metastatic melanoma)
M581	Metastatic	IIIB	01/2013	IIIB	Alive
M575	Metastatic	IIIB	12/2012	IV	Died 12/2013 (pneumonia and metastatic melanoma)
M35	Metastatic	IIIC	04/2012	IV	Died 12/2012 (metastatic melanoma)

Table 3-2: Clinical data for all successfully established patient cell strains.

3.2.2.2 Cell Morphology

To complement the previously described melanoma cell line characterisation (Section 3.2.1.1), the cell shape of patient derived cell strains was recorded. Cell elongation was of special interest as our melanoma cell line findings suggested a decreased elongation in melanoma cells compared to melanocyte controls (Figure 3-1C). The cells were seeded on glass coverslips, incubated overnight and stained for F-actin (Figure 3-11). The cell area and perimeter of the different patient derived cell strains was diverse, with no representative cell area identified (Figure 3-11A and B). Indeed, no consistent difference in cell shape was seen between cells that were from primary or metastatic sites.

In contrast, there was a decrease in elongation across all patient derived cell strains when compared to neonatal melanocytes (1) (Figure 3-11C). However, there was no difference between those strains derived from patients with primary or metastatic melanoma. These findings are in line with the data obtained from the melanoma cell lines and suggest that a less elongated/more circular cell shape is adopted by melanoma cells when compared to wildtype melanocyte cells.

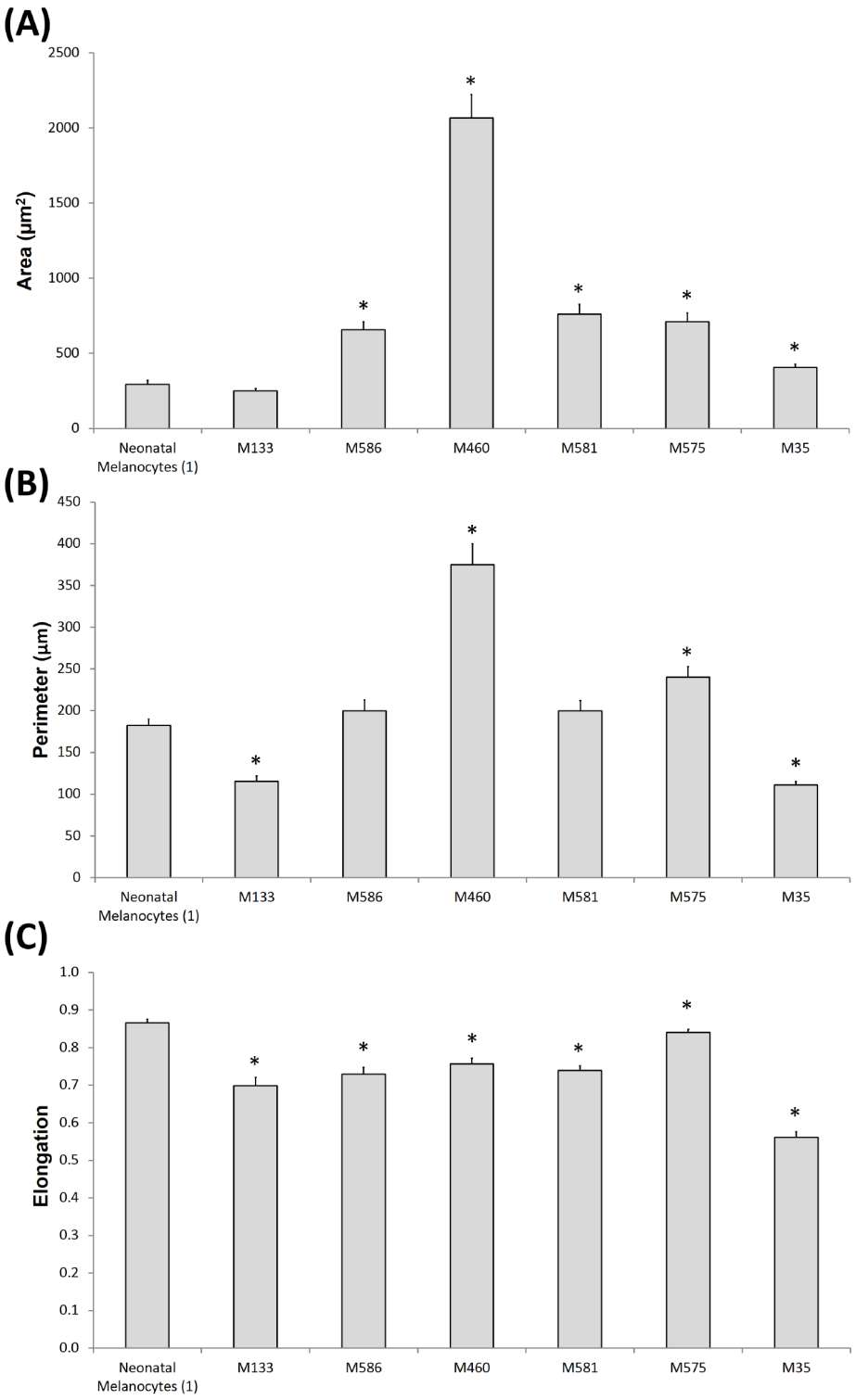

Figure 3-11: Cell shape analysis of patient derived cell strains.
The cell area (A), cell perimeter (B) and cell elongation (C) were calculated for 90 cells, over 3 independent experiments. Cell elongation was represented as a scale from 0 to 1 where 0 = circular and 1 = straight. Significance was calculated to neonatal melanocyte (1). Data are mean values ± S.E.M.; * = $P < 0.05$.

3.2.2.3 Patient Derived Cell Strains Form Invadopodia

Studies in section 3.2.1.2 and 3.2.1.4 demonstrated that a combination of the invadopodia assay and 3D spheroid invasion assay gave a good indication of invasive potential across a variety of melanoma cell lines. Thus, the invasiveness of the patient derived cell strains were tested in the invadopodia assay.

Cells were initially plated on rhodamine conjugated gelatin coverslips and incubated for 3 hrs before fixing and staining for F-actin in line with the previous studies (Figure 3-5). However, in contrast to the melanoma cell lines, only the M35 patient derived cell strain produced invadopodia after a 3 hr incubation (Figure 3-13). Interestingly, the M35 strain (derived from a patient with advanced disease) produced a higher percentage of cells with invadopodia (89%) than any of the melanoma cell lines (74% for WM-115) (Figure 3-5).

Previous studies have analysed invadopodia activity up to 24 hrs post seeding (Artym *et al.*, 2006; Caldieri *et al.*, 2009; Stylli *et al.*, 2009), thus a longer incubation time of 24 hrs was also used. Even, after 24hrs the M133, M581 and M575 cell lines were unable to produce a significant number of invadopodia compared to neonatal melanocytes (1) (Figure 3-12 and Figure 3-13). A small number of M581 cells were able to form invadopodia, however, not at significant levels compared to the control melanocytes.

In contrast, the M586, M460 and M35 cell strains all produced significant percentages of cells with invadopodia when incubated on the gelatin for 24 hrs. Moreover, the M35 cell strain had the highest degradation level per cell (Figure 3-13B), which is particularly noteworthy given it has the smallest cell area of all invasive cell strains (Figure 3-11), thus suggesting a high degree of invasiveness of M35 compared to other cell strains.

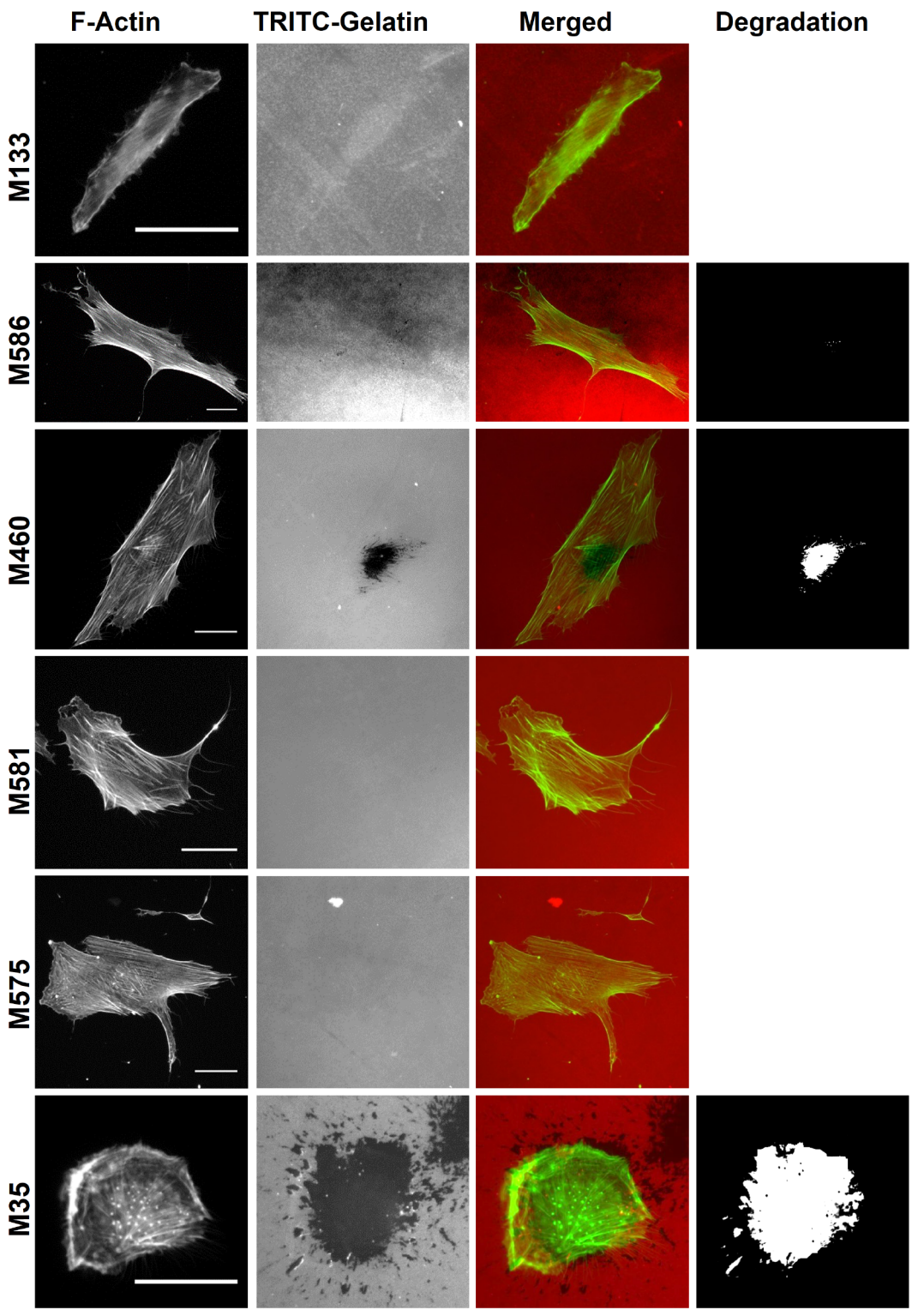

Figure 3-12: Representative images of the patient derived cell strain invadopodia assay at 24 hrs.

Cells were seeded on rhodamine conjugated gelatin for 24hrs and stained for F-actin. Only actin rich dots that corresponded with gelatin degraded dots were counted as invadopodia. The degradation was measured using ImageJ software. Scale bars = 20µm.

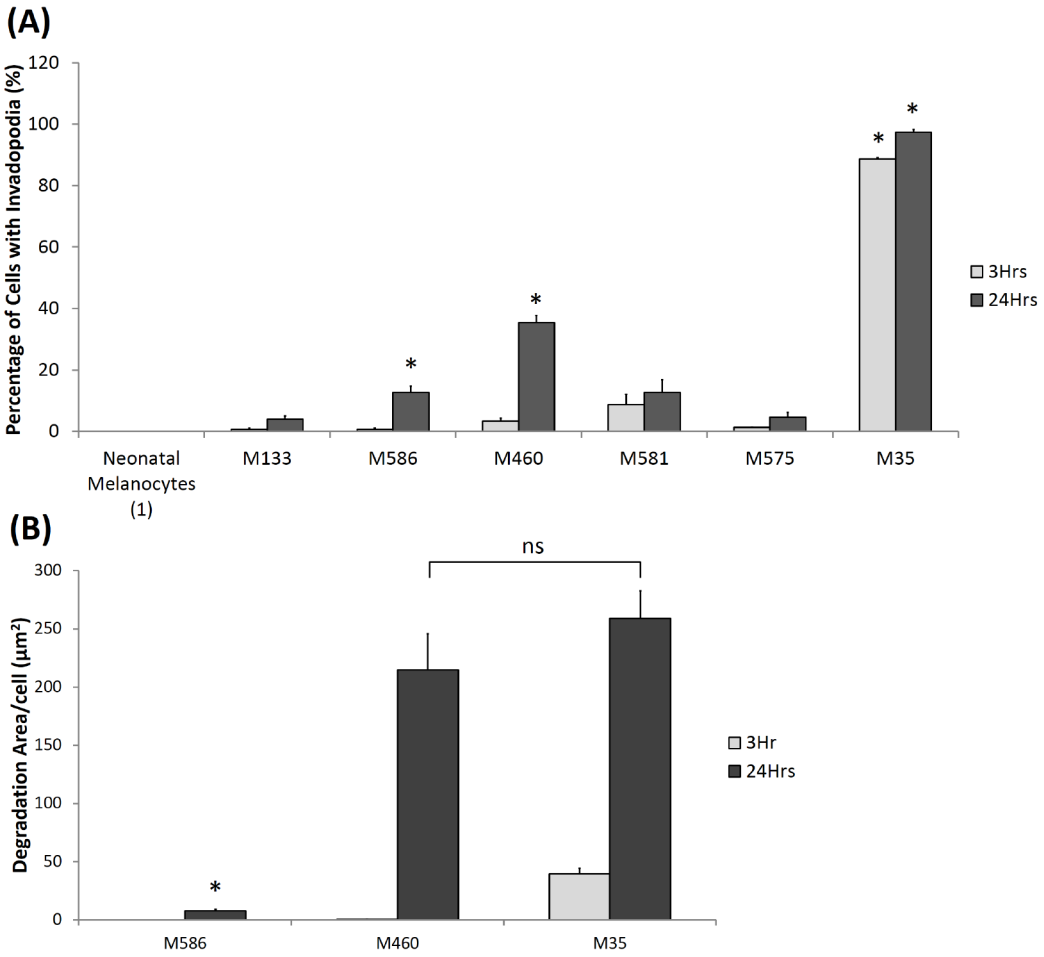

Figure 3-13: 3 hrs and 24 hrs Invadopodia assay of patient derived cell strain and neonatal melanocyte (1) control.

(A) The percentage of cells with invadopodia when cells were plated on gelatin for 3 hrs and 24 hrs. Significance was calculated to neonatal melanocytes (1). Data are mean values ± S.E.M. of 150 cells, over 3 independent experiments; * = $P < 0.05$. (B) The area of degradation per cell when cells were plated on gelatin for 3 hrs and 24 hrs. No degradation was quantified for M586 and M460 at 3 hrs due to the lack of cell number. Significance was calculated between all cell lines at the same time point. Data are mean values ± S.E.M. of 90 invadopodia producing cells, over 3 independent experiments; * = $P < 0.05$, ns = not significant.

3.2.2.4 The Invasion of Patient Derived Cells in the 3D Spheroid Invasion Assay

Following the invadopodia study, the cell strains were subsequently tested in the 3D spheroid assay. The 3D spheroid assay had produced robust, differential invasive phenotypes of the melanoma cell lines compared to melanocyte controls (Section 3.2.1.4), which correlated with the results obtained from the melanoma cell line 2D invadopodia assay (Section 3.2.1.2). The behaviour of the patient derived cell strains was tested in the 3D spheroid assay to ascertain if the result also correlated with invadopodia formation.

As all melanoma cell lines and melanocytes from adult and neonatal melanocytes were able to adhere to collagen I (Section 3.2.1.3) and the major component of the dermis is collagen I, it was assumed that the patient derived cell strains would also adhere to collagen I.

Unlike the 3D spheroid invasion assay performed with the melanoma cells lines, which submerged the spheroid in collagen I matrix over 4 days, the patient derived cell strains were only in the collagen I matrix for 3 days. This timeframe was altered as there were cells outside the field of view on day 4, which would not have been quantified and thus may have skewed the invasion data. All the patient derived cell strains were able to form spheroid masses in the methylcellulose, except for M35, therefore, this strain was not included in the 3D spheroid invasion assay.

Significant numbers of cells invaded away from the spheroid mass for all tested patient derived cell strains, compared to neonatal melanocytes (1) (Figure 3-14A and B). The M575 cell strain had the highest number of invading cells and the highest number of cells that invaded further than 100µm from the spheroid, followed by M460, M586, M581 and lastly M133 (Figure 3-14B). A summary of the patient derived cell strain data can be found in Table 3-3.

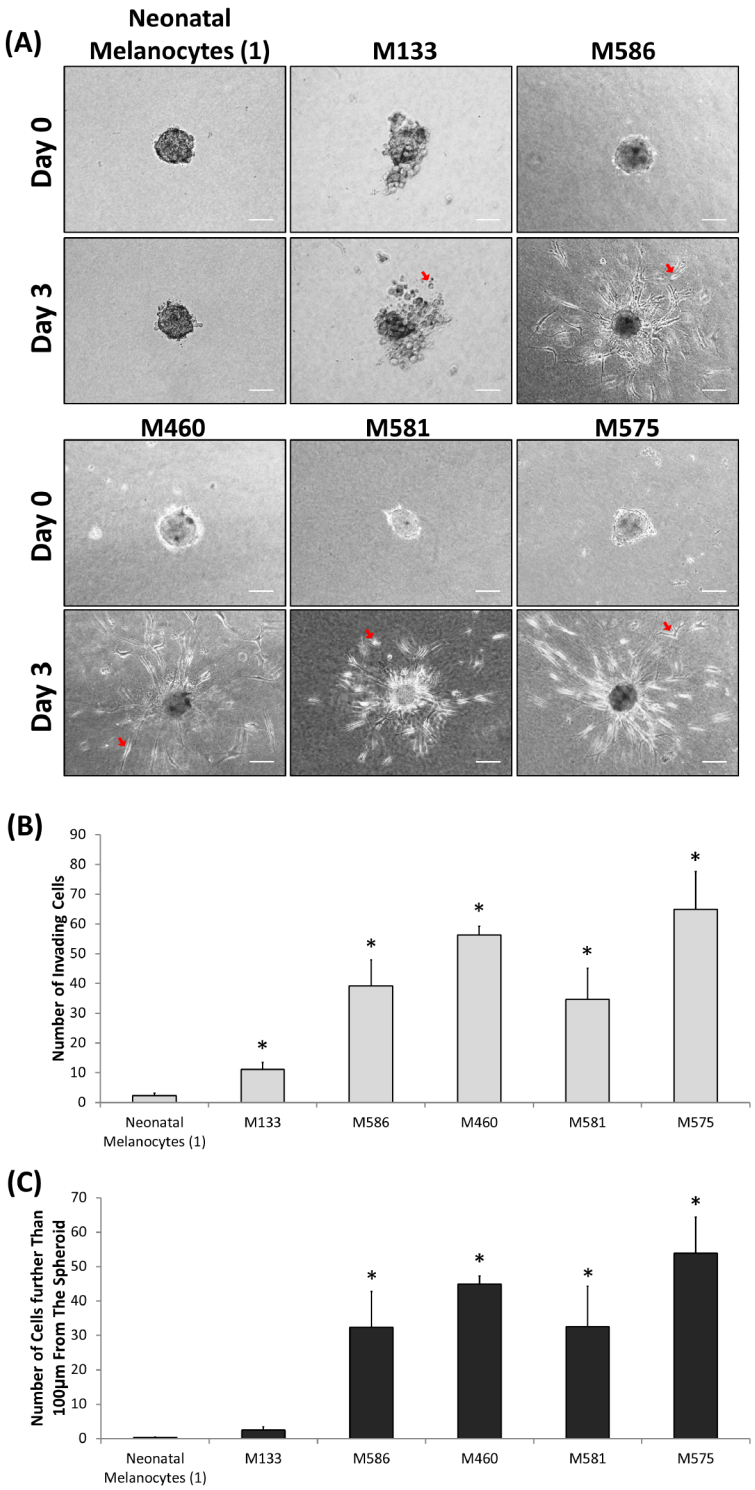

Figure 3-14: 3D spheroid invasion assay of patient derived cell strains compared to neonatal melanocytes (1).

Spheroid were produced in methylcellulose over 3 days, then submerged in collagen I matrix. The cell invasion was measured day 3 from when the spheroids were placed in the collagen I matrix. A) Representative phase contrast images of the spheroids at day 0 and 3 in the collagen I matrix. Examples of invading cells are indicated by red arrows. Scale bar = 100µm (B) The number of cells that invaded away from the spheroid mass. Significance was calculated to neonatal melanocytes (1). Data are mean values ± S.E.M., of 9 spheroids over 3 independent experiments; * = $P < 0.05$. (B) The number of cells that invaded further than 100µm from the spheroid mass. Significance was calculated to neonatal melanocytes (1). Data are mean values ± S.E.M., of 9 spheroids over 3 independent experiments; * = $P < 0.05$.

Cell Line	Disease Progression	Invadopodia Assay	Spheroid Assay	
			Number of Cells	Number of Cells Further than 100µm from the Spheroid
M35	Yes	+++	Ω	Ω
M460	Yes	++	++	+
M586	No	+	++	+
M575	Yes	ns	+++	++
M581	No	ns	++	+
M133	No	ns	+	ns
Neonatal Melanocytes (1)		¥	¥	¥

Table 3-3: Collation of the patient derived cell strains and neonatal melanocytes (1) invasive phenotypes in the 2D and 3D invasion assay.

The trend in invasion is depicted by the number of + symbols (+ = low invasion, +++ = highest invasion). The number of + symbols indicates the trend in invasiveness and may not necessarily indicate significant differences in invasion to other cell lines with the + symbol. ¥ indicates the control cells to which significance was calculated: ns= not significant ($P > 0.05$). Ω symbol indicates the assay was not performed on these cells. Strains were considered to have disease progression if there was an increase in the stage of disease from the time when the tissue was taken to the current stage (further details are found in Table 3-2)

3.3 Discussion

For a cell to metastasise many complex processes must occur, including invading through the basement membrane and the surrounding tissue, intravasation into blood vessels or lymph nodes, extravasation and growth at distant sites (Sahai, 2005). This process undoubtedly relies on various contributing cell characteristics which all play a role in the overall invasiveness of a cell (Friedl and Wolf, 2003). This chapter focuses on optimising the use of a 2D and 3D measure of invasion to characterise the melanoma cell lines and cell strains.

The cell area and perimeter varied greatly in the melanoma cell lines and patient derived cell strains, with most cells differing significantly from the melanocyte controls. These findings indicate that there is no cell area that can be considered representative of melanoma cells when they become tumourous. Furthermore, there were no consistent differences in cell area and perimeter between invasive and non-invasive melanoma cell lines/strains.

The SK-MEL-28 cells were shown to be significantly larger than the melanocytes and the other melanoma cell lines. This is a well known feature of SK-MEL-28 cells (Hoashi *et al.*, 2005; Watabe *et al.*, 2008) and is mostly likely a representative feature of this cell type and therefore not linked to invasiveness.

There was a trend across the cell lines and patient derived cell strains which showed reduced cell elongation, compared to neonatal melanocytes (1). These results indicate that melanoma cells may have a more rounded morphology in 2D. However, there were no consistent differences between invasive and non-invasive melanoma cell lines/strains, therefore, this phenotype is unlikely to indicate cell invasiveness.

However, the 2D invadopodia assay and the 3D spheroid invasion assay provided more reliable results. Cumulatively, the assays performed in this chapter have shown the WM-115, SK-MEL-2 and A-375M2 cell lines to have an invasive phenotype compared to melanocyte controls. Conversely, SK-MEL-28 cells showed little or no invasive phenotype, compared to melanocyte controls. Of the patient derived cell strains the M35, M460, M586, M581 and M575 showed an invasive phenotype in one or more of the invasion assays. The M133 was the only patient derived cell strain that lacked an invasive phenotype in all the assays performed.

The WM-115 cell line, a primary cell line, showed significant levels of invasiveness in 2D and 3D invasion assays, higher than that seen for the metastatic cell lines, A-375M2 and SK-MEL-2. This result was perhaps unexpected due to the primary tumour origins of the WM-115 cell line.

However, the excised tumour was in the vertical growth phase (VGP), which is characterised by vertical invasion through the basement membrane and dermal tissue, the first steps of melanoma invasion (Herlyn *et al.*, 1985; Hsu *et al.*, 2000; Silini *et al.*, 2010). Indeed, in a skin reconstruction assay WM-115 cells were able to breach the basement membrane and invade the dermis (Meier *et al.*, 2000). The lesion from which the WM-115 cell line originated produced metastatic disease in the patient after 16 months post-excision (Silini *et al.*, 2010). Furthermore, studies have shown that WM-115 cells can form lung metastases in mice with a success rate of 80% (Herlyn *et al.*, 1985; Silini *et al.*, 2010), therefore, representing a melanoma in the state of early invasion at the primary site. Additionally, this study shows for the first time that the WM-115 cell line can produce invadopodia protrusions and can invade through a 3D collagen invasion assay. This confirms that these cells can exhibit a robust, highly invasive phenotype in multiple *in vitro* assays. Therefore, this study would define the WM-115 cell line as an invasive primary cell line.

The A-375M2 and SK-MEL-2 cell lines also demonstrated invasive phenotypes in this study, which is confirmed in the literature. The A-375M2 cell line, is a highly metastatic sub-population (isolated from lung metastases) of the parental A-375 cell line and has been shown to form lung metastases in mice (Kozlowski *et al.*, 1984). In addition, the A-375M2 cell line exhibits an invasive phenotype in a range of *in vitro* assays including the invadopodia assay (Baldassarre *et al.*, 2006; Ayala *et al.*, 2008; Md Hashim *et al.*, 2013), collagen I invasion assay (Gadea *et al.*, 2008; Sanz-Moreno *et al.*, 2008; Calvo *et al.*, 2011) and the inverted invasion assay (collagen/Matrigel matrix) (Li *et al.*, 2010a). The SK-MEL-2 cell line was isolated from a skin metastasis and, like A-375M2 cells, has shown the ability to form lung metastases in mice (Fogh and Trempe, 1975; Claffey *et al.*, 1996). SK-MEL-2 cells, have shown invasion in *in vitro* invasion assays including Matrigel transwell invasion assays (Gouon *et al.*, 1996; Knutson *et al.*, 1996) and dermal equivalent invasion assays (collagen I matrix containing dermal fibroblasts) (Bizik *et al.*, 1999). Therefore, the invasive phenotype of A-375M2 and SK-MEL-2 cell lines shown in this study, is very much in line with previous findings.

The SK-MEL-28 cell line was the only melanoma cell line in this study to show no or very low invasive potential. Originally, this cell line was isolated from a primary melanoma lesion (Fogh and Trempe, 1975) and is in fact currently used by many as a non-invasive, early stage, representative for melanoma (Watabe *et al.*, 2008). SK-MEL-28 cells have shown non-invasive phenotypes in multiple invasion assays, including the invadopodia assay (Aoyama and Chen, 1990; Monsky *et al.*, 1994) and the Boyden chamber invasion assay (collagen I or Matrigel

matrix) (Wach *et al.*, 1996). In contrast, there are also reports that the SK-MEL-28 cell line can exhibit invasive characteristics in a Matrigel invasion assay (Liu *et al.*, 2012), dermal equivalent (collagen I matrix containing dermal fibroblasts) and organ-cultured dermal (human neonatal foreskin dermis co-polymerised with dermal equivalents) invasion assays (Bizik *et al.*, 1999). Therefore, depending on the invasion assay used SK-MEL-28 cells may or may not display an invasive phenotype. These findings were also found in this current study, as SK-MEL-28 cells were unable to produce invadopodia protrusions to degrade the gelatin matrix but were able to invade into the collagen I matrix in the 3D spheroid invasion assay (albeit at a distance that was not significant when compared to the melanocyte controls). Therefore, in this study the SK-MEL-28 showed a non-invasive phenotype and was classed thusly.

The six patient derived cell strains were established from primary (M133, M586 and M460) and metastatic (M581, M575 and M35) tissue. However, as with the melanoma cell lines, the invasive capacity was not restricted to those cells produced from metastatic tissue. Indeed, two patient derived cell strains, from primary tissue (M586 and M460) showed a robust invasive phenotype in both the 2D and 3D invasion assays. Therefore, the patient stage and disease outcome may provide a better indication of the potential cell invasiveness.

The M35 patient derived cell strain was shown to have an invasive phenotype as it had the highest percentage of invadopodia producing cells (at both 3 hrs and 24 hrs) of all the strains. Interestingly, M35 was the only strain to have a significant number of cells that produced invadopodia at 3hrs. Furthermore, the percentage of cells with invadopodia at this time point was higher than that seen in the WM-115 melanoma cell line. Unfortunately, no data was obtained for the M35 cells in the 3D spheroid assay as this strain was unable to form spheroids in the methylcellulose. To produce these spheroid masses, cells must be able to form at least a basal level of cell-cell adherence. Over the years, the correlation between invasion/metastasis and reduction in cell adhesion has been well documented (Hirohashi, 1998; Cavallaro and Christofori, 2001). Therefore, M35 cells may not sufficiently adhere to each other to form a spheroid mass due to their high invasive potential. Indeed, the patient clinical data suggests that the M35 cells are extremely invasive, as the disease caused patient death 8 months after the lesion was removed. Consequently, only the invadopodia assay was used to assess the M35 cell invasiveness and the extremely high invasive capacity demonstrated by this assay was firmly in line with the clinical data.

All other patient derived cell strains, other than strain M575, showed a correlation between the phenotype shown in the 2D invadopodia assay and 3D spheroid invasion assay. The M575 strain

was unable to produce invadopodia, but had a highly invasive phenotype in the 3D spheroid invasion assay. Some modes of cell movement can be devoid of matrix degradation (Friedl and Wolf, 2003) and therefore, one explanation for this difference in the invasive phenotype between the two assays may be that the M575 cells invade the collagen I matrix in a protease independent manner. To address this question, the 3D spheroid invasion assay could be performed in the presence of a matrix metalloprotease (MMP) inhibitor to investigate the effect, if any, on the invasive capacity of the M575 cell strain. One suitable inhibitor that could be used is GM6001, a broad-spectrum MMP inhibitor that has been previously used to investigate protease independent invasion in a 3D spheroid invasion assay (Sabeh *et al.*, 2009).

The M133 patient derived cell strain was classified alongside the SK-MEL-28 cell line as demonstrating little to no invasive potential. M133 was in fact the only non-invasive patient derived cell strain in this study, as these cells were unable to form invadopodia and invade further than 100µm from the spheroid (as shown by the invadopodia and 3D spheroid invasion assays respectively). Similar to that which was seen with the non-invasive SK-MEL-28 cell line, the number of M133 patient derived cells invading into the collagen I matrix (in the 3D spheroid invasion assay) was significant, compared to neonatal melanocytes (1). Therefore, non-invasive melanoma cells may still possess a basal level of invasiveness compared to melanocytes (albeit dramatically lower than that of invasive melanoma cells).

The use of the patient derived cell strains has provided data that has both complemented and validated the results obtained from the melanoma cell lines in the 2D and 3D invasion assays. These cell strains provide a valuable tool and their use is highly recommended for any future melanoma studies. Within this study, cell strains were cultured for no more than 6 months, and this limit is recommended for any further work utilising these patient strains. The tumourigenic nature of these cells predisposes them to acquiring mutations that may affect the cell phenotype, which may then not be representative of that present in the patient.

Based on the results obtained with the melanoma cell lines and the patient derived cell strains, it can be concluded that while cell morphology is not a representative indicator of invasiveness, the 2D invadopodia assay and 3D spheroid assay correlate well and can be used to quantitatively measure invasive potential. Moreover, it has now been demonstrated that patient derived cells can both produce invadopodia and invade through a 3D collagen matrix, further validating these *in vitro* assays. The correlation between these two invasion assays was not evident for all cell strains which highlights the importance of using both assays to determine the true invasive potential.

The invadopodia assay and the 3D spheroid invasion assay enabled a level of invasiveness to be assigned to the melanoma cell lines and patient derived cell strains. This will be used in subsequent chapters to assess the potential role of PAK family members in melanoma cell invasion.

4 Chapter 4 – Role of PAK1 and PAK4 in Melanoma Invasion

4.1 Introduction

During invasion and metastasis, cells utilise cytoskeletal remodelling pathways, including the Rho GTPase family, to regulate cell movement (Vega and Ridley, 2008; Yilmaz and Christofori, 2009). Two of the most extensively studied Rho GTPases are Cdc42 and Rac1 which are intimately involved in cell shape and motility, primarily by controlling the polymerisation/depolymerisation and branching of actin filaments (Vega and Ridley, 2008). The most well characterised downstream effectors of Cdc42 and Rac1 are the p21 activated kinase (PAK) family (Bishop and Hall, 2000). PAKs are serine/threonine kinases that consist of 6 isoforms, separated into two groups according to their sequence homology: group I, containing PAK1-3; and group II, containing PAK4-6. PAKs have been shown to be involved in cell cycle control, proliferation, cell motility and apoptosis, therefore, it is not surprising to find that this family of kinases is thought to play a role in cancer growth and progression (King *et al.*, 2014).

The overexpression and/or hyperactivation of PAK isoforms have been found in a variety of tumours, such as brain (PAK1 hyperactivation), breast (PAK1 and PAK4 overexpression), colorectal (PAK5 overexpression) and prostate (PAK6 overexpression) (Dummler *et al.*, 2009; Gong *et al.*, 2009). PAK1 and PAK4 are thought to be the most commonly overexpressed isoforms in cancer (King *et al.*, 2014). Constitutively activated PAK1 has also been shown in previous studies to induce the formation of tumours such as those found in the mammary gland (Wang *et al.*, 2006). In addition, the overexpression of activated PAK4 can transform Rat1 and NIH3T3 fibroblasts and induce anchorage-independent growth, a pivotal stage in tumour progression and metastasis (Qu *et al.*, 2001).

Studies suggest that PAKs may play a role in invadopodia formation. In a model of rat vascular smooth muscle cells, PAK1 can induce the formation of the invadopodia related structures known as podosomes (Webb *et al.*, 2005), while a kinase dead PAK1 open conformation mutant induces the formation of invadopodia-like protrusions in aortic smooth muscle cells (Furmaniak-Kazmierczak *et al.*, 2007). The use of an autoinhibitory domain of PAK1 (PAK1-AID), which can inhibit endogenous PAK1 protein activation, demonstrated that PAK1 activity is required to sustain invadopodia formation and activity during the invasion of the A375MM cell line (Ayala et al., 2008). Indeed, PAK1 can phosphorylate cortactin, a protein vital for invadopodia formation (Ayala *et al.*, 2008). PAKs are also activated by Src, which is known to induce

invadopodia formation (Murphy and Courtneidge, 2011). In addition, PAK4 localises to podosomes in bone-marrow-derived mouse dendritic cells (Wells and Jones, 2010).

Many studies have been conducted in which the involvement of PAKs, in different cancer types, has been investigated. However, the role of PAKs in cutaneous melanoma has not been well studied. In 2006, Pavey and colleagues found that PAK1 overexpression correlated with invasive potential in uveal melanoma cell lines (melanoma of the eye) (Pavey *et al.*, 2006). PAK4 mRNA overexpression is also found in multiple cutaneous melanoma cell lines, including SK-MEL-2 and SK-MEL-28 (Callow *et al.*, 2002). Furthermore, PAK4 is important in the carcinogenesis of squamous cell carcinoma (SCC) (Zanivan *et al.*, 2013). These initial studies suggest a possible role for PAKs in cutaneous melanoma invasion. As discussed previously, during the early stages of metastasis, cells produce the invasive protrusion, invadopodia, to aid matrix degradation and invasion. Indeed, many proteins have been implicated in the promotion of invadopodia formation and degradation. However, the impact of serine/threonine kinases, especially PAKs, is less well studied.

In addition to investigating cell invasion by quantifying invasive structures such as invadopodia, as well as utilising 3D invasion assays, both of which are conducted *in vitro,* studies in an *in vivo* context are extremely important. However, getting useful quantifiable data using mouse models can be quite a challenge. In recent years, the use of zebrafish as an *in vivo* model has become increasingly popular. Single pairs of zebrafish adults can produce many hundreds of embryos in a single spawn (which can be repeated weekly), providing sufficient embryos for several different treatment conditions and experimental repeats. In addition, zebrafish embryos have a very fast developmental process which means that by 5-6 days post-fertilisation (dpf), full embryonic cell migration has occurred and major organs are distinguishable (Rubinstein, 2003). One such zebrafish *in vivo* model, the yolk invasion assay, involves the injection of cancer cell lines into the yolk of 2 dpf embryos (Eguiara *et al.*, 2011; Jung *et al.*, 2012; Teng *et al.*, 2013). The invasiveness of the cancer cell lines can then be quantified by the percentage of embryos with tail invasion after 4-7 days post-injection (dpi). This model has shown great promise in distinguishing the invasive/metastatic potential of xenografted cell lines.

This chapter investigates the expression levels of the PAK family of kinases in melanoma cell lines and patient derived cell strains. The resulting PAK expression is compared to the invasive potential defined in Chapter 3 to identify any correlations. Subsequently, the role of PAKs in melanoma invasion will be investigated.

4.2 Results

4.2.1 PAK Isoform Expression in Melanoma Cell Lines

The overexpression of different PAK isoforms has been found in many human tumours (Dummler *et al.*, 2009; King *et al.*, 2014). However, PAK protein expression in melanoma cells has not been investigated. Thus, PAK isoform expression was quantified in both melanoma cells and melanocyte controls.

As melanoma originates from melanocytes, the latter was used as a wildtype control in this study. In order to determine the best wildtype control for use in western blotting analysis, neonatal and adult melanocyte expression of two representative PAK isoforms from each group, PAK1 and PAK4, were measured (Figure 4-1). As expected, there was variation in protein expression levels between melanocytes from neonatal versus adult origins and in fact, the PAK1 protein expression was significantly higher in the neonatal melanocytes (2) compared to the adult melanocytes (Figure 4-1B). There was, however, no significant difference in PAK4 protein expression between the three wildtype cells (Figure 4-1C). To ensure that any changes in protein levels observed in the melanoma cell lines and patient derived cell strains were in fact robust, the neonatal melanocytes (1) were used as a control in subsequent analyses.

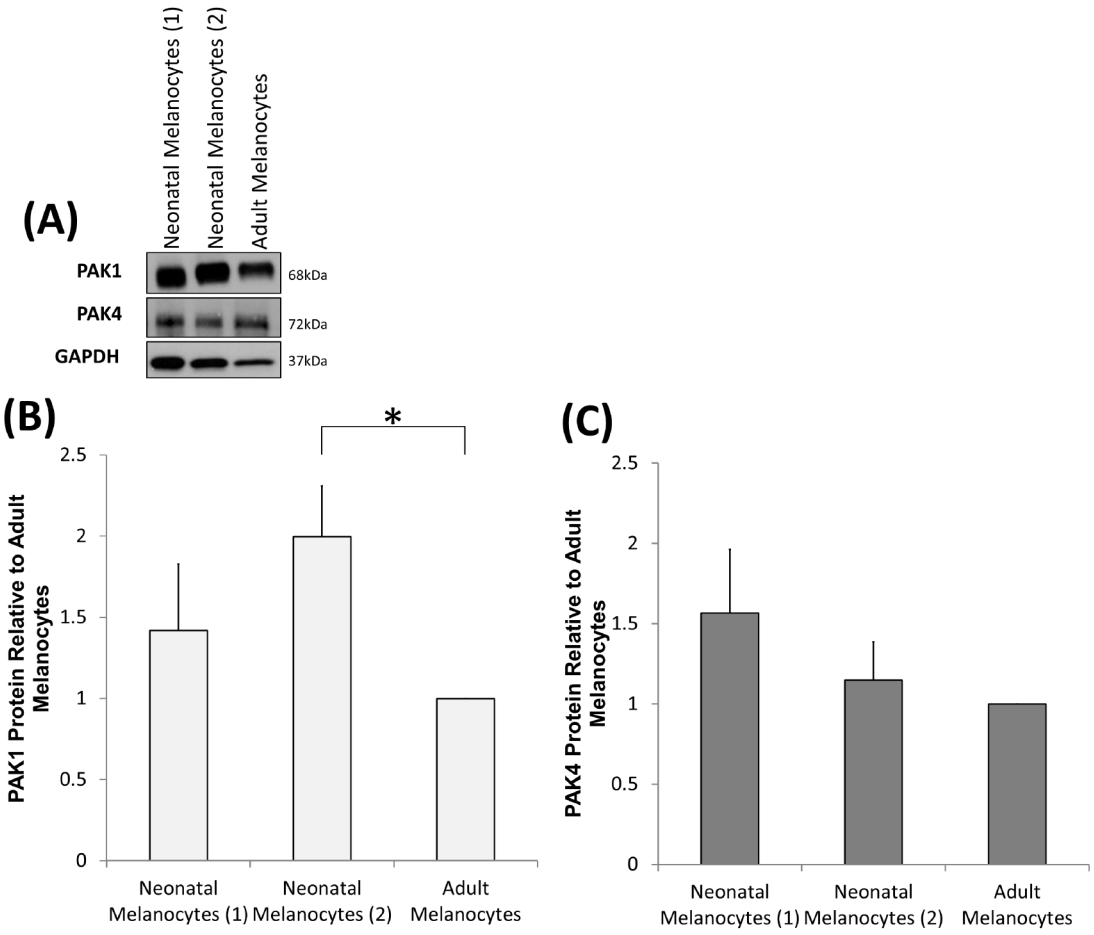

Figure 4-1: PAK Protein expression in neonatal and adult melanocytes.
Western blot of PAK1 and PAK4 expression in neonatal melanocytes (1), neonatal melanocytes (2) and adult melanocytes. (B) Analysis of western blot data via densitometry showing PAK1 expression in neonatal melanocytes (1) and neonatal melanocytes (2) relative to adult melanocytes. (C) Analysis of western blot data via densitometry showing PAK4 expression in neonatal melanocytes (1) and neonatal melanocytes (2) relative to adult melanocytes. Significance was calculated relative to adult melanocytes. Data are the mean values ± S.E.M., over 3 independent experiments; *= $P < 0.05$. Densitometric data were normalized to GAPDH, which was used as a loading control.

4.2.1.1 Group I PAKs - PAK1 and PAK2 are Overexpressed in Melanoma Cell Lines

The protein expression for each PAK isoform in three invasive cell lines (A-375M2, WM-115 and SK-MEL-2) and one non-invasive (SK-MEL-28) cell line was compared to that found in neonatal melanocytes (1). Additionally, representative tumour cell lines were also analysed to determine how melanoma PAK protein expression levels would compare to levels in human breast (MB-231), prostate (DU-145) and bladder (T24) cancers. Furthermore, neural crest oligodendrocyte progenitor cells (OPCs) were included as a positive control in all PAK screening panels because, unlike other cell lines used, they express PAK3 at readily detectable levels (Burbelo *et al.*, 1999).

PAK1 protein expression was found to be overexpressed in three melanoma cell lines, A-37M2, WM-115 and SK-MEL-2 cells, compared to neonatal melanocyte (1) (Figure 4-2). Interestingly, PAK1 was only overexpressed in these melanoma cell lines that were characterised as having an invasive phenotype in Chapter 3 (Figure 4-2B). Indeed, the only cell line (SK-MEL-28) that did not overexpress PAK1 compared to neonatal melanocytes (1), was classed as having a non-invasive phenotype in Chapter 3. Furthermore, the cell line with the most invasive phenotype, WM-115 (Table 3-1), had the highest PAK1 protein expression level of the four melanoma cell lines. It is also interesting to note that PAK1 levels in melanoma cell lines were expressed at similar or higher levels than that seen in other tumour cell lines such as breast (MB-231), prostate (DU-145) and bladder (T24).

The PAK2 protein was found to be overexpressed in all the melanoma cell lines, compared to the neonatal melanocytes (1) (Figure 4-2C). The PAK2 levels were similar to those seen in other cancer cell lines such as breast (MB-231), prostate (DU-145) and bladder (T24). There was an inverse trend (albeit minor) in PAK2 protein expression compared to cell invasiveness in the melanoma cell lines, with the non-invasive SK-MEL-28 cell line having the highest and the three invasive cell lines having lower PAK2 protein levels.

PAK3 is readily detectable in cells of the central nervous system however, is rarely found in other cells, normal or tumourous (Burbelo *et al.*, 1999). Therefore, unsurprisingly, PAK3 protein expression levels in all melanoma cell lines and neonatal melanocytes (1) were undetectable (Figure 4-2D). This suggests that PAK3 is not involved in melanoma cell invasiveness, and is not critical for the pathways that promote melanoma. Likewise, no detectable PAK3 protein levels were found in MB-231 (breast), DU-145 (prostate) and T24 (bladder) tumour cell lines. As expected, high levels of PAK3 were observed in the OPCs, which was used as a positive control.

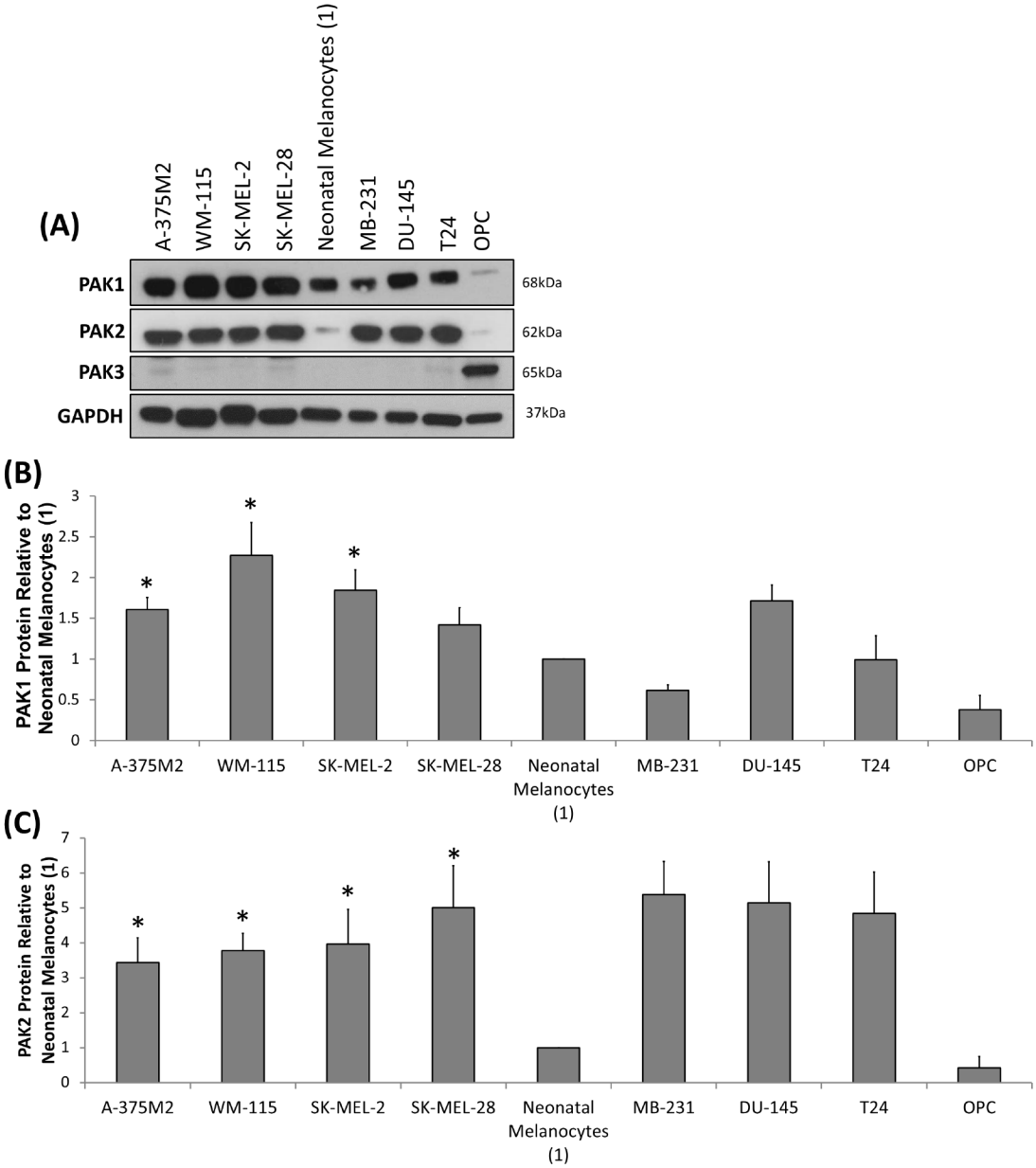

Figure 4-2: Group I PAK protein expression in melanoma cell lines.
(A) Western blot of PAK1, PAK2 and PAK3 expression in melanoma cell lines, neonatal melanocytes (1) and representative tumour cell lines**.** (B-C) Analysis of western blot data via densitometry showing PAK1 (B) and PAK2 (C) protein expression relative to neonatal melanocytes (1). PAK3 protein expression was undetectable and therefore densitometry was not performed for this isoform. Significance was calculated for melanoma cell lines compared to neonatal melanocytes (1). Data are the mean values ± S.E.M., over 3 independent experiments; *= $P < 0.05$. Densitometric data were normalized to GAPDH, which was used as a loading control.

4.2.1.2 Group II PAKs - PAK4 is Overexpressed in Melanoma Cell Lines

All the melanoma cell lines showed a significant increase in PAK4 protein levels compared to the neonatal melanocytes (1) (Figure 4-3). However, there was no correlation with invasive potential as measured here. Furthermore, similar PAK4 protein levels were observed in the different tumour cell lines.

The PAK5 and PAK6 protein levels were undetectable in the neonatal melanocytes (1) and many of the melanoma cell lines (Figure 4-3). Likewise, levels of both proteins were predominantly too low to be quantified in the breast, prostate and bladder tumour cell lines, as well as in OPCs.

Of the group I PAKs, the protein levels of PAK1 and PAK2 (to a lesser extent) correlated with cell invasiveness as characterised in chapter 3 (Table 4-1). In group II, only PAK4 was overexpressed in melanoma cell lines. No correlation was apparent between PAK4 expression and invasive potential, however, there was a robust overexpression of this protein in melanoma cell lines compared to neonatal melanocytes (1). Therefore, PAK4 is clearly important in melanoma, but the extent to which this isoform drives invasion is unclear. Given their prevalence in melanoma cell lines, PAK1 and PAK4 (representing group I and group II PAKs, respectively) were selected for further investigation in patient derived cell strains.

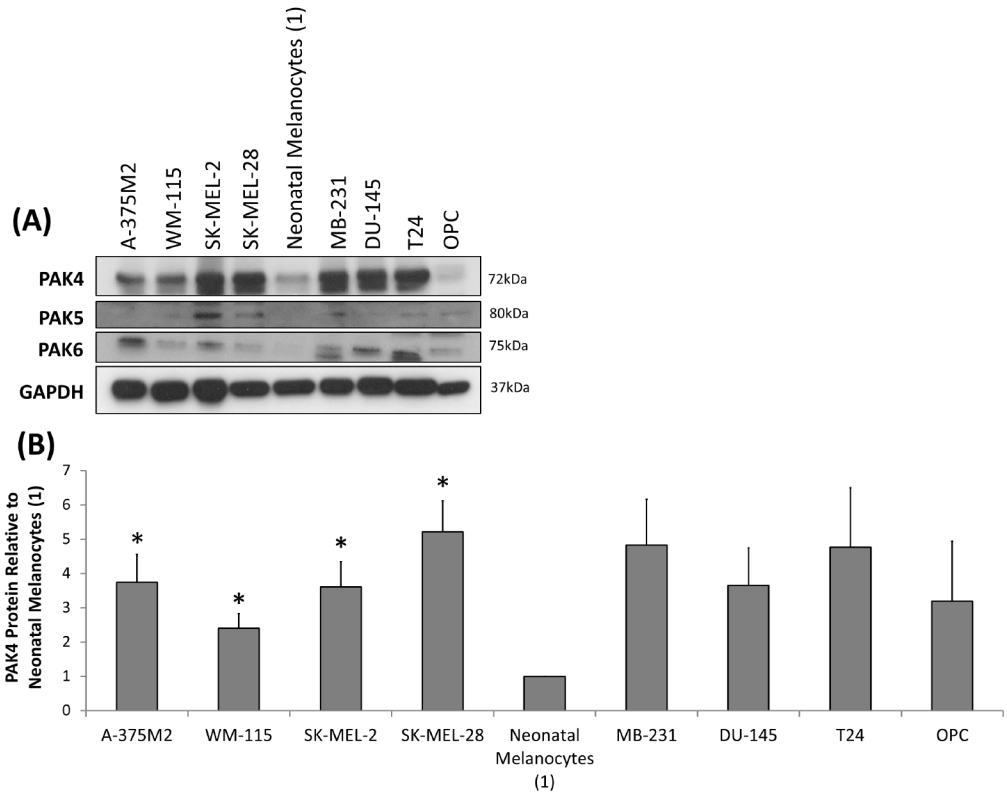

Figure 4-3: Group II PAK protein expression in melanoma cell lines.
(A) Western blot of PAK4, PAK5 and PAK6 expression in melanoma cell lines, neonatal melanocytes (1) and representative tumour cell lines**.** (B) Analysis of western blot data via densitometry showing PAK4 protein expression relative to neonatal melanocytes (1). PAK5 and PAK6 protein expression was unquantifiable and therefore densitometry was not performed for these isoforms. Significance was calculated for melanoma cell lines compared to neonatal melanocytes (1). Data are the mean values ± S.E.M., over 3 independent experiments; *= $P < 0.05$. Densitometric data were normalized to GAPDH, which was used as a loading control.

Cell Line	Invasive phenotype	Invadopodia Invasion	3D Spheroid Invasion (number of invading cells)		Group I PAKs			Group II PAKs		
			Total	>100µm from the spheroid	PAK1	PAK2	PAK3	PAK4	PAK5	PAK6
WM-115	Yes	+++	+++	+++	++	+	§	+	§	§
A-375M2	Yes	++	++	++	+	+	§	++	§	§
SK-MEL-2	Yes	+	+	ns	+	+	§	++	§	§
SK-MEL-28	No	ns	+	ns	ns	++	§	+++	§	§
Neonatal Melanocytes (1)	¥	¥	¥	¥	¥	¥	§	¥	§	§

Table 4-1: Collation of the trends of invasiveness and the PAK expression of melanoma cell lines.
The trend in invasion and PAK expression is depicted by the number of + symbols (+ = lowest, +++ = highest). The number of + symbols indicates the trend in invasiveness and PAK expression and may not necessarily indicate significant differences in invasion and PAK expression to other cell lines with the + symbol. ¥ indicates the control cells to which significance was calculated: ns= not significant ($P > 0.05$). § = unquantifiable protein expression.

4.2.2 PAK1 and PAK4 are Overexpressed in Invasive Patient Derived Cell Strains

PAK1 and PAK4 protein expression were measured in the patient derived cell strains and compared to neonatal melanocytes (1) (Figure 4-4). In addition, A-375M2 and WM-115 were used as melanoma cell line representatives (being the two most invasive in this group) such that the protein levels in the patient derived cell strains could be compared to that of the melanoma cell lines.

PAK1 was found to be overexpressed in three (M586, M460 and M35) patient derived cell strains, compared to neonatal melanocytes (1) (Figure 4-4B) and, interestingly, these were the only strains that produced significant numbers of cells with invadopodia (Section 3.2.2.3 and Table 4-2). Those patient derived cell strains in which PAK1 was over expressed showed similar levels of this protein to that seen in the melanoma cell lines A-375M2 and WM-115. Furthermore M133, the non-invasive patient derived cell strain, had significantly lower PAK protein expression compared to neonatal melanocytes (1). Therefore, these data show a clear correlation between PAK1 and melanoma cell invasiveness in cells derived from patients.

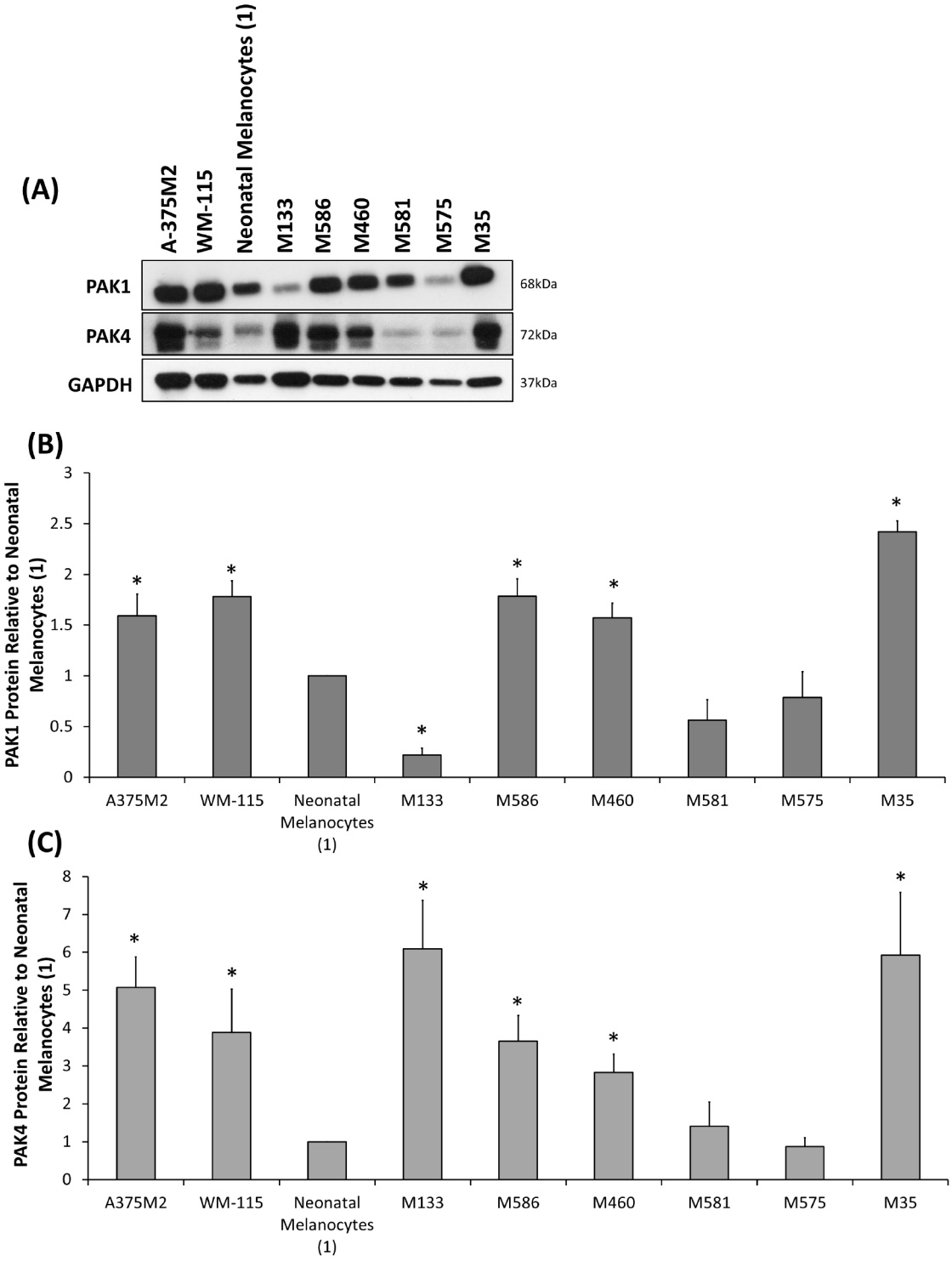

Figure 4-4: PAK1 and PAK4 protein expression in patient derived cell strains.

(A) Western blot of PAK1 and PAK4 protein expression in patient derived cell strains, neonatal melanocytes (1) and representative melanoma cell lines (A-375M2 and WM-115)**.** (B-C) Analysis of western blot data via densitometry showing PAK1 (B) and PAK4 (C) protein expression relative to neonatal melanocytes (1). Significance was calculated for patient derived cell strains and melanoma cell lines compared to neonatal melanocytes (1). Data are the mean values ± S.E.M., over 3 independent experiments; *= $P < 0.05$. Densitometric data were normalized to GAPDH, which was used as a loading control.

PAK4 protein was overexpressed in four (M133, M586, M460 and M35) patient derived cell strains when compared to the neonatal melanocytes (1) (Figure 4-4C), with protein levels in these cell strains being similar to that seen in the melanoma cell lines A-375M2 and WM-115. M586, M460 and M35 are classed as invasive cell strains (Section 3.2.2.3 and Table 4-2), and all showed elevated levels of PAK1 and PAK4. In contrast, the M133 non-invasive patient derived cell strain, had significantly lower levels of PAK1 and elevated levels of PAK4.

Cell Strain	Invasive phenotype	Invadopodia Invasion	3D Spheroid Invasion (number of invading cells)		PAK1	PAK4
			Total	>100µm from the spheroid		
M35	Yes	+++	Ω	Ω	++	++
M460	Yes	++	++	+	+	+
M586	Yes	+	++	+	+	+
M575	Yes	ns	+++	++	ns	ns
M581	Yes	ns	++	+	ns	ns
M133	No	ns	+	ns	-	++
Neonatal Melanocytes (1)	¥	¥	¥	¥	¥	¥

Table 4-2: Collation of the patient derived cell strains and neonatal melanocytes (1) invasive phenotypes and PAK1 and PAK4 protein expression.
The trend in invasion and PAK expression is depicted by the number of + symbols (+ = lowest, +++ = highest). The number of + symbols indicates the trend in invasiveness and PAK expression and may not necessarily indicate significant differences in invasion and PAK expression to other cell lines with the + symbol. ¥ indicates the control cells to which significance was calculated: ns= not significant ($P > 0.05$). The Ω symbol shows the assay was not performed for these cells.

4.2.3 siRNA Oligonucleotides can Transiently Reduce PAK1 and PAK4 Expression in A-375M2 and WM-115 Melanoma Cell Lines

Our data suggests that PAK1 may be involved in melanoma invasiveness, with the picture being less clear for PAK4. Therefore, to investigate the involvement (or lack thereof) of these proteins in melanoma invasiveness, our established invasion assays were performed with cells that had transiently reduced expression of PAK1 and PAK4. As well as the reduction of PAK1 and PAK4 individually, double knockdown experiments were also performed to simultaneously reduce the levels of both proteins in the same cell. Of the melanoma cell lines investigated in this study,

WM-115 and A-375M2 had the most consistent invasive phenotype in both the 2D invadopodia assay and the 3D spheroid assay (Table 4-1) and were the cell lines chosen for the transient depletion of PAK1 and PAK4 expression and subsequent invasion studies.

In WM-115 cells, PAK1 and PAK4 protein expression was significantly reduced from day four when targeted siRNA oligonucleotides were used compared to wildtype and control siRNA cells (Figure 4-5). The depletion of PAK1 and PAK4 expression was still present at day seven, with >50% reduction for all the oligonucleotides compared to the wildtype and control siRNA cells. The double knockdown of PAK1 and PAK4 also showed a protein depletion of >70% at four and seven days after siRNA oligonucleotide transfection, compared to wildtype and siRNA control cells. The sustained depletion of PAK1 and PAK4 proteins enabled these cells to be used in the 3D spheroid invasion assay.

In A-375M2 cells, reduced PAK1 and PAK4 expression was achieved from day four post siRNA oligonucleotide transfection and was sustained until day seven for the majority of the oligonucleotides (Figure 4-6). The double depletion of PAK1 and PAK4 also showed a protein reduction of >40% at four and seven days after siRNA oligonucleotide transfection, compared to wildtype and siRNA control cells.

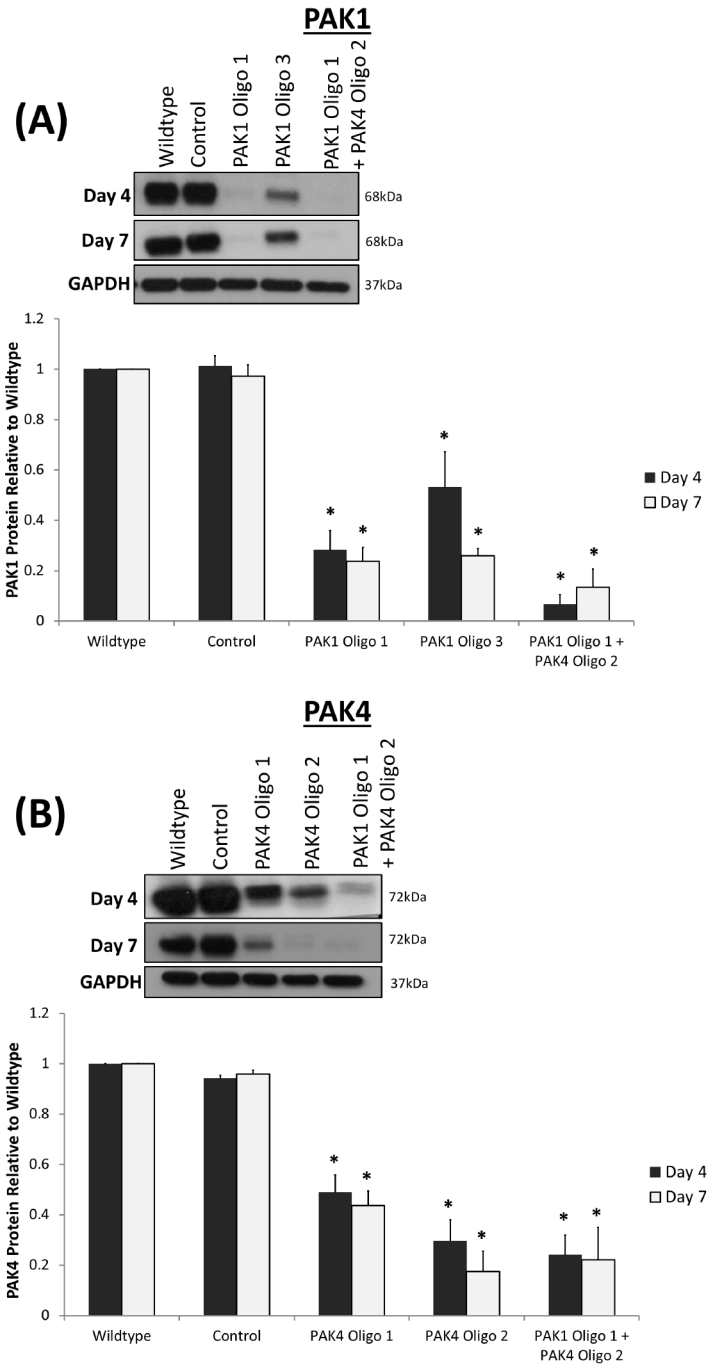

Figure 4-5: Transient reduction of PAK1 and PAK4 expression in the WM-115 cell line.
Cells plated at a concentration of $2x10^4$ in a 6 well plate were transiently depleted using siRNA oligonucleotides and HiPerfect transfection reagent (2 oligonucleotides for each protein). A double knockdown was performed using PAK1 Oligo 1 and PAK4 Oligo 2 oligonucleotides. Control cells were transfected with a control siRNA non targeting oligonucleotide. The reduction in protein expression was quantified 4 and 7 days after transfection using western blotting and densitometry. The reduction in (A) PAK1 and (B) PAK4 protein expression in WM-115 cells. Significance was calculated for protein depleted cell lines compared to wildtype and control siRNA transfected cells. Data are the mean values ± S.E.M., over 3 independent experiments; *= $P < 0.05$. Densitometric data were normalized to GAPDH, which was used as a loading control.

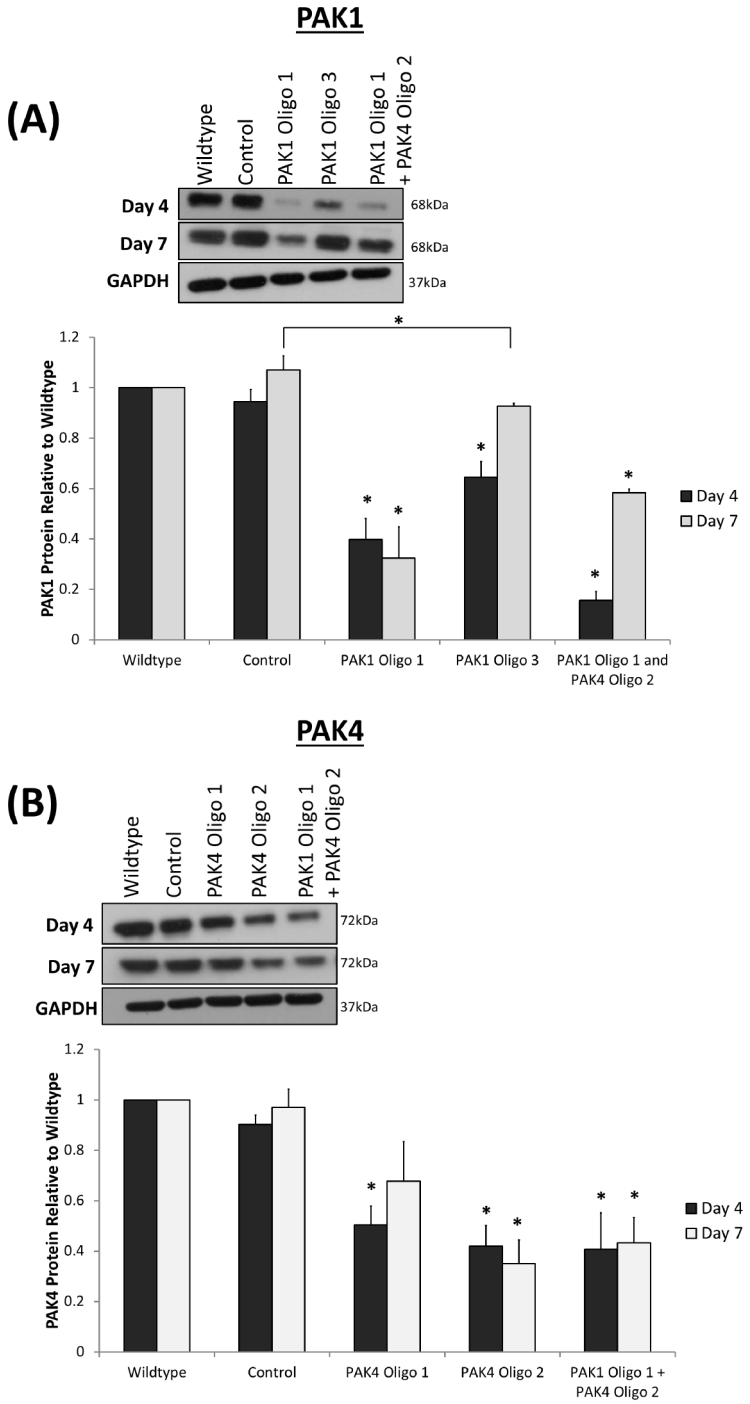

Figure 4-6: Transient reduction of PAK1 and PAK4 expression in the A-375M2 cell line.
Cells plated at a concentration of $2x10^4$ in a 6 well plate were transiently depleted using siRNA oligonucleotides and HiPerfect transfection reagent (2 oligonucleotides for each protein). A double knockdown was performed using PAK1 Oligo 1 and PAK4 Oligo 2 oligonucleotides. Control cells were transfected with a control siRNA non targeting oligonucleotide. The reduction in protein expression was quantified 4 and 7 days after transfection using western blotting and densitometry. The reduction in (A) PAK1 and (B) PAK4 protein expression in A-375M2 cells. Significance was calculated for protein depleted cell lines compared to wildtype and control siRNA transfected cells. Data are the mean values ± S.E.M., over 3 independent experiments; *= $P < 0.05$. Densitometric data were normalized to GAPDH, which was used as a loading control.

4.2.4 PAK1 and PAK4 Depletion Reduces Invadopodia Formation and Degradation

PAK1 and PAK4 were overexpressed in melanoma cell lines and patient derived cell strains that were able to produce invadopodia (Table 4-1 and Table 4-2). To investigate this further, the invadopodia assay was performed using PAK1 and PAK4 depleted cells (Figure 4-7 and Figure 4-8).

WM-115 and A-375M2 cells with reduced PAK1 expression, had a significant decrease in the percentage of cells with invadopodia, compared to control and wildtype cells (Figure 4-9A). Additionally, the cells that produced invadopodia, had a reduction in the area of degradation per invadopodia producing cell compared to wildtype and control invadopodia producing cells (Figure 4-9B). A similar phenotype was observed when PAK4 expression was diminished in WM-115 and A-375M2 cells, with a reduction in the percentage of cells with invadopodia and a reduction in the degradation area per invadopodia producing cell compared to wildtype and control cells. These data indicate that depleting the expression of PAK1 and PAK4 reduces the cell invasiveness not only by decreasing the number of cells with invadopodia but also by reducing the ability of the few invadopodia that do form, to degrade gelatin.

WM-115 and A-375M2 cells in which the expression of PAK1 and PAK4 were simultaneously reduced showed a decrease in the percentage of cells with invadopodia and the area of invadopodia induced degradation compared to wildtype and control cells. However, this was not significantly different to that observed when PAK1 and PAK4 expression was diminished individually.

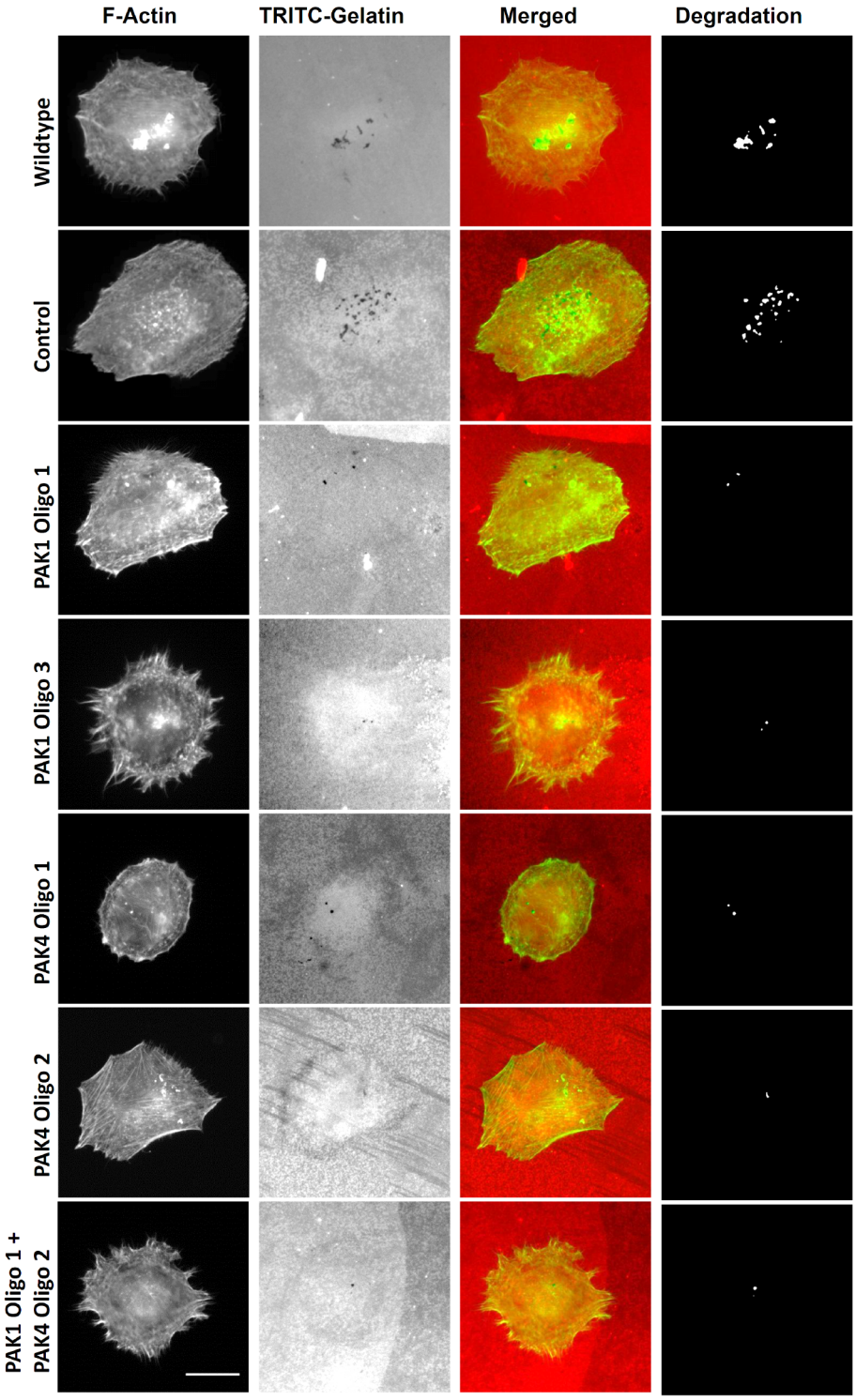

Figure 4-7: Representative invadopodia assay images of WM-115 cells in which PAK1 and PAK4 proteins are knocked down (individually and simultaneously).

Four days after siRNA oligonucleotide transfection the cells were seeded on rhodamine conjugated gelatin for 3 hrs and stained for F-actin. Only actin rich dots that corresponded with gelatin degraded dots were counted as invadopodia. The degradation was measured using ImageJ software. Scale bars = 10µm. Control = cells transfected with non-specific siRNA.

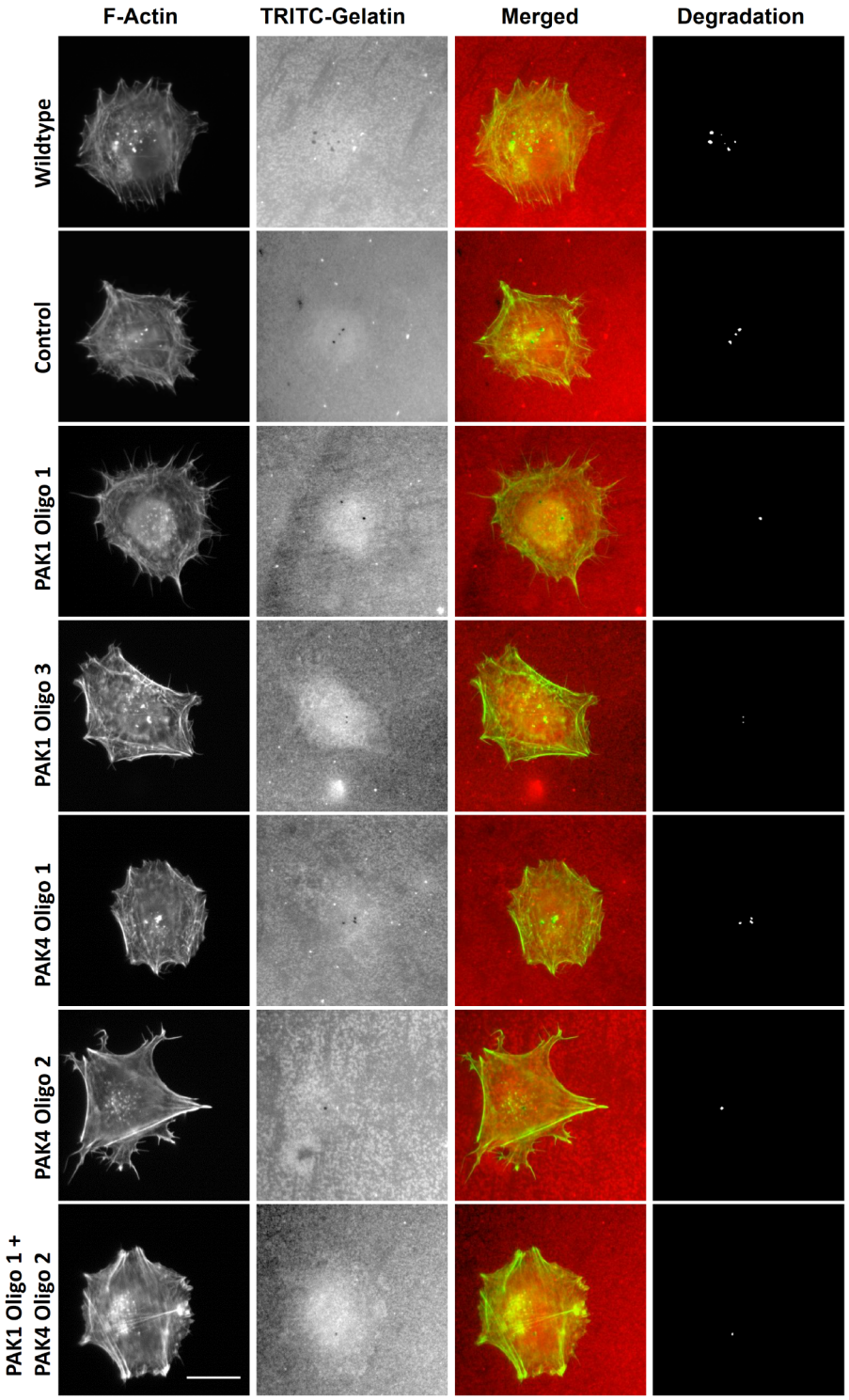

Figure 4-8: Representative invadopodia assay images of A-375M2 in which PAK1 and PAK4 proteins are depleted (individually and simultaneously).

Four days after siRNA oligonucleotide transfection the cells were seeded on rhodamine conjugated gelatin for 3 hrs and stained for F-actin. Only actin rich dots that corresponded with gelatin degraded dots were counted as invadopodia. The degradation was measured using ImageJ software. Scale bars = 10µm. Control = cells transfected with non-specific siRNA.

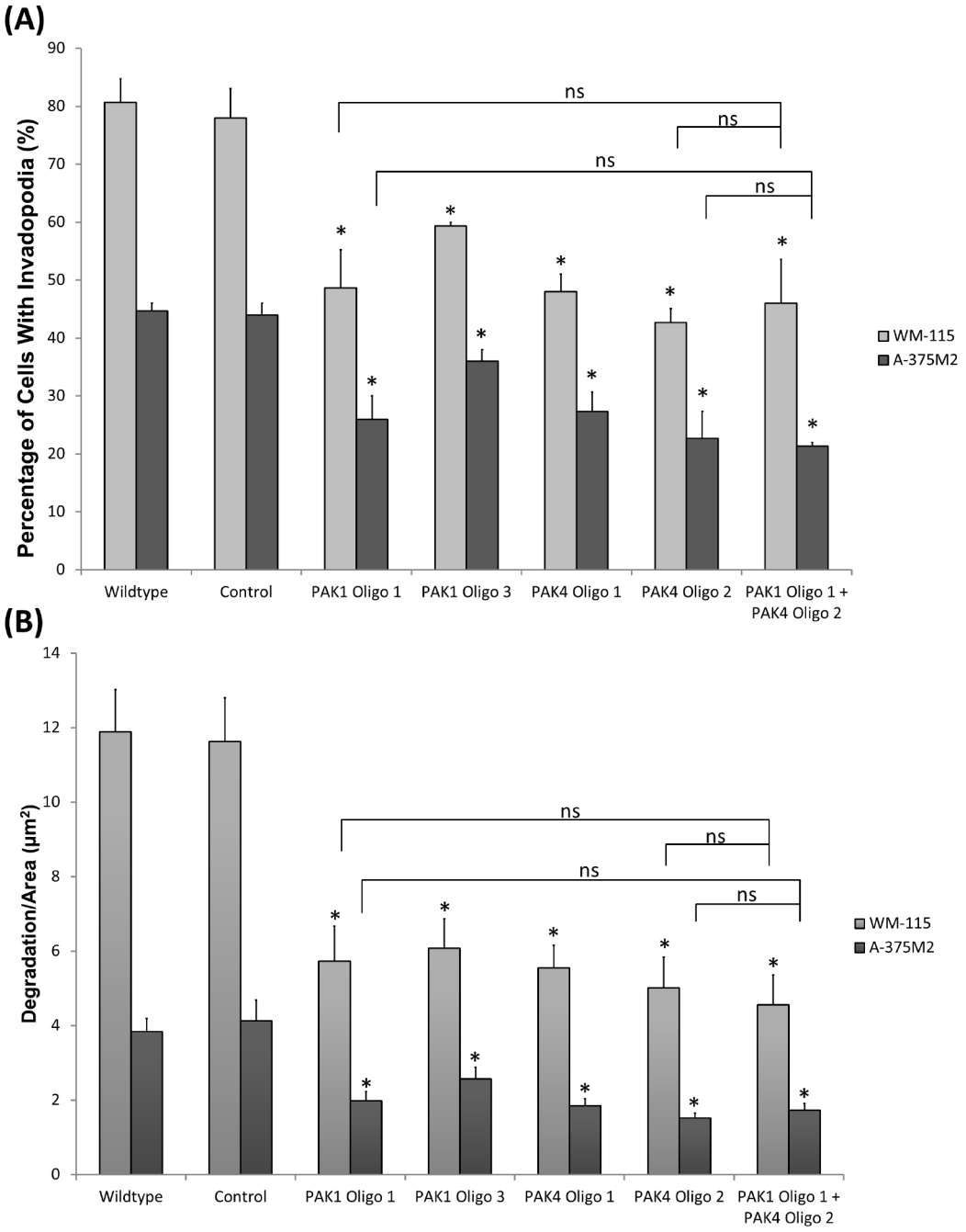

Figure 4-9: Invadopodia assay with WM-115 and A-375M2 cells in which PAK1 and PAK4 expression was depleted (individually and simultaneously).

(A) The percentage of cells with invadopodia. Significance was calculated to wildtype and control cells. The double knockdown significance was also calculated to the corresponding single siRNA knockdown oligonucleotides. Data are mean values ± S.E.M. of 150 cells, over 3 independent experiments; * = $P < 0.05$. (B) The area of degradation from invadopodia per cell. Significance was calculated to wildtype and control cells. The double knockdown significance was also calculated to the corresponding single siRNA knockdown oligonucleotides. Data are mean values ± S.E.M. of 90 invadopodia producing cells, over 3 independent experiments; * = $P < 0.05$. ns = not significant. Control = cells transfected with non-specific siRNA.

4.2.5 PAK1 and PAK4 Depletion Reduces 3D Melanoma Invasion

The depletion of PAK1 and PAK4 protein expression revealed a reduction in invadopodia formation (Section 4.2.4). To expand the study the cells were subsequently tested in the spheroid assay (Figure 4-10 and Figure 4-11). As protein recovery was observed with some of the oligonucleotides in A-375M2 cells at day seven, the length of the assay (originally eight days), was reduced to seven days in subsequent experiments (one day for the transfection of the siRNA oligonucleotides, three days in methylcellulose and three days in the collagen I matrix) to ensure that most of the assay was performed in the presence of protein knockdown.

The depletion of PAK1 expression in WM-115 and A-375M2 cells reduced the total number of invading cells and the number that invaded further than 100µm from the spheroid, compared to wildtype and control cells. Likewise, when PAK4 expression was depleted in WM-115 and A-375M2 cells a reduction in the total number of cells as well as the number of cells invading further than 100µm was observed, compared to wildtype and control cells. These data show that decreasing either PAK1 or PAK4 protein expression reduces the cell invasiveness of melanoma cell lines in a 3D collagen matrix.

Interestingly, the double depletion of PAK1 and PAK4 expression resulted in a further reduction in the number of invading cells and the number of cells that invaded further than 100µm, compared to when PAK1 or PAK4 expression were decreased individually (Figure 4-11). This is in contrast to that which was observed in the invadopodia assay in which there was no additive effect in the double knockdown experiments (Figure 4-9).

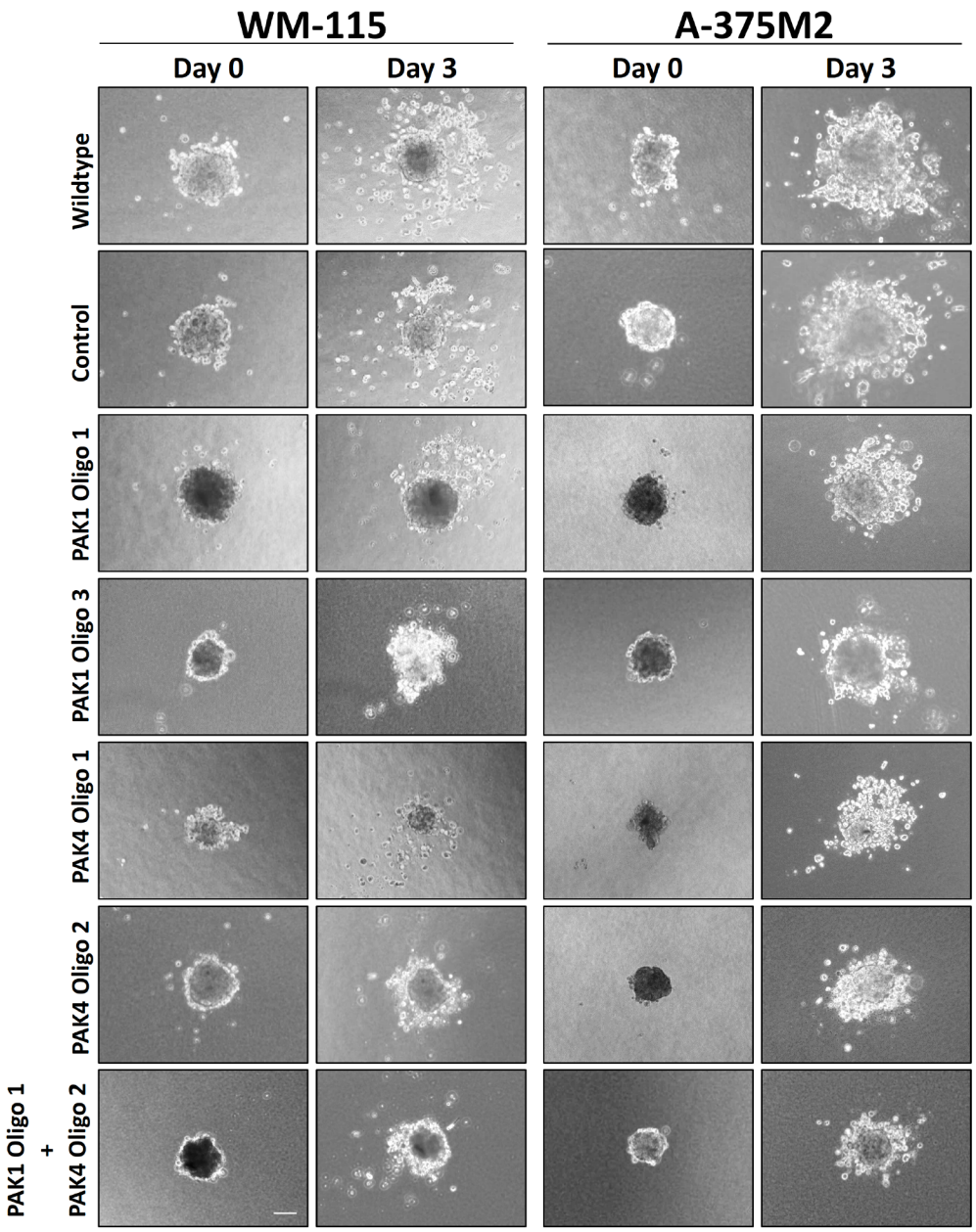

Figure 4-10: Representative images at day 0 and day 3 of the 3D spheroid invasion assay in WM-115 and A-375M2 cells in which PAK1 and PAK4 have been knocked down (individually and simultaneously). Spheroids were produced in media containing methylcellulose for 3 days, then submerged in a collagen I matrix. Phase contrast images were taken at day 0 and day 3. The cell invasion was measured at day 3, commencing when the spheroids were placed in the collagen I matrix. Scale bar = 100µm.

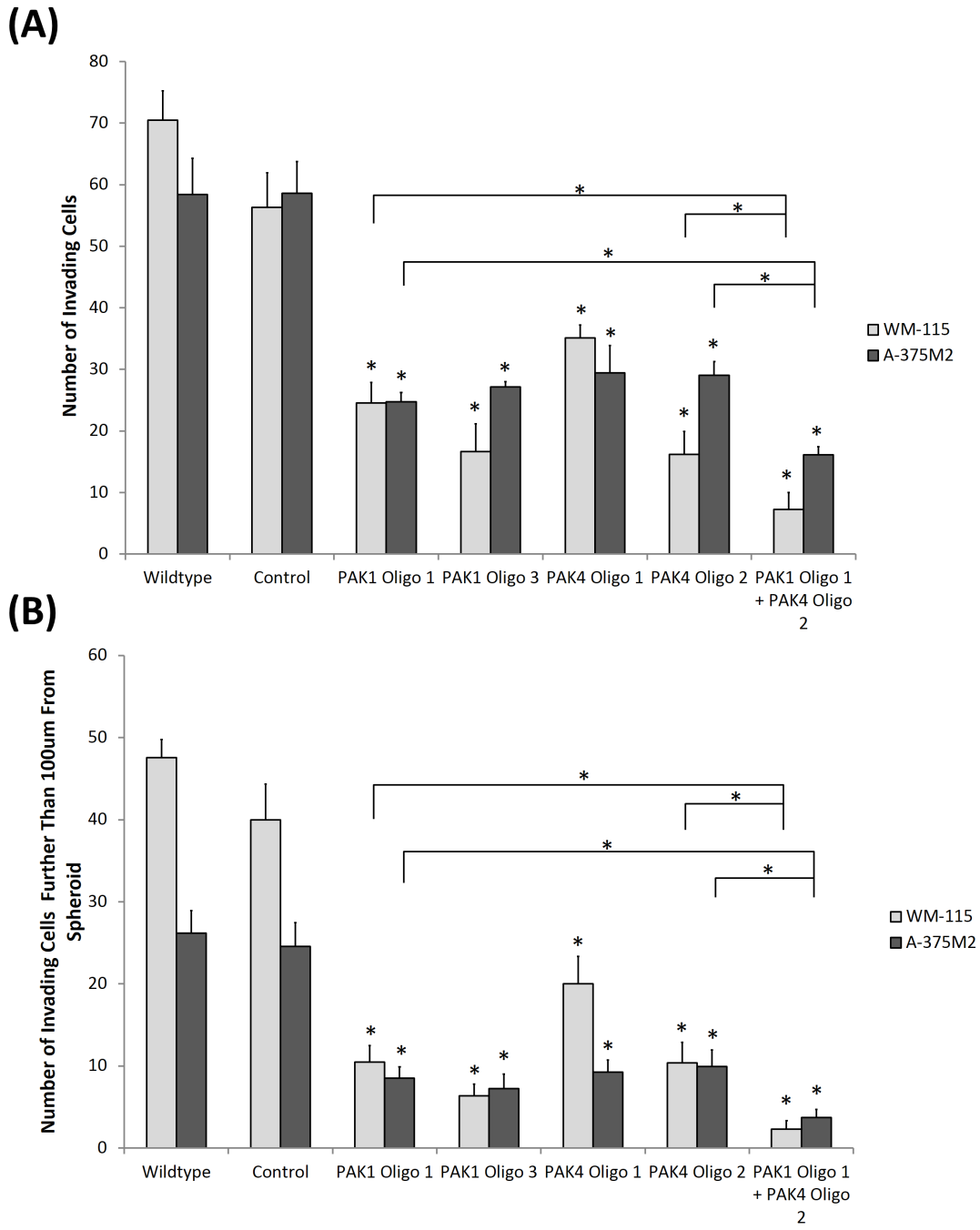

Figure 4-11: 3D spheroid invasion assay of WM-115 and A-375M2 cell lines in which PAK1 and PAK4 have been knocked down (individually and simultaneously).

Spheroid were produced in methylcellulose for 3 days, then submerged in a collagen I matrix. The cell invasion was measured at day 3, commencing when the spheroids were placed in the collagen I matrix. (A) The total number of cell that invaded away from the spheroid mass. Significance was calculated to wildtype and control cells. Data are mean values ± S.E.M., of 9 spheroids over 3 independent experiments; * = $P < 0.05$. Control = cells transfected with non-specific siRNA. (B) The number of cells that invaded further than 100µm from the spheroid mass. Significance was calculated to wildtype and control cells. Data are mean values ± S.E.M., of 9 spheroids over 3 independent experiments; * = $P < 0.05$. Control = cells transfected with non-specific siRNA.

4.2.6 Construction of GFPPAK1r Rescue Vector

To verify that the reduction in invasion observed in PAK1 and PAK4 depleted cells was due to the specific decrease in PAK1 or PAK4 expression, rescue experiments were performed. The GFPPAK4r (PAK4 oligo 2 siRNA resistant) rescue vector was previously created in the Wells lab and therefore available for use.

The GFPPAK1r rescue construct was generated by site directed mutagenesis. The wildtype GFPPAK1 construct was used as template DNA in two PCR reactions to create two DNA fragments (Figure 4-12A). The first fragment incorporated the 5' region of the PAK1 cDNA up to the desired mutated sequence (PAK1r 5' primer set) and the second fragment contained the mutated sequence and the remaining 3' sequence of the PAK1 cDNA (PAK1r 3' primer set). These two fragments were purified, mixed and used as template DNA for another PCR reaction using primers located at the 5' and 3' of the PAK1 cDNA (PAK1 *att*B primer set) (Figure 4-12B). In this PCR reaction the mutated region, located in both PCR fragments, provided a complementary sequence to allow for binding, thus producing the full length PAK1 cDNA (including the mutated sequence), which was then amplified. The full length PAK1r rescue fragment was also flanked by *att*B sequences to allow for the creation of the GFPPAK1r rescue expression vector via Gateway® cloning (Figure 4-12C).

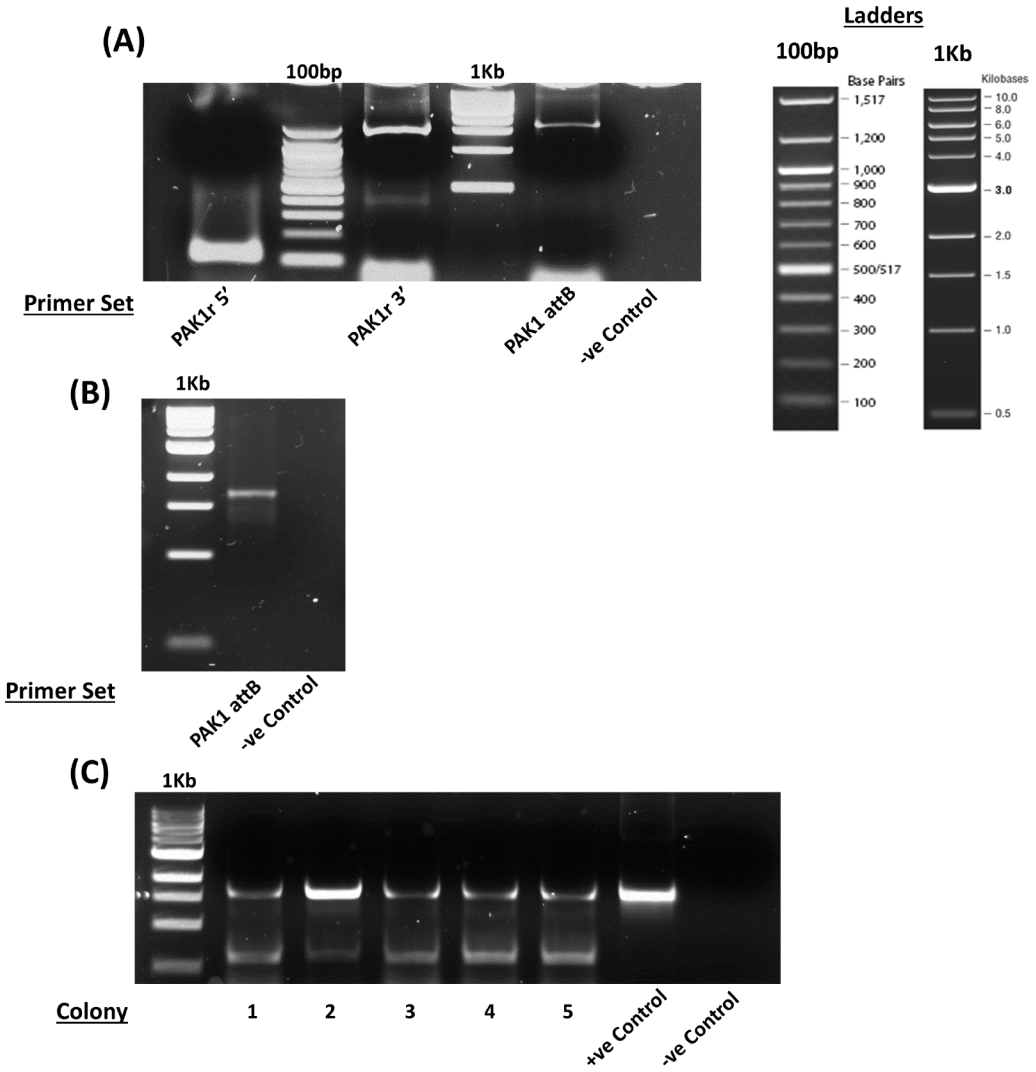

Figure 4-12: Construction of the GFPPAK1r rescue vector.
The GFPPAK1r (PAK1 oligo 1 siRNA resistant) rescue vector was created using traditional molecular cloning techniques and Gateway® cloning. (A) PCR to construct two fragments of PAK1 containing the mutated sequence (all using the GFPPAK1 vector as a DNA template). The primer set PAK1r 5' (PAK1 Fwd and PAK1Rescue Rev) produce the 5' region of the PAK1-mutated site (predicted fragment size = ~100bp). The PAK1r 3' primer set (PAK1Rescue Fwd and PAK1 Rev) produce the 3' region of PAK1 from the mutated sequence (predicted fragment size = ~1.7Kbp). The PAK1 *att*B primer set (PAK1 Fwd and PAK1 Rev) was used as a positive (+ve) control (predicted fragment size = ~1.8Kbp). (B) PCR to create the PAK1r rescue construct using the PAK1 *att*B primer set with the fragments from the PAK1r 5' and PAK1r 3' PCR reaction as template DNA (predicted fragment size = ~1.8Kbp). (C) PCR screen of PAK1r entry clones produced from the Gateway® BP reaction. Primer set PAK1 *att*B was used for all samples (predicted fragment size = ~1.8Kbp). A positive (+ve) control was performed using GFPPAK1 as template DNA. For all experiments a negative (-ve) control was used containing no DNA. 100bp or 1Kbp DNA ladders were used as a size reference (size of fragments are shown in figure).

Following the construction of GFPPAK1r, the GFPPAK1r and GFPPAK4r rescue constructs were transfected in PAK1 or PAK4 depleted WM-115 cells, respectively, and the rescue of protein expression confirmed (Figure 4-13). The rescue construct was 27kDa heavier due to the fused GFP biomarker, therefore allowing it to be readily distinguished from the endogenous protein. The GFPPAK1r and GFPPAK4r rescue constructs were expressed in cells that had reduced PAK1 and PAK4 expression, respectively, validating their use in the rescue experiments.

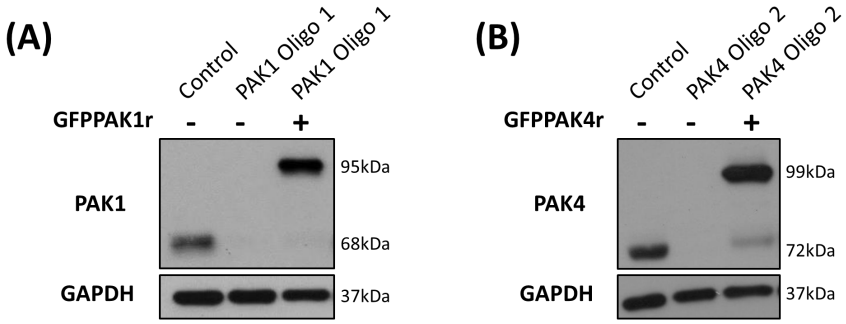

Figure 4-13: Confirmation of siRNA resistant proteins in siRNA depleted WM-115 cells.
Cells were seeded at a concentration of $2x10^4$ in a 6 well plate and transfected with PAK1 oligo 1, PAK4 oligo 2 or a control siRNA oligonucleotide. After three days, cells were transfected with either GFPPAK1r or GFPPAK4r rescue constructs and lysed after 48 hrs. (A) The expression of GFPPAK1r rescue construct in WM-115 cells in which PAK1 expression was reduced. (B) The expression of GFPPAK4r rescue construct in WM-115 cells in which PAK4 was reduced. GAPDH was used as a loading control in all experiments.

4.2.7 GFPPAK1r Rescues Invadopodia Formation and Degradation in WM-115 Cells with Reduced PAK4 Expression

PAK1 knockdown in WM-115 cells reduces both the percentage of cells with invadopodia and the degradation area per invadopodia producing cell (Figure 4-14). The specificity of this PAK1 depletion was validated by the expression of the GFPPAK1r siRNA resistant vector in WM-115 cells with diminished PAK1 expression. The expression of the GFPPAK1r rescue construct in WM-115 cells with depleted PAK1 was able to rescue the invasive phenotype to levels seen in the control cells, both in the percentage of cells with invadopodia and the degradation area. This further validates the role of PAK1 in invadopodia formation in invasive cells.

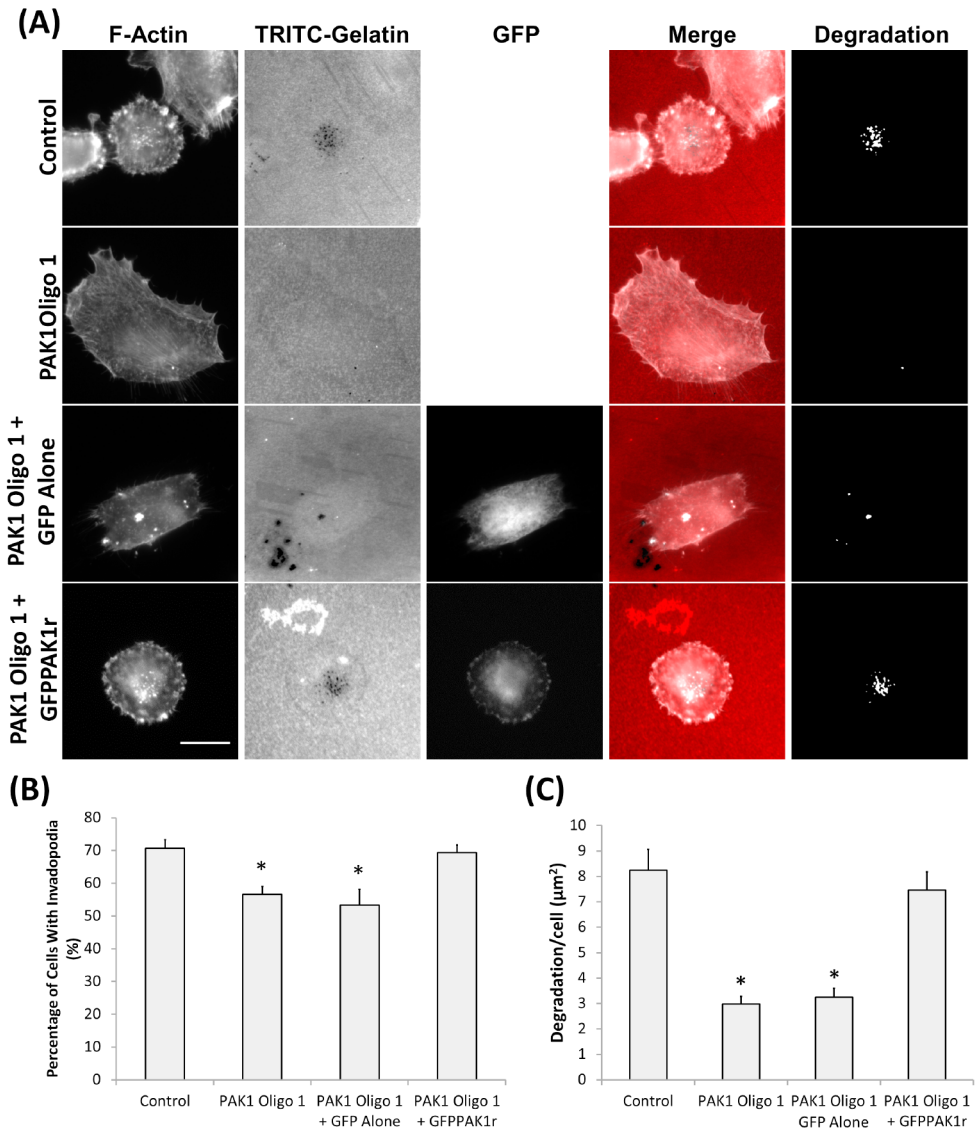

Figure 4-14: Invadopodia assay of PAK1 depleted WM-115 cells expressing GFPPAK1r.
Three days after siRNA oligonucleotide transfection, cells were transfected with DNA expression vectors and incubated for 48hrs. Following this, the cells were seeded on rhodamine conjugated gelatin for 3 hrs and stained for F-actin. Only actin rich dots that corresponded with gelatin degraded dots were counted as invadopodia. The degradation was measured using ImageJ software. (A) Representative invadopodia assay images of WM-115 depleted cells transfected with GFP alone or GFPPAK1r. Scale bars = 10µm. (B) The percentage of cells with invadopodia. Significance was calculated to control siRNA transfected cells. Data are mean values ± S.E.M. of 150 cells, over 3 independent experiments; * = $P < 0.05$. (C) The area of degradation from invadopodia per cell. Significance was calculated to control siRNA transfected cells. Data are mean values ± S.E.M. of 90 invadopodia producing cells, over 3 independent experiments; * = $P < 0.05$. Control = cells transfected with non-specific siRNA.

4.2.8 GFPPAK4r Rescues Invadopodia Formation and Degradation in WM-115 Cells with Reduced PAK4 Expression

The expression of the GFPPAK4r siRNA resistant vector in a PAK4 knockdown background rescued both the percentage of cells with invadopodia and the degradation, to values seen by the control cells (Figure 4-15). This further validates the importance of PAK4 in invadopodia formation and degradation.

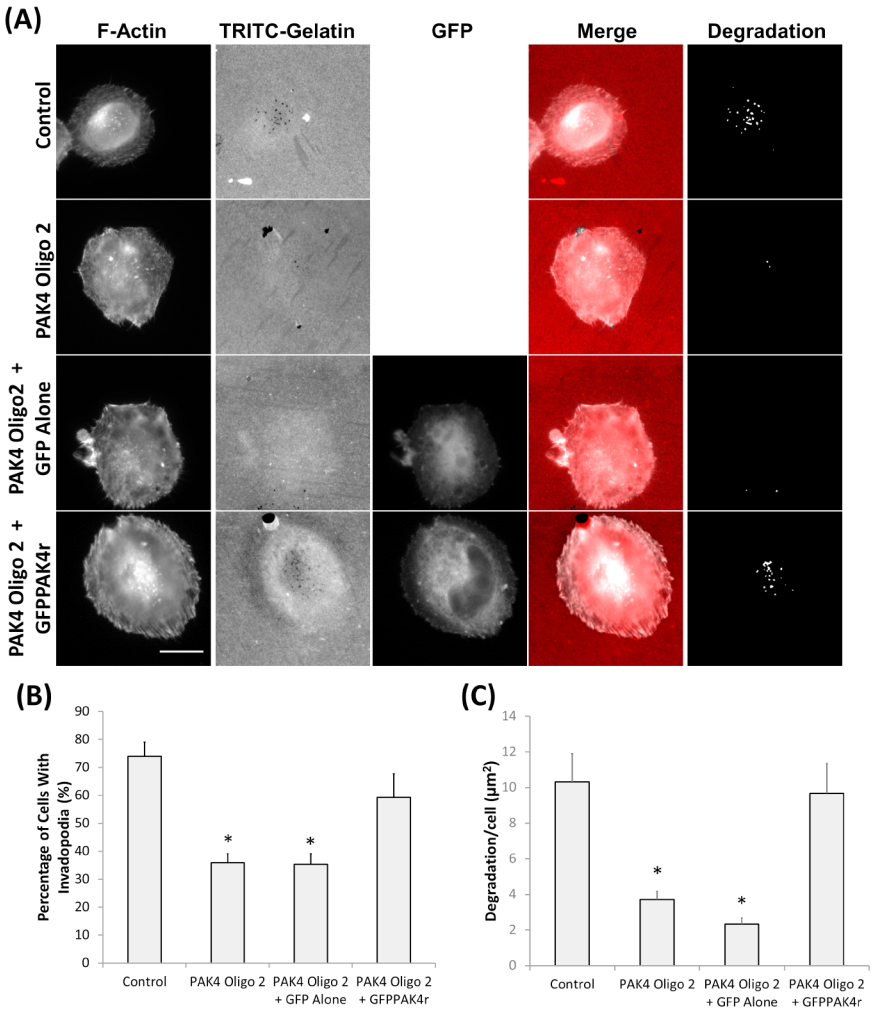

Figure 4-15: Invadopodia assay of PAK4 depleted WM-115 cells expressing GFPPAK4r.
Three days after siRNA oligonucleotide transfection, cells were transfected with DNA expression vectors and incubated for 48hrs. Following this, the cells were seeded on rhodamine conjugated gelatin for 3 hrs and stained for F-actin. Only actin rich dots that corresponded with gelatin degraded dots were counted as invadopodia. The degradation was measured using ImageJ software. (A) Representative invadopodia assay images of WM-115 PAK4 depleted cells transfected with GFP alone or GFPPAK4r. Scale bars = 10µm. (B) The percentage of cells with invadopodia. Significance was calculated to control siRNA transfected cells. Data are mean values ± S.E.M. of 150 cells, over 3 independent experiments; * = $P < 0.05$. (C) The area of degradation from invadopodia per cell. Significance was calculated to control siRNA transfected cells. Data are mean values ± S.E.M. of 90 invadopodia producing cells, over 3 independent experiments; * = $P < 0.05$. Control = cells transfected with non-specific siRNA.

4.2.9 Reduction of PAK1 and PAK4 Expression in an *In Vivo* Zebrafish Yolk Invasion Assay

The knockdown of PAK1 and PAK4 reduced the invasion of WM-115 and A-375M2 cells in 2D and 3D invasion assays (Section 4.2.4 and Section 4.2.5). To complement these *in vitro* assays, invasion was investigated in an *in vivo* zebrafish yolk invasion assay.

4.2.9.1 Stable Reduction of PAK1 and PAK4 Expression in A-375M2 cells

The zebrafish yolk invasion assay requires the injection of a high number of fluorescently labelled knockdown cells into the zebrafish embryos. To create these stable knockdown A-375M2 cell lines a bi-cistronic DNA vector containing an shRNA sequence to reduce either PAK1 or PAK4 expression, and a GFP fluorescence biomarker for cell visualisation in the zebrafish, was used.

The protein expression was reduced with two different shRNA constructs each targeted at either PAK1 or PAK4. An off target shRNA construct, with a non-targeting shRNA sequence, was transfected for use as a control. Both PAK1 and PAK4 constructs resulted in a significant reduction in the expression of the targeted protein compared to wildtype and control shRNA cells (Figure 4-16). These PAK1 and PAK4 stable knockdown A-375M2 cells were then used to investigate the effects of PAK1 and PAK4 expression on invasive capacity *in vivo* using the zebrafish yolk invasion assay.

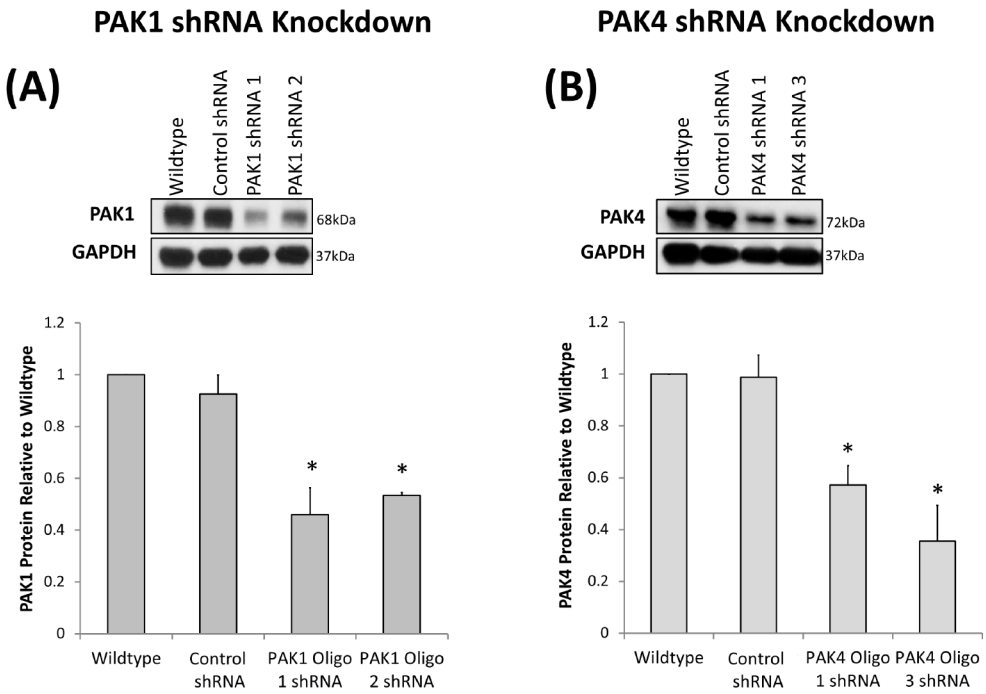

Figure 4-16: Stable Reduction of PAK1 and PAK4 in the A-375M2 cell line.
Stable knockdown A-375M2 cells were created by transfecting cells with shRNA DNA constructs and selecting the cells with depleted protein expression using puromycin antibiotic. Protein depletion was quantified using western blotting and densitometric analysis. (A) PAK1 and (B) PAK4 reduction in A-375M2 cells. Significance was calculated for depleted cell lines compared to wildtype cells. Data are the mean values ± S.E.M., over 3 independent experiments; *= $P < 0.05$. Densitometric data were normalized to GAPDH, which was used as a loading control.

4.2.9.2 PAK1 and PAK4 Depletion Reduces Invasion of A-375M2 cells *In Vivo*

A-375M2 cells stably transfected with the control shRNA construct were able to invade through the yolk and into the embryo where they lodged in the tail and either proliferated or invaded into the surrounding tissue (Figure 4-17). Cell invasion in the head was also seen (Figure 4-17C), but, only embryos with GFP positive cells in the tail were recorded in this assay.

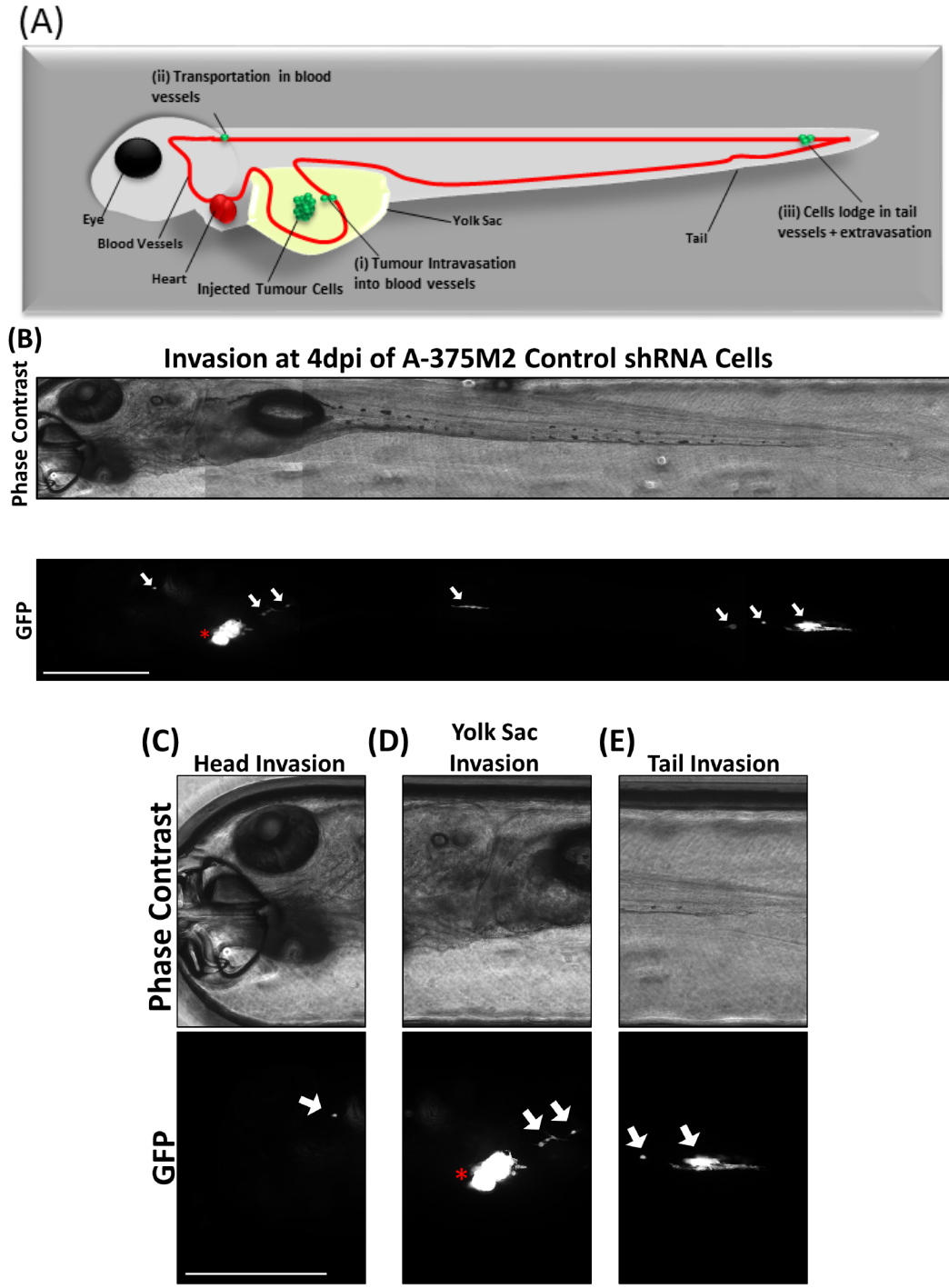

Figure 4-17: Cell invasion in a zebrafish embryo 4 dpi with A-375M2 control shRNA.
(A) Diagram of *in vivo* zebrafish yolk invasion assay. Tumour cells were injected into the yolk sac of 2 dpf zebrafish embryos. Tumour cells invade the yolk and intravasate into blood vessels (i), travel through the blood system (ii) and lodge in the tail vessels where they can grow or extravasate (iii). (B) A representative phase contrast and fluorescent image of a zebrafish (lateral view) 4 dpi with A-375M2 control shRNA cells to show cell invasion. Image is a tiled reconstruction of multiple small images. (C-E) The invasion of cells was evident in several different parts of the embryo including the head (C), within the yolk sac (D) and in the tail (E). Red stars indicate cell mass in yolk sac (original injection site). White arrows indicate invaded cells. Scale bar = 500µm.

When the A-375M2 cells with stably depleted PAK1 expression were injected into the zebrafish yolk sac the percentage of embryos with tail invasions significantly decreased compared to the control (Figure 4-18 and Figure 4-19). A similar reduction was also seen with PAK4 stably depleted A-375M2 cells. Therefore, reducing PAK1 or PAK4 expression can inhibit the invasion of melanoma cells *in vivo*, thus validating the work performed *in vitro* (Section 4.2.4 and Section 4.2.5) and demonstrating the importance of these proteins in cell invasion.

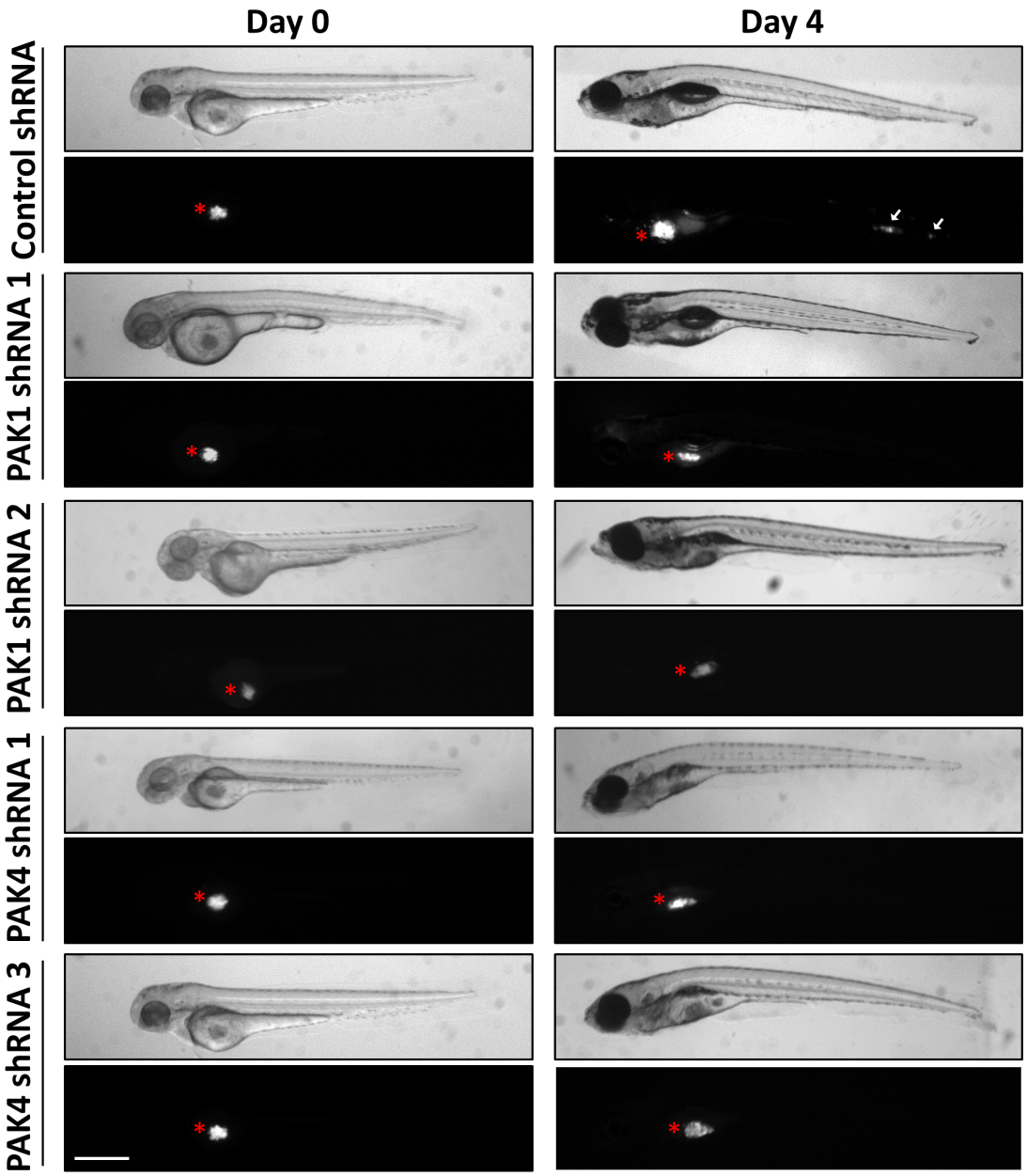

Figure 4-18: Representative phase contrast and fluorescent images of the *In vivo* zebrafish yolk invasion assay.

Phase contrast and fluorescent images of zebrafish embryos (lateral view) at 0 and 4 dpi for embryos injected with A-375M2 control cells (control shRNA), PAK1 depleted (PAK1 shRNA 1 and PAK1 shRNA2) and PAK4 depleted (PAK4 shRNA 1 and PAK4 shRNA 3). Red stars indicate cell mass in yolk sac (original injection site). White arrows indicate tail invasion of GFP labelled A-375M2 cells. Scale bar = 500µm.

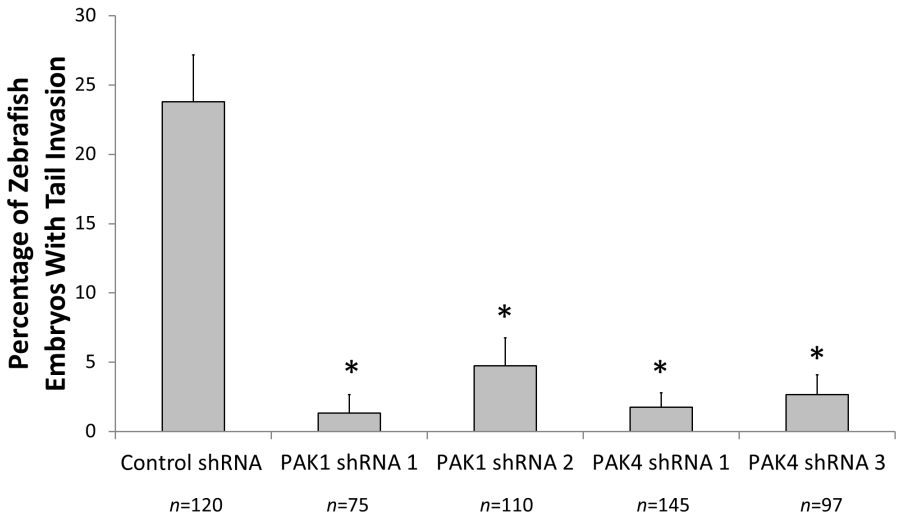

Figure 4-19: *In vivo* zebrafish yolk invasion assay using PAK1 and PAK4 stably depleted A-375M2 cells. 2 dpf zebrafish embryos were injected into the yolk sac with approximately 500 cells and incubated at 35^{o}C for 4 days. The percentage of embryos with A-375M2 cell tail invasion was measured. Significance was calculated for knockdown cell lines compared to the control shRNA cells. Data are the mean values ± S.E.M., over at least 3 independent experiments; *n* = total number of embryos, *= P < 0.05.

4.3 Discussion

The PAK family of kinases are the major downstream effectors of Rac1 and Cdc42. PAK isoforms (of which there are 6) have been shown to be overexpressed in many human tumours such as breast, colon, prostate and ovarian cancer (Radu *et al.*, 2014). This chapter investigated the expression of the PAK isoforms in a panel of melanoma cell lines and patient derived cell strains (PAK1 and PAK4) compared to melanocyte controls - the aim being to identify any correlating trends between PAK protein expression and the invasive capacity, as characterised in chapter 3. Following this, the knockdown of PAK1 and PAK4 expression was used as a tool to verify their involvement in melanoma cell invasiveness *in vitro* and *in vivo*.

There was a direct correlation between the level of PAK1 expression and the level of invasiveness defined in chapter 3. These findings complement previous studies that have linked PAK1 overexpression with increased invasiveness of uveal melanoma, a cancer of melanocytes located in the eye (Pavey *et al.*, 2006). This suggests a global melanoma requirement for PAK1 irrespective of the melanocyte origin, be it cutaneous or uveal. Furthermore, melanoma may not be the only form of skin cancer in which PAK1 overexpression occurs. Indeed, PAK1 was also found to be overexpressed in malignant SCC mouse tissue but not in benign papilloma, in a two stage chemically induced tumourigenesis (7,12-dimethylbenz(a)anthracene (DMBA) and 12-O-tetradecanoylphor- bol-13-acetate (TPA)) mouse model (Zanivan *et al.*, 2013).

PAK4 was robustly overexpressed in the melanoma cell lines including the invasive cells. An increase in PAK4 mRNA in SK-MEL-2 and SK-MEL-28 cells, compared to melanocytes, suggest that the upregulation may also be occurring at the transcriptional level (Callow *et al.*, 2002). Furthermore, PAK4 is important for the carcinogenesis of SCC, which shows both an increase in phosphorylation at Ser^{181}, in a two stage chemically induced tumourigenesis (DMBA and TPA) mouse model, and an importance in protein expression for SCC cell line invasion in both a 3D collagen invasion assay (A431 cell line) and a 3D organotypic invasion model (SCC9 cell line) (Zanivan *et al.*, 2013). This requirement of PAK4 in the invasion of other skin cancers validates the choice to investigate PAK4 in melanoma invasion despite overexpression being evident in the non-invasive SK-MEL-28 cells. In tumourigenesis and progression, PAK4 can play a role in multiple cellular processes including cell cycle progression (Siu *et al.*, 2010a; Zhang *et al.*, 2011; Tabusa *et al.*, 2013) and inhibition of apoptosis (Gnesutta and Minden, 2003; Kesanakurti *et al.*, 2012). Therefore, this protein may enhance other pathways distinct from invasion which may mask any correlating trends between PAK4 protein expression and cellular invasion.

To complement the results found in melanoma cell lines, PAK1 and PAK4 expression was measured in the patient derived cell strains. Both proteins were overexpressed in a variety of cell strains, emphasising that PAK1 and PAK4 overexpression is not only observed in melanoma cell lines, but also in cells isolated from patient tissue. Furthermore, the invasive strains that were able to produce invadopodia (M586, M460 and M35) showed overexpression of PAK1 and PAK4. Interestingly, the M35 strain showed the highest expression of both PAK1 and PAK4, which correlated with both the high invasion of this strain as characterised in chapter 3 and also with the clinical data which revealed that this patient progressed to stage IV metastatic melanoma and died 8 months from when the tissue was taken. Similarly, the M460 cell strain (derived from primary tissue from a patient with stage IIIA progressive metastatic melanoma) had a PAK1 and PAK4 expression profile that matched that of the invasive phenotype.

Interestingly, the non-invasive patient derived cell strain (M133) did, in fact, overexpress PAK4. However, PAK1 levels were significantly lower than that seen for neonatal melanocytes (1). This finding phenocopies that seen for the non-invasive SK-MEL-28 cell line that overexpressed PAK4 but lacked a significant increase in PAK1 expression compared to the neonatal melanocytes (1). The inverse combination of high PAK1 with low PAK4 was not detected in any of the melanoma cell lines panel or the patient derived cell strains. This suggests that both PAK1 and PAK4 are important in melanoma.

However, a correlation between PAK1 and PAK4 overexpression and invasion was not evident in all patient derived cell strains, with the M581 and M575 strains showing no correlation. Therefore, the data obtained from the patient derived cell strains show that overexpression of both PAK1 and PAK4 is not deleterious to cell invasion, complementing that of the melanoma cell lines. However, a larger data set would be required to accurately validate any link between these proteins and the invasion potential or clinical data of patient derived cells.

Our findings of PAK1 overexpression in invasive melanoma cells and in the most invasive patient derived cell strain complement published data for other cancer cell types and a study conducted using uveal melanoma cell lines (Pavey *et al.*, 2006; Kamai *et al.*, 2010; Siu *et al.*, 2010b). However, one contradictory study, using primary melanoma tissue and cell lines found that PAK1 overexpression was restricted to a wildtype BRAF subset and was not present in BRAF mutated melanomas (Ong *et al.*, 2013). However, the melanoma cell lines used in this current study contained the BRAF mutation (A-375M2, WM-115 and SK-MEL-28) and also overexpressed PAK1. Of the patient derived cell strains, the BRAF mutational status was only available for M35 (mutated), M460 (Wildtype) and M581 (wildtype). Once again in contrast to the data presented

in Ong *et al* M35 showed PAK1 overexpression, while M581 did not. Interestingly, if only the primary tissue is taken into account in this study, the data complements that seen by Ong and colleagues, with M460 (wildtype BRAF) overexpressing PAK1 and SK-MEL28 (mutated BRAF) lacking PAK1 overexpression. Therefore, increased levels of PAK1 may be restricted to wildtype BRAF in primary melanoma. However, our study has shown that this is not the case when investigating metastatic melanoma, where PAK1 overexpression correlates with invasion (rather than BRAF mutational status).

To further elucidate the role that PAK1 and PAK4 play in melanoma invasion these proteins were reduced in the two most invasive melanoma cell lines, WM-115 and A-375M2 and the effect on invasive capacity was subsequently assessed. Depleting PAK1 and PAK4 expression resulted in a reduction in invasion in both the 2D invadopodia assay and the 3D spheroid invasion assay. Reduced expression of PAK1 can inhibit the invasion of colon cancer cell lines (DLD1 and HCT116) in a boyden chamber assay (Huynh *et al.*, 2010). In addition, PAK1 inhibition reduces Matrigel invasion of the T47D breast cancer cell line (Coniglio *et al.*, 2008). Similarly, the depletion of PAK4 expression inhibits the invasion of choriocarcinoma cell lines (JEG3 and JAR cells) (Zhang *et al.*, 2011) and endometrial cancer cell lines (AN3CA and Ishikawa cells) (Lu *et al.*, 2013) in Matrigel transwell invasion assays. These findings show that the overexpression of PAK1 and PAK4 play an important role in invasion in many different tumour types (including melanoma as has been shown in this study). PAK4 is important for the invasion of SCC skin cancer (Zanivan *et al.*, 2013), while PAK1 is overexpressed and plays a role in uveal melanoma invasion as shown in a Matrigel transwell invasion assay (Pavey *et al.*, 2006). Therefore, the data in this study complements previously published studies with other cancer types and suggests that PAK1 and PAK4 are involved in melanoma invasion *in vitro*.

Some evidence has linked PAK1 to the formation of both invadopodia and the invadopodia related protrusion, podosomes. PAK1 and kinase dead PAK1 mutants can induce the formation of podosomes in rat vascular smooth muscle cells and aortic smooth muscle cells, respectively (Webb *et al.*, 2005; Furmaniak-Kazmierczak *et al.*, 2007). Furthermore, PAK1 localises to invadopodia (Moshfegh *et al.*, 2014) and the inhibition of endogenous PAK1 via a PAK1 autoinhibitory domain fragment, can reduce the formation and degradation of invadopodia in A375MM cells demonstrating the importance of PAK1 activity for invasive protrusions (Ayala et al., 2008). One suggested PAK1 pathway in invadopodia formation is via the phosphorylation of cortactin at Ser^{113} (Ayala *et al.*, 2008). In contrast, an alternate study indicates that PAK1 is involved in invadopodia dissolution, with the knockdown of PAK1 increasing matrix degradation

of MTLn3 and MDA-MB-231 cells (Moshfegh *et al.*, 2014). The differences found by this study may be accounted for by a differing method of matrix degradation quantification, with Mosfegh *et al* quantifying the entire field of view, in contrast to the method used in this study of quantifying the degradation under each cell that corresponded with actin puncta. Furthermore, this effect may be cell type specific as another tested cell line, MCF10A, had no increase in matrix degradation when PAK1 was depleted in this system. Therefore, our findings regarding the role of PAK1 in the promotion of invadopodia formation and degradation complements other studies and solidifies the hypothesis that PAK1 is important in invadopodia.

PAK4 localises to podosomes in bone-marrow-derived mouse dendritic cells (Wells and Jones, 2010) and primary human macrophages (Gringel *et al.*, 2006). Moreover, the kinase activity of PAK4 is important in podosome formation as kinase dead and active forms of PAK4 can inhibit and enhance respectively, individual podosome size and number in primary human macrophages (Gringel *et al.*, 2006). However, this is the first comprehensive study to show that PAK4 is involved in invadopodia formation and degradation.

PAK1 and PAK4 double knockdowns were also performed to identify any additive effects that could suggest separate roles/pathways that these PAK isoforms may be involved in. Our findings showed no additive reduction in invadopodia percentage or degradation, suggesting that PAK1 and PAK4 are either: 1) in overlapping pathways, or 2) in different pathways that are equally important for invadopodia formation such that the elimination of one pathway reduces the invadopodia production to the lowest limit. Interestingly, cells were less invasive in the double knockdown 3D spheroid invasion assay compared to single PAK1 and PAK4 depletion, suggesting that PAK1 and PAK4 are involved in different pathways in 3D invasion. Where, these different PAK1 and PAK4 pathways, each contribute to the total invasive capacity through a 3D collagen I matrix. However, this does not indicate that PAK1 and PAK4 are exclusive to these distinct pathways, as these proteins may be involved in multiple 3D invasion signalling pathways. This is not surprising as invasion of cells through a 3D matrix relies on more than just the matrix degradation seen in the invadopodia assay, but also utilises multiple pathways that are involved in cell motility and cell-matrix adhesion amongst others (Friedl and Wolf, 2003). Therefore, to further elucidate the roles of PAK1 and PAK4 in 3D invasion additional assays could be performed with PAK1, PAK4, and PAK1/4 double, knockdown cells, including timelapse microscopy on collagen I to investigate cell movement and cell adhesion assays on collagen I to investigate cell matrix adhesion.

This study not only investigated the role of PAK1 and PAK4 in melanoma cell lines using *in vitro* invasion assays, but in fact, showed that PAK1 and PAK4 are important for invasion in an *in vivo* context as well. This was achieved using the zebrafish yolk invasion assay, in which it was found that zebrafish injected with PAK1 or PAK4 knockdown cells had a significantly reduced tumour cell invasion.

Compared to other studies, the percentage of embryos with tail invasion in this assay was low (~25% for injection with control A-375M2 cells compared to >75% seen in other studies, in which different cell types were injected) (Haldi *et al.*, 2006; Eguiara *et al.*, 2011). This difference could be due to the use of different cell types used in this study.

The zebrafish yolk invasion assay has several advantages over other *in vivo* models that are used to investigate metastasis and invasion, such as the tail vein injection of mice. These advantages include, the production of hundreds of zebrafish embryos from each spawn allowing a high embryo number for injection and quantification, the transparency of the embryos which means that the fluorescently labelled xenografted cells can be easily visualised and the fast zebrafish development which means that the entire experiment can be completed within 2 weeks (Amatruda *et al.*, 2002; Mimeault and Batra, 2013). Furthermore, the injection of the cells into the yolk sac ensures that metastasis into the tail can only occur if the cells invade through the yolk into the surrounding blood vessels or tissue, thus providing a representative model of tumour cell invasion. In fact, the importance of a functional circulatory system in this assay was shown in a recent study in which cells were unable to form tail invasion in *cloche* mutated embryos that lack functional vasculature (Marques *et al.*, 2009).

The most commonly used mouse metastasis model involves the injection of cells into the tail vein and quantification of the number of lung metastases. However, this model is not truly representative of metastasis as the initial stages (invasion away from the primary mass and intravasation) are bypassed and the injected cells lodge in the next capillary bed, in this case the lungs, then simply proliferate (Khanna and Hunter, 2005). Therefore the zebrafish yolk invasion assay offers clear advantages over the mouse tail vein injection. However, there are some caveats that are associated with the zebrafish yolk invasion assay, the main one being that though there is high conservation of genes between fish and humans, little is known about the differences in the microenvironment and how this could influence the human cell invasion and thus translate to human metastasis (Konantz *et al.*, 2012). Despite this, the zebrafish yolk invasion assay provides a good model to investigate the invasive/metastatic capacity of cancer cells *in vivo*.

5 Chapter 5 – PAK1 and PAK4 have Converging and Unique Pathways in Melanoma Cell Invasion

5.1 Introduction

In the previous chapter reductions in the expression of PAK1 and PAK4 delivered the same phenotypes, despite the fact that PAK1 and PAK4 belong to two different groups in this family of proteins. This is interesting as pharmaceutical companies are currently developing group or isoform specific inhibitors (Viaud and Peterson, 2009; Murray *et al.*, 2010; Zhang *et al.*, 2012). However, if both groups contribute to invasion and metastasis, cross reactive inhibitors may be particularly beneficial in treating some cancers types.

PAK1 and PAK4 are members of the group I and group II subdivision of PAKs, respectively. These two proteins, though both PAK isoforms, differ in many ways including the protein sequence. All the PAK isoforms contain a conserved N-terminal p21 binding domain (PBD) and a C-terminal kinase domain (Dummler *et al.*, 2009). However, the PBD and the kinase domain sequence have less than 40% and 54% homology, respectively, between PAKs of group I and II (Jaffer and Chernoff, 2002). Furthermore, PAK1 and PAK4 also differ in their kinase activation. Within the PBD of PAK1 there is an autoinhibitory domain (AID), which binds to the PBD of another PAK1 protein, forming a homodimer and blocking protein activation (Lei et al., 2000; Parrini et al., 2002). PAK1 has a low basal kinase activity which is increased by the binding of Cdc42 and Rac1 to the PBD, dissociating the inhibitory PAK1 homodimer (Zenke et al., 1999). In contrast, PAK4 lacks an AID. Recent findings suggest that PAK4 is constitutively phosphorylated and that kinase activity is controlled by conformational changes in the N-terminal region by the binding of Cdc42 (Baskaran *et al.*, 2012; Ha *et al.*, 2012; King *et al.*, 2014). These differences in sequence and kinase regulation may suggest that PAK1 and PAK4 could have divergent functions in cells, driven by differing substrates (Jaffer and Chernoff, 2002). Moreover, PAK4 knockout mice are embryonically lethal while PAK1 knockout mice remain viable, further emphasising that these two proteins may have distinct functions (Qu *et al.*, 2003; Arias-Romero and Chernoff, 2008).

A 2007 positional scanning peptide library study by Rennefahrt and colleagues demonstrated differing optimal phosphorylation sequences between PAK1 and PAK4, suggesting differential substrate specificities (Rennefahrt et al., 2007). However, despite the structural and biochemical differences, PAK1 and PAK4 share the majority of their substrates with little evidence to date suggesting that these isoforms are involved in different pathways (Arias-Romero and Chernoff,

2008). Furthermore, these two proteins are rarely directly compared in the same cell type which poses difficulty in differentiating unique substrates.

Whilst PAK1 and PAK4 can both bind, phosphorylate and inhibit the function of GEF-H1 (Zenke *et al.*, 2004; Callow *et al.*, 2005; Wells *et al.*, 2010; King *et al.*, 2014), the interactions between these proteins is not clearly defined with PAK1 and GEF-H1 interactions in particular revealing contradictory findings (Zenke *et al.*, 2004; Coniglio *et al.*, 2008; Tian *et al.*, 2014). The PAK4 interactions are thought to be more consistent, with phosphorylation of GEF-H1 leading to a down regulation of RhoA activity (Callow *et al.*, 2005; Wells *et al.*, 2010). The PAK1 and PAK4 proteins have differential binding to PDZ-RhoGEF - PAK1 does not bind, whilst PAK4 both binds and inhibits protein function (Barac *et al.*, 2004; Rosenfeldt *et al.*, 2006). However, this interaction with PDZ-RhoGEF has to date not been linked to any distinct PAK4 cellular processes.

This chapter investigates both shared and diverging PAK1 and PAK4 pathways in melanoma invasion.

5.2 Results

This study, so far has found that both PAK1 and PAK4 protein reduction in melanoma cell lines reduced invasion *in vitro* and *in vivo*. In the invadopodia assay, no additive reduction in the percentage of cells with invadopodia or invadopodia degradation was seen when PAK1 and PAK4 were simultaneously knocked down (Section 4.2.4). This may suggest that PAK1 and PAK4 are involved in the same signalling pathways. To investigate this further, cross rescues were performed by expressing GFPPAK1 and GFPPAK4 constructs in cells with reduced expression of PAK4 and PAK1, respectively.

5.2.1 GFPPAK4 Can Rescue Invadopodia Degradation in WM-115 Cells with Reduced PAK1 Expression

The expression of GFPPAK4 in WM-115 cells with diminished PAK1 expression had no effect on the percentage of cells with invadopodia (Figure 5-1). However, GFPPAK4 expression resulted in an increase in, and thus a rescue of, the degradation area in these knockdown cells. This result suggests, PAK4 may play an important role in degradation.

In contrast, expression of GFPPAK1 in WM-115 cells that had depleted PAK4 expression did not rescue the invasive phenotype, with no increase in either the percentage of cells with invadopodia or area of degradation, compared to cells with reduced PAK4 expression (Figure 5-2). These findings suggest that PAK1 and PAK4 have distinct roles in invadopodia formation and degradation.

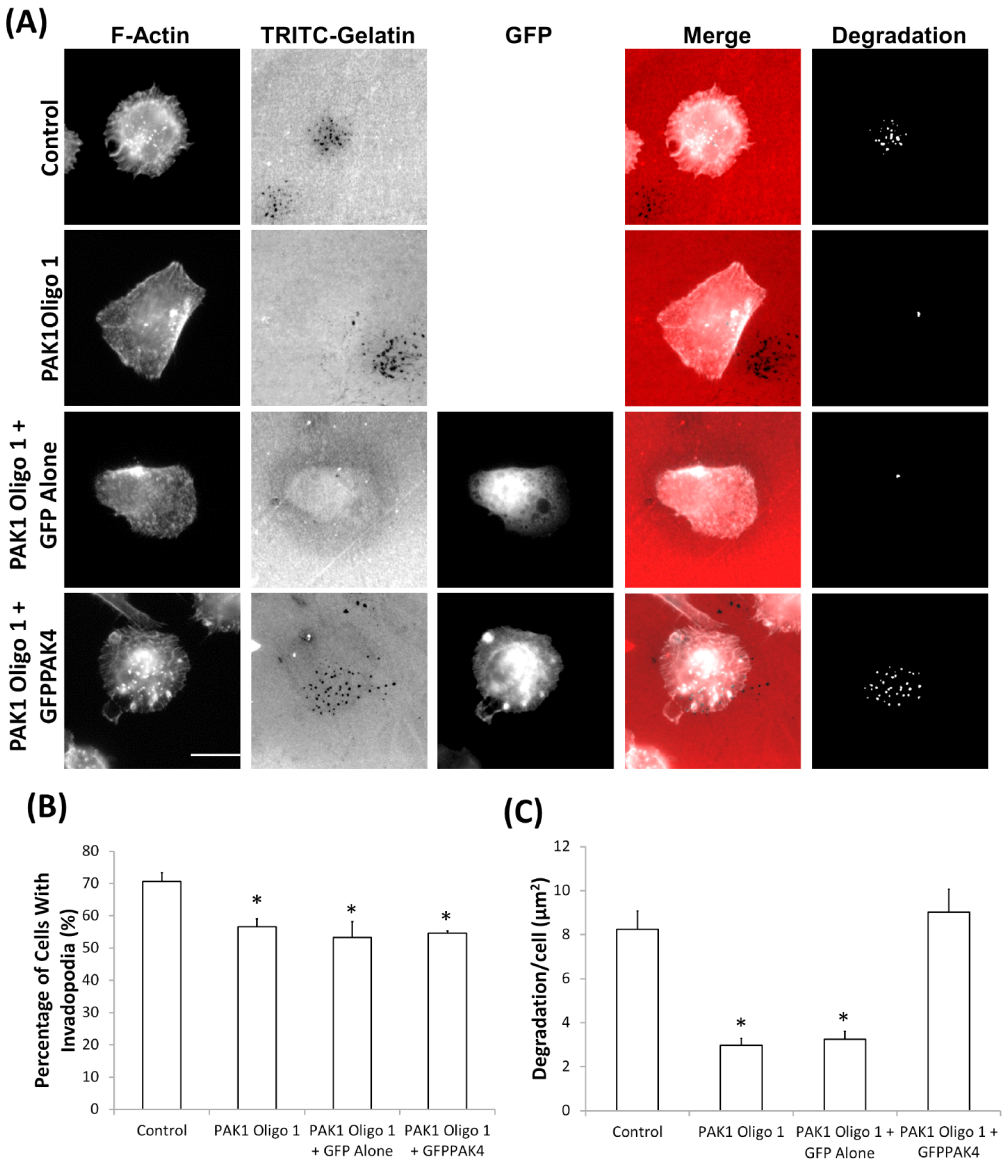

Figure 5-1: Invadopodia assay of WM-115 cells with diminished PAK1 protein expressing GFPPAK4.

Three days after siRNA oligonucleotide transfection, cells were transfected with DNA expression vectors and incubated for 48hrs. Following this, the cells were seeded on rhodamine conjugated gelatin for 3 hrs and stained for F-actin. Only actin rich dots that corresponded with gelatin degraded dots were counted as invadopodia. The degradation was measured using ImageJ software. (A) Representative invadopodia assay images of WM-115 PAK1 knockdown cells transfected with GFP alone or GFPPAK4. Scale bars = 10µm. (B) The percentage of cells with invadopodia. Significance was calculated to control siRNA transfected cells. Data are mean values ± S.E.M. of 150 cells, over 3 independent experiments; * = $P < 0.05$. (C) The area of degradation from invadopodia per cell. Significance was calculated to control siRNA transfected cells. Data are mean values ± S.E.M. of 90 invadopodia producing cells, over 3 independent experiments; * = $P < 0.05$. Control = cells transfected with non-specific siRNA.

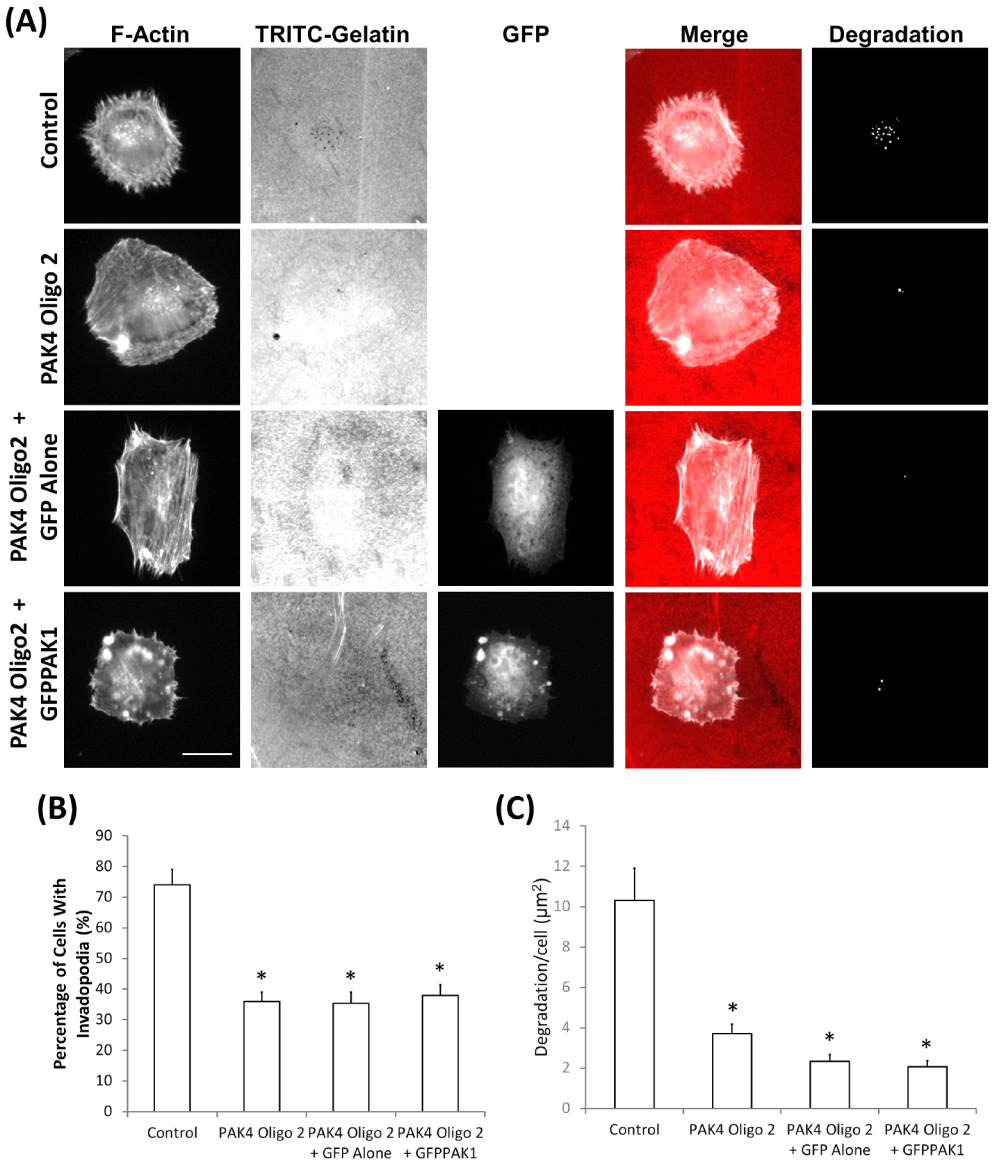

Figure 5-2: Invadopodia assay of WM-115 cells with diminished PAK4 protein expressing GFPPAK1.

Three days after siRNA oligonucleotide transfection, cells were transfected with DNA expression vectors and incubated for 48hrs. Following this, the cells were seeded on rhodamine conjugated gelatin for 3 hrs and stained for F-actin. Only actin rich dots that corresponded with gelatin degraded dots were counted as invadopodia. The degradation was measured using ImageJ software. (A) Representative invadopodia assay images of WM-115 PAK4 knockdown cells transfected with GFP alone or GFPPAK1. Scale bars = 10µm. (B) The percentage of cells with invadopodia. Significance was calculated to control siRNA transfected cells. Data are mean values ± S.E.M. of 150 cells, over 3 independent experiments; * = $P < 0.05$. (C) The area of degradation from invadopodia per cell. Significance was calculated to control siRNA transfected cells. Data are mean values ± S.E.M. of 90 invadopodia producing cells, over 3 independent experiments; * = $P < 0.05$. Control = cells transfected with non-specific siRNA.

5.2.2 Overexpression of PAK4 Does Not Increase Invadopodia Formation or Degradation

As the expression of GFPPAK4 in PAK1 knockdown WM-115 cells rescued the invadopodia degradation phenotype, investigations were conducted to determine whether overexpression of PAK4 in wildtype WM-115 cells could increase invadopodia formation or degradation.

The percentage of cells with invadopodia and the area of degradation did not change when GFPPAK4 was expressed in WM-115 cells compared to the wildtype and GFP alone control cells (Figure 5-3). Therefore, this shows that the expression of GFPPAK4 in WM-115 does not enhance invadopodia formation or degradation.

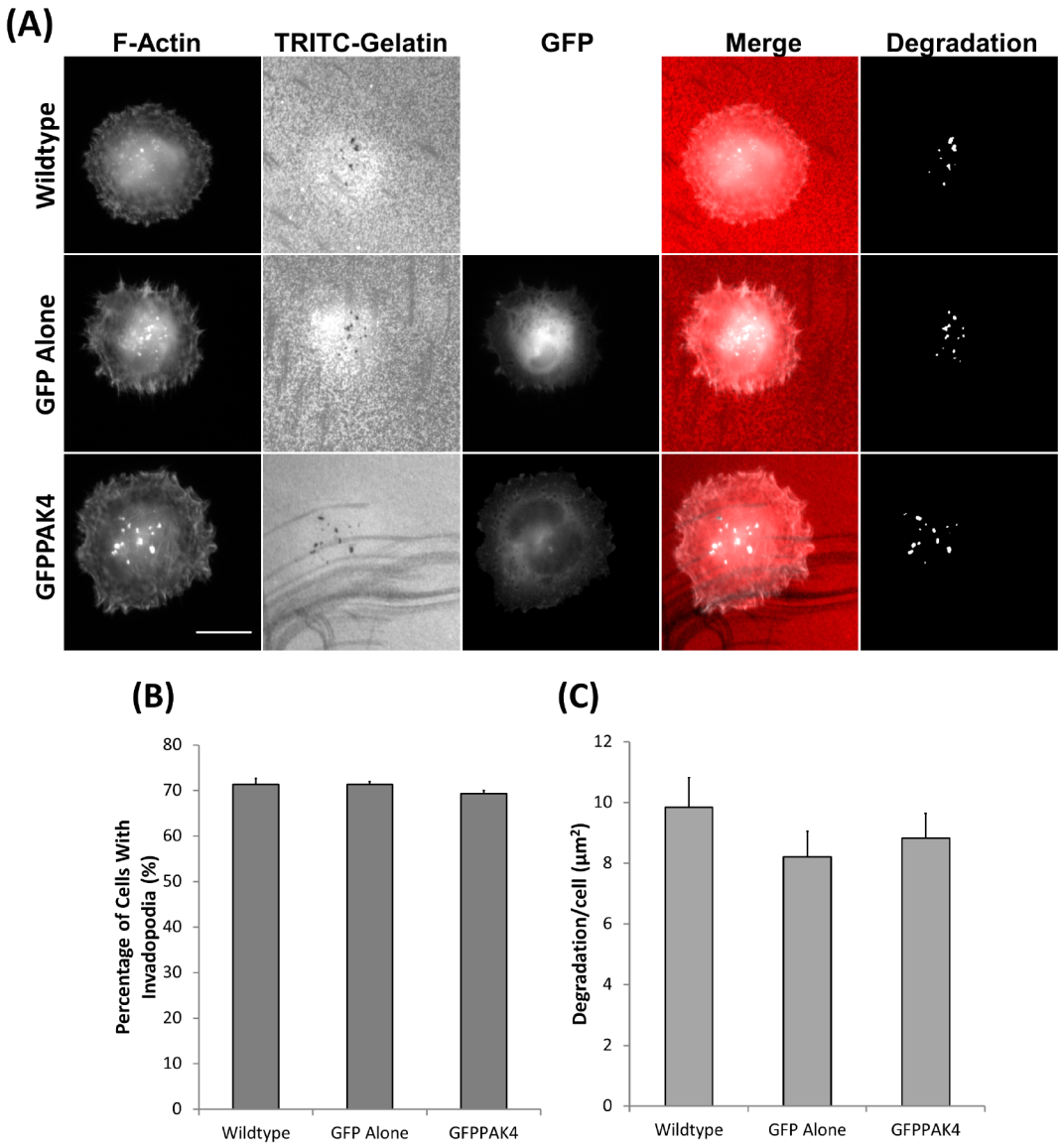

Figure 5-3: Invadopodia assay of WM-115 cells expressing GFPPAK4.
WM-115 cells were transfected with either GFP alone or GFPPAK4 constructs and incubated for 48hrs. Following this, the cells were seeded on rhodamine conjugated gelatin for 3 hrs and stained for F-actin. Only actin rich dots that corresponded with gelatin degraded dots were counted as invadopodia. The degradation was measured using ImageJ software. (A) Representative invadopodia assay images of WM-115 cells transfected with no construct (wildtype), GFP alone or GFPPAK4. Scale bars = 10µm. (B) The percentage of cells with invadopodia. Significance was calculated to wildtype WM-115 cells. Data are mean values ± S.E.M. of 150 cells, over 3 independent experiments; * = $P < 0.05$. (C) The area of degradation from invadopodia per cell. Significance was calculated to wildtype WM-115 cells. Data are mean values ± S.E.M. of 90 invadopodia producing cells, over 3 independent experiments; * = $P < 0.05$.

5.2.3 Depletion of PAK4 Expression Does Not Reduce the Percentage of Cells with Actin Puncta on Gelatin

To investigate if PAK1 and PAK4 function in invadopodia development from the early/nascent stages to the mature degradative protrusion, the percentage of cells with actin puncta when plated on gelatin was calculated. The depletion of PAK1 expression reduced the percentage of cells with actin puncta, compared to wildtype and control cells (Figure 5-4), whilst a reduction of PAK4 expression had no effect on the percentage of cells with actin puncta.

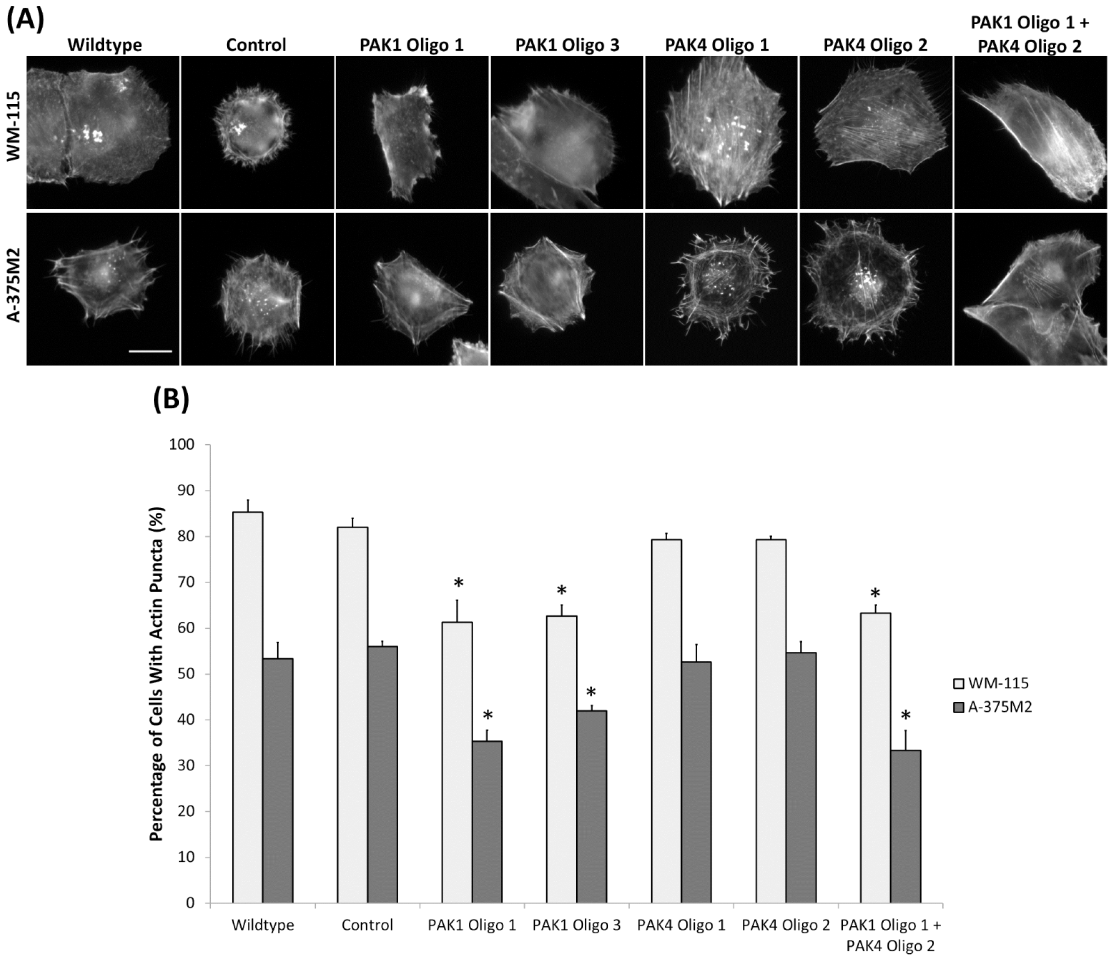

Figure 5-4: The percentage of WM-115 and A-375M2 cells with actin puncta on gelatin when PAK1 and PAK4 expression was depleted (individually and simultaneously).
Cells were plated on gelatin matrix coated coverslips 4 days post-transfection of siRNA oligonucleotides to reduce PAK1 and PAK4. (A) Representative images of WM-115 and A-375M2 cells for each condition. Scale bar = 10µm. (B) The percentage of cells with actin puncta on gelatin. Significance was calculated to wildtype and control cells. Data are mean values ± S.E.M. of 150 cells, over 3 independent experiments; * = $P < 0.05$.

5.2.4 Cell Shape is Unaffected by the Depletion of PAK1 and PAK4 Expression in WM-115 and A-375M2 Cells

All the invasion assays conducted in this study, utilising cells with diminished PAK1 and PAK4 expression (Section 4.2.4 and Section 4.2.5), found that no phenotypic differences existed between these two knockdown groups, with reduced invasion present in both groups. This data however, gives little insight into the specific role of PAK1 and PAK4 in melanoma invasion and progression. Therefore, to elucidate the role of these proteins additional assays were conducted to identify any phenotypic differences between PAK1 and PAK4 knockdown cells.

As discussed in chapter 3, cell shape may indicate the mode by which cells migrate and invade, e.g. a less elongated phenotype may indicate amoeboid migration rather than mesenchymal. Therefore, the cell shape was measured in WM-155 and A-375M2 cells in which PAK1, PAK4 and both proteins simultaneously, were reduced to identify any differences between these two isoforms (Figure 5-5). There was no significant difference in cell area, perimeter or elongation when PAK1, PAK4 or both PAK1 and PAK4 simultaneously, were reduced in WM-115 and A-375M2 cells, compared to wildtype and control cells.

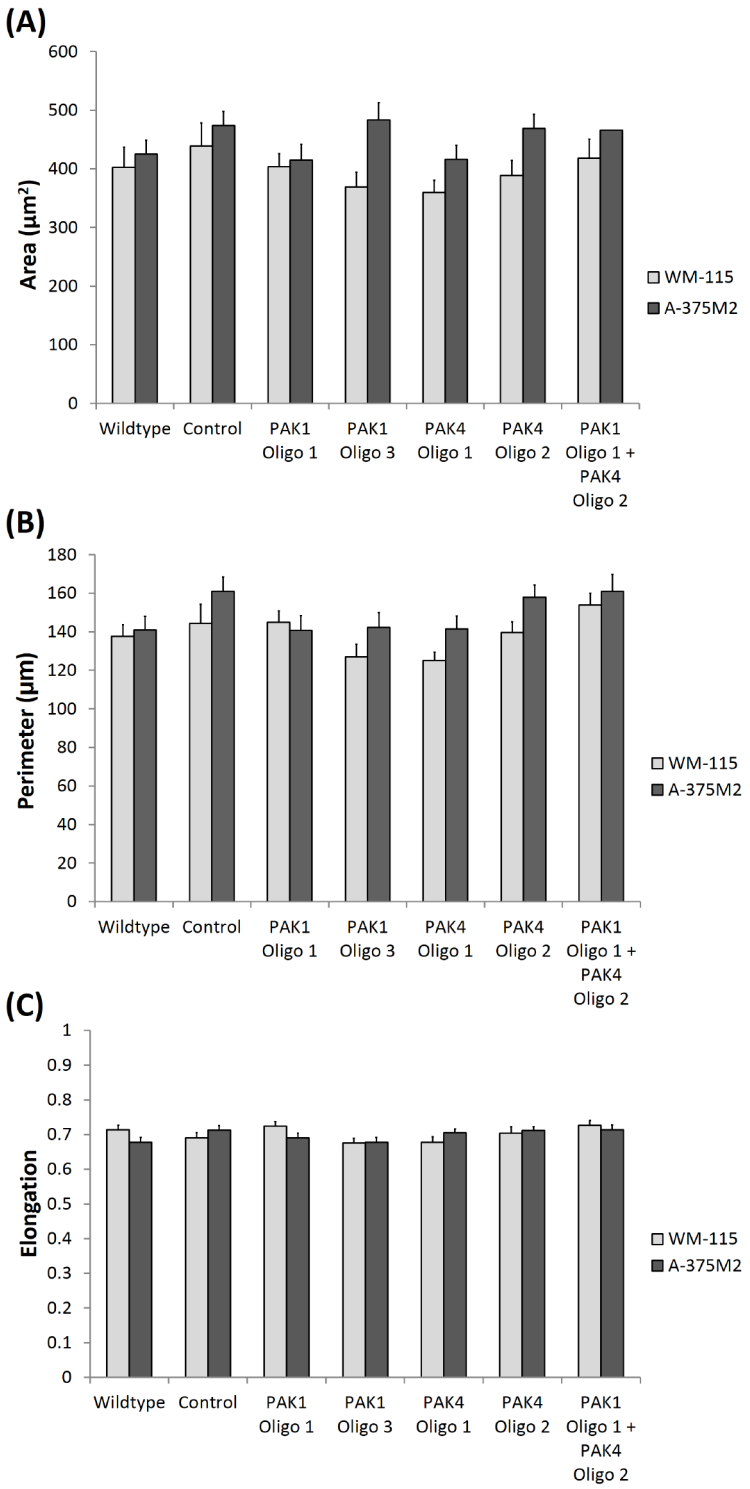

Figure 5-5: Cell shape analysis of PAK1, PAK4 and PAK1&PAK4 depleted WM-115 and A-375M2 cells. Four days post-transfection of siRNA oligonucleotides, cells were seeded on glass coverslips, incubated overnight, and stained for F-actin. The cell area (A), cell perimeter (B) and cell elongation (C) were calculated for 90 cells, over 3 independent experiments. Cell elongation was represented as a scale from 0 to 1 where 0 = circular and 1 = straight. Significance was calculated to wildtype and control cells. Data are mean values ± S.E.M.; * = $P < 0.05$. Control = cells transfected with non-specific siRNA.

5.2.5 Reduced PAK4 Expression Increases Prominent Actin Fibres in WM-115 and A-375M2 Cells

An increase in prominent actin fibres has been linked to cell rigidity and reduced cell invasion (Friedl and Wolf, 2003). Indeed, within this study few prominent actin fibres were found in the most invasive WM-115 cell line (Section 3.2.1.1). Furthermore, previous experiments have shown an increase in prominent actin fibres in PAK4 diminished DU-145 prostate cancer cells and in PAK1 diminished REF-52 rat embryo fibroblast cells (Frost *et al.*, 1998; Wells *et al.*, 2010). However, no direct comparison of prominent actin fibre formation in PAK1 and PAK4 depleted melanoma cell lines has previously been conducted.

An increase in prominent actin fibres was detected compared to wildtype and control cells in PAK4 depleted cells, whilst a loss of PAK1 expression did not increase the percentage of cells with prominent actin fibres (Figure 5-6). The simultaneous reduction of PAK1 and PAK4 also increased the percentage of cells with prominent actin fibres. In addition, these different PAK1 and PAK4 depleted phenotypes were observed on gelatin (the substrate used in the invadopodia assay).

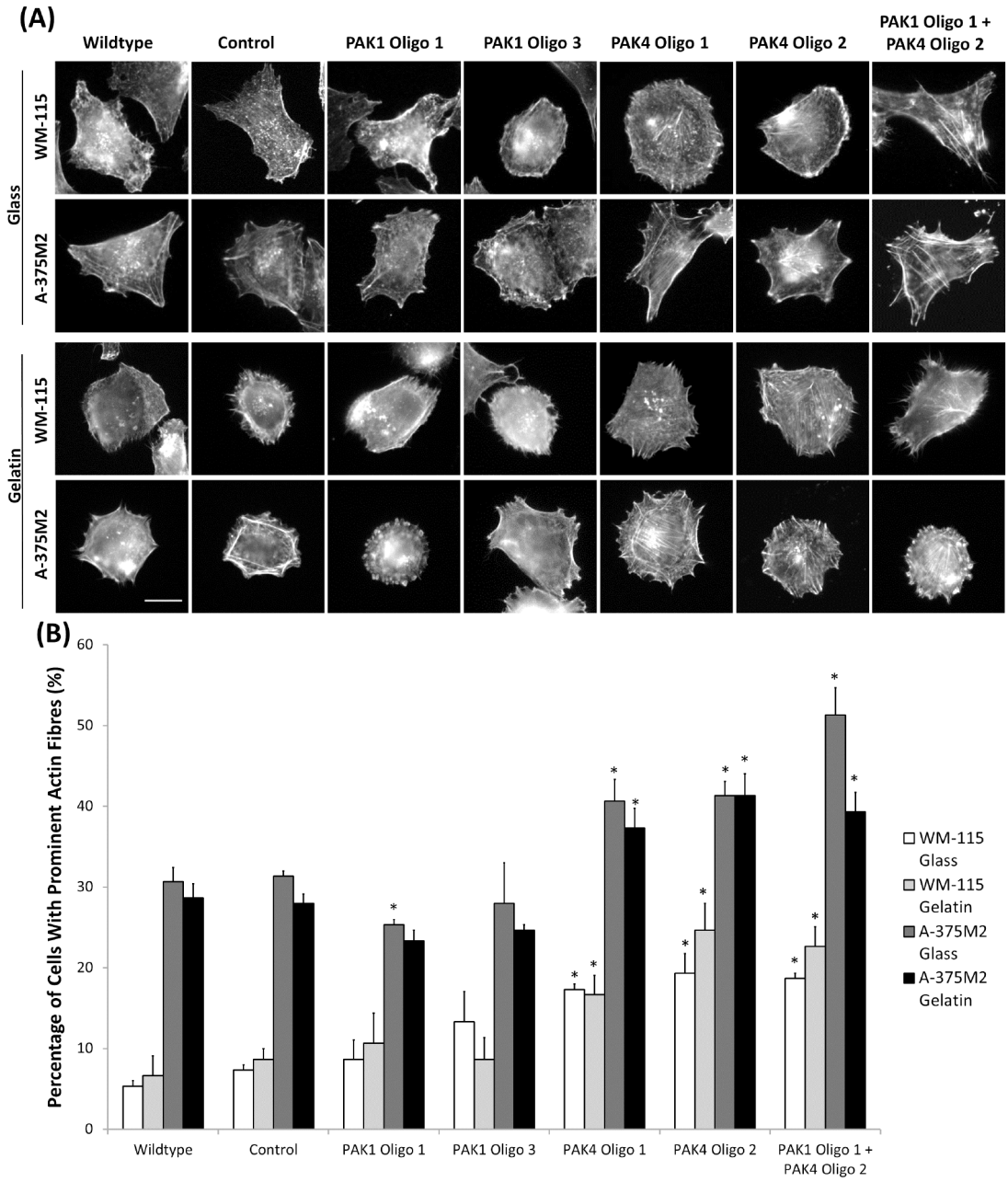

Figure 5-6: Percentage of WM-115 and A-375M2 cells with prominent actin fibres in PAK1 and PAK4 knockdown (individually and simultaneously) on glass and gelatin.

Cells were plated on glass or gelatin matrix coated coverslips 4 days post-transfection of siRNA oligonucleotides to reduce PAK1 and PAK4. (A) Representative images of WM-115 and A-375M2 cells on glass and gelatin for each condition. Scale bar = 10µm (B) Quantification of the percentage of cells with prominent actin fibres. Significance was calculated to wildtype and control cells. Data are mean values ± S.E.M. of 150 cells, over 3 independent experiments; * = $P < 0.05$. Control = cells transfected with non-specific siRNA.

5.2.6 GFPPAK4r siRNA Resistant Vector Rescued the Prominent Actin Fibre Phenotype in PAK4 Diminished WM-115 Cells

In the previous section, the depletion of PAK4 in WM-115 and A-375M2 cells increased the percentage of prominent actin fibres (Section 5.2.5). To validate that this phenotype is PAK4 specific, the prominent actin fibres were quantified for cells in which the GFPPAK4r siRNA resistant construct was expressed. As the wildtype A-375M2 cell line had a higher percentage of cells with prominent actin fibres compared to WM-115 cells, and therefore was able to show a larger differential in the percentage of cells with prominent actin fibres between wildtype and PAK4 knockdown cells, this cell line was used in the rescue experiments.

The expression of GFPPAK4 in PAK4 knockdown A-375M2 cells rescued the percentage of cells with prominent actin fibres back to that seen by the control cells (Figure 5-7). This further verified the importance of PAK4 in prominent actin fibre formation.

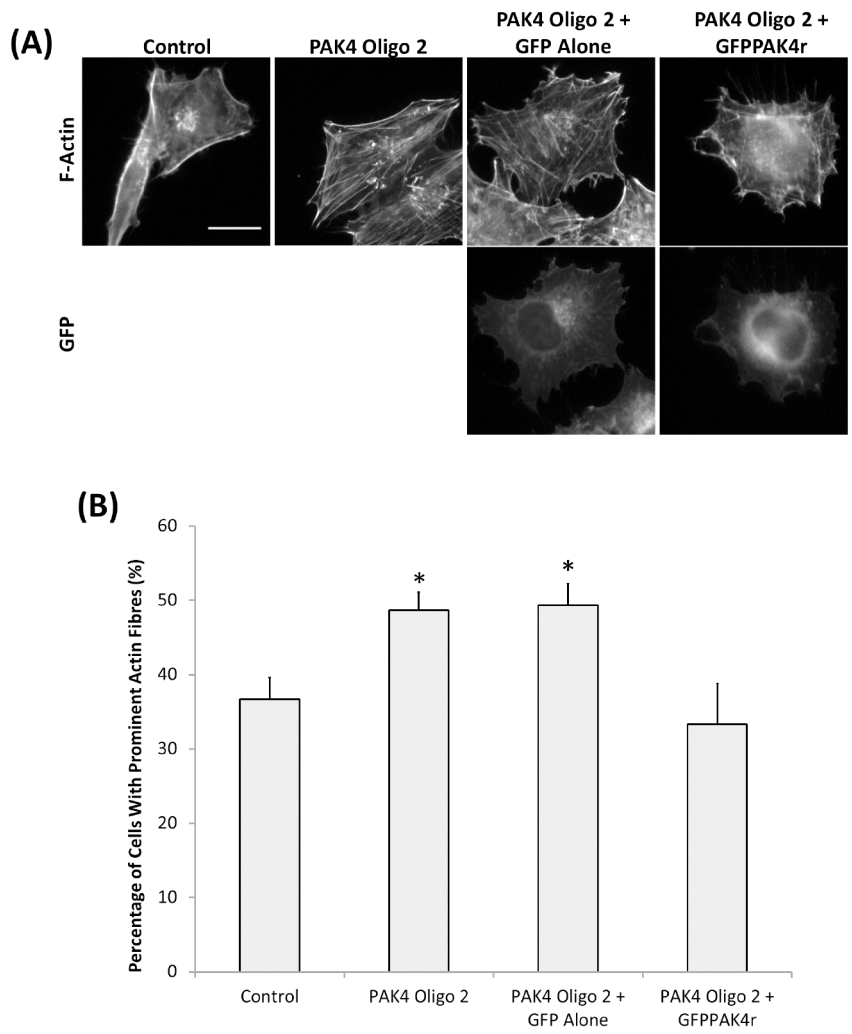

Figure 5-7: Percentage of cells with prominent actin fibres in PAK4 knockdown A-375M2 cells transfected with GFPPAK4r siRNA resistant rescue construct.

Cells were plated in 6 well plates and transfected with siRNA oligonucleotides to reduce PAK4. Two days post-transfection the cells were transfected with GFP alone or GFPPAK4 constructs. After 48 hrs, these cells were seeded on glass coverslips and incubated overnight, fixed and stained for F-actin. (A) Representative images of A-375M2 cells for each condition. Scale bar = 10µm (B) Quantification of the percentage of cells with prominent actin fibres. Significance was calculated to control cells. Data are mean values ± S.E.M. of 150 cells, over 3 independent experiments; * = $P < 0.05$. Control = cells transfected with non-specific siRNA.

5.2.7 A Reduction in PAK4 Protein Expression Leads to an Increase in RhoA Activation

An increase in RhoA activity has previously been shown to increase prominent actin fibres (Ridley and Hall, 1992). In addition, a reduction of PAK4 leads to an increase in the percentage of prominent actin fibres via an increase in RhoA activity in the DU-145 prostate cancer cell line (Wells *et al.*, 2010). Therefore, an investigation of the effects of PAK1 and PAK4 knockdown on RhoA activation was conducted, using a RhoA biosensor (named A-375M2 RhoA cells) (Fritz *et al.*, 2013).

A-375M2 cells stably expressing the RhoA biosensor (A-375M2 RhoA cells) were generated. Initially, the effect of PAK1 and PAK4 knockdown on prominent actin fibre formation was measured in A-375M2 RhoA cells to confirm that the presence of the RhoA biosensor does not change this phenotype.

The knockdown of PAK4 increased the percentage of cells with prominent actin fibres in agreement with our previous findings (Figure 5-6) whilst, the reduction of PAK1 expression had no effect (Figure 5-8). Thus the presence of the RhoA biosensor does not change the knockdown phenotype.

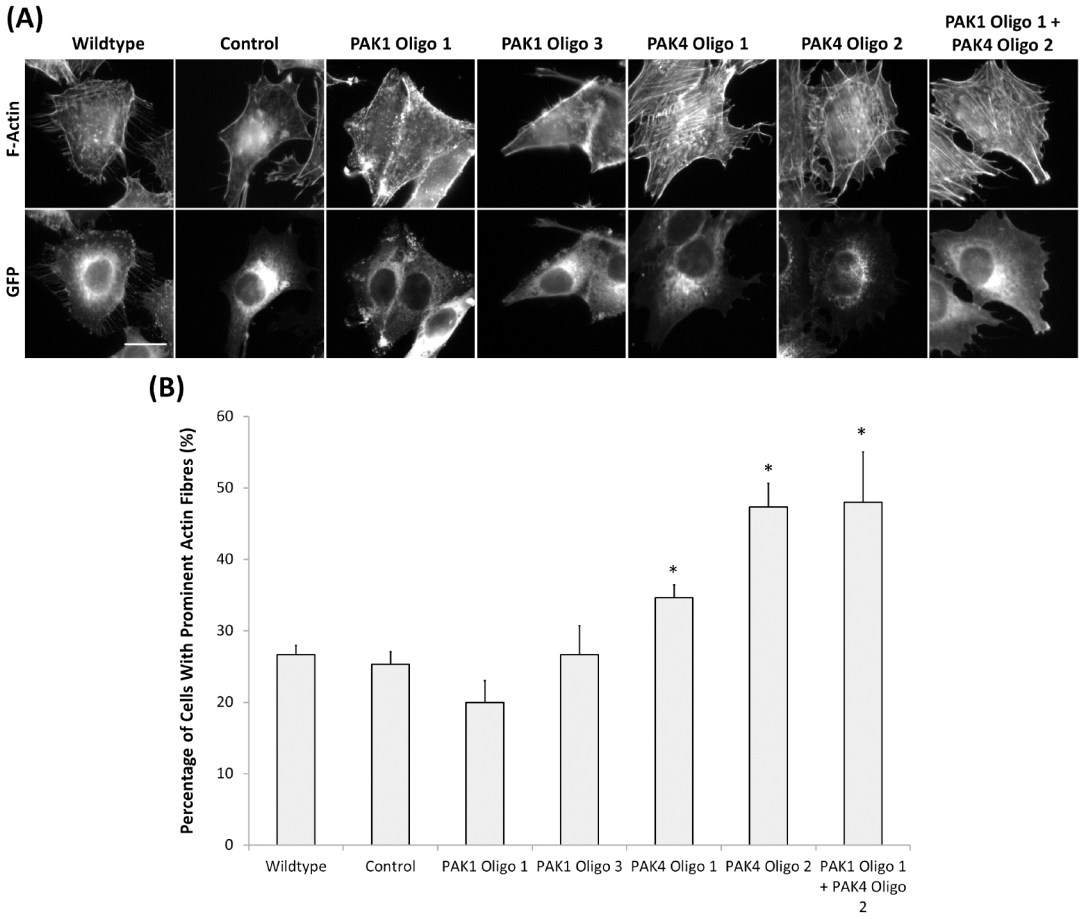

Figure 5-8: Percentage of cells with prominent actin fibres in PAK1 and PAK4 knockdown (both individually and simultaneously) in A-375M2 RhoA cells.
A-375M2 RhoA cells were plated on glass coverslips four days post-transfection of siRNA oligonucleotides. (A) Representative images of A-375M2 RhoA cells for each condition. Scale bar = 10µm. (B) Quantification of the percentage of cells with prominent actin fibres. Significance was calculated to wildtype and control cells. Data are mean values ± S.E.M. of 150 cells, over 3 independent experiments; * = $P < 0.05$. Control = cells transfected with non-specific siRNA.

An increase in FRET efficiency was observed in A-375M2 RhoA cells in which PAK4 levels were reduced (using either PAK4 oligo 1 or PAK4 oligo 2) compared to the control (Figure 5-9). This indicates that an increase in RhoA activation does occur when PAK4 expression is reduced. Interestingly, when PAK1 levels were diminished (using either PAK1 oligo 1 or PAK1 oligo 3) in A-375M2 RhoA cells there was a decrease in FRET efficiency compared to the control. Therefore, the level of RhoA activation differs in PAK1 and PAK4 knockdown A-375M2 RhoA cells. This suggests that the differential signalling pathways employed by PAK1 and PAK4 may occur via RhoA.

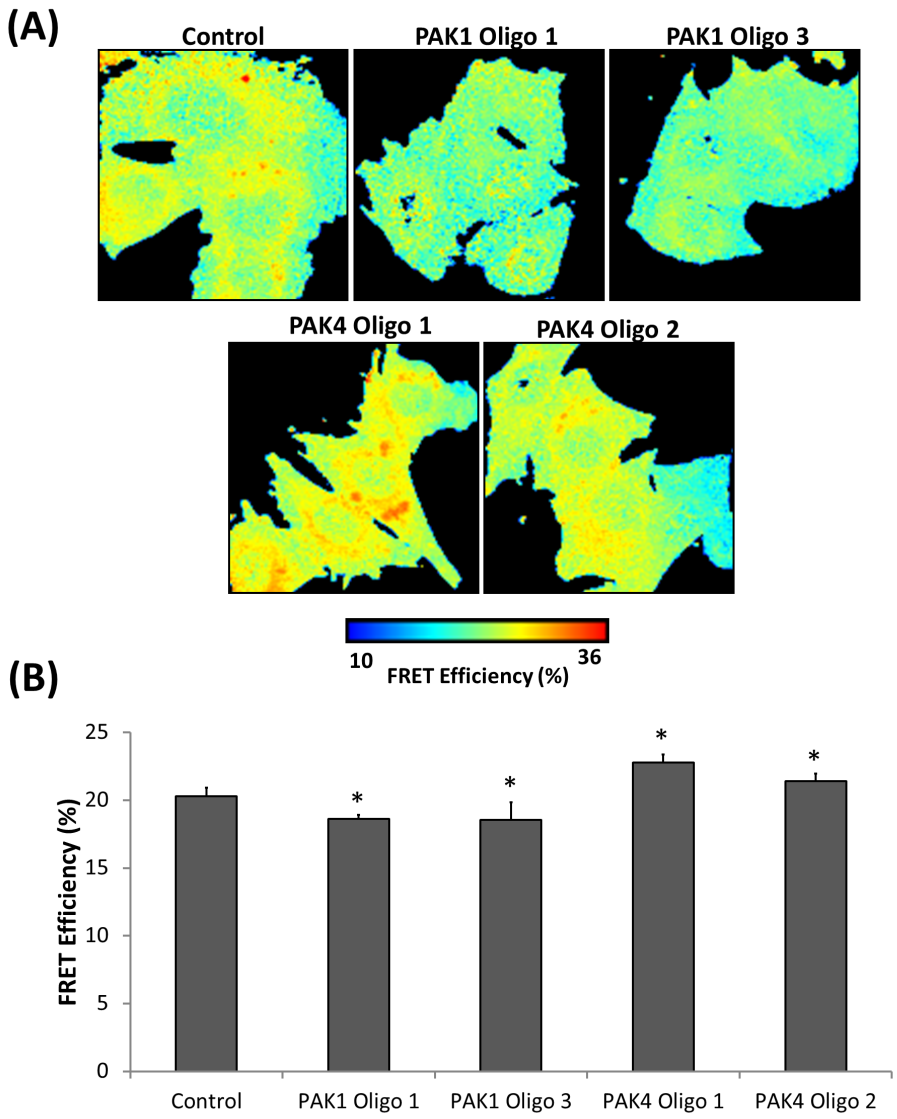

Figure 5-9: FRET analysis of RhoA activation in A-375M2 RhoA cells in which PAK1 and PAK4 expression was diminished.
A-375M2 RhoA cells were plated on glass coverslips four days post-transfection of siRNA oligonucleotides and the FRET was measured using a multiphoton, time-correlated single-photon counting (TCSPC) fluorescence lifetime imaging microscope (FLIM). FRET efficiency was calculated using TRI2. (A) Representative FRET efficiency images of A-375M2 RhoA cells for each condition. (B) Quantification of the FRET efficiency of A-375M2 RhoA cells in which PAK1 or PAK4 was reduced. Significance was calculated to control cells. Data are mean values ± S.E.M. over 3 independent experiments; * = $P < 0.05$. Control = cells transfected with non-specific siRNA.

5.2.8 PAK4 Does Not Signal Through GEF-H1 in WM-115 Cells

These results suggest PAK4 but not PAK1 signals via inhibition of RhoA. PAK4 has previously been shown to inhibit the activation of RhoA via the phosphorylation and inhibition of GEF-H1 at Ser^{885} (Callow *et al.*, 2005; Wells *et al.*, 2010). However, the findings regarding PAK1 signalling through

GEF-H1 to RhoA are conflicting (Zenke *et al.*, 2004; Coniglio *et al.*, 2008; Tian *et al.*, 2014). To date the extent to which PAK1 and PAK4 phosphorylate GEF-H1 has not been directly compared. Therefore, the level of pGEF-H1 phosphorylation at Ser^{885} was quantified using western blot in PAK1 and PAK4 knockdown cells.

There was no significant difference in the phosphorylation of GEF-H1 at Ser^{885} when PAK1 and PAK4 were knocked down (individually and simultaneously) in WM-115 cells when compared to control cells (Figure 5-10). This data indicates that the unique signalling of PAK4 to RhoA does not occur through the phosphorylation of GEF-H1 at Ser^{885} in melanoma cells.

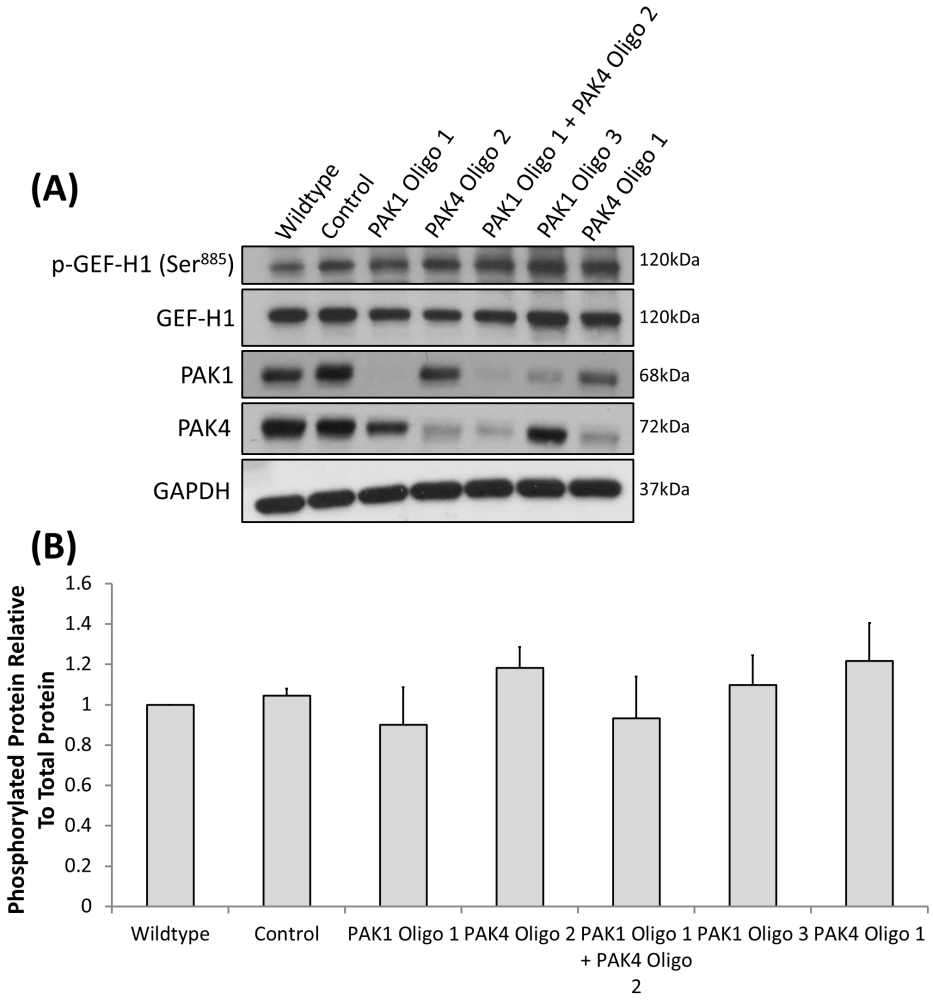

Figure 5-10: The expression of p-GEF-H1 (Ser^{885}) in WM-115 cells with reduced expression of PAK1 and PAK4 (individually or simultaneously).
(A) Western blot of p-GEF-H1 (Ser^{885}), total GEF-H1, PAK1 and PAK4 in WM-115 cells in which PAK1 and PAK4 expression was reduced (individually and simultaneously). (B) Analysis of western blot data via densitometry showing p-GEF-H1 (Ser^{885}) levels compared to the total GEF-H1 protein. Significance was calculated compared to control WM-115 cells. Data are the mean values ± S.E.M., over 3 independent experiments; *= $P < 0.05$. Densitometric data were normalized to total GEF-H1. GAPDH was also used as a loading control. Control = cells transfected with non-specific siRNA.

5.2.9 PDZ-RhoGEF Dominant Negative Mutant Can Rescue the PAK4 Knockdown Prominent Actin Fibre Phenotype

The activity of RhoA can be controlled via other GEFs including PDZ-RhoGEF. Interestingly, only PAK4 (and not PAK1) can bind to, and inhibit the GEF activity of, PDZ-RhoGEF (Barac *et al.*, 2004; Rosenfeldt *et al.*, 2006). Therefore, the inhibition of the activation of RhoA by PAK4 may signal via PDZ-RhoGEF in melanoma cells. To investigate this possibility, a dominant negative PDZ-RhoGEF mutant (myc-PDZ-RhoGEFΔDH) was expressed in cells with reduced PAK4 expression and the percentage of cells with prominent actin fibres was subsequently calculated (Figure 5-11). This myc-PDZ-RhoGEFΔDH mutant, lacks the DH domain essential for GTPase activation (Hart *et al.*, 1994), and competes with the wildtype PDZ-RhoGEF to bind Rho, but, is unable to activate the GTPase (Driessens *et al.*, 2002; Kasai *et al.*, 2004). If reducing PAK4 expression allows increased PDZ-RhoGEF activity, this mutant should repress this effect and deliver a rescue of phenotype. The expression of myc-PDZ-RhoGEFΔDH in PAK4 diminished WM-115 cells did indeed decrease the percentage of cells with prominent actin fibres to levels seen by the control cells.

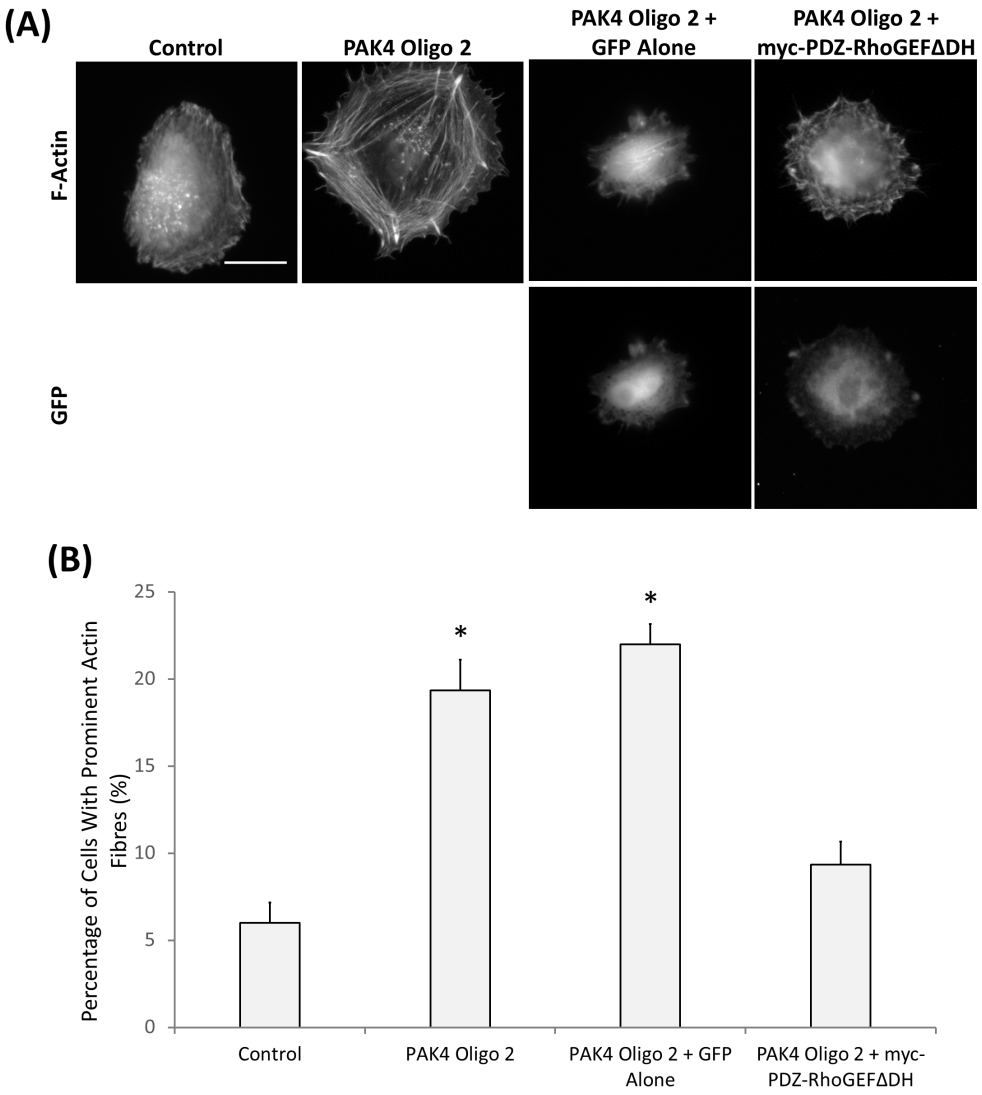

Figure 5-11: Percentage of cells with prominent actin fibres in PAK4 reduced WM-115 cells expressing myc-PDZ-RhoGEFΔDH on gelatin.

Three days after siRNA oligonucleotide transfection, WM-115 cells were transfected with DNA expression vectors and incubated for 48hrs. Following this, the cells were seeded on rhodamine conjugated gelatin for 3 hrs and stained for F-actin. (A) Representative images of WM-115 cells for each condition. Scale bar = 10µm. (B) Quantification of the percentage of cells with prominent actin fibres. Significance was calculated to control cells. Data are mean values ± S.E.M. of 150 cells, over 3 independent experiments; * = $P < 0.05$. Control = cells transfected with non-specific siRNA.

5.2.10 PDZ-RhoGEFΔDH Dominant Negative Mutant Can Rescue the Invadopodia Formation and Degradation in PAK4 Diminished Cells

As myc-PDZ-RhoGEFΔDH was able to rescue the PAK4 knockdown prominent actin fibre phenotype, the effect of this dominant negative PDZ-RhoGEF mutant on the invasion of WM-115 PAK4 knockdown cells was investigated.

The expression of myc-PDZ-RhoGEFΔDH in WM-115 cells in which PAK4 expression levels were reduced, rescued the invasive phenotype as measured by the invadopodia assay. In fact, both the percentage of cells with invadopodia and the degradation from invadopodia producing cells increased, returning to levels seen by the control cells (Figure 5-12).

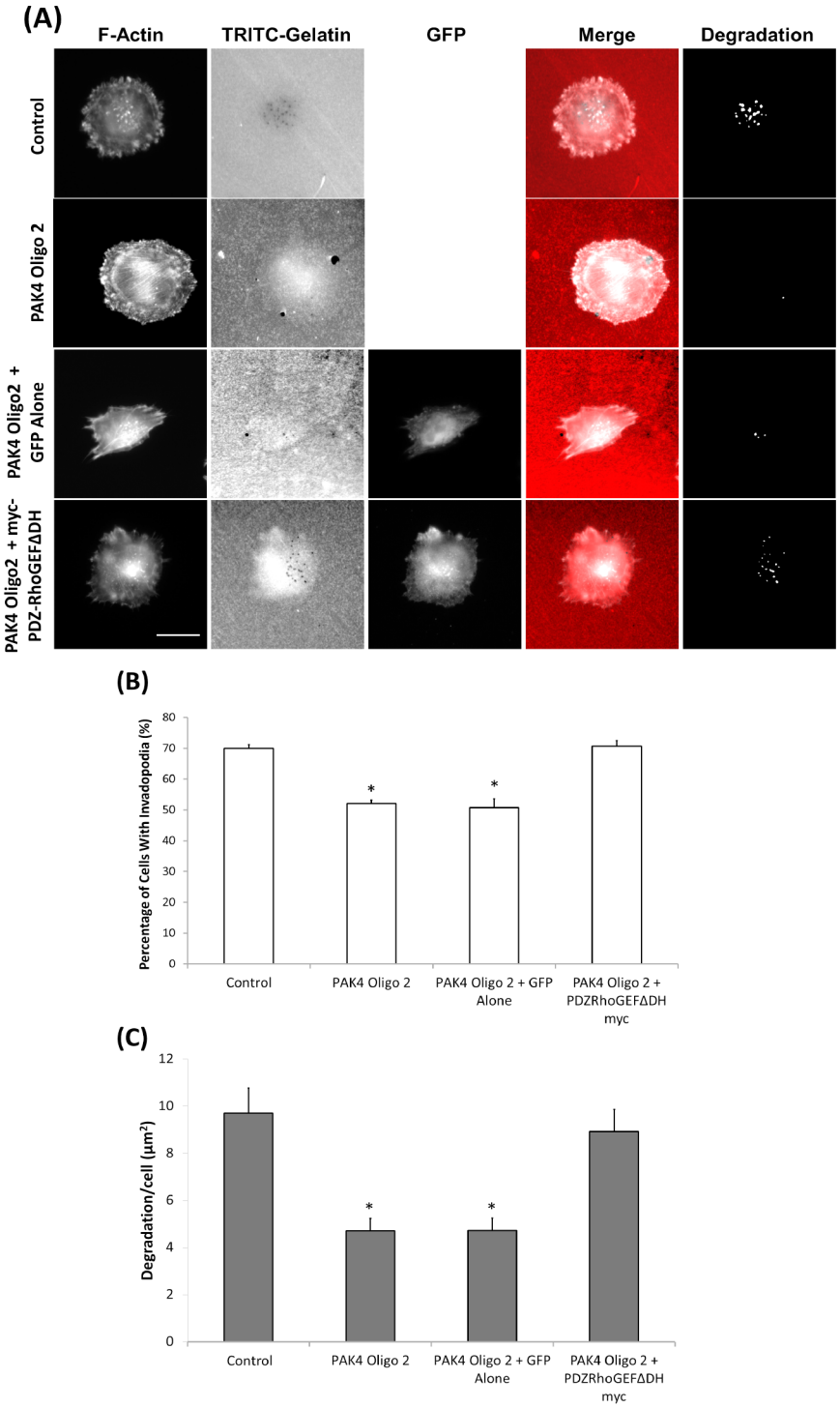

Figure 5-12: Invadopodia assay of PAK4 knockdown WM-115 cells expressing myc-PDZ-RhoGEFΔDH. Three days after siRNA oligonucleotide transfection, cells were transfected with DNA expression vectors and incubated for 48hrs. Following this, the cells were seeded on rhodamine conjugated gelatin for 3 hrs and stained for F-actin. Only actin rich dots that corresponded with gelatin degraded dots were counted as invadopodia. The degradation was measured using ImageJ software. (A) Representative invadopodia assay images of WM-115 PAK4 knockdown cells for each condition. Scale bars = 10µm. (B) The percentage of cells with invadopodia. Significance was calculated to control cells. Data are mean values ± S.E.M. of 150 cells, over 3 independent experiments; * = $P < 0.05$. (B) The area of degradation from invadopodia per cell. Significance was calculated to control cells. Data are mean values ± S.E.M. of 90 invadopodia producing cells, over 3 independent experiments; * = $P < 0.05$. Control = cells transfected with non-specific siRNA.

5.2.11 Overexpression of PDZ-RhoGEF Mimics PAK4 Knockdown in Wildtype WM-115 Cells

Given that the dominant negative myc-PDZ-RhoGEFΔDH mutant rescues the invasive phenotype (as measured by the invadopodia assay) in PAK4 diminished cells, it was thought that an increase in the expression of wildtype myc-PDZ-RhoGEF in WM-115 cells may mimic the PAK4 knockdown phenotype. This would further validate the PAK4 signalling pathway via inhibition of PDZ-RhoGEF.

The overexpression of myc-PDZ-RhoGEF did in fact reduce the percentage of cells with invadopodia and the degradation from invadopodia producing cells compared to wildtype and GFP Alone transfected cells (Figure 5-13), thus mimicking the PAK4 knockdown phenotype. Therefore, this data further validates the conclusion that PAK4 signalling in invadopodia formation and degradation occurs by inhibiting PDZ-RhoGEF activity.

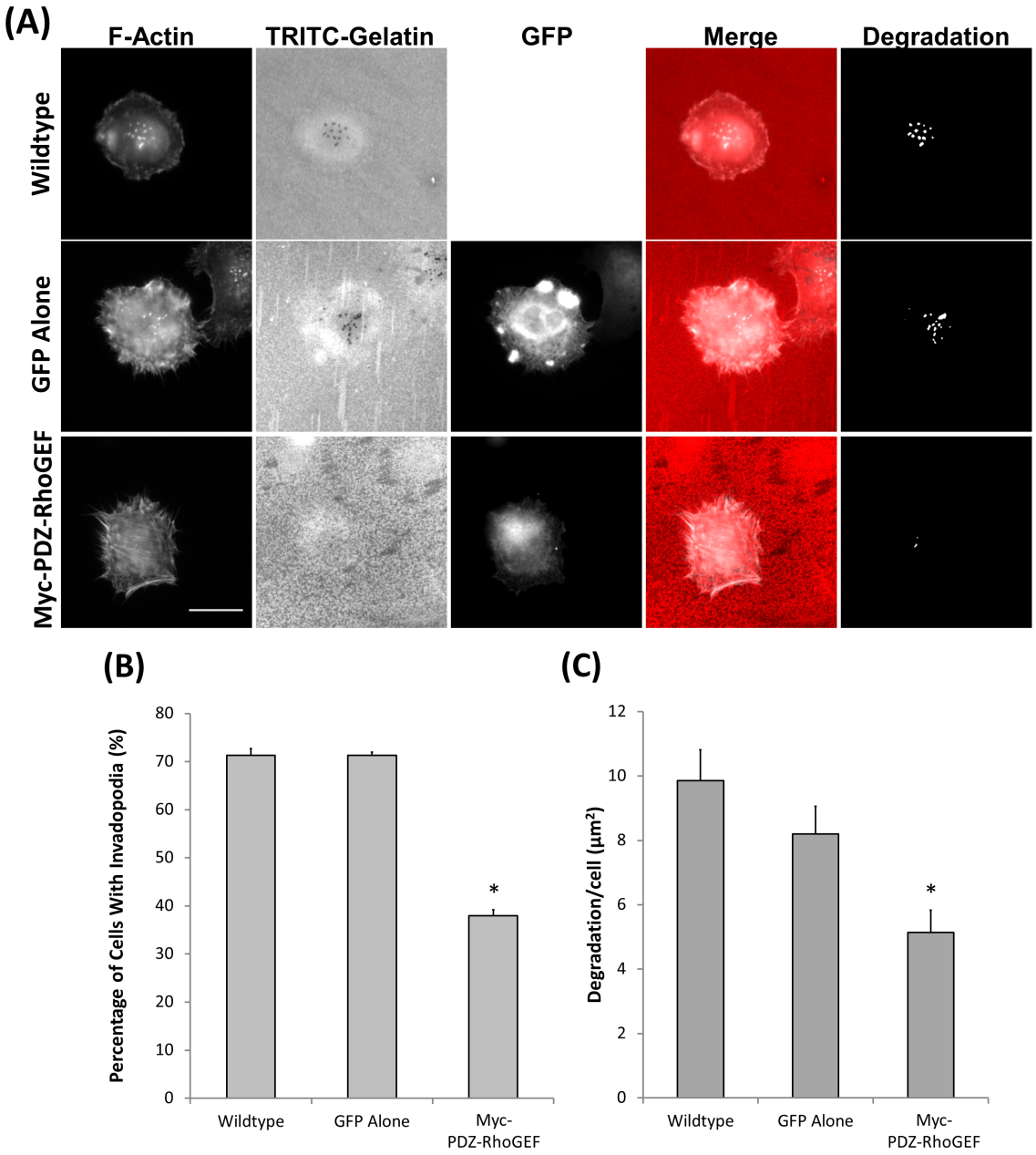

Figure 5-13: Invadopodia assay of WM-115 cells expressing myc-PDZ-RhoGEF.

WM-115 cells were transfected with either GFP alone or myc-PDZ-RhoGEF constructs and incubated for 48hrs. Following this, the cells were seeded on rhodamine conjugated gelatin for 3 hrs and stained for F-actin. Only actin rich dots that corresponded with gelatin degraded dots were counted as invadopodia. The degradation was measured using ImageJ software. (A) Representative invadopodia assay images of WM-115 cells for each condition. Scale bars = 10µm. (B) The percentage of cells with invadopodia. Significance was calculated to wildtype WM-115 cells. Data are mean values ± S.E.M. of 150 cells, over 3 independent experiments; * = $P < 0.05$. (B) The area of degradation from invadopodia per cell. Significance was calculated to wildtype WM-115 cells. Data are mean values ± S.E.M. of 90 invadopodia producing cells, over 3 independent experiments; * = $P < 0.05$.

5.2.12 PDZ-RhoGEF and PAK4 Localise to Invadopodia

Our findings suggest that PAK4 signals through PDZ-RhoGEF during invadopodia formation and degradation. Thus, it might be expected that these proteins are localised to invadopodia. Therefore, myc-PDZ-RhoGEF (both wildtype and ΔDH mutant) and GFPPAK4 were overexpressed in WM-115 cells and protein localisation was observed using confocal microscopy.

Both GFPPAK4 and myc-PDZ-RhoGEF (wildtype and ΔDH mutant) localised to invadopodia structures (Figure 5-14). Furthermore, the localisation of PDZ-RhoGEF at invadopodia is independent of the GEF activity as the myc-PDZ-RhoGEFΔDH dominant mutant retained the invadopodia localisation (Figure 5-14C and D).

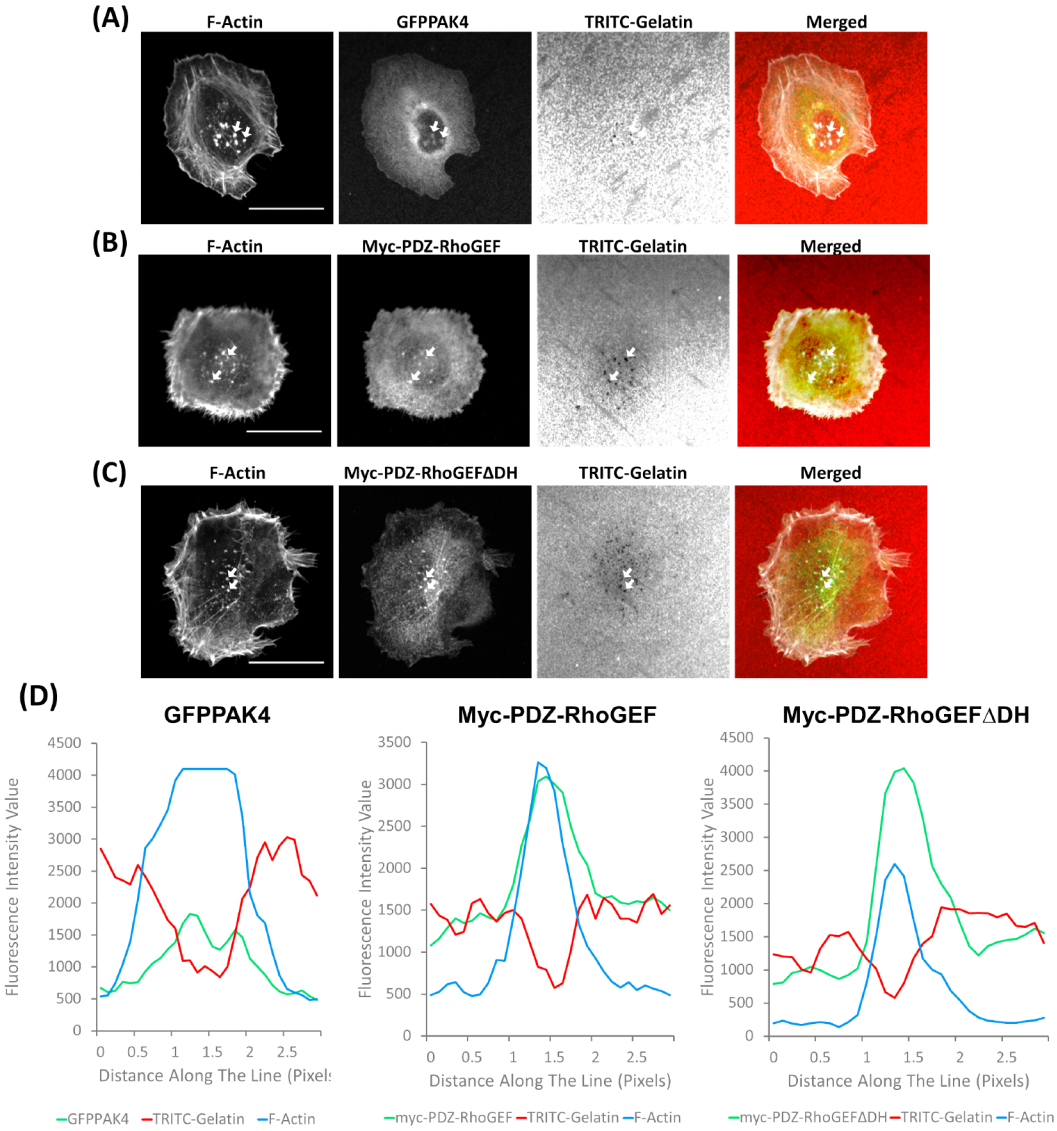

Figure 5-14: Co-localisation of GFPPAK4 and myc-PDZ-RhoGEF (wildtype and ΔDH mutant) with F-actin and TRITC gelatin degradation.

WM-115 cells transfected with GFPPAK4 or myc-PDZ-RhoGEF were seeded on TRITC gelatin coated coverslips for 3 hrs and then fixed and stained for F-actin. (A) Representative confocal images showing co-localisation of GFPPAK4 and myc-PDZ-RhoGEF (wildtype and ΔDH mutant) with F-actin and gelatin degradation. Scale bar = 10µm. (B) A representative fluorescence intensity plot showing co-localisation of GFPPAK4 and myc-PDZ-RhoGEF (wildtype and ΔDH mutant) with F-actin and gelatin degradation. Fluorescence intensity was measured at each image pixel along an arbitrary line that crossed through an invadopodia structure.

5.3 Discussion

This chapter has identified for the first time a unique PAK4 pathway (not used by PAK1) that signals via PDZ-RhoGEF to promote invadopodia formation and degradation, in addition to demonstrating a converging PAK1 and PAK4 pathway utilised in invadopodia degradation. These findings reveal the importance of both PAK1 and PAK4 in melanoma invasion and invadopodia structures.

The rescue by GFPPAK4 of the degradation area of WM-115 cells in which PAK1 was diminished, suggests that PAK4 signals later in the lifecycle of the invadopodia than PAK1. Furthermore, when the percentage of cells on gelatin with actin puncta (presumed to be early/nascent invadopodia) was analysed, the reduction of PAK4 did not reduce the formation of these puncta. This differed from cells with depleted PAK1 levels which had a reduction in the percentage of cells with actin puncta. This suggests that PAK1 enhances the formation of invadopodia, which is supported by a previous study which found that PAK1 is involved in the early stages of invadopodia formation via the phosphorylation of cortactin at Ser^{113} (Ayala *et al.*, 2008). However, the function that cortactin phosphorylation plays in invadopodia is currently in dispute with a recent study suggesting a key role for this phosphorylated protein in the disassembly of invadopodia (Moshfegh *et al.*, 2014). In contrast, PAK4 may function during the maturation of invadopodia to a degradative protrusion, or during the degradation process.

Both PAK1 and PAK4 have previously been implicated in pathways involved in matrix degradation. Prolactin induced secretion of MMP-1 and MMP-3 by TMX2-28 breast cancer cell lines in collagen IV matrix, signals via PAK1, while the expression and secretion of MMP-9 in collagen I, and MMP-2 in collagen IV, is down regulated by this PAK isoform (Rider *et al.*, 2013). Conversely, the inhibition of PAK1 reduces MMP-9 expression in the PC3 prostate cancer cell line (Goc *et al.*, 2013). PAK4 inhibition reduces MMP-2 expression in the 4910 glioma cell line and OVCA420 ovarian cancer cell line (Siu *et al.*, 2010a; Kesanakurti *et al.*, 2012). Furthermore, PAK4 knockdown down regulates MT1-MMP expression in CCA choriocarcinoma cells (Zhang *et al.*, 2011), while its overexpression enhances the expression of MMP-2 (Siu *et al.*, 2010a). Due to the key role played by matrix metalloproteinases in matrix degradation and the regulation of the expression and secretion of these proteins by PAK4, it is likely that the signalling pathway utilised by this isoform in invadopodia degradation occurs via MMPs.

This study has also found PAK4 to have a unique pathway, not shared by PAK1, in invasion. This pathway involves the inhibition of PDZ-RhoGEF by PAK4 in invadopodia. In addition, our findings

suggest that it is the RhoA isoform which is involved in this pathway, as PAK4 knockdown increases RhoA activity while PAK1 depletion does not.

PDZ-RhoGEF is classed as a RhoA specific activator and signalling of this protein via the activation of RhoA has been widely published (Rumenapp *et al.*, 1999; Rossman *et al.*, 2005; Oleksy *et al.*, 2006; Wong *et al.*, 2007). However, PDZ-RhoGEF may also play a role in signalling through other Rho isoforms, as evidenced by the fact that this protein was able to promote the activation of RhoB and RhoC in an *in vitro* GDP dissociation assay, albeit to a lesser extent than that seen with RhoA (Jaiswal *et al.*, 2011). Therefore, further experiments are required to validate that PAK4 signalling through PDZ-RhoGEF in invadopodia occurs via RhoA. This could be achieved by measuring RhoA activity at invadopodia structures (Bravo-Cordero *et al.*, 2011) when expressing PAK4, PDZ-RhoGEF or PDZ-RhoGEFΔDH, either using fixed cells or more interestingly, timelapse microscopy on live cells. In addition, to confirm the results obtained with the dominant negative mutant were specifically due to reduced PDZ-RhoGEF activity, the depletion of PDZ-RhoGEF protein expression (using siRNA oligonucleotides) could be performed in PAK4 knockdown cells in the invadopodia assay.

Within this study, both PAK4 and PDZ-RhoGEF were shown to localise to invadopodia structures which indicates that Rho activity is spatiotemporally controlled in these structures. This also suggests that activation of this GTPase is likely to be required for additional stages of either invadopodia formation or dissolution, as the requirement for low levels of Rho activity throughout the invadopodia life cycle, could simply be achieved by the localisation of PDZ-RhoGEF away from the invadopodia structure.

Other invadopodia proteins exhibit spatiotemporal functions, such as cortactin and cofilin (Artym *et al.*, 2006; Oser *et al.*, 2009). In invadopodia cortactin forms an inhibitory complex with cofilin, N-WASP, Arp2/3 and other proteins (Oser *et al.*, 2009). During the early formation of invadopodia, cortactin is phosphorylated, which results in the release of cofilin, allowing the creation of free barbed ends for actin polymerisation (Oser *et al.*, 2009). After the formation of invadopodia, cortactin is de-phosphorylated, exerts an inhibitory function on cofilin leading to invadopodia stabilisation and matrix degradation.

RhoC also demonstrates spatiotemperal activity in invadopodia which is controlled by the localisation of RhoC GEFs and GAPs (Bravo-Cordero *et al.*, 2011). p190RhoGAP localises to the invadopodia core while p190RhoGEF localises around this core in MTLn3 cells, to spatiotemporally control RhoC activity in invadopodia, ultimately influencing spatial cofilin

phosphorylation. Indeed, a RhoA GAP, ARAP3, also localises to the core of podosomes, an invadopodia related structure (Yu *et al.*, 2013). The presence of p190RhoGEF, p190RhoGAP and ARAP3 in invadopodia and related structures highlights the importance of GEFs and GAPs in the formation of these invasive structures.

Little is known about the role that PDZ-RhoGEF plays in tumour invasion. Gene amplification of PDZ-RhoGEF is evident in gallbladder cancer specimens, compared to normal tissue (Kim *et al.*, 2008). In addition, PDZ-RhoGEF has higher tissue expression in more advanced stages of breast cancer, with this GEF being essential for the spatial activation of RhoA in CXCR4 induced cell migration of MDA-MB-231 breast cancer cells (Struckhoff *et al.*, 2013). These findings are in line with the results obtained in this current study in which the localisation of PDZ-RhoGEF to invadopodia indicates that activity of this protein, is required at some stage of the invadopodia life cycle. This study indicates that the spatiotemporal inhibition (via PAK4) of PDZ-RhoGEF is essential for the invadopodia function and degradation that promotes cell invasion. Therefore, the presence of global PDZ-RhoGEF overexpression in advanced tumours emphasises the importance of PAK4 in providing an inhibitory function at invadopodia for successful invasion.

Studies on the function of RhoA in cell invasion and invadopodia formation have produced contradictory results depending on the cell type and experimental technique. RhoA expression and activity has been shown to both promote and hinder cell invasion. The depletion of RhoA in MDA-MB-231 cells and the prostate cancer cell lines DU-145, PC3 and LnCaP, increased cellular invasion both in a 3D Matrigel matrix and in a transwell invasion assay (coated with Matrigel) (Vega *et al.*, 2011). Similarly, RhoA protein depletion in the breast cancer cell lines, SUM-159 and MCF-7, increased cell invasion in a transwell invasion assay (Matrigel coated) (Simpson *et al.*, 2004). Moreover, the reduction in β1 integrin in MDA-MB-231 breast cancer cells is associated with decreased RhoA activity and increased invasion (Costa *et al.*, 2013). An enhancement of cortactin was observed at the invasive front of cells invading through Matrigel and a collagen I/Matrigel mix when RhoA expression was diminished in MDA-MB-231 cells. This supports the hypothesis that RhoA reduction enhances invasiveness (Vega *et al.*, 2011).

Contradictory results found that a reduction in RhoA expression in MDA-MB-231 cells reduces the lung metastasis in an *in vivo* murine tail injection assay (Valastyan *et al.*, 2009) and RhoA overexpression in rat MM1 hepatoma cells enhances peritoneal invasion (Yoshioka *et al.*, 1999). These differing findings suggest that the role of RhoA in invasion is complex and may be dependent on the assay itself, and the length of time that is given for invasion. Interestingly, of the three Rho isoforms, RhoA is the only isoform that can cause a reduction in cell invasion when

overexpressed (Ridley, 2013). This further validates the results of this study which indicate that PAK4 inhibition of PDZ-RhoGEF signals downstream to reduce the activation of RhoA in invadopodia.

RhoA is overexpressed in many different tumour types, including breast, colon and lung cancer tissue (Fritz *et al.*, 1999; Kamai *et al.*, 2001; Sahai and Marshall, 2002). In invasive melanoma cell lines such as A-375M2, the Rho-ROCK-MLC2 pathway is vital for invasion by promoting a highly contractile and motile, amoeboid phenotype in both a 3D *in vitro* assay and *in vivo* (Sahai and Marshall, 2003; Sanz-Moreno and Marshall, 2010). While this is in line with the findings in the current study which suggest that RhoA activity is regulated within invadopodia, a localised lapse in cell contractility would be required to allow for the outgrowth of the membrane and the formation of these invasive protrusions. This may be achieved through the spatiotemporal reduction in RhoA via PAK4 inhibition of PDZ-RhoGEF.

As with the global impact of RhoA, studies investigating the role played by this protein in invadopodia formation provide contradictory results. Bravo-Cordero and colleagues, detected no localised variation in RhoA activity at invadopodia structures in the MTLn3 rat mammary adenocarcinoma cell line (Bravo-Cordero *et al.*, 2011). However, observation of the published FRET timelapse images, reveal the cells to have very high global RhoA activity which may result in signal saturation, preventing the observation of subtle changes in RhoA activity. Furthermore, a decrease in RhoA expression in these cells reduced invadopodia formation and degradation. This is not surprising given that RhoA activity promotes the interaction of the Ras GTPase-activating-like protein IQGAP1 with Sec3 and Sec8 exocyst subunits to tether cargo, such as vesicles containing MMPs, to invadopodia for matrix degradation (Sakurai-Yageta *et al.*, 2008).

In contrast, other studies using active and dominant negative RhoA indicated that this protein had no effect on invadopodia degradation in RPMI7951 melanoma cells (Nakahara *et al.*, 2003), while PIP3 induced RhoA inactivation (via the recruitment of ARAP3) resulted in podosome formation in rat embryonic fibroblast (REF52) cells (Yu *et al.*, 2013). Furthermore, expression of constitutively active RhoA in NIH3T3 cells reduced v-Src induced podosomes (Schramp *et al.*, 2008) and this was supported by a later study in which a constitutively active RhoA mutant or the stimulation of RhoA via LPA eliminated podosome formation (Yu *et al.*, 2013). The importance of RhoA in invasive protrusions is further supported by the fact that the stimulation of dendritic cells with prostaglandin E2 (PGE_2) activates the RhoA-ROCK pathway which promotes the dissolution of podosomes (van Helden *et al.*, 2008). Interestingly, the expression of a dominant negative RhoA mutant results in disorganisation of v-Src induced podosomes in

NIH3T3 cells (Berdeaux *et al.*, 2004). Furthermore, both a constitutively active and dominant negative RhoA mutant reduced the podosome induced degradation by v-Src NIH3T3 cells (Berdeaux *et al.*, 2004). These findings suggest that a balance of RhoA activity and inactivation may be important for podosome function. Therefore, it is likely that RhoA and its activity, play a complex role in invadopodia formation, with differing activation states being present during the life cycle of the protrusion.

Invadopodia formation is controlled by actin polymerisation and microtubule dynamics, which are both influenced by RhoA activity (Schoumacher *et al.*, 2010; O'Connor and Chen, 2013). RhoA is a central player in membrane protrusions and cell contractility, and thus there are multiple pathways that this GTPase may influence in invadopodia formation. One such pathway involves the promotion of ROCK phosphorylation by RhoA and subsequent phosphorylation of LIMK (Maekawa *et al.*, 1999). LIMK phosphorylates and inhibits cofilin, a protein that binds and severs actin filaments, allowing the binding of the Arp2/3 complex to form a nucleation core for branched actin polymerisation. This nucleation core also promotes actin depolymerisation to provide a pool of free actin for new actin polymerisation (Carlier *et al.*, 1999; Ridley, 2011). The importance of cofilin function was recently reported *in vivo,* using *C. elegans* (Hagedorn *et al.*, 2014). In this study, active cofilin was found to be essential for the creation of discrete invadopodia-like structures and to promote actin recycling for protrusion turnover. However, despite cofilin being a target for RhoA, the depletion of this GTPase did not change the p-Cofilin levels in invasive MTLn3 cells (Bravo-Cordero *et al.*, 2011).

As discussed previously, RhoA is a central protein in controlling cell contractility with RhoA activated ROCK activating MLC by direct phosphorylation and by phosphorylating and inhibiting myosin phosphatase (an inactivator of MLC) to enhance myosin induced actin contractility (O'Connor and Chen, 2013). Therefore, localised inhibition of this contractility (by inhibiting RhoA activity) at invadopodia would allow for the membrane to extend away from the cell body to form the protrusion. However, additional investigations, which could include the inhibition of myosin II contractility using blebbistatin (Sanz-Moreno *et al.*, 2008) in cells with reduced PAK4 expression, are needed to elucidate this pathway further.

This study demonstrates that PAK1 and PAK4 are involved in key pathways in melanoma cell invasion, with some of these pathways being shared by both proteins while others are distinct. While we have begun to tease out the details of these pathways including signalling through PDZ-RhoGEF and RhoA, additional studies are required to provide further insight. However, the data obtained so far certainly suggests that PAK1 and PAK4 are potential therapeutic targets for

treating metastatic melanoma, with targeting of both isoforms likely to be a more effective treatment than targeting either protein individually.

6 Chapter 6 - Concluding Remarks

The majority of deaths from cancer are as a result of metastasis (>90%) (Valastyan and Weinberg, 2011). This is particularly true for melanoma in which a dramatic reduction in patient five year survival is evident from primary (98%) to regional (62%) to distant (16%) metastatic disease (American Cancer Society, 2014). This considerable drop in survival in melanoma patients with metastatic disease highlights the importance of understanding this invasive process. This study used the invadopodia assay as an indicator of invasive potential, along with a 3D and an *in vivo* invasion assay, to investigate the role of PAK1 and PAK4 in melanoma invasion. Invadopodia are actin rich protrusions that secrete proteases to degrade the ECM and are formed by many invasive tumour cell lines in 2D invadopodia assays (Artym *et al.*, 2006; Ayala *et al.*, 2008; Schoumacher *et al.*, 2010). However, there is still debate about whether these protrusions are formed and used by cells *in vivo,* and are not therefore artefacts of long term cell culture.

Conflicting views exist over the presence and use of invadopodia in 3D matrices and *in* vivo, primarily due to the difficultly in visualising this protrusion. In 3D, new techniques have been utilised to allow the high resolution imaging of invadopodia-like degradative structures in cells, embedded in collagen (Yu and Machesky, 2012). In addition, recent studies have visualised invadopodia-like protrusions that were positive for cortactin and had local degradation (proteolytic activity) in xenografted mammary fat pad tumours (MTLn3 cell line) (Gligorijevic *et al.*, 2012). Furthermore, these cells formed invadopodia-like structures that extended into blood vessels during intravasation, suggesting a role for this invasive protrusion *in vivo* (Yamaguchi *et al.*, 2005b). In an additional study, glioma cells derived from the tissue of two patients (with metastatic disease) had the ability to form invadopodia *in vitro* (Stylli *et al.*, 2008). Though these studies provide some indication that invadopodia do occur in an *in vivo* setting, they still utilise cell lines rather than native tumour cells. However, in a recent study, anchor cells utilising invadopodial-like protrusions were imaged invading through the basement membrane in *C. Elegans* (Hagedorn *et al.*, 2014). This study demonstrated that native invasive cells use invasive protrusions to cross the basement membrane, thus providing evidence that invasive protrusions do occur *in vivo*. In this study patient derived cell strains were established from both human primary and metastatic melanoma tissue and it was demonstrated that melanoma cells from patients can produce invadopodia protrusions in culture (Chapter 3). The ability of these patient derived cells to form invadopodia *in vitro* suggests that these cells may also have the capacity to do so when in the patient. These findings therefore complement the previous studies described

above which suggest a role for invadopodia *in* vivo and highlight the need for a better understanding of these structures as a potential therapeutic target.

There is some evidence that PAKs are involved in invadopodia function (Ayala *et al.*, 2008; Moshfegh *et al.*, 2014). PAK isoforms (of which there are 6) are overexpressed in a wide variety of human tumours such as breast, colon, prostate and ovarian cancer (Radu *et al.*, 2014). However, the role of these proteins in melanoma invasion is undefined. Therefore, this study firstly looked at the PAK isoform protein expression in melanoma, with initial experiments being focused on the quantification of protein expression of the six PAK isoforms in melanoma cells compared to a melanocyte control. Of the PAK family of proteins, PAK1, PAK2 and PAK4 were overexpressed in melanoma cell lines (Chapter 4). These expression levels were subsequently compared to the previously characterised invasive potential (Chapter 3) to identify any correlations that may suggest a role for these proteins in melanoma invasion. PAK1overexpression correlated with melanoma cell line invadopodia formation capacity. A correlation with invadopodia capacity was also seen with PAK2, however this was a weaker, inverse correlation and thus PAK1 was chosen over PAK2 for further investigation of the group I PAKs. PAK4 showed a general overexpression in all melanoma cells. In line with these results, PAK1 and PAK4 were also found to be overexpressed in the patient derived cell strains that formed invadopodia. Thus, further exploration of the role of PAK1 and PAK4 in invadopodia was undertaken. Depletion of PAK1 and PAK4 protein expression in melanoma cell lines reduced the percentage of cells with invadopodia and the invadopodial induced matrix degradation, suggesting that both proteins are important in promoting invadopodia function (Section 4.2.4). The effect of PAK1 and PAK4 on the global invasive capacity was also confirmed in complementary 3D invasion and *in vivo* assays, which showed a reduction in melanoma invasion when both proteins were depleted (Chapter 4).

PAK1 has been previously found to promote the cell invasion of colon cancer (Huynh *et al.*, 2010) and breast cancer cell lines (Coniglio *et al.*, 2008). Similarly, PAK4 promotes the cell invasion of choriocarcinoma (Zhang *et al.*, 2011) and endometrial cancer (Lu *et al.*, 2013). Moreover, in skin cancer specifically, PAK1 and PAK4 promote cell invasion of uveal melanoma (Pavey *et al.*, 2006) and SCC (Zanivan *et al.*, 2013) cell lines, respectively. Therefore, the data obtained from this study, is in line with that produced in other investigations. This provides key evidence that these two proteins are important in melanoma cell invasion and solidifies the data obtained in other studies which suggest that these proteins are globally important in cancer invasion.

This study suggests that both PAK1 and PAK4 play a role in melanoma invasion. But do these proteins function through the same pathway? The PAKs from group I and group II (including PAK1 and PAK4, respectively), are activated differently (King *et al.*, 2014). However little is known about the unique signalling pathways or the substrates of these two groups and how these differences may impact on the effect that these proteins have on the invasive potential of tumours (Arias-Romero and Chernoff, 2008). Research into these potential differences could help guide the further development of therapeutic drugs. Currently, pharmaceutical companies are focused on developing group or isoform specific inhibitors (Viaud and Peterson, 2009; Murray *et al.*, 2010; Zhang *et al.*, 2012). Therefore, data indicating whether both groups contribute to invasion and metastasis in the same way, may determine whether the use of cross reactive inhibitors is more beneficial than isoform specific inhibitors in treating some cancers types. This study seeks to help address this question by identifying differences in PAK1 and PAK4 (representing the group I and group II PAKs respectively) signalling pathways. Our findings revealed distinct functional roles for PAK1 and PAK4 in invadopodia, with PAK1 promoting the formation of this protrusion while PAK4 functions in the maturation and/or degradation stage of the invadopodial lifecycle (Figure 6-1).

Our hypothesis (Figure 6-1) of a differential function is defined by our specific findings. Depletion of PAK1 reduced both the percentage of cells with invadopodia and also the matrix degradation for those cells that formed invadopodia (Section 4.2.4). In addition, reduction of PAK1 protein expression also reduced the number of nascent invadopodia actin puncta, suggesting an important role for this protein in the initial stages of the invadopodial lifecycle (Section 5.2.3). Together, our results indicate that PAK1 promotes the initial formation of invadopodia protrusions. Several investigations have been conducted into the function of PAK1 in the invadopodia-like protrusion, podosomes. Within these studies reduced PAK1 activity resulted in a decrease in podosome formation (Furmaniak-Kazmierczak *et al.*, 2007) and increased PAK1 expression enhanced the formation of this protrusion (Webb *et al.*, 2005). However, while it is known that PAK1 localises to invadopodia (Moshfegh *et al.*, 2014), recent findings have suggested several contradictory roles for PAK1 in invadopodia function. Some studies suggest that PAK1 is important for the formation of invadopodia - inhibition of endogenous PAK1 protein (using the PAK1 AID) reduced the formation of invadopodia in the A-375MM melanoma cell line, via the phosphorylation of cortactin at Ser^{113} (Ayala *et al.,* 2008). In contrast a more recent study suggests that PAK1 (once again via the phosphorylation of cortactin at Ser^{113}), promotes the disassembly of invadopodia protrusions, with a depletion of PAK1 resulting in an increase in

matrix degradation (Moshfegh *et al.*, 2014). Therefore, this study strengthens the argument that PAK1 is important for the formation of invadopodia protrusions.

In addition, PAK1 may also contribute to the maturation/degradation stage of the invadopodia lifecycle as the depletion of PAK1 also reduced matrix degradation (Section 4.2.4). This complements previous studies which suggest that PAK1 promotes MMP-9 expression (Goc *et al.*, 2013) and the secretion of MMP-1 and MMP-3 (Rider *et al.*, 2013).

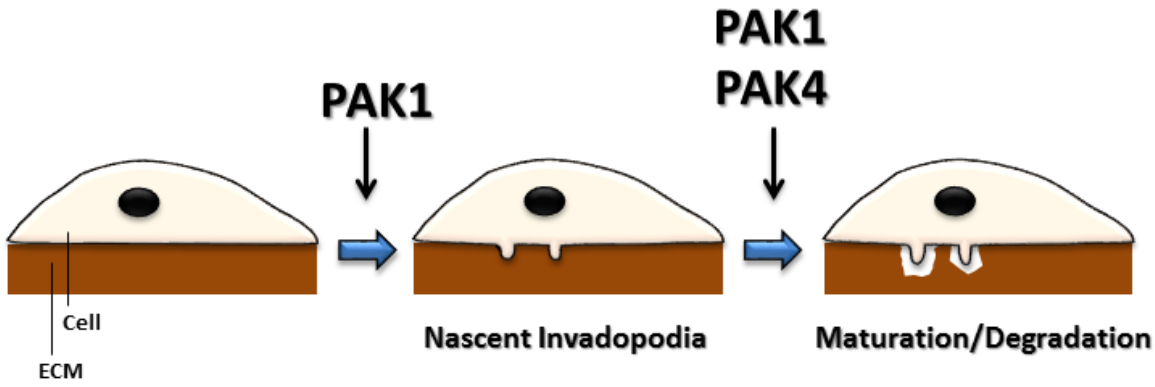

Figure 6-1: Possible functions for PAK1 and PAK4 in the invadopodial lifecycle.
PAK1 plays a role in the formation of nascent invadopodia. PAK1 and PAK4 both function in the maturation/degradation stage of the invadopodial lifecyle.

Findings here suggest that PAK4 does not play a role in the initial stages of invadopodia formation, as a reduction in PAK4 protein expression did not reduce the formation of nascent invadopodial actin puncta (Section 5.2.3). This study does show for the first time that PAK4 promotes invadopodia function and is likely to be important in invadopodial maturation and degradation (Figure 6-1). These claims are supported by the localisation of PAK4 to invadopodia (Section 5.2.12) and the fact that the depletion of PAK4 in melanoma cell lines resulted in a reduction in the percentage of cells with invadopodia and invadopodial induced matrix degradation (Section 4.2.4). In addition, the overexpression of GFPPAK4 in cells with depleted PAK1 expression rescued the matrix degradation capacity of those invadopodia that still formed, back to that seen by control cells, further suggesting an important role for PAK4 in invadopodia matrix degradation (Section 5.2.1). This complements previous studies in which PAK4 was found to promote the expression of proteases involved in matrix degradation such as MMP-2 (Siu *et*

al., 2010a; Kesanakurti *et al.*, 2012) and MT1-MMP (Zhang *et al.*, 2011). Our data is also in line with the role of PAK4 in podosomes, in which this kinase was shown to localise to podosomes as well as promote their function (Gringel *et al.*, 2006; Wells and Jones, 2010).

In addition to demonstrating that PAK1 and PAK4 promote invadopodial function, this study has identified a signalling pathway, unique to PAK4 (and not shared by PAK1), utilized during the invadopodia lifecycle in melanoma cells (Chapter 5). Our findings suggest that PAK4 (localised to invadopodia), inhibits the function of PDZ-RhoGEF (a Rho GEF) to promote the formation and degradation of invadopodia. This is unique to PAK4 as the binding and inhibition of PDZ-RhoGEF by PAK4 is not shared by PAK1 (Barac *et al.*, 2004; Rosenfeldt *et al.*, 2006). In addition, it is proposed that this pathway may signal via RhoA (Figure 6-2). This study is the first time that the relevance of these differing interactions has been investigated in the context of cancer invasion.

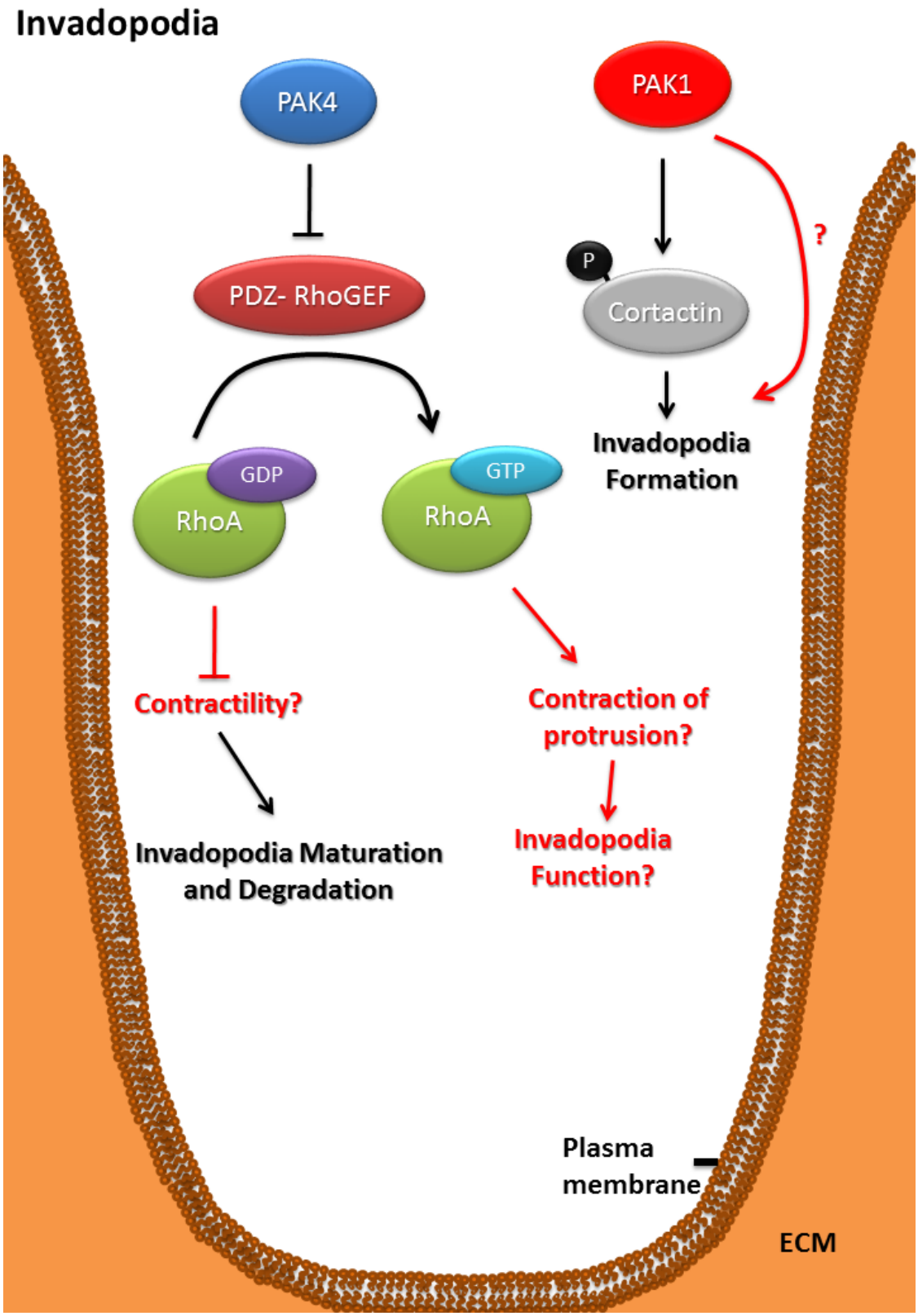

Figure 6-2: Unique PAK4 pathway in the function of invadopodia protrusions.
PAK4, localised to the invadopodia protrusion, inhibits the function of PDZ-RhoGEF. This in turn prevents the activation of RhoA to promote invadopodial maturation and degradation. This may be through the inhibition of membrane contraction. Active RhoA may function in invadopodia to retract the protrusion during disassembly. Speculative pathways are labelled in red. PAK1 does not signal through PDZ-RhoGEF in invadopodia. It may function via the phosphorylation of cortactin or another substrate.

The unique PAK4/PDZ-RhoGEF pathway was confirmed by the use of a dominant negative mutant of PDZ-RhoGEF which could bind, but not activate Rho (Hart *et al.*, 1994; Driessens *et al.*, 2002; Kasai *et al.*, 2004). The expression of this mutant in cells with depleted PAK4 protein resulted in the rescue of invadopodia formation and degradation back to levels seen by wildtype cells (Section 5.2.10). Furthermore, the expression of wildtype PDZ-RhoGEF mimicked a PAK4 depletion phenotype, reducing the percentage of cells with invadopodia and the invadopodial induced matrix degradation (Section 5.2.11). PDZ-RhoGEF, along with PAK4 was found to be localised to invadopodia supporting the suggestion that the proposed signalling pathway occurs within these protrusions (Section 5.2.12). This localisation also suggests that RhoA activation is likely required at some stage during the lifecycle of the protrusion (low levels of Rho activity in invadopodia can be easily achieved by the localisation of PDZ-RhoGEF away from the protrusion).

This study proposes that RhoA is the GTPase downstream of the PAK4/PDZ-RhoGEF pathway, in invadopodia. Several findings support this proposal including the fact that PAK4 depleted cells had an increased RhoA activity while PAK1 depleted cells did not (Section 5.2.7). Furthermore PDZ-RhoGEF is known to be specific for Rho, with no binding to Cdc42 or Rac1, with this GEF preferentially activating RhoA, over RhoB and RhoC (Jaiswal *et al.*, 2011).

Investigations into the function of RhoA in invadopodia have yielded contradictory results. Some studies have suggested that reduced RhoA expression decreases invadopodia formation and degradation (Bravo-Cordero *et al.*, 2011), while others have found no effect on invadopodia degradation when RhoA activation is inhibited or activated (Nakahara *et al.*, 2003). However, work with podosomes have indicated that RhoA inactivation is required for podosome formation (Yu *et al.*, 2013) and that the constitutive activation of this protein reduces podosome formation (Schramp *et al.*, 2008; Yu *et al.*, 2013). It has been suggested that a balance of RhoA activation and inactivation is important for podosome function with both the constitutive activation and reduction of RhoA activity resulting in reduced podosome degradation (Berdeaux *et al.*, 2004). Our findings suggest that the same may be true for invadopodia function and provide additional evidence that the control of RhoA activity is important in invadopodia function.

To date, the mechanism by which the PAK4/PDZ-RhoGEF/RhoA pathway functions in invadopodia is unknown. RhoA plays a key role in the actin cytoskeletal dynamics and actomyosin contractility which is important in the formation of protrusions such as invadopodia (Schoumacher *et al.*, 2010; O'Connor and Chen, 2013). Therefore, one potential mechanism by

which the inhibition of RhoA brought about by the PAK4/PDZ-RhoGEF/RhoA pathway can function at invadopodia, is through a reduction in the contractile force exerted on the protrusion to allow for the extension of the membrane. Furthermore, with RhoA activation being important for focal adhesions (incorporation of stress fibres), which is often associated with invadopodia dissolution, RhoA inactivation at invadopodia may tip the balance away from focal adhesion formation to promote invadopodia formation.

In conclusion, this study had provided evidence that PAK1 and PAK4 play an important role in melanoma cell invasion. In addition it has been demonstrated that these two isoforms have distinct pathways in invadopodia function, with PAK4 promoting maturation and/or degradation through the localised inhibition of PDZ-RhoGEF. Very crucially, this study suggests a potential key role for inhibitors that bind to, and thus block the function of, both the group I and group II PAKs, as a treatment for melanoma. One such candidate could be the PF-3758309 inhibitor, which has *in vitro* activity towards both PAK1 (~14nM) and PAK4 (~19nM) (Murray *et al.*, 2010). Such inhibitors may reduce the metastasis of this cancer type, thus potentially improving patient prognosis.

6.1 Future Work

Based on the findings in this study, PAK1 and PAK4 both promote melanoma cell invasion. To further validate the role that these two proteins play in melanoma, staining (using immunohistochemistry) of primary and metastatic tissue samples could be performed and correlated with patient clinical outcomes. This would give insight into the prognostic implications that overexpression of these protein have in melanoma.

There remains controversy over the function that PAK1 plays in invadopodia formation (Ayala *et al.*, 2008; Moshfegh *et al.*, 2014). Further experiments utilising the melanoma cell lines could be performed to investigate the effect of PAK1 depletion on cortactin phosphorylation at Ser^{113}. Moreover, the use of a PAK1 biosensor, in conjunction with FRET and timelapse microscopy, could reveal the extent of PAK1 participation throughout the lifecycle of the invadopodia protrusion. This would help determine whether PAK1 activation is important during invadopodia formation, disassembly, or even both.

This study found that PAK4 and PDZ-RhoGEF are localised to invadopodia and that PDZ-RhoGEF can rescue the formation and degradation of invadopodia in PAK4 knockdown cells, suggesting

an interaction between these proteins. To validate the requirement of RhoA, supplemental experiments can be performed, including the depletion of RhoA protein expression to investigate the effect on invadopodia function, as well as the quantification of RhoA activity through the invadopodia lifecycle using a RhoA biosensor with FRET and timelapse microscopy. The FRET experiments could also be performed with cells that have depleted PAK4 expression. In addition, the effect of PDZ-RhoGEF protein knockdown on invadopodia function could also provide valuable information to validate the role of PDZ-RhoGEF in the activity of this protrusion. A significant amount of the data generated in this study point to the importance of PAK4 in the maturation and degradation stage of the invadopodia lifecycle. This could be further explored by quantifying both the MMP expression levels and the secreted proteins (in cultured media) in melanoma cells that have PAK4 depletion, in cells that have expression of PDZ-RhoGEFΔDH in a PAK4 depleted background, and in cells overexpressing PDZ-RhoGEF. An investigation into whether the PAK4/PDZ-RhoGEF pathway also plays a central role in the 3D spheroid invasion assay would provide valuable confirmation as to the importance of this pathway in invasion. This can be done by depleting both PDZ-RhoGEF and PAK4 expression simultaneously (using siRNA oligonucleotide transfection) and investigating in a 3D spheroid assay, whether this can rescue the invasive phenotype of melanoma cells in which only PAK4 is depleted.

Additional further work would certainly shed more light on, and increase our understanding of the signalling pathways involved in invadopodia formation and melanoma invasion. However, this current study offers key insights into the role of PAK1 and PAK4 in melanoma invasion and can therefore help guide the future direction of research into metastatic melanoma.

7 References

American Cancer Society. Cancer Facts and Figures, 2011. American Cancer Society. Accessed 24/04/2014. Available online: http://www.cancer.org/research/cancerfactsstatistics/cancerfactsfigures2011/index.

Melanoma Research Foundation Staging Melanoma - Melanoma Diagnostic Indicators, 2011. Accessed 28/06/2014. Available online: http://www.melanoma.org/learn-more/melanoma-101/staging-melanoma

American Cancer Society. Cancer Facts and Figures, 2014. American Cancer Society. Accessed 24/04/2014. Available online: http://www.cancer.org/research/cancerfactsstatistics/cancerfactsfigures2014/index.

Cancer Research UK. Skin cancer Key Facts, 2014. Accessed 22/05/2014. Available online: http://www.cancerresearchuk.org/cancer-info/cancerstats/keyfacts/skin-cancer/.

Abo, A., Qu, J., Cammarano, M. S., Dan, C., Fritsch, A., Baud, V., Belisle, B. and Minden, A. (1998). "PAK4, a novel effector for Cdc42Hs, is implicated in the reorganization of the actin cytoskeleton and in the formation of filopodia." EMBO J **17**(22): 6527-6540.

Adam, L., Vadlamudi, R., Kondapaka, S. B., Chernoff, J., Mendelsohn, J. and Kumar, R. (1998). "Heregulin regulates cytoskeletal reorganization and cell migration through the p21-activated kinase-1 via phosphatidylinositol-3 kinase." J Biol Chem **273**(43): 28238-28246.

Adam, L., Vadlamudi, R., Mandal, M., Chernoff, J. and Kumar, R. (2000). "Regulation of microfilament reorganization and invasiveness of breast cancer cells by kinase dead p21-activated kinase-1." J Biol Chem **275**(16): 12041-12050.

Ahmed, T., Shea, K., Masters, J. R., Jones, G. E. and Wells, C. M. (2008). "A PAK4-LIMK1 pathway drives prostate cancer cell migration downstream of HGF." Cell Signal **20**(7): 1320-1328.

Ahn, H. K., Jang, J., Lee, J., Se Hoon, P., Park, J. O., Park, Y. S., Lim, H. Y., Kim, K. M. and Kang, W. K. (2011). "P21-activated kinase 4 overexpression in metastatic gastric cancer patients." Transl Oncol **4**(6): 345-349.

Alahari, S. K., Reddig, P. J. and Juliano, R. L. (2004). "The integrin-binding protein Nischarin regulates cell migration by inhibiting PAK." EMBO J **23**(14): 2777-2788.

Alblas, J., Ulfman, L., Hordijk, P. and Koenderman, L. (2001). "Activation of Rhoa and ROCK are essential for detachment of migrating leukocytes." Mol Biol Cell **12**(7): 2137-2145.

Alexander, N. R., Branch, K. M., Parekh, A., Clark, E. S., Iwueke, I. C., Guelcher, S. A. and Weaver, A. M. (2008). "Extracellular matrix rigidity promotes invadopodia activity." Curr Biol **18**(17): 1295-1299.

Amatruda, J. F., Shepard, J. L., Stern, H. M. and Zon, L. I. (2002). "Zebrafish as a cancer model system." Cancer Cell **1**(3): 229-231.

Aoyama, A. and Chen, W. T. (1990). "A 170-kDa membrane-bound protease is associated with the expression of invasiveness by human malignant melanoma cells." Proc Natl Acad Sci U S A **87**(21): 8296-8300.

Arias-Romero, L. E. and Chernoff, J. (2008). "A tale of two Paks." Biol Cell **100**(2): 97-108.

Artym, V. V., Zhang, Y., Seillier-Moiseiwitsch, F., Yamada, K. M. and Mueller, S. C. (2006). "Dynamic interactions of cortactin and membrane type 1 matrix metalloproteinase at invadopodia: defining the stages of invadopodia formation and function." Cancer Res **66**(6): 3034-3043.

Ayala, I., Baldassarre, M., Giacchetti, G., Caldieri, G., Tete, S., Luini, A. and Buccione, R. (2008). "Multiple regulatory inputs converge on cortactin to control invadopodia biogenesis and extracellular matrix degradation." J Cell Sci **121**(Pt 3): 369-378.

Balch, C. M., Buzaid, A. C., Soong, S. J., Atkins, M. B., Cascinelli, N., Coit, D. G., Fleming, I. D., Gershenwald, J. E., Houghton, A., Jr., Kirkwood, J. M., McMasters, K. M., Mihm, M. F., Morton, D. L., Reintgen, D. S., Ross, M. I., Sober, A., Thompson, J. A. and Thompson, J. F. (2001). "Final version of the American Joint Committee on Cancer staging system for cutaneous melanoma." J Clin Oncol **19**(16): 3635-3648.

Balch, C. M., Gershenwald, J. E., Soong, S. J., Thompson, J. F., Atkins, M. B., Byrd, D. R., Buzaid, A. C., Cochran, A. J., Coit, D. G., Ding, S., Eggermont, A. M., Flaherty, K. T., Gimotty, P. A., Kirkwood, J. M., McMasters, K. M., Mihm, M. C., Jr., Morton, D. L., Ross, M. I., Sober, A. J. and Sondak, V. K. (2009). "Final version of 2009 AJCC melanoma staging and classification." J Clin Oncol **27**(36): 6199-6206.

Baldassarre, M., Ayala, I., Beznoussenko, G., Giacchetti, G., Machesky, L. M., Luini, A. and Buccione, R. (2006). "Actin dynamics at sites of extracellular matrix degradation." Eur J Cell Biol **85**(12): 1217-1231.

Baldassarre, M., Pompeo, A., Beznoussenko, G., Castaldi, C., Cortellino, S., McNiven, M. A., Luini, A. and Buccione, R. (2003). "Dynamin participates in focal extracellular matrix degradation by invasive cells." Mol Biol Cell **14**(3): 1074-1084.

Barac, A., Basile, J., Vazquez-Prado, J., Gao, Y., Zheng, Y. and Gutkind, J. S. (2004). "Direct interaction of p21-activated kinase 4 with PDZ-RhoGEF, a G protein-linked Rho guanine exchange factor." J Biol Chem **279**(7): 6182-6189.

Barber, P. R., Ameer-Beg, S. M., Gilbey, J., Carlin, L. M., Keppler, M., Ng, T. C. and Vojnovic, B. (2009). "Multiphoton time-domain fluorescence lifetime imaging microscopy: practical application to protein-protein interactions using global analysis." Journal of the Royal Society Interface **6**: S93-S105.

Baskaran, Y., Ng, Y. W., Selamat, W., Ling, F. T. and Manser, E. (2012). "Group I and II mammalian PAKs have different modes of activation by Cdc42." EMBO Rep **13**(7): 653-659.

Beaty, B. T., Sharma, V. P., Bravo-Cordero, J. J., Simpson, M. A., Eddy, R. J., Koleske, A. J. and Condeelis, J. (2013). "beta1 integrin regulates Arg to promote invadopodial maturation and matrix degradation." Mol Biol Cell **24**(11): 1661-1675, S1661-1611.

Becker, J. C., Kampgen, E. and Brocker, E. (2000). "Classical chemotherapy for metastatic melanoma." Clin Exp Dermatol **25**(6): 503-508.

Berdeaux, R. L., Diaz, B., Kim, L. and Martin, G. S. (2004). "Active Rho is localized to podosomes induced by oncogenic Src and is required for their assembly and function." J Cell Biol **166**(3): 317-323.

Bishop, A. L. and Hall, A. (2000). "Rho GTPases and their effector proteins." Biochem J **348 Pt 2**: 241-255.

Bishop, J. N., Bataille, V., Gavin, A., Lens, M., Marsden, J., Mathews, T. and Wheelhouse, C. (2007). "The prevention, diagnosis, referral and management of melanoma of the skin: concise guidelines." Clin Med **7**(3): 283-290.

Bizik, J., Trancikova, D., Felnerova, D., Sedlakova, O., Kudela, P. and Vaheri, A. (1999). Invasion of human melanoma cells into dermal equivalents. Intermolecular Cross-Talk in Tumor Metastasis. G. G. Skouteris and G. L. Nicolson, IOS Press. **311:** 79-93.

Bokoch, G. M. (2003). "Biology of the p21-activated kinases." Annu Rev Biochem **72**: 743-781.

Bokoch, G. M., Wang, Y., Bohl, B. P., Sells, M. A., Quilliam, L. A. and Knaus, U. G. (1996). "Interaction of the Nck adapter protein with p21-activated kinase (PAK1)." J Biol Chem **271**(42): 25746-25749.

Bowden, E. T., Barth, M., Thomas, D., Glazer, R. I. and Mueller, S. C. (1999). "An invasion-related complex of cortactin, paxillin and PKCmu associates with invadopodia at sites of extracellular matrix degradation." Oncogene **18**(31): 4440-4449.

Bravo-Cordero, J. J., Oser, M., Chen, X., Eddy, R., Hodgson, L. and Condeelis, J. (2011). "A novel spatiotemporal RhoC activation pathway locally regulates cofilin activity at invadopodia." Curr Biol **21**(8): 635-644.

Breslow, A. (1970). "Thickness, cross-sectional areas and depth of invasion in the prognosis of cutaneous melanoma." Ann Surg **172**(5): 902-908.

Bright, M. D., Garner, A. P. and Ridley, A. J. (2009). "PAK1 and PAK2 have different roles in HGF-induced morphological responses." Cell Signal **21**(12): 1738-1747.

Bromann, P. A., Korkaya, H. and Courtneidge, S. A. (2004). "The interplay between Src family kinases and receptor tyrosine kinases." Oncogene **23**(48): 7957-7968.

Buccione, R., Caldieri, G. and Ayala, I. (2009). "Invadopodia: specialized tumor cell structures for the focal degradation of the extracellular matrix." Cancer Metastasis Rev **28**(1-2): 137-149.

Buccione, R., Orth, J. D. and McNiven, M. A. (2004). "Foot and mouth: podosomes, invadopodia and circular dorsal ruffles." Nat Rev Mol Cell Biol **5**(8): 647-657.

Burbelo, P. D., Kozak, C. A., Finegold, A. A., Hall, A. and Pirone, D. M. (1999). "Cloning, central nervous system expression and chromosomal mapping of the mouse PAK-1 and PAK-3 genes." Gene **232**(2): 209-215.

Caldieri, G., Giacchetti, G., Beznoussenko, G., Attanasio, F., Ayala, I. and Buccione, R. (2009). "Invadopodia biogenesis is regulated by caveolin-mediated modulation of membrane cholesterol levels." J Cell Mol Med **13**(8B): 1728-1740.

Callow, M. G., Clairvoyant, F., Zhu, S., Schryver, B., Whyte, D. B., Bischoff, J. R., Jallal, B. and Smeal, T. (2002). "Requirement for PAK4 in the anchorage-independent growth of human cancer cell lines." J Biol Chem **277**(1): 550-558.

Callow, M. G., Zozulya, S., Gishizky, M. L., Jallal, B. and Smeal, T. (2005). "PAK4 mediates morphological changes through the regulation of GEF-H1." J Cell Sci **118**(Pt 9): 1861-1872.

Calvo, F., Sanz-Moreno, V., Agudo-Ibanez, L., Wallberg, F., Sahai, E., Marshall, C. J. and Crespo, P. (2011). "RasGRF suppresses Cdc42-mediated tumour cell movement, cytoskeletal dynamics and transformation." Nat Cell Biol **13**(7): 819-826.

Carlier, M. F., Ressad, F. and Pantaloni, D. (1999). "Control of actin dynamics in cell motility. Role of ADF/cofilin." J Biol Chem **274**(48): 33827-33830.

Cau, J. and Hall, A. (2005). "Cdc42 controls the polarity of the actin and microtubule cytoskeletons through two distinct signal transduction pathways." J Cell Sci **118**(Pt 12): 2579-2587.

Cavallaro, U. and Christofori, G. (2001). "Cell adhesion in tumor invasion and metastasis: loss of the glue is not enough." Biochim Biophys Acta **1552**(1): 39-45.

Chambers, A. F., Groom, A. C. and MacDonald, I. C. (2002). "Dissemination and growth of cancer cells in metastatic sites." Nat Rev Cancer **2**(8): 563-572.

Chan, K. T., Cortesio, C. L. and Huttenlocher, A. (2009). "FAK alters invadopodia and focal adhesion composition and dynamics to regulate breast cancer invasion." J Cell Biol **185**(2): 357-370.

Chen, H., Miao, J., Li, H., Wang, C., Li, J., Zhu, Y., Wang, J., Wu, X. and Qiao, H. (2014). "Expression and prognostic significance of p21-activated kinase 6 in hepatocellular carcinoma." J Surg Res **189**(1): 81-88.

Chen, W. T. (1989). "Proteolytic activity of specialized surface protrusions formed at rosette contact sites of transformed cells." J Exp Zool **251**(2): 167-185.

Chen, W. T., Chen, J. M., Parsons, S. J. and Parsons, J. T. (1985). "Local degradation of fibronectin at sites of expression of the transforming gene product pp60src." Nature **316**(6024): 156-158.

Chen, W. T., Lee, C. C., Goldstein, L., Bernier, S., Liu, C. H., Lin, C. Y., Yeh, Y., Monsky, W. L., Kelly, T., Dai, M. and et al. (1994). "Membrane proteases as potential diagnostic and therapeutic targets for breast malignancy." Breast Cancer Res Treat **31**(2-3): 217-226.

Chen, W. T., Olden, K., Bernard, B. A. and Chu, F. F. (1984). "Expression of transformation-associated protease(s) that degrade fibronectin at cell contact sites." J Cell Biol **98**(4): 1546-1555.

Chiang, A. C. and Massague, J. (2008). "Molecular basis of metastasis." N Engl J Med **359**(26): 2814-2823.

Ching, Y. P., Leong, V. Y., Lee, M. F., Xu, H. T., Jin, D. Y. and Ng, I. O. (2007). "P21-activated protein kinase is overexpressed in hepatocellular carcinoma and enhances cancer metastasis involving c-Jun NH2-terminal kinase activation and paxillin phosphorylation." Cancer Res **67**(8): 3601-3608.

Ching, Y. P., Leong, V. Y., Wong, C. M. and Kung, H. F. (2003). "Identification of an autoinhibitory domain of p21-activated protein kinase 5." J Biol Chem **278**(36): 33621-33624.

Chrzanowska-Wodnicka, M. and Burridge, K. (1996). "Rho-stimulated contractility drives the formation of stress fibers and focal adhesions." J Cell Biol **133**(6): 1403-1415.

Chuang, Y. Y., Tran, N. L., Rusk, N., Nakada, M., Berens, M. E. and Symons, M. (2004). "Role of synaptojanin 2 in glioma cell migration and invasion." Cancer Res **64**(22): 8271-8275.

Claffey, K. P., Brown, L. F., del Aguila, L. F., Tognazzi, K., Yeo, K. T., Manseau, E. J. and Dvorak, H. F. (1996). "Expression of vascular permeability factor/vascular endothelial growth factor by melanoma cells increases tumor growth, angiogenesis, and experimental metastasis." Cancer Res **56**(1): 172-181.

Clark, E. S. and Weaver, A. M. (2008). "A new role for cortactin in invadopodia: regulation of protease secretion." Eur J Cell Biol **87**(8-9): 581-590.

Clark, E. S., Whigham, A. S., Yarbrough, W. G. and Weaver, A. M. (2007). "Cortactin is an essential regulator of matrix metalloproteinase secretion and extracellular matrix degradation in invadopodia." Cancer Res **67**(9): 4227-4235.

Coniglio, S. J., Zavarella, S. and Symons, M. H. (2008). "Pak1 and Pak2 mediate tumor cell invasion through distinct signaling mechanisms." Mol Cell Biol **28**(12): 4162-4172.

Coopman, P. J., Do, M. T., Thompson, E. W. and Mueller, S. C. (1998). "Phagocytosis of cross-linked gelatin matrix by human breast carcinoma cells correlates with their invasive capacity." Clin Cancer Res **4**(2): 507-515.

Costa, P., Scales, T. M., Ivaska, J. and Parsons, M. (2013). "Integrin-specific control of focal adhesion kinase and RhoA regulates membrane protrusion and invasion." PLoS One **8**(9): e74659.

Davis, S. J., Sheppard, K. E., Pearson, R. B., Campbell, I. G., Gorringe, K. L. and Simpson, K. J. (2013). "Functional analysis of genes in regions commonly amplified in high-grade serous and endometrioid ovarian cancer." Clin Cancer Res **19**(6): 1411-1421.

Delorme-Walker, V. D., Peterson, J. R., Chernoff, J., Waterman, C. M., Danuser, G., DerMardirossian, C. and Bokoch, G. M. (2011). "Pak1 regulates focal adhesion strength, myosin IIA distribution, and actin dynamics to optimize cell migration." J Cell Biol **193**(7): 1289-1303.

Desai, B., Ma, T. and Chellaiah, M. A. (2008). "Invadopodia and matrix degradation, a new property of prostate cancer cells during migration and invasion." J Biol Chem **283**(20): 13856-13866.

Destaing, O., Planus, E., Bouvard, D., Oddou, C., Badowski, C., Bossy, V., Raducanu, A., Fourcade, B., Albiges-Rizo, C. and Block, M. R. (2010). "beta1A integrin is a master regulator of invadosome organization and function." Mol Biol Cell **21**(23): 4108-4119.

Dharmawardhane, S., Sanders, L. C., Martin, S. S., Daniels, R. H. and Bokoch, G. M. (1997). "Localization of p21-activated kinase 1 (PAK1) to pinocytic vesicles and cortical actin structures in stimulated cells." J Cell Biol **138**(6): 1265-1278.

Driessens, M. H., Olivo, C., Nagata, K., Inagaki, M. and Collard, J. G. (2002). "B plexins activate Rho through PDZ-RhoGEF." FEBS Lett **529**(2-3): 168-172.

Dummler, B., Ohshiro, K., Kumar, R. and Field, J. (2009). "Pak protein kinases and their role in cancer." Cancer Metastasis Rev **28**(1-2): 51-63.

Eguiara, A., Holgado, O., Beloqui, I., Abalde, L., Sanchez, Y., Callol, C. and Martin, A. G. (2011). "Xenografts in zebrafish embryos as a rapid functional assay for breast cancer stem-like cell identification." Cell Cycle **10**(21): 3751-3757.

Elloul, S., Vaksman, O., Stavnes, H. T., Trope, C. G., Davidson, B. and Reich, R. (2010). "Mesenchymal-to-epithelial transition determinants as characteristics of ovarian carcinoma effusions." Clin Exp Metastasis **27**(3): 161-172.

Etienne-Manneville, S. and Hall, A. (2003). "Cell polarity: Par6, aPKC and cytoskeletal crosstalk." Curr Opin Cell Biol **15**(1): 67-72.

Fogh, J. and Trempe, G. (1975). New Human Tumor Cell Lines. Human Tumor Cells *In Vitro*. J. Fogh, Springer US**:** 115-159.

Friedl, P. and Alexander, S. (2011). "Cancer invasion and the microenvironment: plasticity and reciprocity." Cell **147**(5): 992-1009.

Friedl, P. and Wolf, K. (2003). "Tumour-cell invasion and migration: diversity and escape mechanisms." Nat Rev Cancer **3**(5): 362-374.

Fritz, G., Just, I. and Kaina, B. (1999). "Rho GTPases are over-expressed in human tumors." Int J Cancer **81**(5): 682-687.

Fritz, R. D., Letzelter, M., Reimann, A., Martin, K., Fusco, L., Ritsma, L., Ponsioen, B., Fluri, E., Schulte-Merker, S., van Rheenen, J. and Pertz, O. (2013). "A versatile toolkit to produce sensitive FRET biosensors to visualize signaling in time and space." Sci Signal **6**(285): rs12.

Frost, J. A., Khokhlatchev, A., Stippec, S., White, M. A. and Cobb, M. H. (1998). "Differential effects of PAK1-activating mutations reveal activity-dependent and -independent effects on cytoskeletal regulation." J Biol Chem **273**(43): 28191-28198.

Furmaniak-Kazmierczak, E., Crawley, S. W., Carter, R. L., Maurice, D. H. and Cote, G. P. (2007). "Formation of extracellular matrix-digesting invadopodia by primary aortic smooth muscle cells." Circ Res **100**(9): 1328-1336.

Gadea, G., Sanz-Moreno, V., Self, A., Godi, A. and Marshall, C. J. (2008). "DOCK10-mediated Cdc42 activation is necessary for amoeboid invasion of melanoma cells." Curr Biol **18**(19): 1456-1465.

Galisteo, M. L., Chernoff, J., Su, Y. C., Skolnik, E. Y. and Schlessinger, J. (1996). "The adaptor protein Nck links receptor tyrosine kinases with the serine-threonine kinase Pak1." J Biol Chem **271**(35): 20997-21000.

Garcia-Mata, R., Boulter, E. and Burridge, K. (2011). "The 'invisible hand': regulation of RHO GTPases by RHOGDIs." Nat Rev Mol Cell Biol **12**(8): 493-504.

Gardiner, E. M., Pestonjamasp, K. N., Bohl, B. P., Chamberlain, C., Hahn, K. M. and Bokoch, G. M. (2002). "Spatial and temporal analysis of Rac activation during live neutrophil chemotaxis." Curr Biol **12**(23): 2029-2034.

Geiger, T. R. and Peeper, D. S. (2009). "Metastasis mechanisms." Biochim Biophys Acta **1796**(2): 293-308.

Gimona, M., Buccione, R., Courtneidge, S. A. and Linder, S. (2008). "Assembly and biological role of podosomes and invadopodia." Curr Opin Cell Biol **20**(2): 235-241.

Gligorijevic, B., Wyckoff, J., Yamaguchi, H., Wang, Y., Roussos, E. T. and Condeelis, J. (2012). "N-WASP-mediated invadopodium formation is involved in intravasation and lung metastasis of mammary tumors." J Cell Sci **125**(Pt 3): 724-734.

Gnesutta, N. and Minden, A. (2003). "Death receptor-induced activation of initiator caspase 8 is antagonized by serine/threonine kinase PAK4." Mol Cell Biol **23**(21): 7838-7848.

Goc, A., Al-Azayzih, A., Abdalla, M., Al-Husein, B., Kavuri, S., Lee, J., Moses, K. and Somanath, P. R. (2013). "P21 activated kinase-1 (Pak1) promotes prostate tumor growth and microinvasion via inhibition of transforming growth factor beta expression and enhanced matrix metalloproteinase 9 secretion." J Biol Chem **288**(5): 3025-3035.

Goicoechea, S. M., Awadia, S. and Garcia-Mata, R. (2014). "I'm coming to GEF you: Regulation of RhoGEFs during cell migration." Cell Adh Migr **8**(4).

Gong, W., An, Z., Wang, Y., Pan, X., Fang, W., Jiang, B. and Zhang, H. (2009). "P21-activated kinase 5 is overexpressed during colorectal cancer progression and regulates colorectal carcinoma cell adhesion and migration." Int J Cancer **125**(3): 548-555.

Goswami, S., Sahai, E., Wyckoff, J. B., Cammer, M., Cox, D., Pixley, F. J., Stanley, E. R., Segall, J. E. and Condeelis, J. S. (2005). "Macrophages promote the invasion of breast carcinoma cells via a colony-stimulating factor-1/epidermal growth factor paracrine loop." Cancer Res **65**(12): 5278-5283.

Gouon, V., Tucker, G. C., Kraus-Berthier, L., Atassi, G. and Kieffer, N. (1996). "Up-regulated expression of the beta3 integrin and the 92-kDa gelatinase in human HT-144 melanoma cell tumors grown in nude mice." Int J Cancer **68**(5): 650-662.

Gringel, A., Walz, D., Rosenberger, G., Minden, A., Kutsche, K., Kopp, P. and Linder, S. (2006). "PAK4 and alphaPIX determine podosome size and number in macrophages through localized actin regulation." J Cell Physiol **209**(2): 568-579.

Guo, Q., Su, N., Zhang, J., Li, X., Miao, Z., Wang, G., Cheng, M., Xu, H., Cao, L. and Li, F. (2014). "PAK4 kinase-mediated SCG10 phosphorylation involved in gastric cancer metastasis." Oncogene **33**(25): 3277-3287.

Ha, B. H., Davis, M. J., Chen, C., Lou, H. J., Gao, J., Zhang, R., Krauthammer, M., Halaban, R., Schlessinger, J., Turk, B. E. and Boggon, T. J. (2012). "Type II p21-activated kinases (PAKs) are regulated by an autoinhibitory pseudosubstrate." Proc Natl Acad Sci U S A **109**(40): 16107-16112.

Hagedorn, E. J., Kelley, L. C., Naegeli, K. M., Wang, Z., Chi, Q. and Sherwood, D. R. (2014). "ADF/cofilin promotes invadopodial membrane recycling during cell invasion in vivo." J Cell Biol **204**(7): 1209-1218.

Haldi, M., Ton, C., Seng, W. L. and McGrath, P. (2006). "Human melanoma cells transplanted into zebrafish proliferate, migrate, produce melanin, form masses and stimulate angiogenesis in zebrafish." Angiogenesis **9**(3): 139-151.

Hart, M. J., Eva, A., Zangrilli, D., Aaronson, S. A., Evans, T., Cerione, R. A. and Zheng, Y. (1994). "Cellular transformation and guanine nucleotide exchange activity are catalyzed by a common domain on the dbl oncogene product." J Biol Chem **269**(1): 62-65.

Heasman, S. J. and Ridley, A. J. (2008). "Mammalian Rho GTPases: new insights into their functions from in vivo studies." Nat Rev Mol Cell Biol **9**(9): 690-701.

Hegerfeldt, Y., Tusch, M., Brocker, E. B. and Friedl, P. (2002). "Collective cell movement in primary melanoma explants: plasticity of cell-cell interaction, beta1-integrin function, and migration strategies." Cancer Res **62**(7): 2125-2130.

Herlyn, M., Thurin, J., Balaban, G., Bennicelli, J. L., Herlyn, D., Elder, D. E., Bondi, E., Guerry, D., Nowell, P., Clark, W. H. and et al. (1985). "Characteristics of cultured human melanocytes isolated from different stages of tumor progression." Cancer Res **45**(11 Pt 2): 5670-5676.

Hirohashi, S. (1998). "Inactivation of the E-cadherin-mediated cell adhesion system in human cancers." Am J Pathol **153**(2): 333-339.

Hoashi, T., Watabe, H., Muller, J., Yamaguchi, Y., Vieira, W. D. and Hearing, V. J. (2005). "MART-1 is required for the function of the melanosomal matrix protein PMEL17/GP100 and the maturation of melanosomes." J Biol Chem **280**(14): 14006-14016.

Holm, C., Rayala, S., Jirstrom, K., Stal, O., Kumar, R. and Landberg, G. (2006). "Association between Pak1 expression and subcellular localization and tamoxifen resistance in breast cancer patients." J Natl Cancer Inst **98**(10): 671-680.

Hoshino, D., Branch, K. M. and Weaver, A. M. (2013). "Signaling inputs to invadopodia and podosomes." J Cell Sci **126**(Pt 14): 2979-2989.

Howe, A. K. and Juliano, R. L. (2000). "Regulation of anchorage-dependent signal transduction by protein kinase A and p21-activated kinase." Nat Cell Biol **2**(9): 593-600.

Hsu, M. Y., Meier, F. E., Nesbit, M., Hsu, J. Y., Van Belle, P., Elder, D. E. and Herlyn, M. (2000). "E-cadherin expression in melanoma cells restores keratinocyte-mediated growth control and down-regulates expression of invasion-related adhesion receptors." Am J Pathol **156**(5): 1515-1525.

Huynh, N., Liu, K. H., Baldwin, G. S. and He, H. (2010). "P21-activated kinase 1 stimulates colon cancer cell growth and migration/invasion via ERK- and AKT-dependent pathways." Biochim Biophys Acta **1803**(9): 1106-1113.

Ito, M., Nishiyama, H., Kawanishi, H., Matsui, S., Guilford, P., Reeve, A. and Ogawa, O. (2007). "P21-activated kinase 1: a new molecular marker for intravesical recurrence after transurethral resection of bladder cancer." J Urol **178**(3 Pt 1): 1073-1079.

Jaffe, A. B. and Hall, A. (2005). "Rho GTPases: biochemistry and biology." Annu Rev Cell Dev Biol **21**: 247-269.

Jaffer, Z. M. and Chernoff, J. (2002). "p21-activated kinases: three more join the Pak." Int J Biochem Cell Biol **34**(7): 713-717.

Jaiswal, M., Gremer, L., Dvorsky, R., Haeusler, L. C., Cirstea, I. C., Uhlenbrock, K. and Ahmadian, M. R. (2011). "Mechanistic insights into specificity, activity, and regulatory elements of the regulator of G-protein signaling (RGS)-containing Rho-specific guanine nucleotide exchange factors (GEFs) p115, PDZ-RhoGEF (PRG), and leukemia-associated RhoGEF (LARG)." J Biol Chem **286**(20): 18202-18212.

Joyce, J. A. (2005). "Therapeutic targeting of the tumor microenvironment." Cancer Cell **7**(6): 513-520.

Jung, D. W., Oh, E. S., Park, S. H., Chang, Y. T., Kim, C. H., Choi, S. Y. and Williams, D. R. (2012). "A novel zebrafish human tumor xenograft model validated for anti-cancer drug screening." Mol Biosyst **8**(7): 1930-1939.

Kam, Y., Guess, C., Estrada, L., Weidow, B. and Quaranta, V. (2008). "A novel circular invasion assay mimics in vivo invasive behavior of cancer cell lines and distinguishes single-cell motility in vitro." BMC Cancer **8**: 198.

Kamai, T., Arai, K., Tsujii, T., Honda, M. and Yoshida, K. (2001). "Overexpression of RhoA mRNA is associated with advanced stage in testicular germ cell tumour." BJU Int **87**(3): 227-231.

Kamai, T., Shirataki, H., Nakanishi, K., Furuya, N., Kambara, T., Abe, H., Oyama, T. and Yoshida, K. (2010). "Increased Rac1 activity and Pak1 overexpression are associated with lymphovascular invasion and lymph node metastasis of upper urinary tract cancer." BMC Cancer **10**: 164.

Kasai, K., Takahashi, M., Osumi, N., Sinnarajah, S., Takeo, T., Ikeda, H., Kehrl, J. H., Itoh, G. and Arnheiter, H. (2004). "The G12 family of heterotrimeric G proteins and Rho GTPase mediate Sonic hedgehog signalling." Genes Cells **9**(1): 49-58.

Katz, S. I., Cooper, K. D., Iijima, M. and Tsuchida, T. (1985). "The role of Langerhans cells in antigen presentation." J Invest Dermatol **85**(1 Suppl): 96s-98s.

Kaur, R., Yuan, X., Lu, M. L. and Balk, S. P. (2008). "Increased PAK6 expression in prostate cancer and identification of PAK6 associated proteins." Prostate **68**(14): 1510-1516.

Kesanakurti, D., Chetty, C., Rajasekhar Maddirela, D., Gujrati, M. and Rao, J. S. (2012). "Functional cooperativity by direct interaction between PAK4 and MMP-2 in the regulation of anoikis resistance, migration and invasion in glioma." Cell Death Dis **3**: e445.

Khanna, C. and Hunter, K. (2005). "Modeling metastasis in vivo." Carcinogenesis **26**(3): 513-523.

Kikuchi, T., Hassanein, M., Amann, J. M., Liu, Q., Slebos, R. J., Rahman, S. M., Kaufman, J. M., Zhang, X., Hoeksema, M. D., Harris, B. K., Li, M., Shyr, Y., Gonzalez, A. L., Zimmerman, L. J., Liebler, D. C., Massion, P. P. and Carbone, D. P. (2012). "In-depth proteomic analysis of nonsmall cell lung cancer to discover molecular targets and candidate biomarkers." Mol Cell Proteomics **11**(10): 916-932.

Kim, J. H., Kim, H. N., Lee, K. T., Lee, J. K., Choi, S. H., Paik, S. W., Rhee, J. C. and Lowe, A. W. (2008). "Gene expression profiles in gallbladder cancer: the close genetic similarity seen for early and advanced gallbladder cancers may explain the poor prognosis." Tumour Biol **29**(1): 41-49.

Kimmelman, A. C., Hezel, A. F., Aguirre, A. J., Zheng, H., Paik, J. H., Ying, H., Chu, G. C., Zhang, J. X., Sahin, E., Yeo, G., Ponugoti, A., Nabioullin, R., Deroo, S., Yang, S., Wang, X., McGrath, J. P., Protopopova, M., Ivanova, E., Zhang, J., Feng, B., Tsao, M. S., Redston, M., Protopopov, A., Xiao, Y., Futreal, P. A., Hahn, W. C., Klimstra, D. S., Chin, L. and DePinho, R. A. (2008). "Genomic alterations link Rho family of GTPases to the highly invasive phenotype of pancreas cancer." Proc Natl Acad Sci U S A **105**(49): 19372-19377.

King, C. C., Gardiner, E. M., Zenke, F. T., Bohl, B. P., Newton, A. C., Hemmings, B. A. and Bokoch, G. M. (2000). "p21-activated kinase (PAK1) is phosphorylated and activated by 3-phosphoinositide-dependent kinase-1 (PDK1)." J Biol Chem **275**(52): 41201-41209.

King, H., Nicholas, N. S. and Wells, C. M. (2014). "Role of p-21-activated kinases in cancer progression." Int Rev Cell Mol Biol **309**: 347-387.

Kissil, J. L., Wilker, E. W., Johnson, K. C., Eckman, M. S., Yaffe, M. B. and Jacks, T. (2003). "Merlin, the product of the Nf2 tumor suppressor gene, is an inhibitor of the p21-activated kinase, Pak1." Mol Cell **12**(4): 841-849.

Knutson, J. R., Iida, J., Fields, G. B. and McCarthy, J. B. (1996). "CD44/chondroitin sulfate proteoglycan and alpha 2 beta 1 integrin mediate human melanoma cell migration on type IV collagen and invasion of basement membranes." Mol Biol Cell **7**(3): 383-396.

Koh, C. G., Tan, E. J., Manser, E. and Lim, L. (2002). "The p21-activated kinase PAK is negatively regulated by POPX1 and POPX2, a pair of serine/threonine phosphatases of the PP2C family." Curr Biol **12**(4): 317-321.

Konantz, M., Balci, T. B., Hartwig, U. F., Dellaire, G., Andre, M. C., Berman, J. N. and Lengerke, C. (2012). "Zebrafish xenografts as a tool for in vivo studies on human cancer." Ann N Y Acad Sci **1266**: 124-137.

Kozlowski, J. M., Hart, I. R., Fidler, I. J. and Hanna, N. (1984). "A human melanoma line heterogeneous with respect to metastatic capacity in athymic nude mice." J Natl Cancer Inst **72**(4): 913-917.

Kreis, P., Rousseau, V., Thevenot, E., Combeau, G. and Barnier, J. V. (2008). "The four mammalian splice variants encoded by the p21-activated kinase 3 gene have different biological properties." J Neurochem **106**(3): 1184-1197.

Lammermann, T. and Sixt, M. (2009). "Mechanical modes of 'amoeboid' cell migration." Curr Opin Cell Biol **21**(5): 636-644.

Le Clainche, C. and Carlier, M. F. (2008). "Regulation of actin assembly associated with protrusion and adhesion in cell migration." Physiol Rev **88**(2): 489-513.

Lei, M., Lu, W., Meng, W., Parrini, M. C., Eck, M. J., Mayer, B. J. and Harrison, S. C. (2000). "Structure of PAK1 in an autoinhibited conformation reveals a multistage activation switch." Cell **102**(3): 387-397.

Li, A., Dawson, J. C., Forero-Vargas, M., Spence, H. J., Yu, X., Konig, I., Anderson, K. and Machesky, L. M. (2010a). "The actin-bundling protein fascin stabilizes actin in invadopodia and potentiates protrusive invasion." Curr Biol **20**(4): 339-345.

Li, F., Adam, L., Vadlamudi, R. K., Zhou, H., Sen, S., Chernoff, J., Mandal, M. and Kumar, R. (2002). "p21-activated kinase 1 interacts with and phosphorylates histone H3 in breast cancer cells." EMBO Rep **3**(8): 767-773.

Li, L. H., Zheng, M. H., Luo, Q., Ye, Q., Feng, B., Lu, A. G., Wang, M. L., Chen, X. H., Su, L. P. and Liu, B. Y. (2010b). "P21-activated protein kinase 1 induces colorectal cancer metastasis involving ERK activation and phosphorylation of FAK at Ser-910." Int J Oncol **37**(4): 951-962.

Li, X. and Minden, A. (2003). "Targeted disruption of the gene for the PAK5 kinase in mice." Mol Cell Biol **23**(20): 7134-7142.

Li, X., Wen, W., Liu, K., Zhu, F., Malakhova, M., Peng, C., Li, T., Kim, H. G., Ma, W., Cho, Y. Y., Bode, A. M., Dong, Z. and Dong, Z. (2011). "Phosphorylation of caspase-7 by p21-activated protein kinase (PAK) 2 inhibits chemotherapeutic drug-induced apoptosis of breast cancer cell lines." J Biol Chem **286**(25): 22291-22299.

Li, Y., Shao, Y., Tong, Y., Shen, T., Zhang, J., Gu, H. and Li, F. (2012). "Nucleo-cytoplasmic shuttling of PAK4 modulates beta-catenin intracellular translocation and signaling." Biochim Biophys Acta **1823**(2): 465-475.

Li, Z., Hannigan, M., Mo, Z., Liu, B., Lu, W., Wu, Y., Smrcka, A. V., Wu, G., Li, L., Liu, M., Huang, C. K. and Wu, D. (2003). "Directional sensing requires G beta gamma-mediated PAK1 and PIX alpha-dependent activation of Cdc42." Cell **114**(2): 215-227.

Li, Z., Zhang, H., Lundin, L., Thullberg, M., Liu, Y., Wang, Y., Claesson-Welsh, L. and Stromblad, S. (2010c). "p21-activated kinase 4 phosphorylation of integrin beta5 Ser-759 and Ser-762 regulates cell migration." J Biol Chem **285**(31): 23699-23710.

Liu, F., Gomez Garcia, A. M. and Meyskens, F. L., Jr. (2012). "NADPH oxidase 1 overexpression enhances invasion via matrix metalloproteinase-2 and epithelial-mesenchymal transition in melanoma cells." J Invest Dermatol **132**(8): 2033-2041.

Liu, K. H., Huynh, N., Patel, O., Shulkes, A., Baldwin, G. and He, H. (2013). "P21-activated kinase 1 promotes colorectal cancer survival by up-regulation of hypoxia-inducible factor-1alpha." Cancer Lett **340**(1): 22-29.

Liu, R. X., Wang, W. Q., Ye, L., Bi, Y. F., Fang, H., Cui, B., Zhou, W. W., Dai, M., Zhang, J., Li, X. Y. and Ning, G. (2010a). "p21-activated kinase 3 is overexpressed in thymic neuroendocrine tumors (carcinoids) with ectopic ACTH syndrome and participates in cell migration." Endocrine **38**(1): 38-47.

Liu, S., Yamashita, H., Weidow, B., Weaver, A. M. and Quaranta, V. (2010b). "Laminin-332-beta1 integrin interactions negatively regulate invadopodia." J Cell Physiol **223**(1): 134-142.

Liu, Y., Xiao, H., Tian, Y., Nekrasova, T., Hao, X., Lee, H. J., Suh, N., Yang, C. S. and Minden, A. (2008). "The pak4 protein kinase plays a key role in cell survival and tumorigenesis in athymic mice." Mol Cancer Res **6**(7): 1215-1224.

Lizarraga, F., Poincloux, R., Romao, M., Montagnac, G., Le Dez, G., Bonne, I., Rigaill, G., Raposo, G. and Chavrier, P. (2009). "Diaphanous-related formins are required for invadopodia formation and invasion of breast tumor cells." Cancer Res **69**(7): 2792-2800.

Lorenz, M., Yamaguchi, H., Wang, Y., Singer, R. H. and Condeelis, J. (2004). "Imaging sites of N-wasp activity in lamellipodia and invadopodia of carcinoma cells." Curr Biol **14**(8): 697-703.

Lozano, E., Frasa, M. A., Smolarczyk, K., Knaus, U. G. and Braga, V. M. (2008). "PAK is required for the disruption of E-cadherin adhesion by the small GTPase Rac." J Cell Sci **121**(Pt 7): 933-938.

Lu, W., Katz, S., Gupta, R. and Mayer, B. J. (1997). "Activation of Pak by membrane localization mediated by an SH3 domain from the adaptor protein Nck." Curr Biol **7**(2): 85-94.

Lu, W., Xia, Y. H., Qu, J. J., He, Y. Y., Li, B. L., Lu, C., Luo, X. and Wan, X. P. (2013). "p21-activated kinase 4 regulation of endometrial cancer cell migration and invasion involves the ERK1/2 pathway mediated MMP-2 secretion." Neoplasma **60**(5): 493-503.

Machacek, M., Hodgson, L., Welch, C., Elliott, H., Pertz, O., Nalbant, P., Abell, A., Johnson, G. L., Hahn, K. M. and Danuser, G. (2009). "Coordination of Rho GTPase activities during cell protrusion." Nature **461**(7260): 99-103.

Machesky, L. M. and Li, A. (2010). "Fascin: Invasive filopodia promoting metastasis." Commun Integr Biol **3**(3): 263-270.

Maekawa, M., Ishizaki, T., Boku, S., Watanabe, N., Fujita, A., Iwamatsu, A., Obinata, T., Ohashi, K., Mizuno, K. and Narumiya, S. (1999). "Signaling from Rho to the actin cytoskeleton through protein kinases ROCK and LIM-kinase." Science **285**(5429): 895-898.

Mak, A. S. (2014). "p53 in cell invasion, podosomes, and invadopodia." Cell Adh Migr **8**(3).

Manser, E., Huang, H. Y., Loo, T. H., Chen, X. Q., Dong, J. M., Leung, T. and Lim, L. (1997). "Expression of constitutively active alpha-PAK reveals effects of the kinase on actin and focal complexes." Mol Cell Biol **17**(3): 1129-1143.

Manser, E., Loo, T. H., Koh, C. G., Zhao, Z. S., Chen, X. Q., Tan, L., Tan, I., Leung, T. and Lim, L. (1998). "PAK kinases are directly coupled to the PIX family of nucleotide exchange factors." Mol Cell **1**(2): 183-192.

Maricich, S. M., Wellnitz, S. A., Nelson, A. M., Lesniak, D. R., Gerling, G. J., Lumpkin, E. A. and Zoghbi, H. Y. (2009). "Merkel cells are essential for light-touch responses." Science **324**(5934): 1580-1582.

Marques, I. J., Weiss, F. U., Vlecken, D. H., Nitsche, C., Bakkers, J., Lagendijk, A. K., Partecke, L. I., Heidecke, C. D., Lerch, M. M. and Bagowski, C. P. (2009). "Metastatic behaviour of primary human tumours in a zebrafish xenotransplantation model." BMC Cancer **9**: 128.

Marsden, J. R., Newton-Bishop, J. A., Burrows, L., Cook, M., Corrie, P. G., Cox, N. H., Gore, M. E., Lorigan, P., MacKie, R., Nathan, P., Peach, H., Powell, B. and Walker, C. (2010). "Revised U.K. guidelines for the management of cutaneous melanoma 2010." Br J Dermatol **163**(2): 238-256.

Md Hashim, N. F., Nicholas, N. S., Dart, A. E., Kiriakidis, S., Paleolog, E. and Wells, C. M. (2013). "Hypoxia-induced invadopodia formation: a role for beta-PIX." Open Biol **3**(6): 120159.

Meier, F., Nesbit, M., Hsu, M. Y., Martin, B., Van Belle, P., Elder, D. E., Schaumburg-Lever, G., Garbe, C., Walz, T. M., Donatien, P., Crombleholme, T. M. and Herlyn, M. (2000). "Human melanoma progression in skin reconstructs : biological significance of bFGF." Am J Pathol **156**(1): 193-200.

Meng, J., Meng, Y., Hanna, A., Janus, C. and Jia, Z. (2005). "Abnormal long-lasting synaptic plasticity and cognition in mice lacking the mental retardation gene Pak3." J Neurosci **25**(28): 6641-6650.

Mimeault, M. and Batra, S. K. (2013). "Emergence of zebrafish models in oncology for validating novel anticancer drug targets and nanomaterials." Drug Discov Today **18**(3-4): 128-140.

Monsky, W. L., Lin, C. Y., Aoyama, A., Kelly, T., Akiyama, S. K., Mueller, S. C. and Chen, W. T. (1994). "A potential marker protease of invasiveness, seprase, is localized on invadopodia of human malignant melanoma cells." Cancer Res **54**(21): 5702-5710.

Moshfegh, Y., Bravo-Cordero, J. J., Miskolci, V., Condeelis, J. and Hodgson, L. (2014). "A Trio-Rac1-Pak1 signalling axis drives invadopodia disassembly." Nat Cell Biol.

Mueller, S. C., Ghersi, G., Akiyama, S. K., Sang, Q. X., Howard, L., Pineiro-Sanchez, M., Nakahara, H., Yeh, Y. and Chen, W. T. (1999). "A novel protease-docking function of integrin at invadopodia." J Biol Chem **274**(35): 24947-24952.

Murphy, D. A. and Courtneidge, S. A. (2011). "The 'ins' and 'outs' of podosomes and invadopodia: characteristics, formation and function." Nat Rev Mol Cell Biol **12**(7): 413-426.

Murray, B. W., Guo, C., Piraino, J., Westwick, J. K., Zhang, C., Lamerdin, J., Dagostino, E., Knighton, D., Loi, C. M., Zager, M., Kraynov, E., Popoff, I., Christensen, J. G., Martinez, R., Kephart, S. E., Marakovits, J., Karlicek, S., Bergqvist, S. and Smeal, T. (2010). "Small-molecule p21-activated kinase inhibitor PF-3758309 is a potent inhibitor of oncogenic signaling and tumor growth." Proc Natl Acad Sci U S A **107**(20): 9446-9451.

Nakahara, H., Howard, L., Thompson, E. W., Sato, H., Seiki, M., Yeh, Y. and Chen, W. T. (1997). "Transmembrane/cytoplasmic domain-mediated membrane type 1-matrix metalloprotease docking to invadopodia is required for cell invasion." Proc Natl Acad Sci U S A **94**(15): 7959-7964.

Nakahara, H., Mueller, S. C., Nomizu, M., Yamada, Y., Yeh, Y. and Chen, W. T. (1998). "Activation of beta1 integrin signaling stimulates tyrosine phosphorylation of p190RhoGAP and membrane-protrusive activities at invadopodia." J Biol Chem **273**(1): 9-12.

Nakahara, H., Otani, T., Sasaki, T., Miura, Y., Takai, Y. and Kogo, M. (2003). "Involvement of Cdc42 and Rac small G proteins in invadopodia formation of RPMI7951 cells." Genes Cells **8**(12): 1019-1027.

Nayal, A., Webb, D. J., Brown, C. M., Schaefer, E. M., Vicente-Manzanares, M. and Horwitz, A. R. (2006). "Paxillin phosphorylation at Ser273 localizes a GIT1-PIX-PAK complex and regulates adhesion and protrusion dynamics." J Cell Biol **173**(4): 587-589.

Neila, J. and Soyer, H. P. (2011). "Key points in dermoscopy for diagnosis of melanomas, including difficult to diagnose melanomas, on the trunk and extremities." J Dermatol **38**(1): 3-9.

Nekrasova, T., Jobes, M. L., Ting, J. H., Wagner, G. C. and Minden, A. (2008). "Targeted disruption of the Pak5 and Pak6 genes in mice leads to deficits in learning and locomotion." Dev Biol **322**(1): 95-108.

Nguyen, D. X., Bos, P. D. and Massague, J. (2009). "Metastasis: from dissemination to organ-specific colonization." Nat Rev Cancer **9**(4): 274-284.

Nobes, C. D. and Hall, A. (1995). "Rho, rac, and cdc42 GTPases regulate the assembly of multimolecular focal complexes associated with actin stress fibers, lamellipodia, and filopodia." Cell **81**(1): 53-62.

Nobes, C. D. and Hall, A. (1999). "Rho GTPases control polarity, protrusion, and adhesion during cell movement." J Cell Biol **144**(6): 1235-1244.

O'Connor, K. and Chen, M. (2013). "Dynamic functions of RhoA in tumor cell migration and invasion." Small GTPases **4**(3): 141-147.

Oleksy, A., Opalinski, L., Derewenda, U., Derewenda, Z. S. and Otlewski, J. (2006). "The molecular basis of RhoA specificity in the guanine nucleotide exchange factor PDZ-RhoGEF." J Biol Chem **281**(43): 32891-32897.

Ong, C. C., Jubb, A. M., Haverty, P. M., Zhou, W., Tran, V., Truong, T., Turley, H., O'Brien, T., Vucic, D., Harris, A. L., Belvin, M., Friedman, L. S., Blackwood, E. M., Koeppen, H. and Hoeflich, K. P. (2011). "Targeting p21-activated kinase 1 (PAK1) to induce apoptosis of tumor cells." Proc Natl Acad Sci U S A **108**(17): 7177-7182.

Ong, C. C., Jubb, A. M., Jakubiak, D., Zhou, W., Rudolph, J., Haverty, P. M., Kowanetz, M., Yan, Y., Tremayne, J., Lisle, R., Harris, A. L., Friedman, L. S., Belvin, M., Middleton, M. R., Blackwood, E. M., Koeppen, H. and Hoeflich, K. P. (2013). "P21-activated kinase 1 (PAK1) as a therapeutic target in BRAF wild-type melanoma." J Natl Cancer Inst **105**(9): 606-607.

Orgaz, J. L. and Sanz-Moreno, V. (2013). "Emerging molecular targets in melanoma invasion and metastasis." Pigment Cell Melanoma Res **26**(1): 39-57.

Oser, M., Yamaguchi, H., Mader, C. C., Bravo-Cordero, J. J., Arias, M., Chen, X., Desmarais, V., van Rheenen, J., Koleske, A. J. and Condeelis, J. (2009). "Cortactin regulates cofilin and N-WASp activities to control the stages of invadopodium assembly and maturation." J Cell Biol **186**(4): 571-587.

Overall, C. M. and Dean, R. A. (2006). "Degradomics: systems biology of the protease web. Pleiotropic roles of MMPs in cancer." Cancer Metastasis Rev **25**(1): 69-75.

Parrini, M. C., Lei, M., Harrison, S. C. and Mayer, B. J. (2002). "Pak1 kinase homodimers are autoinhibited in trans and dissociated upon activation by Cdc42 and Rac1." Mol Cell **9**(1): 73-83.

Pavey, S., Zuidervaart, W., van Nieuwpoort, F., Packer, L., Jager, M., Gruis, N. and Hayward, N. (2006). "Increased p21-activated kinase-1 expression is associated with invasive potential in uveal melanoma." Melanoma Res **16**(4): 285-296.

Paz, H., Pathak, N. and Yang, J. (2013). "Invading one step at a time: the role of invadopodia in tumor metastasis." Oncogene.

Pegtel, D. M., Ellenbroek, S. I., Mertens, A. E., van der Kammen, R. A., de Rooij, J. and Collard, J. G. (2007). "The Par-Tiam1 complex controls persistent migration by stabilizing microtubule-dependent front-rear polarity." Curr Biol **17**(19): 1623-1634.

Pichot, C. S., Arvanitis, C., Hartig, S. M., Jensen, S. A., Bechill, J., Marzouk, S., Yu, J., Frost, J. A. and Corey, S. J. (2010). "Cdc42-interacting protein 4 promotes breast cancer cell invasion and formation of invadopodia through activation of N-WASp." Cancer Res **70**(21): 8347-8356.

Poincloux, R., Lizarraga, F. and Chavrier, P. (2009). "Matrix invasion by tumour cells: a focus on MT1-MMP trafficking to invadopodia." J Cell Sci **122**(Pt 17): 3015-3024.

Qu, J., Cammarano, M. S., Shi, Q., Ha, K. C., de Lanerolle, P. and Minden, A. (2001). "Activated PAK4 regulates cell adhesion and anchorage-independent growth." Mol Cell Biol **21**(10): 3523-3533.

Qu, J., Li, X., Novitch, B. G., Zheng, Y., Kohn, M., Xie, J. M., Kozinn, S., Bronson, R., Beg, A. A. and Minden, A. (2003). "PAK4 kinase is essential for embryonic viability and for proper neuronal development." Mol Cell Biol **23**(20): 7122-7133.

Radu, M., Semenova, G., Kosoff, R. and Chernoff, J. (2014). "PAK signalling during the development and progression of cancer." Nat Rev Cancer **14**(1): 13-25.

Rayala, S. K. and Kumar, R. (2007). "Sliding p21-activated kinase 1 to nucleus impacts tamoxifen sensitivity." Biomed Pharmacother **61**(7): 408-411.

Rennefahrt, U. E., Deacon, S. W., Parker, S. A., Devarajan, K., Beeser, A., Chernoff, J., Knapp, S., Turk, B. E. and Peterson, J. R. (2007). "Specificity profiling of Pak kinases allows identification of novel phosphorylation sites." J Biol Chem **282**(21): 15667-15678.

Rettig, M., Trinidad, K., Pezeshkpour, G., Frost, P., Sharma, S., Moatamed, F., Tamanoi, F. and Mortazavi, F. (2012). "PAK1 kinase promotes cell motility and invasiveness through CRK-II serine phosphorylation in non-small cell lung cancer cells." PLoS One **7**(7): e42012.

Reymond, N., d'Agua, B. B. and Ridley, A. J. (2013). "Crossing the endothelial barrier during metastasis." Nat Rev Cancer **13**(12): 858-870.

Reymond, N., Im, J. H., Garg, R., Vega, F. M., Borda d'Agua, B., Riou, P., Cox, S., Valderrama, F., Muschel, R. J. and Ridley, A. J. (2012). "Cdc42 promotes transendothelial migration of cancer cells through beta1 integrin." J Cell Biol **199**(4): 653-668.

Rider, L., Oladimeji, P. and Diakonova, M. (2013). "PAK1 regulates breast cancer cell invasion through secretion of matrix metalloproteinases in response to prolactin and three-dimensional collagen IV." Mol Endocrinol **27**(7): 1048-1064.

Ridley, A. J. (2011). "Life at the leading edge." Cell **145**(7): 1012-1022.

Ridley, A. J. (2013). "RhoA, RhoB and RhoC have different roles in cancer cell migration." J Microsc **251**(3): 242-249.

Ridley, A. J. and Hall, A. (1992). "The small GTP-binding protein rho regulates the assembly of focal adhesions and actin stress fibers in response to growth factors." Cell **70**(3): 389-399.

Rook, A. (2004). Rook's Textbook of Dermatology. T. Burns, S. Breathnach, N. Cox and C. Griffiths. Wiley-Blackwell. **1+3**:

Rook, A. (2010). Rook's Textbook of Dermatology. T. Burns, S. Breathnach, N. Cox and C. Griffiths. Wiley-Blackwell. **1**: 3-35.

Rosai, J. and Ackerman, L. V. (2004). Rosai and Ackerman's Surgical Pathology. Mosby.

Rosenfeldt, H., Castellone, M. D., Randazzo, P. A. and Gutkind, J. S. (2006). "Rac inhibits thrombin-induced Rho activation: evidence of a Pak-dependent GTPase crosstalk." J Mol Signal **1**: 8.

Rossman, K. L., Der, C. J. and Sondek, J. (2005). "GEF means go: turning on RHO GTPases with guanine nucleotide-exchange factors." Nat Rev Mol Cell Biol **6**(2): 167-180.

Rubinstein, A. L. (2003). "Zebrafish: from disease modeling to drug discovery." Curr Opin Drug Discov Devel **6**(2): 218-223.

Rumenapp, U., Blomquist, A., Schworer, G., Schablowski, H., Psoma, A. and Jakobs, K. H. (1999). "Rho-specific binding and guanine nucleotide exchange catalysis by KIAA0380, a dbl family member." FEBS Lett **459**(3): 313-318.

Sabeh, F., Shimizu-Hirota, R. and Weiss, S. J. (2009). "Protease-dependent versus -independent cancer cell invasion programs: three-dimensional amoeboid movement revisited." J Cell Biol **185**(1): 11-19.

Sahai, E. (2005). "Mechanisms of cancer cell invasion." Curr Opin Genet Dev **15**(1): 87-96.

Sahai, E. (2007). "Illuminating the metastatic process." Nat Rev Cancer **7**(10): 737-749.

Sahai, E., Garcia-Medina, R., Pouyssegur, J. and Vial, E. (2007). "Smurf1 regulates tumor cell plasticity and motility through degradation of RhoA leading to localized inhibition of contractility." J Cell Biol **176**(1): 35-42.

Sahai, E. and Marshall, C. J. (2002). "RHO-GTPases and cancer." Nat Rev Cancer **2**(2): 133-142.

Sahai, E. and Marshall, C. J. (2003). "Differing modes of tumour cell invasion have distinct requirements for Rho/ROCK signalling and extracellular proteolysis." Nat Cell Biol **5**(8): 711-719.

Sakurai-Yageta, M., Recchi, C., Le Dez, G., Sibarita, J. B., Daviet, L., Camonis, J., D'Souza-Schorey, C. and Chavrier, P. (2008). "The interaction of IQGAP1 with the exocyst complex is required for tumor cell invasion downstream of Cdc42 and RhoA." J Cell Biol **181**(6): 985-998.

Sanz-Moreno, V., Gadea, G., Ahn, J., Paterson, H., Marra, P., Pinner, S., Sahai, E. and Marshall, C. J. (2008). "Rac activation and inactivation control plasticity of tumor cell movement." Cell **135**(3): 510-523.

Sanz-Moreno, V. and Marshall, C. J. (2010). "The plasticity of cytoskeletal dynamics underlying neoplastic cell migration." Curr Opin Cell Biol **22**(5): 690-696.

Schnaeker, E. M., Ossig, R., Ludwig, T., Dreier, R., Oberleithner, H., Wilhelmi, M. and Schneider, S. W. (2004). "Microtubule-dependent matrix metalloproteinase-2/matrix metalloproteinase-9 exocytosis: prerequisite in human melanoma cell invasion." Cancer Res **64**(24): 8924-8931.

Schoumacher, M., Goldman, R. D., Louvard, D. and Vignjevic, D. M. (2010). "Actin, microtubules, and vimentin intermediate filaments cooperate for elongation of invadopodia." J Cell Biol **189**(3): 541-556.

Schramp, M., Ying, O., Kim, T. Y. and Martin, G. S. (2008). "ERK5 promotes Src-induced podosome formation by limiting Rho activation." J Cell Biol **181**(7): 1195-1210.

Sells, M. A., Boyd, J. T. and Chernoff, J. (1999). "p21-activated kinase 1 (Pak1) regulates cell motility in mammalian fibroblasts." J Cell Biol **145**(4): 837-849.

Sells, M. A., Pfaff, A. and Chernoff, J. (2000). "Temporal and spatial distribution of activated Pak1 in fibroblasts." J Cell Biol **151**(7): 1449-1458.

Silini, A., Ghilardi, C., Ardinghi, C., Bernasconi, S., Oliva, P., Carraro, F., Naldini, A., Bani, M. R. and Giavazzi, R. (2010). "Protease-activated receptor-1 (PAR-1) promotes the motility of human melanomas and is associated to their metastatic phenotype." Clin Exp Metastasis **27**(1): 43-53.

Simpson, K. J., Dugan, A. S. and Mercurio, A. M. (2004). "Functional analysis of the contribution of RhoA and RhoC GTPases to invasive breast carcinoma." Cancer Res **64**(23): 8694-8701.

Siu, M. K., Chan, H. Y., Kong, D. S., Wong, E. S., Wong, O. G., Ngan, H. Y., Tam, K. F., Zhang, H., Li, Z., Chan, Q. K., Tsao, S. W., Stromblad, S. and Cheung, A. N. (2010a). "p21-activated kinase 4 regulates ovarian cancer cell proliferation, migration, and invasion and contributes to poor prognosis in patients." Proc Natl Acad Sci U S A **107**(43): 18622-18627.

Siu, M. K., Wong, E. S., Chan, H. Y., Kong, D. S., Woo, N. W., Tam, K. F., Ngan, H. Y., Chan, Q. K., Chan, D. C., Chan, K. Y. and Cheung, A. N. (2010b). "Differential expression and phosphorylation of Pak1 and Pak2 in ovarian cancer: effects on prognosis and cell invasion." Int J Cancer **127**(1): 21-31.

Struckhoff, A. P., Rana, M. K., Kher, S. S., Burow, M. E., Hagan, J. L., Del Valle, L. and Worthylake, R. A. (2013). "PDZ-RhoGEF is essential for CXCR4-driven breast tumor cell motility through spatial regulation of RhoA." J Cell Sci **126**(Pt 19): 4514-4526.

Stylli, S. S., Kaye, A. H. and Lock, P. (2008). "Invadopodia: at the cutting edge of tumour invasion." J Clin Neurosci **15**(7): 725-737.

Stylli, S. S., Stacey, T. T., Verhagen, A. M., Xu, S. S., Pass, I., Courtneidge, S. A. and Lock, P. (2009). "Nck adaptor proteins link Tks5 to invadopodia actin regulation and ECM degradation." J Cell Sci **122**(Pt 15): 2727-2740.

Tabusa, H., Brooks, T. and Massey, A. J. (2013). "Knockdown of PAK4 or PAK1 inhibits the proliferation of mutant KRAS colon cancer cells independently of RAF/MEK/ERK and PI3K/AKT signaling." Mol Cancer Res **11**(2): 109-121.

Takkunen, M., Hukkanen, M., Liljestrom, M., Grenman, R. and Virtanen, I. (2010). "Podosome-like structures of non-invasive carcinoma cells are replaced in epithelial-mesenchymal transition by actin comet-embedded invadopodia." J Cell Mol Med **14**(6B): 1569-1593.

Tehrani, S., Tomasevic, N., Weed, S., Sakowicz, R. and Cooper, J. A. (2007). "Src phosphorylation of cortactin enhances actin assembly." Proc Natl Acad Sci U S A **104**(29): 11933-11938.

Teng, Y., Xie, X., Walker, S., White, D. T., Mumm, J. S. and Cowell, J. K. (2013). "Evaluating human cancer cell metastasis in zebrafish." BMC Cancer **13**: 453.

Tian, X., Tian, Y., Gawlak, G., Sarich, N., Wu, T. and Birukova, A. A. (2014). "Control of vascular permeability by atrial natriuretic peptide via a GEF-H1-dependent mechanism." J Biol Chem **289**(8): 5168-5183.

Valastyan, S., Benaich, N., Chang, A., Reinhardt, F. and Weinberg, R. A. (2009). "Concomitant suppression of three target genes can explain the impact of a microRNA on metastasis." Genes Dev **23**(22): 2592-2597.

Valastyan, S. and Weinberg, R. A. (2011). "Tumor metastasis: molecular insights and evolving paradigms." Cell **147**(2): 275-292.

van Helden, S. F., Oud, M. M., Joosten, B., Peterse, N., Figdor, C. G. and van Leeuwen, F. N. (2008). "PGE2-mediated podosome loss in dendritic cells is dependent on actomyosin contraction downstream of the RhoA-Rho-kinase axis." J Cell Sci **121**(Pt 7): 1096-1106.

Vega, F. M., Fruhwirth, G., Ng, T. and Ridley, A. J. (2011). "RhoA and RhoC have distinct roles in migration and invasion by acting through different targets." J Cell Biol **193**(4): 655-665.

Vega, F. M. and Ridley, A. J. (2008). "Rho GTPases in cancer cell biology." FEBS Lett **582**(14): 2093-2101.

Viaud, J. and Peterson, J. R. (2009). "An allosteric kinase inhibitor binds the p21-activated kinase autoregulatory domain covalently." Mol Cancer Ther **8**(9): 2559-2565.

Vitale, S., Avizienyte, E., Brunton, V. G. and Frame, M. C. (2008). "Focal adhesion kinase is not required for Src-induced formation of invadopodia in KM12C colon cancer cells and can interfere with their assembly." Eur J Cell Biol **87**(8-9): 569-579.

Wach, F., Eyrich, A. M., Wustrow, T., Krieg, T. and Hein, R. (1996). "Comparison of migration and invasiveness of epithelial tumor and melanoma cells in vitro." J Dermatol Sci **12**(2): 118-126.

Wang, R. A., Zhang, H., Balasenthil, S., Medina, D. and Kumar, R. (2006). "PAK1 hyperactivation is sufficient for mammary gland tumor formation." Oncogene **25**(20): 2931-2936.

Wang, W., Lim, L., Baskaran, Y., Manser, E. and Song, J. (2013). "NMR binding and crystal structure reveal that intrinsically-unstructured regulatory domain auto-inhibits PAK4 by a mechanism different from that of PAK1." Biochem Biophys Res Commun **438**(1): 169-174.

Wang, Y. and McNiven, M. A. (2012). "Invasive matrix degradation at focal adhesions occurs via protease recruitment by a FAK-p130Cas complex." J Cell Biol **196**(3): 375-385.

Watabe, H., Valencia, J. C., Le Pape, E., Yamaguchi, Y., Nakamura, M., Rouzaud, F., Hoashi, T., Kawa, Y., Mizoguchi, M. and Hearing, V. J. (2008). "Involvement of dynein and spectrin with early melanosome transport and melanosomal protein trafficking." J Invest Dermatol **128**(1): 162-174.

Webb, B. A., Eves, R., Crawley, S. W., Zhou, S., Cote, G. P. and Mak, A. S. (2005). "PAK1 induces podosome formation in A7r5 vascular smooth muscle cells in a PAK-interacting exchange factor-dependent manner." Am J Physiol Cell Physiol **289**(4): C898-907.

Wells, C. M., Abo, A. and Ridley, A. J. (2002). "PAK4 is activated via PI3K in HGF-stimulated epithelial cells." J Cell Sci **115**(Pt 20): 3947-3956.

Wells, C. M. and Jones, G. E. (2010). "The emerging importance of group II PAKs." Biochem J **425**(3): 465-473.

Wells, C. M., Whale, A. D., Parsons, M., Masters, J. R. and Jones, G. E. (2010). "PAK4: a pluripotent kinase that regulates prostate cancer cell adhesion." J Cell Sci **123**(Pt 10): 1663-1673.

Wheeler, A. P., Wells, C. M., Smith, S. D., Vega, F. M., Henderson, R. B., Tybulewicz, V. L. and Ridley, A. J. (2006). "Rac1 and Rac2 regulate macrophage morphology but are not essential for migration." J Cell Sci **119**(Pt 13): 2749-2757.

Whiteman, D. C., Pavan, W. J. and Bastian, B. C. (2011). "The melanomas: a synthesis of epidemiological, clinical, histopathological, genetic, and biological aspects, supporting distinct subtypes, causal pathways, and cells of origin." Pigment Cell Melanoma Res **24**(5): 879-897.

Wiercinska, E., Naber, H. P., Pardali, E., van der Pluijm, G., van Dam, H. and ten Dijke, P. (2011). "The TGF-beta/Smad pathway induces breast cancer cell invasion through the up-regulation of matrix metalloproteinase 2 and 9 in a spheroid invasion model system." Breast Cancer Res Treat **128**(3): 657-666.

Wolf, K., Wu, Y. I., Liu, Y., Geiger, J., Tam, E., Overall, C., Stack, M. S. and Friedl, P. (2007). "Multi-step pericellular proteolysis controls the transition from individual to collective cancer cell invasion." Nat Cell Biol **9**(8): 893-904.

Wong, K., Van Keymeulen, A. and Bourne, H. R. (2007). "PDZRhoGEF and myosin II localize RhoA activity to the back of polarizing neutrophil-like cells." J Cell Biol **179**(6): 1141-1148.

Wong, L. E., Chen, N., Karantza, V. and Minden, A. (2013). "The Pak4 protein kinase is required for oncogenic transformation of MDA-MB-231 breast cancer cells." Oncogenesis **2**: e50.

Wu, X., Gan, B., Yoo, Y. and Guan, J. L. (2005). "FAK-mediated src phosphorylation of endophilin A2 inhibits endocytosis of MT1-MMP and promotes ECM degradation." Dev Cell **9**(2): 185-196.

Wyckoff, J. B., Wang, Y., Lin, E. Y., Li, J. F., Goswami, S., Stanley, E. R., Segall, J. E., Pollard, J. W. and Condeelis, J. (2007). "Direct visualization of macrophage-assisted tumor cell intravasation in mammary tumors." Cancer Res **67**(6): 2649-2656.

Xia, C., Ma, W., Stafford, L. J., Marcus, S., Xiong, W. C. and Liu, M. (2001). "Regulation of the p21-activated kinase (PAK) by a human Gbeta -like WD-repeat protein, hPIP1." Proc Natl Acad Sci U S A **98**(11): 6174-6179.

Yamaguchi, H. (2012). "Pathological roles of invadopodia in cancer invasion and metastasis." Eur J Cell Biol **91**(11-12): 902-907.

Yamaguchi, H., Lorenz, M., Kempiak, S., Sarmiento, C., Coniglio, S., Symons, M., Segall, J., Eddy, R., Miki, H., Takenawa, T. and Condeelis, J. (2005a). "Molecular mechanisms of invadopodium formation: the role of the N-WASP-Arp2/3 complex pathway and cofilin." J Cell Biol **168**(3): 441-452.

Yamaguchi, H., Wyckoff, J. and Condeelis, J. (2005b). "Cell migration in tumors." Curr Opin Cell Biol **17**(5): 559-564.

Yamazaki, D., Kurisu, S. and Takenawa, T. (2009). "Involvement of Rac and Rho signaling in cancer cell motility in 3D substrates." Oncogene **28**(13): 1570-1583.

Yilmaz, M. and Christofori, G. (2009). "EMT, the cytoskeleton, and cancer cell invasion." Cancer Metastasis Rev **28**(1-2): 15-33.

Yoshioka, K., Nakamori, S. and Itoh, K. (1999). "Overexpression of small GTP-binding protein RhoA promotes invasion of tumor cells." Cancer Res **59**(8): 2004-2010.

Yu, C. H., Rafiq, N. B., Krishnasamy, A., Hartman, K. L., Jones, G. E., Bershadsky, A. D. and Sheetz, M. P. (2013). "Integrin-matrix clusters form podosome-like adhesions in the absence of traction forces." Cell Rep **5**(5): 1456-1468.

Yu, X. and Machesky, L. M. (2012). "Cells assemble invadopodia-like structures and invade into matrigel in a matrix metalloprotease dependent manner in the circular invasion assay." PLoS One **7**(2): e30605.

Yu, X., Zech, T., McDonald, L., Gonzalez, E. G., Li, A., Macpherson, I., Schwarz, J. P., Spence, H., Futo, K., Timpson, P., Nixon, C., Ma, Y., Anton, I. M., Visegrady, B., Insall, R. H., Oien, K., Blyth, K., Norman, J. C. and Machesky, L. M. (2012). "N-WASP coordinates the delivery and F-actin-mediated capture of MT1-MMP at invasive pseudopods." J Cell Biol **199**(3): 527-544.

Zaman, M. H., Trapani, L. M., Sieminski, A. L., Mackellar, D., Gong, H., Kamm, R. D., Wells, A., Lauffenburger, D. A. and Matsudaira, P. (2006). "Migration of tumor cells in 3D matrices is governed by matrix stiffness along with cell-matrix adhesion and proteolysis." Proc Natl Acad Sci U S A **103**(29): 10889-10894.

Zanivan, S., Meves, A., Behrendt, K., Schoof, E. M., Neilson, L. J., Cox, J., Tang, H. R., Kalna, G., van Ree, J. H., van Deursen, J. M., Trempus, C. S., Machesky, L. M., Linding, R., Wickstrom, S. A., Fassler, R. and Mann, M. (2013). "In vivo SILAC-based proteomics reveals phosphoproteome changes during mouse skin carcinogenesis." Cell Rep **3**(2): 552-566.

Zegers, M. M., Forget, M. A., Chernoff, J., Mostov, K. E., ter Beest, M. B. and Hansen, S. H. (2003). "Pak1 and PIX regulate contact inhibition during epithelial wound healing." EMBO J **22**(16): 4155-4165.

Zenke, F. T., King, C. C., Bohl, B. P. and Bokoch, G. M. (1999). "Identification of a central phosphorylation site in p21-activated kinase regulating autoinhibition and kinase activity." J Biol Chem **274**(46): 32565-32573.

Zenke, F. T., Krendel, M., DerMardirossian, C., King, C. C., Bohl, B. P. and Bokoch, G. M. (2004). "p21-activated kinase 1 phosphorylates and regulates 14-3-3 binding to GEF-H1, a microtubule-localized Rho exchange factor." J Biol Chem **279**(18): 18392-18400.

Zhan, Q., Ge, Q., Ohira, T., Van Dyke, T. and Badwey, J. A. (2003). "p21-activated kinase 2 in neutrophils can be regulated by phosphorylation at multiple sites and by a variety of protein phosphatases." J Immunol **171**(7): 3785-3793.

Zhang, H., Li, Z., Viklund, E. K. and Stromblad, S. (2002). "P21-activated kinase 4 interacts with integrin alpha v beta 5 and regulates alpha v beta 5-mediated cell migration." J Cell Biol **158**(7): 1287-1297.

Zhang, H. J., Siu, M. K., Yeung, M. C., Jiang, L. L., Mak, V. C., Ngan, H. Y., Wong, O. G., Zhang, H. Q. and Cheung, A. N. (2011). "Overexpressed PAK4 promotes proliferation, migration and invasion of choriocarcinoma." Carcinogenesis **32**(5): 765-771.

Zhang, J., Wang, J., Guo, Q., Wang, Y., Zhou, Y., Peng, H., Cheng, M., Zhao, D. and Li, F. (2012). "LCH-7749944, a novel and potent p21-activated kinase 4 inhibitor, suppresses proliferation and invasion in human gastric cancer cells." Cancer Lett **317**(1): 24-32.